รายงานวิจัยฉบับสมบูรณ์

โครงการ

การยับยั้งการขนส่งโปรตีนในเซลล์เพื่อลดการสร้างไวรัสเดงกี่

โดย

รองศาสตราจารย์ ดร.นพ.ถาวรชัย ลิ้มจินดาพร

ธันวาคม 2560

สัญญาเลขที่ RSA 5780012

รายงานวิจัยฉบับสมบูรณ์

โครงการ

การยับยั้งการขนส่งโปรตีนในเซลล์เพื่อลดการสร้างไวรัสเดงกี่

	คณะผู้วิจัย	สังกัด
หัวหน้าโครงการ	รศ.ดร.นพ.ถาวรชัย ลิ้มจินดาพร	มหาวิทยาลัยมหิดล
ผู้ร่วมโครงการ	ศ.ดร.เพทาย เย็นจิตโสมนัส	มหาวิทยาลัยมหิดล
	ดร.ศันสนีย น้อยสคราญ	ศูนย์พันธุวิศวกรรม และเทคโนโลยีชีวภาพแห่งชาติ

สนับสนุนโดยสำนักงานกองทุนสนับสนุนการวิจัย

Abstract

Project code: RSA 5780012

Project title: Targeting intracellular membrane trafficking to combat dengue virus

Investigator: Associate professor Thawornchai Limjindaporn, MD, PhD

Email address: thawornchai.lim@mahidol.ac.th

Project period: July 2014-June 2017

Once inside the cells, virus hijacks intracellular trafficking mechanisms to generate sheltered compartments to prepare for its own replication. The assembly and budding process of enveloped virus utilizes cellular factors to facilitate transport from one membrane bound compartment to the others. Recent development has led to the design of compounds targeting keys of these membrane trafficking pathways to prevent infection. In this study, RNA interference was performed to identify host proteins contributing to each step of trafficking of dengue viral protein from endocytosis to exocytosis. The candidate host proteins involving in intracellular trafficking mechanisms include COPs, APs and SNAREs proteins. Then, protein protein interaction study was used to identify interacting domains between DENV E and identified host proteins. Finally, peptides were designed to inhibit interactions between DENV E and identified host proteins. This study provides not only cell biology of DENV but also highlight the potential development of mimetic peptides as inhibitors by targeting specifically to interacting domains between DENV-host proteins.

Keywords: Dengue virus, Intracellular membrane trafficking, RNA interference, Protein-Protein Interaction, Peptides

บทคัดย่อ

รหัสโครงการ: RSA 5780012

ชื่อโครงการ: การยับยั้งการขนส่งโปรตีนในเซลล์เพื่อลดการสร้างไวรัสเดงกี่

ชื่อนักวิจัย: รศ.ดร.นพ.ถาวรชัย ลิ้มจินดาพร

Email address: thawornchai.lim@mahidol.ac.th

ระยะเวลาโครงการ: กรกฎาคม 2557 ถึง มิถุนายน 2560

ไวรัสสามารถใช้ขบวนการขนส่งภายในเซลล์ให้เป็นประโยชน์ในการเพิ่มจำนวนของตัวเอง เมื่ออยู่ในเซลล์ ดังนั้นในการพัฒนายาที่มีผลต่อการขนส่งโปรตีนในเซลล์เป็นอีกทางหนึ่งในการกำจัดไวรัสภายในเซลล์ได้ ในการศึกษาครั้งนี้เทคนิค RNA interference ถูกนำมาใช้ในการค้นหาโปรตีนของมนุษย์ที่ไวรัสนำไปใช้ให้เป็นประโยชน์ในการเพิ่มจำนวนของตัวเอง พบว่าโปรตีนในกลุ่ม Aps, COPs และ SNAREs เป็นกลุ่มโปรตีนที่สำคัญ เทคนิคในการหาความสัมพันธ์ระหว่างโปรตีนถูกนำมาทดสอบความสำคัญระหว่างโปรตีนของไวรัสและโปรตีนของมนุษย์ในเซลล์และนำไปสู่การค้นหา peptide ที่สามารยับยั้งปฏิสัมพันธ์ระหว่างโปรตีนของไวรัสและโปรตีนของมนุษย์ อันจะสามารถพัฒนาต่อไปใช้ในการกำจัดไวรัสเดงกี่ในเซลล์ได้ในอนาคต

Keywords: ไวรัสเดงกี่, การขนส่งโปรตีนในเซลล์, RNA interference, ปฏิสัมพันธ์ระหว่างโปรตีน, Peptide

Introduction

Dengue virus (DENV) is a positive-stranded RNA virus in the *Flaviviridae* family, which is transmitted by mosquito vectors. The genome of DENV has sequences encoding structural proteins including capsid (C), pre-membrane protein (prM), and envelope (E), and non-structural proteins (NS) including NS1, NS2A, NS2B, NS3, NS4A, NS4B and NS5[1]. DENV consists of four serotypes, and secondary infection by different serotypes of DENV contributes to severe dengue [2]. Patients with dengue hemorrhagic fever often present with plasma leakage, hemoconcentration, thrombocytopenia, and hemorrhagic tendencies. Additionally, serious complications of dengue hemorrhagic fever, such as organ failure, may lead to dengue shock syndrome [1-3]. Currently, there are no effective vaccines or antiviral drugs available; therefore, a better understanding of dengue pathogenesis is required.

DENV needs host cellular machinery for its replication. It binds to receptors and enters host cells by clathrin-mediated endocytosis [4-16]. Reduced pH in the endosomes induces fusion of viral and host cell membranes, thereby releasing DENV RNA into the cytoplasm [17]. Viral replication occurs on the network of modified endoplasmic reticulum (ER) membranes, including vesicular packets, virus-induced vesicles, and convoluted membranes [18-20]. Immature viral particles are transported through the trans-Golgi network (TGN) and mature virions are generated after cleavage of prM protein by host furin. Mature viruses are finally released from the host cells by exocytosis [21]. Host proteins are important for the viral life cycle, including endocytosis, virus-induced membrane rearrangement, viral RNA replication and translation, and virion assembly and production.

Adaptor protein complex (AP) was originally identified as a component of the clathrin-coated vesicles in the brain [22, 23]. Each member of AP has two large subunits (γ/β1, α/β2, δ/β3, ε/β4 or ζ/β5), one medium subunit (μ1–μ5), and one small subunit (σ1–σ5). AP-1A consists of one medium subunit (μ1A), two large subunits (β1 and γ), and one

small subunit (σ1). In contrast, AP-1B consists of one medium subunit (μ1B), two large subunits (β1 and γ), and one small subunit (σ1). The μ subunit mediates a selection of cargo proteins via its binding with tyrosine-based sorting motif on the cargo protein [24-26]. AP-1A is expressed ubiquitously and regulates the TGN-basolateral plasma membrane transport. However, AP-1B is expressed in epithelial cells and regulates the basolateral transport of proteins from the recycling endosomes. AP-1A, AP-2, AP-3A, AP-4 and AP-5 are expressed ubiquitously. In contrast, AP-1B and AP-3B are expressed in a tissue-specific manner [23]. Each member of AP has two large subunits (γ/β1, α/β2, δ/β3, ε/β4 or ζ/β5), one medium subunit (μ1–μ5), and one small subunit (σ1–σ5). AP-1A consists of two large subunits (β1 and γ), one medium subunit (μ1A), and one small subunit (σ1). The μ subunit mediates a selection of cargo proteins via its binding with tyrosine-based sorting motif on the cargo protein [24-26]. AP-1 can be recruited to components required for membrane rearrangement and interactions between AP-1A and viral proteins are reported in several viruses [27-30]. Dysfunction of AP-1 may affect membrane organization, thereby decreasing viral replication in infected cells.

Coat proteins and soluble *N*-ethylmaleimide-sensitive factor attachment protein receptors (SNAREs) are the components of the vesicle trafficking process in cells. There are 3 basic types of coat proteins, including coat protein complex I (COPI), coat protein complex II (COPII), and clathrin [31]. Clathrin mediates endocytosis while COPII-coated vesicle mediates anterograde transport from the ER to the Golgi apparatus, and COPI-coated vesicle mediates retrograde transport from the Golgi apparatus to the ER [32]. SNAREs are important for vesicular fusion on the target membrane, and they are formed as the specific determinant to mediate fusion events in different intracellular membrane trafficking pathways. SNAREs are structurally classified as either Q-SNAREs or R-SNAREs, according to the central residue

of SNARE motif, which is glutamine or arginine, respectively [33, 34]. SNAREs are functionally classified as either v-SNAREs or t-SNAREs, depending on whether they are found on the vesicle membrane or the target membrane, respectively. Previous studies have demonstrated the role of coat protein complex in several virus infections, including poliovirus [35, 36], enterovirus 71 (EV71) [37], alphavirus [38], HIV [39], HCV [40], and DENV [41].

In this study, RNA interference was performed to identify host proteins contributing to each step of trafficking of dengue viral protein from endocytosis to exocytosis. The candidate host proteins involving in intracellular trafficking mechanisms include Adaptor proteins (AP-1A, AP-2), Coat proteins (COPI, COPII), and SNAREs proteins (STX 5, NSF) Then, protein protein interaction study was used to identify interacting domains between DENV E and AP-1A. Finally, peptides were designed to inhibit interactions between DENV E and AP-1A. This study provides not only cell biology of DENV but also highlight the potential development of mimetic peptides as inhibitors by targeting specifically to interacting domains between DENV-host proteins.

Materials and Methods

Part I: Adaptor Protein 1A Facilitates Dengue Virus Replication

Cell lines, virus, and antibodies

Human hepatocellular carcinoma (Huh7) cells were obtained from the JCRB Cell Bank (Osaka, Japan) and cultured in RPMI 1640 (Gibco, Carlsbad, CA, USA) supplemented with 10% heat-inactivated fetal bovine serum (FBS; Gibco), 1% non-essential amino acid (Gibco), 37 μg/ml penicillin (Sigma, St Louis, MO, USA) and 60 μg/ml streptomycin (Sigma) at 37°C in a 5% CO_2 incubator with a humidified atmosphere. Propagation of DENV-1 (Hawaii), DENV-2 strain 16681, DENV-3 (H87), and DENV-4 (H241) was performed in C6/36

mosquito cells. Mouse monoclonal antibodies specific for DENV E (clones 3H5 and 4G2), DENV prM (clone 1C3), and DENV NS1 (clone NS1-3F.1) were produced from previously established hybridoma cells [42-44]. Mouse polyclonal antibody specific for AP1M1 (μ1A subunit) was purchased from Abnova (Taipei, Taiwan). Mouse monoclonal antibody specific for β-actin was purchased from Santa Cruz Biotechnology (Santa Cruz, CA, USA).

AP-1-dependent traffic inhibitor and DENV infection

Huh7 cells were infected with DENV-2 at a multiplicity of infection (MOI) of 1 for 2 h. Excess viruses were removed and cells were washed three times with PBS. DENV-infected or mock-infected Huh7 cells were incubated with AP-1-dependent traffic inhibitor (A5) (Merck KGaA, Darmstadt, Germany) [45] at a final concentration of 0, 25, 50, 100 or 200 μM in 2% FBS–RPMI 1640 for 24 h. DENV-infected Huh7 cells were harvested for measuring viral protein expression by western blotting using antibody to DENV E (4G2). The culture supernatants were also collected to measure the amount of DENV production by a focus forming unit (FFU) assay, as described previously[46]. Cell viability was determined by PrestoBlue cell viability assay (Invitrogen, Carlsbad, CA, USA). To establish whether AP-1-mediated traffic was involved in production of four serotypes of DENV, Huh7 cells were infected with DENV-1, -2, -3 or -4 at a MOI of 1 for 2 h. Unbound virus was removed by washing with PBS. DENV-infected Huh7 cells were incubated with A5 (200 μM) or culture medium (control) for 24 h. Virus titer in culture supernatants was measured by FFU assay [46].

Knockdown of AP-1A

Huh7 cells were seeded onto a 24-well plate in culture medium without antibiotics at a concentration of 8×10^4 cells/well. Twenty-four hours later, the medium was replaced with fresh RPMI 1640 medium and the cells were transfected with duplex AP-1A-specific siRNA (AP1M1 (μ1A) siRNA: 5′-CCGAAGGCAUCAAGUAUCGGAAGAA-3′, Invitrogen) or

control siRNA (Cat.No. 12935-300; Invitrogen) using Lipofectamine RNAi Max (Invitrogen). After incubation with siRNA (100 nM) for 6 h, the cells were supplemented with maintenance medium and incubated for a further 24 h. The second round of siRNA transfection was performed. mRNA and protein expression of AP-1A and β-actin was subsequently verified by real-time reverse transcription polymerase chain reaction (RT-PCR) (Lightcycler RNA Amplification Kit; Roche, Basel, Switzerland) using primers including AP1M1-Forward: 5′-CTAGTGTGGAGGCCGAAGAC-3′; AP1M1-Reverse: 5′-CGGAGCTGGTAATCTCCATT-3′; ACTB-Forward: 5′-AGAAAATCTGGCACCACACC-3′; ACTB-Reverse: 5′-CTCCTTAATGTCACGCACGA-3′, and western blot analysis [47] using AP1M1 and β-actin antibodies, respectively. Cell viability was measured by trypan blue exclusion, as described previously [48].

Binding assay

Huh7 cells transfected with AP-1A siRNA or control siRNA were detached by trypsinization. After washing three times with PBS, cells were blocked with 1% bovine serum albumin (BSA)–PBS for 30 min and incubated with DENV-2 at a MOI of 1 for 30 min on ice to prevent endocytosis. Cells were washed twice with 1% BSA–PBS and incubated with anti-DENV E antibody (3H5) for 30 min on ice. After washing, rabbit anti-mouse IgG conjugated with fluorescein isothiocyanate (dilution 1:50) was added and incubated for 30 min on ice. Cells were washed three times with 1% BSA–PBS and resuspended in 350 μl of 1% paraformaldehyde–PBS. Virus binding was finally counted by the percentage of surface DENV-E-positive cells analyzed by flow cytometry.

Internalization assay

Huh7 cells transfected with AP-1A siRNA or control siRNA were incubated with DENV-2 at a MOI of 1 for 2 h at 37°C to allow penetration of DENV. To remove excess virus, cells were washed three times with PBS. RNA was extracted from DENV-infected Huh7 cells using the

High Pure RNA isolation kit (Roche) and 0.5 μg RNA was reverse transcribed by random hexamer primers from the Superscript III cDNA synthesis kit (Invitrogen). cDNA was amplified by PCR using SYBR Green I Master Mix and primers specific to DENV E (DENV E-Forward: 5′-ATCCAGATGTCATCAGGAAAC-3′; DENV E-Reverse: 5′-CCGGCTCTACTCCTATGATG-3′). Real-time RT-PCR was performed by LightCycler 480 II (Roche) with: (i) 40 amplification cycles of denaturation at 95°C for 10 s, annealing at 60°C for 10 s, and extension at 72°C for 10 s; and (ii) melting curve and cooling steps as recommended by the manufacturer. Relative levels of human AP1M1 mRNA and viral RNA expression were determined by normalization to the expression levels of human β-actin according to the $2^{-\Delta\Delta Ct}$ method [49].

Real-time RT-PCR

RNA was extracted from DENV-infected Huh7 cells, which were transfected with AP-1A-specific siRNA or control siRNA using the High Pure RNA isolation kit (Roche). Reverse transcription was performed using total RNA (1 μg) and SuperScript III reverse transcriptase (Invitrogen). Oligo(dT) 20 primer or random hexamer primers were used for synthesis of cDNA template for determination of human AP-1A and β-actin mRNA, as well as DENV RNA. Real-time RT-PCR was performed by LightCycler 480 II (Roche) with: (i) 40 amplification cycles of denaturation at 95°C for 10 s, annealing at 60°C for 10 s, and extension at 72°C for 10 s; and (ii) melting curve and cooling steps as recommended by the manufacturer's instructions. Relative levels of human AP-1A mRNA and viral RNA expression were determined by normalization to the expression levels of human β-actin according to the $2^{-\Delta\Delta Ct}$ method [49].

Viral RNA transfection

DENV RNA was isolated from culture supernatant of DENV-infected C6/36 cells using the High Pure RNA isolation kit (Roche). In a 24-well plate, cells transfected with AP-1A siRNA

or control siRNA were transfected with DENV RNA (0.5 μg) using Lipofectamine 2000. At 4 h post-transfection, transfection reagent was removed and replaced with complete RPMI 1640 medium. Cells were harvested at 6 and 24 h post-transfection for detection of viral RNA by real-time RT-PCR. The culture supernatant was collected at 24 h post-transfection for FFU assay [46].

Western blotting

Clear lysates prepared from Huh7 cells transfected with AP-1A siRNA or control siRNA were mixed with 4× loading buffer [50 mM Tris–HCl (pH 6.8), 2% SDS, 0.1% bromophenol blue and 10% glycerol] and heated at 95°C for 5 min. Proteins in the samples were subjected to 10% SDS-PAGE and transferred to nitrocellulose membranes (GE Healthcare Life Sciences, Freiburg, Germany) as described previously [50]. The membranes were incubated with 5% skimmed milk in PBS or in Tris-buffered saline with 0.1% Tween 20 (TBST) for 1 h to block non-specific binding and with mouse monoclonal antibodies specific for DENV E (clones 4G2), DENV PrM (clone 1C3), and DENV NS1 (clone NS1-3F.1) or human β-actin at 4°C overnight. The membranes were washed three times with PBS or TBST and incubated with horseradish peroxidase (HRP)-conjugated rabbit anti-mouse immunoglobulin antibody (DAKO, Santa Clara, CA, USA) at a dilution of 1:1000 for 1 h at room temperature, followed by three further washes. Proteins were visualized using an enhanced chemiluminescence detection kit (SuperSignal West Pico Chemiluminescent Substrate; Thermo Scientific, Waltham, MA, USA). Relative expression levels of human AP-1A, and DENV proteins were assessed by normalization of their protein band intensities to human β-actin intensity using ImageJ software (National Institutes of Health, Bethesda, MD, USA).

FFU assay

Supernatants collected from DENV-infected Huh7 cells transfected with AP-1A siRNA or control siRNA were assessed for DENV production. Vero cells were seeded onto a 96-well

plate (Sigma) at 3×10^4 cells/well in minimal essential medium (MEM) supplemented with 10% FBS, 2 mM L-glutamine, 36 µg/ml penicillin and 60 µg/ml streptomycin, and cultured at 37°C in a 5% CO_2 incubator for 24 h. The medium was removed from each well. DENV was serially diluted 10-fold in MEM containing 3% FBS, 2 mM L-glutamine, 36 µg/ml penicillin and 60 µg/ml streptomycin, added to each well (100 µl/well), and incubated at 37°C in a 5% CO_2 incubator for 2 h. Overlay medium (MEM containing 3% FBS, 2 mM L-glutamine, 2% carboxy methyl cellulose, 10% tryptose phosphate broth, 37 µg/ml penicillin and 60 µg/ml streptomycin was added to each well (100 µl/well), and the culture was incubated for 3 days. The medium was discarded from DENV-infected cells. The adherent cells were washed three times with PBS (pH 7.4), fixed with 3.7% formaldehyde (BDH Laboratory Supplies, Poole, UK) in PBS at room temperature for 10 min, followed by an additional 10 min permeabilization with 1% Triton X-100 (Fluka, Steinheim, Switzerland). The cells were incubated sequentially with mouse anti-DENV E monoclonal antibody (clone 4G2) at 37°C for 1 h and HRP-conjugated rabbit anti-mouse immunoglobulins (DAKO; at a dilution of 1:1000 in PBS containing 2% FBS and 0.05% Tween-20 in the dark at 37°C for 30 min. To develop an enzymatic reaction, the cells were incubated with a substrate solution containing 0.6 mg/ml diaminobenzidine, 0.03% H_2O_2 and 0.08% $NiCl_2$ in PBS at room temperature in the dark for 5 min. After washing three times with PBS, dark brown foci of the DENV-infected cells were counted under a light microscope. Virus titers were reported as FFU/ml.

Transmission electron microscopy (TEM)

Huh7 cells transfected with AP-1A siRNA or control siRNA were infected with DENV-2 at a MOI of 10 for 2 h. Cells were washed three times with PBS and incubated in maintenance medium (2% FBS–RPMI 1640) for 24 h. Cells were fixed with 2% paraformaldehyde/2% glutaraldehyde in PBS for 24 h at 4°C, post-fixed with 1% osmium tetroxide and 1% potassium ferrocyanide for 1 h at room temperature, followed by dehydration in a graded

series of ethanol (25%, 50%, 75%, 95% and 100%) for 20 min. Cells were embedded in LRW resin and incubated at 60°C for polymerization for 48 h. Sections were obtained with a Reichert–Jung Ultracut E Ultramicrotome and diamond knife, counterstained with uranyl acetate and lead citrate for 10 min each, and examined with a JEOL-1010 transmission electron microscope (JEOL USA, Peabody, MA, USA).

YFP-PCA mammalian two-hybrid system

Mammalian two hybrid system can be used to map the domains required for protein-protein interaction. The full length of DENV E and host trafficking proteins were constructed. HEK293T cells were grown in complete Dulbecco's modified eagle's medium (DMEM) (GIBCO) supplemented with 10% fetal bovine serum (GIBCO), 100 U/ml penicillin and 100 µg/ml streptomycin at 37 $^{\circ}$C in 5% CO_2 incubator. On the day before transfection, cells were plated in 6-well plate with 50% confluence per well. The cultured cells were individually transfected with 1 µg each of the following constructs; pcDNA3.1/Zeo-YFP[2]-AP-1 mu1A, pcDNA3.1/Zeo-YFP[2]-AP-1 mu1B, pcDNA3.1/Zeo-YFP[1]-E_III , pcDNA3.1/Zeo-YFP[1] and pcDNA3.1/Zeo-YFP[2] by using Lipofectamine 2000 (Invitrogen) and according to the manufacture's protocol. The cultured cells were co-transfected with different pair of the construct (1 µg each) including pcDNA3.1/Zeo-YFP[1] and pcDNA3.1/Zeo-YFP[2] (as a negative control), pcDNA3.1/Zeo-YFP[1]-kAE1 and pcDNA3.1/Zeo-YFP[2]- AP-1 mu1A (as a positive control), pcDNA3.1/Zeo-YFP[1]-EDIII and pcDNA3.1/Zeo-YFP[2]-AP-1 mu1A and pcDNA3.1/Zeo-YFP[1]-EDIII and pcDNA3.1/Zeo-YFP[2]-AP-1 mu1B by using Lipofectamine 2000 (Invitrogen) and according to the manufacture's protocol. At 5 hours post-co-transfection, transfection mixture was removed and replaced with complete DMEM medium. After 48 h after transfection, cells were observed under fluorescence microscope. They were detached, centrifugation 2000 rpm 5 minutes at 4º C and then fixed in 2%

paraformaldehyde. Cells were re-suspended again and analyzed by using FACSort flow cytometer**.**

Peptide blocking

Peptides were designed base on the sequences of domain III of DENV E including RRRRRRRR-MKGMSYSMCTGKFKVVKEIAETQHGTIVIRVQY and RRRRRRRR-MRGMSYSMCTGKFKVVKEIAETQHGTIVIRVQY, respectively. Mammalian two hybrid system was performed as previously described. After 24 h after co-transfection, cells were incubated with 10 μM of peptides. After 48 h after transfection, cells were observed under fluorescence microscope. They were detached, centrifugation 2000 rpm 5 minutes at 4º C and then fixed in 2% paraformaldehyde. Cells were re-suspended again and analyzed by using FACSort flow cytometer**.**

Statistical analysis

Data were statistically analyzed by unpaired *t* test, with the use of GraphPad Prism version 5.0 (San Diego, CA, USA). Results were expressed as mean and standard error of the mean (SEM) and $P<0.05$ was considered significant.

Part II: Exocytosis Role of Adaptor Protein 2 in Dengue Virus Infection

Cell lines, viruses, antibodies and inhibitor

Human hepatocellular carcinoma (Huh7) cells were obtained from the JCRB Cell Bank (Osaka, Japan) and cultured in RPMI 1640 (Gibco, Carlsbad, CA, USA) supplemented with 10% heat-inactivated fetal bovine serum (FBS; Gibco), 1% non-essential amino acid (Gibco), 37 μg/ml penicillin (Sigma, St Louis, MO, USA) and 60 μg/ml streptomycin (Sigma) at 37°C in a 5% CO_2 incubator with a humidified atmosphere. DENV strains used in this study were DENV-1 (Hawaii), DENV-2 (16681), DENV-3 (H87) and DENV-4 (H241). Mouse monoclonal antibodies specific to DENV E (clones 3H5) were kindly provided by Dr.

Chunya Puttikhunt. Sunitinib malate, AAK1 inhibitor was purchased from Sigma-Aldrich, USA.

siRNA and primers

Control siRNA: Stealth RNAi Negative Control Duplexes, Cat.No. 12935-300

AP2M1 siRNA: 5'-CAGCAGTCACCAAGCAGAATGTCAA-3'

AP2M1-Forward: 5'-CAGCAGGGCATCAAGAGTCAGCA-3'

AP2M1-Reverse: 5'-CACCTGCCCTTGTGGGGACATGA-3'

DENV E-Forward: 5'-ATCCAGATGTCATCAGGAAAC-3'

DENV E-Reverse: 5'-CCGGCTCTACTCCTATGATG-3'

ACTB-Forward: 5'-AGAAAATCTGGCACCACACC-3'

ACTB-Reverse: 5'-CTCCTTAATGTCACGCACGA-3'

Control and AP2M1 siRNA were purchased from Invitrogen, USA.

Time-of-addition studies of sunitinib

Time-of-addition assay was performed to study an anti-DENV activity of sunininib in DENV replication cycle. For DENV infection, Huh7 cells were infected with DENV-2 at an MOI of 1 for 2 h. The virus inoculum was removed and cells were washed with PBS for three times. The fresh growth medium was added and incubated at 37°C in 5% CO_2 incubator for 24 h. Cells were treated with sunitinib at concentration 0.5, 1, 2.5, 5 and 10 µM. Time-of-addition studies including pre-treatment (2 h before DENV inoculation), co-treatment (0 h, during 2 h inoculation) and post-treatment (2 h after inoculation) were performed. After 24 h post infection, culture supernatants were collected for determining virus titer by focus forming assay (FFA).

siRNA transfection

Huh7 cells were transfected with duplex AP2M1 specific siRNA or control siRNA using Lipofectamine 2000 (Invitrogen). After 6 h post transfection, cells were supplemented with

fresh growth medium and incubated for a further 24 h. siRNA transfection was performed twice in 24 h interval.

DENV naked RNA transfection

DENV RNA was isolated from culture supernatant of DENV-2-infected C6/36 cells using High Pure RNA isolation kit (Roche). Control or AP2M1 knockdown Huh7 cells were transfected with 0.5 μg DENV naked RNA by Lipofectamine 2000 (Invitrogen). At 4 h post-transfection, transfection reagent was removed and replaced with complete RPMI 1640 medium. Cells were harvested at 24 h post-transfection.

Reverse transcription and real-time PCR

Total RNA was extracted from cells using the High Pure RNA isolation kit (Roche). Reverse transcription was performed using total RNA (1 μg) and SuperScript III reverse transcriptase (Invitrogen). Real-time RT-PCR was performed using SYBR Green I based detection. And analyzed by LightCycler480 II instrument (Roche) with: (i) 40 amplification cycles of denaturation at 95°C for 10 s, annealing at 60°C for 10 s, and extension at 72°C for 10 s; and (ii) melting curve and cooling steps as recommended by the manufacturer's instructions. Relative levels of human AP2M1 mRNA and viral RNA expression were determined by normalization to the expression levels of human β-actin according to the $2^{-\Delta\Delta Ct}$ method.

Indirect immunofluorescence staining

DENV naked RNA transfected Huh7 cells, which were transfected with AP2M1 specific siRNA or control siRNA were fixed with 4% paraformaldehyde-PBS, permeabilized with 500 μl of 0.2% Triton X-100-PBS for 10 min each at RT. Subsequently, cells were incubated with mouse monoclonal antibody to DENV (clone 3H5) for 1 h at RT. After washing three times with PBS, cells were incubated with donkey anti-mouse IgG conjugated with Alexa Fluor 594 for 30 min at RT. Nuclei were stained with Hoechst 33342 dye. The staining cells were visualized by a confocal microscopy.

Statistical analysis

Data were statistically analyzed by one-way ANOVA or unpaired *t* test using GraphPad Prism version 5.0 (San Diego, CA, USA). Results were expressed as mean and standard error of the mean (SEM) and $P<0.05$ was considered significant.

Part III: Coat Protein Complex I Facilitates Dengue Virus Production

Cell lines and virus strains

Human hepatocellular carcinoma Huh7 cell line was grown in RPMI-1640 medium (Gibco, Carlsbad, CA, USA) complemented with 10% heat-inactivated fetal bovine serum (FBS; Gibco), 1% non-essential amino acid (Gibco), 100 U/ml penicillin (Sigma Aldrich, St. Louis, MO, USA), and 100 µg/ml streptomycin (Sigma Aldrich) at 37°C in a 5% CO_2 incubator. EA.hy926 cells (human endothelial cell line) were cultured in Dulbecco's Modified Eagle Medium/Nutrient Mixture F-12 (DMEM/F-12; Gibco) supplemented with 10% heat-inactivated FBS (Gibco), 100 U/ml penicillin (Sigma Aldrich), and 100 µg/ml streptomycin (Sigma Aldrich) at 37°C in a humidified 5% CO2 incubator. DENV serotype 1 (strain Hawaii), DENV serotype 2 (strain 16681), DENV serotype 3 (strain H87), and DENV serotype 4 (strain H241) were propagated in mosquito C6/36 cells, which were grown in Leibovitz's L-15 Medium (Gibco, CA, USA), complemented with 10% heat-inactivated FBS (Gibco), 10% tryptose phosphate broth (Sigma Aldrich), 100 U/ml penicillin, and 100 µg/ml streptomycin (Sigma Aldrich) at 28°C in an incubator without CO_2.

Antibodies

Mouse monoclonal antibodies against DENV E (clone 4G2), C (clone 1C4), prM (clone 1C3), and NS1 (clone 2G6) were generated from hybridoma cells, as described previously [42-44]. Mouse monoclonal antibody against GAPDH and goat polyclonal antibody against COPG (COPI subunit) were purchased from Santa Cruz Biotechnology, Inc. (Santa Cruz, CA, USA).

siRNA transfection and DENV infection

Huh7 cell line was seeded in complete RPMI medium. On the second and third days, cells were separately transfected with specific siRNA (Invitrogen) or control siRNA (Invitrogen) using Lipofectamine™ 2000 (Invitrogen) and incubated in a 37°C 5% CO_2 incubator for 48 hours. Target sequences of siRNA included siCOPI (5′GAGUUCAUCGAGGACUGCGAGUUCA3′),siCOPII(5′GGGCAGAUCCUUAUCGCC GACCUCA3′), siSTX5(5′GAGUUGGGCUCCAUCUUUCAGCAGU3′), siNSF (5′GCACCACAATTGCACAGCAAGTCAA3′). Knockdown cells were then infected with DENV at a multiplicity of infection (MOI) of 1. At 2 hours post-infection, unabsorbed viruses were removed by washing with PBS three times and further incubated. At 24-hours post-infection, cells were collected to verify their knockdown efficiencies by real-time RT-PCR (Lightcycler® RNA Amplification Kit; Roche, Basel, Switzerland) and by Western blot analysis. Infectious virus production in culture supernatants was determined by focus forming unit (FFU) assay [51]. Cell viability was detected by trypan blue exclusion, as described previously [51].

Binding assay

COPI-silenced Huh7 cells and control cells were trypsinized and washed with PBS three times. Cells were incubated on ice with DENV-2 at an MOI of 1 for 30 minutes. After removal of unbound virus by washing with 1% BSA-PBS twice, cells were incubated on ice with mouse anti-DENV E antibody (clone 4G2) for 30 minutes. Upon washing, cells were incubated on ice with rabbit anti-mouse IgG conjugated with fluorescein isothiocyanate (dilution 1:50) for 30 minutes. After washing three times, cells were resuspended with 1% paraformaldehyde-PBS. Finally, virus binding on the cell surface was analyzed by flow cytometry.

Internalization assay

COPI-silenced Huh7 cells and control cells were incubated with DENV-2 at an MOI of 1 at 37°C for 2 hours, after which excessive viruses were removed by washing. Total RNA was extracted using High Pure RNA Isolation Kit (Roche). Random hexamer primers of the Superscript III cDNA Synthesis Kit (Invitrogen) were used for reverse transcription of total RNA to cDNA. Real-time RT-PCR was then performed using SYBR Green I Master Mix (Roche) with primers specific to DENV E in a LightCycler® 480 Instrument (Roche). Fold change of DENV E relative to the GAPDH endogenous control was determined by applying the $2^{-\Delta(\Delta CT)}$ method.

qRT-PCR

qRT-PCR was performed using SYBR Green I Reaction Mix (Roche) with primers specific to individual genes in a LightCycler® 480 Instrument (Roche). cDNA samples were amplified

for 40 cycles using the following temperature and time protocol: denaturation at 95°C for 30 seconds, annealing at 60°C for 40 seconds, and extension at 72°C for 25 seconds. The threshold cycle (Ct) was obtained and used for calculation. The fold change of target genes relative to the GAPDH endogenous control was determined using the equation $2^{-\Delta(\Delta CT)}$.

Indirect immunofluorescence staining and Western blot analysis

Huh7 cells were seeded on coverslips and incubated for 24 hours. Later, these cells were individually transfected with COPI-specific siRNA or control siRNA twice at 24-hour intervals. At 48 hours after the first round of siRNA transfection, cells were infected with DENV-2 at an MOI of 1. At 24-hours post-infection, cells were washed once with PBS, fixed with 4% paraformaldehyde-PBS, and permeabilized with 0.2% Triton X-100-PBS. Cells on coverslips were incubated with primary antibody specific to either COPI or DENV E protein at room temperature for 1 hour. Cells were washed to remove excessive primary antibody, incubated with secondary antibody at room temperature for 30 minutes, and cell nuclei were stained by Hoechst (Thermo Fisher Scientific). Fluorescence staining was observed under a laser scanning confocal microscope (Zeiss LSM 510 META). Western blot analysis was performed, as described in a previous report [51].

Statistical analysis

GraphPad Prism version 5.0 (La Jolla, CA, USA) was used to analyze statistical significance by unpaired t-test. A *p*-value of less than 0.05 was regarded as being statistically significant for all tests.

Results

Part I: Adaptor Protein 1A Facilitates Dengue Virus Replication

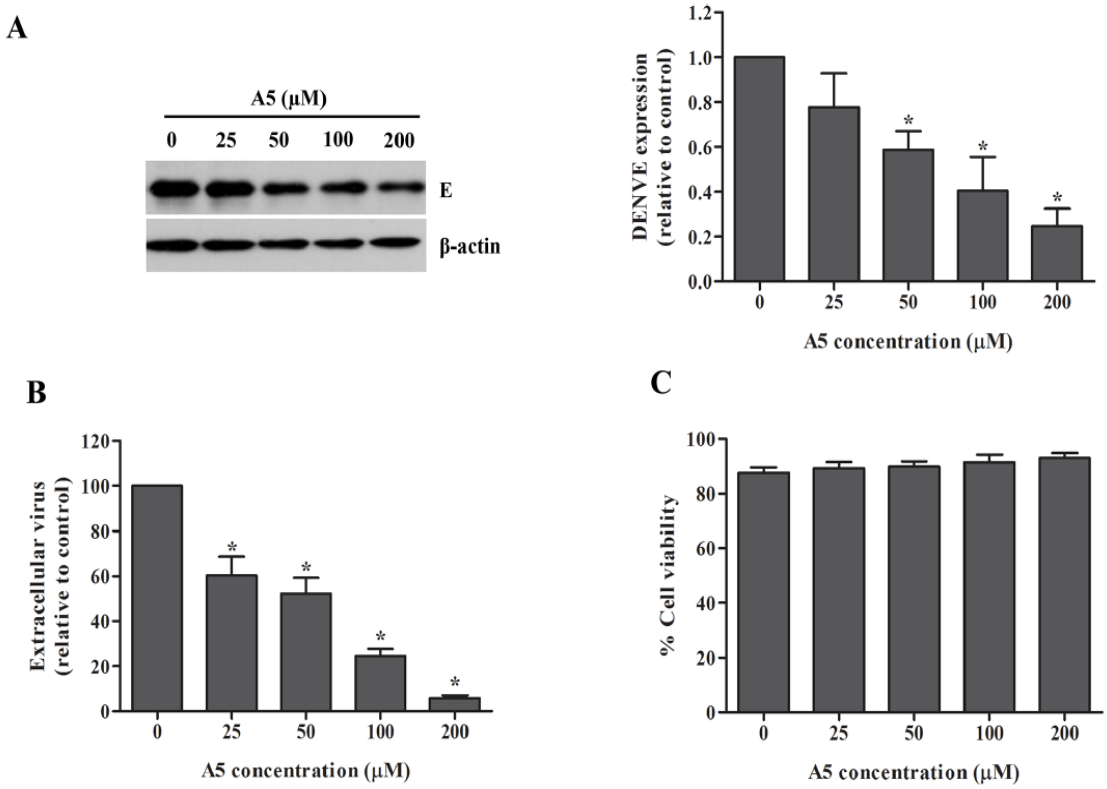

Figure 1. AP-1-dependent traffic inhibitor, A5, inhibited DENV production in Huh7 cells. Huh7 cells were infected with DENV-2 at a MOI of 1 for 2 h. Unbound virus was removed by washing with PBS. Mock- or DENV-infected cells were incubated with A5 at 0, 25, 50, 100 and 200 μM for 24 h. (A) DENV envelope protein in cell lysates was examined at 24 h post-treatment with A5 by western blotting.Band intensity of DENV envelope protein was quantified using Image J software.(B)Virus titer in culture supernatants was measured by FFU assay.(C)Viability of DENV-infected cells was measured using PrestoBlue cell viability reagent. Statistical significance was analyzed using the unpaired *t* test. *P<0.05. Error bars represent SEM from three independent experiments.

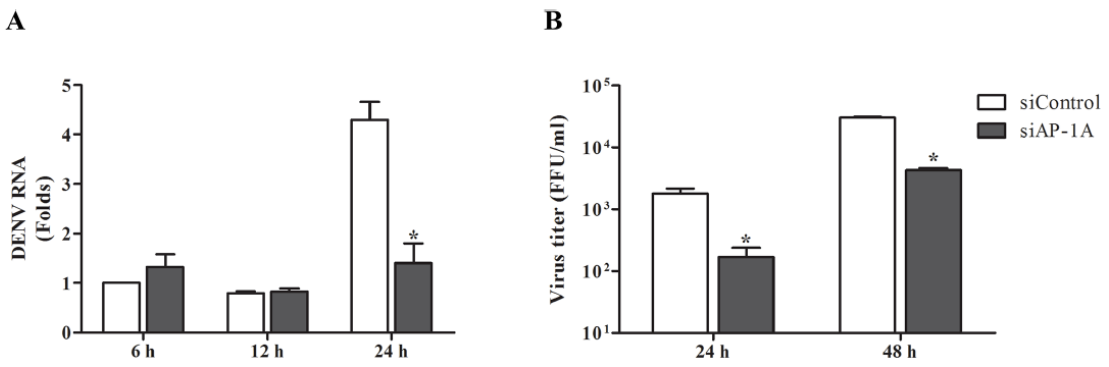

Figure 2. Depletion of AP-1A impaired DENV genome replication. (A) Effect of AP-1A siRNA on DENV RNA synthesis. Cells transfected with control and AP-1A siRNA were transfected with 0.5 µg DENV RNA using Lipofectamine 2000. Viral RNA level was determined by real-time RT-PCR at 6 and 24 h post-transfection. (B) Quantification of virions released from cells transfected with DENV RNA. At 24 h post-transfection, culture supernatants were collected for titration by FFU assay. The results were plotted relative to cells transfected with control siRNA. Statistical significance was analyzed using unpaired *t* test (*P<0.05). Error bars represent SEM from three independent experiments.

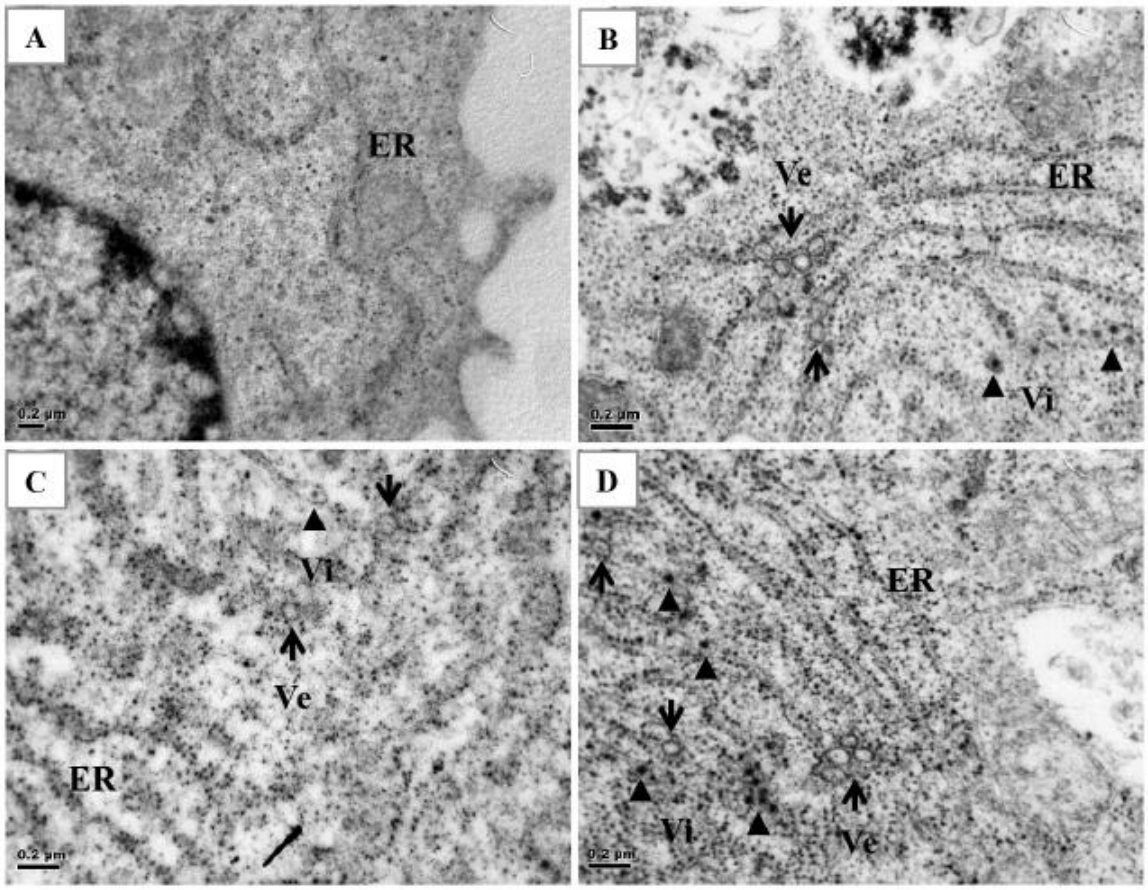

Figure 3. AP-1A knockdown affected the DENV replication site. (A) Ultrastructural analysis of Huh7 cells transfected with control siRNA was observed by TEM at 48 h after second transfection. (B) Cells transfected with control siRNA. (C) Cells transfected with AP-1A siRNA. (D) Cells transfected with AP-2siRNA were infected with DENV-2 at a MOI of 10 for 24 h. Cells were fixed, processed and analyzed by TEM. Ve, virus-induced vesicles (arrow); Vi, virus particles (arrowhead).

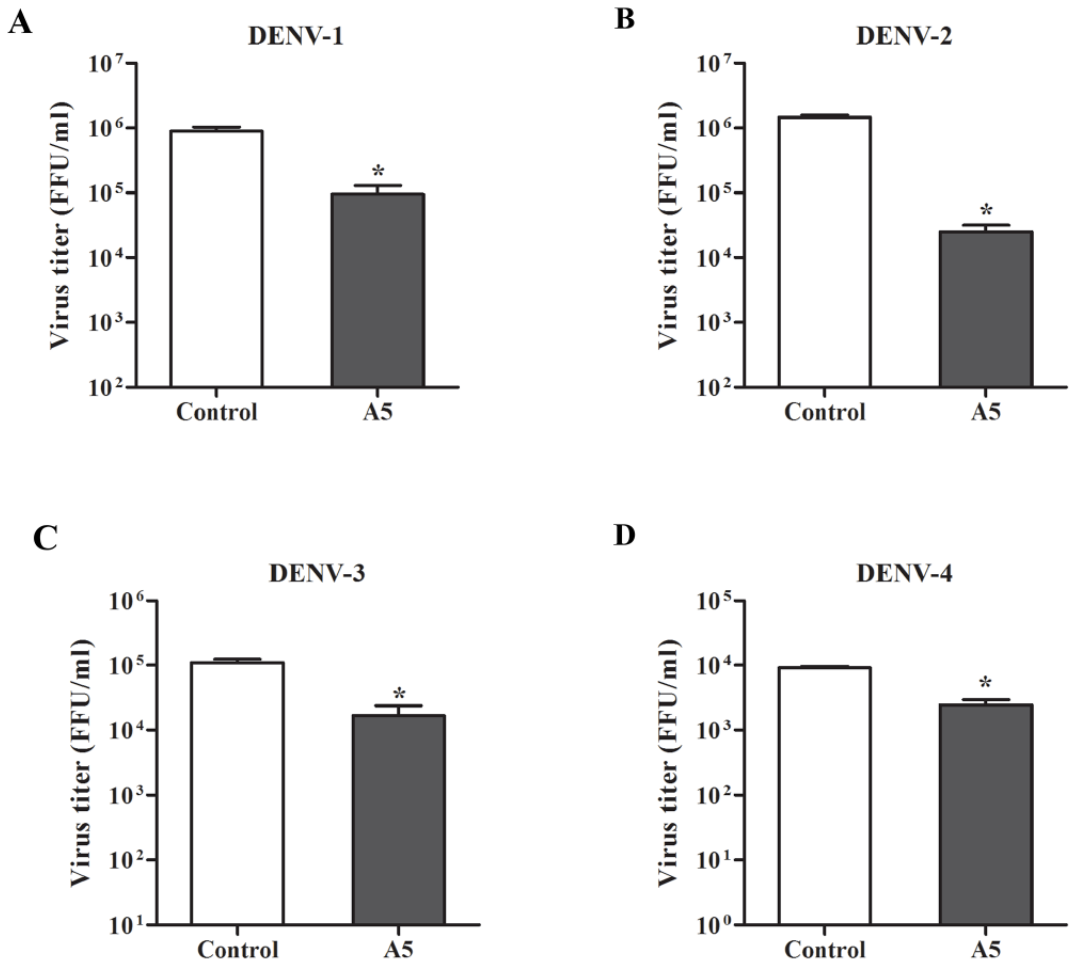

Figure 4. AP-1 was involved in production of four serotypes of DENV. Inhibitory effect of A5 on virus replication was determined in all four serotypes of DENV. Huh7 cells were infected with DENV-1, -2, -3 and -4 at a MOI of 1 for 2 h. Unbound virus was removed by washing with PBS. DENV-infected cells were incubated with A5 (200 μM) or culture medium (control) for 24 h. Virus titer in culture supernatants was measured by FFU assay. (A) Titer of DENV-1; (B) titer of DENV-2; (C) titer of DENV-3; (D) titer of DENV-4. Statistical significance was analyzed using unpaired *t* test (*P<0.05). Error bars represent SEM from three independent experiments.

Conditions	Times						Average (%)
	1	2	3	4	5	6	
GFP	75.23	60.06	65.18	61.98	60.45	63.15	64.34
AP1A-EDIII	26.18	28.42	20	28.72	21.67	18.15	23.86
AP1B-EDIII	20.59	34.97	20.6	23.95	24.91	20.65	24.28
AP1A-kAE1	25.77	43.75	19.9	17.7	18.34	14.63	23.35
V1C-V2N	20.8	7.45	16.02	16.39	13.64	12.65	14.49
pcDNA3.1	ND	3.11	6.37	4.04	4.08	2.27	3.46

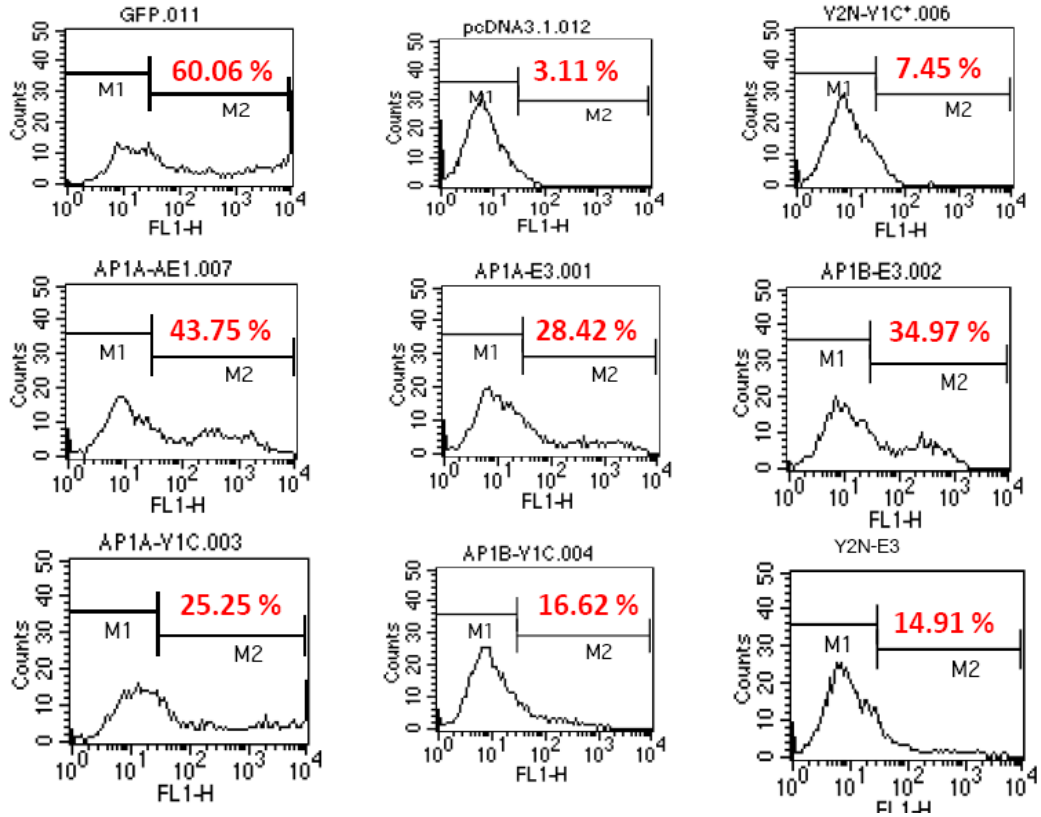

Figure 5. Domain 3 of DENV binds to AP1A, and AP1B by YFP-PCA mammalian two-hybrid system. The cultured cells were co-transfected with different pair of the construct including pcDNA3.1/Zeo-YFP[1] and pcDNA3.1/Zeo-YFP[2] (as a negative control), pcDNA3.1/Zeo-YFP[1]-kAE1 and pcDNA3.1/Zeo-YFP[2]- AP-1 mu1A (as a positive control), pcDNA3.1/Zeo-YFP[1]-EDIII and pcDNA3.1/Zeo-YFP[2]-AP-1 mu1A and

pcDNA3.1/Zeo-YFP[1]-EDIII and pcDNA3.1/Zeo-YFP[2]-AP-1 mu1B by using Lipofectamine 2000 (Invitrogen) and according to the manufacture's protocol. At 5 hours post-co-transfection, transfection mixture was removed and replaced with complete DMEM medium. After 48 h after transfection, cells were observed under fluorescence microscope. They were detached, centrifugation 2000 rpm 5 minutes at 4º C and then fixed in 2% paraformaldehyde. Cells were re-suspended again and analyzed by using FACSort flow cytometer**.**

Conditions	Times			Average (%)
	1	2	3	
AP1A-EDIII	21.26	20.61	20.22	20.70
AP1A-EDIII + peptide I	11.67	11.62	10.50	11.26
AP1A-EDIII + peptide II	12.59	12.91	13.09	12.86

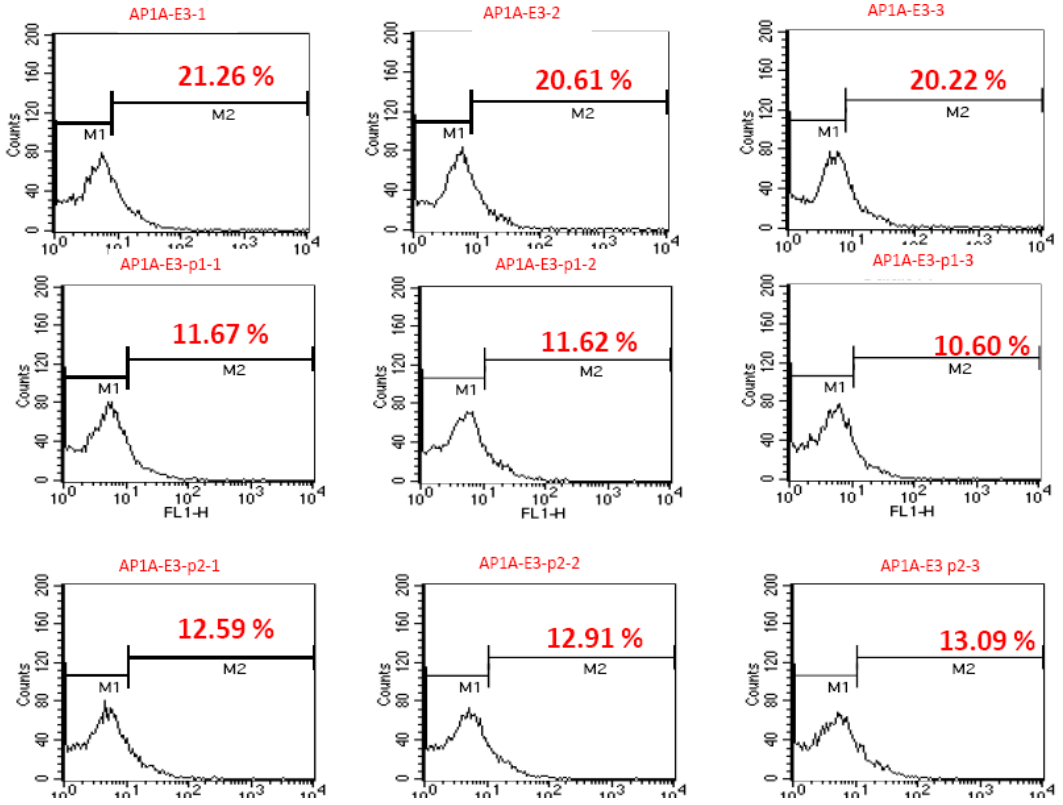

Figure 6. Peptide blocking of DENV E binding to AP1A by YFP-PCA mammalian two-hybrid system. Peptides were designed base on the sequences of domain III of DENV E including RRRRRRRR-MKGMSYSMCTGKFKVVKEIAETQHGTIVIRVQY and RRRRRRRR-MRGMSYSMCTGKFKVVKEIAETQHGTIVIRVQY, respectively. Mammalian two hybrid system was performed as previously described. After 24 h after co-transfection, cells were incubated with 10 μM of peptides. After 48 h after transfection, cells were observed under fluorescence microscope. They were detached, centrifugation 2000 rpm 5 minutes at 4º C and then fixed in 2% paraformaldehyde. Cells were re-suspended again and analyzed by using FACSort flow cytometer**.**

Part II: Exocytosis Role of Adaptor Protein 2 in Dengue Virus Infection

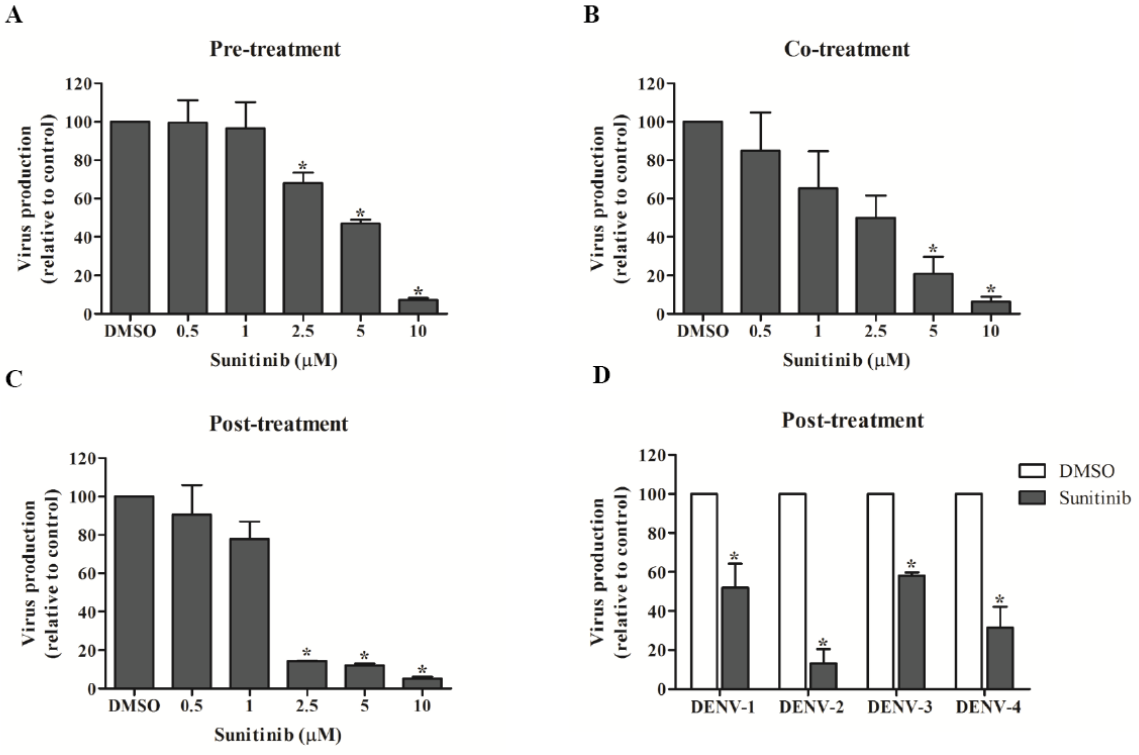

Figure 1. Time-of-addition studies of sunitinib. Activity of AP-2 is regulated by AP-2-associated protein kinase 1 (AAK1). To determine the role of AP-2 in DENV replication cycle, time-of-addition studies of sunitinib, AAK1 inhibitor was performed. Huh7 cells were

treated with sunitinib as following pre-treatment (2 h before infection, -2 h), co-treatment (during infection, 0 h) and post-treatment (2 h after infection, +2 h) and infected with DENV-2 for 24 h. Culture supernatant was harvested for determining viral titer by focus forming assay (FFA). The results showed that sunitinib reduced virus production in all time-of-addition (Fig. 1A-C). Moreover, post-treatment of sunitinib inhibited DENV production in all serotypes (Fig. 1D). These results suggested that AP-2 plays role in DENV replication cycle.

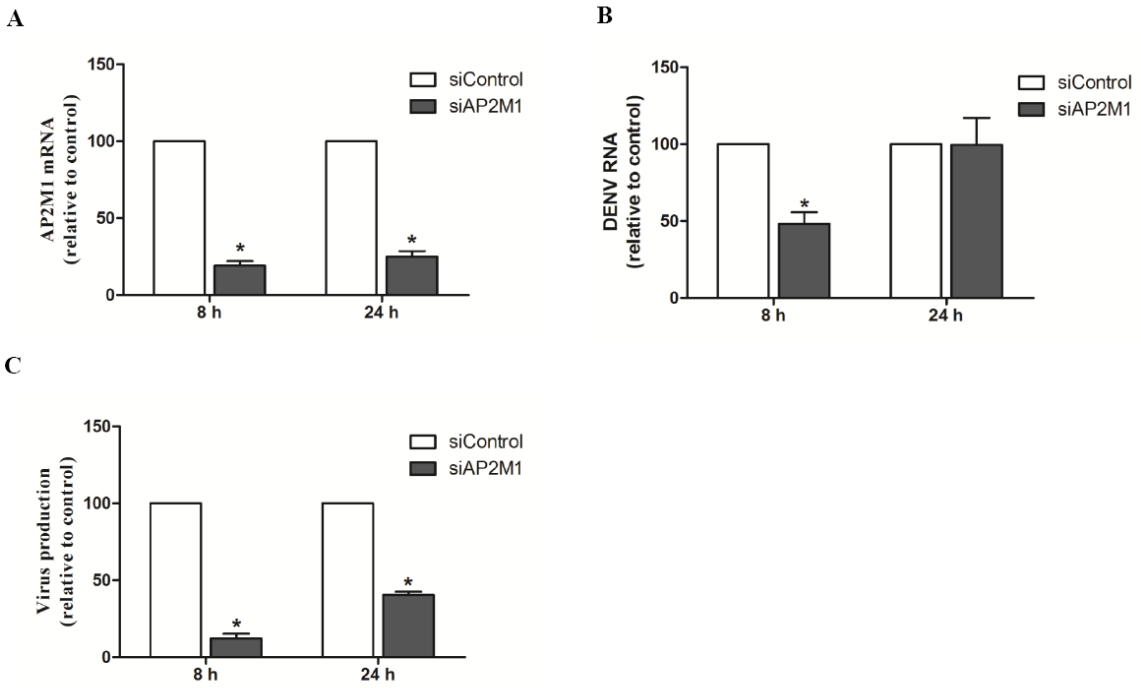

Figure 2. Knockdown of AP2M1 reduces dengue virus production. To confirm the role of AP-2 in DENV production, the μ subunit of AP-2 (AP2M1) was silenced by AP2M1 siRNA before infection. Knockdown efficiency was determined by real-time RT-PCR (Fig. 2A). Control and AP2M1 knockdown cells were infected with DENV-2 at the MOI of 1. Intracellular DENV RNA and extracellular virus were examined at 8 h and 24 h post infection by real-time RT-PCR and focus forming assay (FFA), respectively. At 8 h post infection, intracellular DENV RNA was decreased in AP2M1 knockdown cells (Fig. 2B). At 24 h post infection, intracellular DENV RNA was not changed but extracellular virus was

reduced in AP2M1 knockdown cells compared with those in control siRNA-transfected cells (Fig. 2C). These results suggested that AP-2 plays role in DENV production. Altogether, AP-2 may play an additional role in post-entry stage of DENV replication cycle.

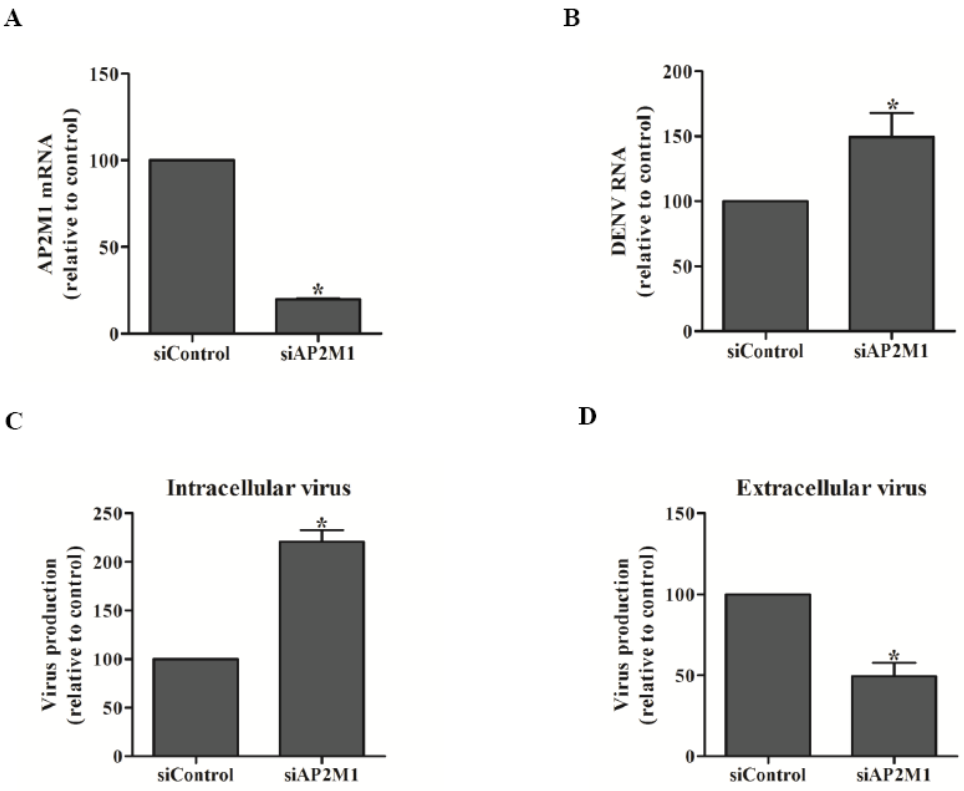

Figure 3. Knockdown of AP2M1 increases intracellular DENV RNA and virions. To characterize the role of AP-2 in post-entry stage, the effect of AP2M1 knockdown on distinct steps of viral replication cycle was determined in DENV naked RNA transfected cells. Huh7 cells were transfected with control or AP2M1 siRNA twice, 24 h interval. Knockdown efficiency was determined by real-time RT-PCR (Fig. 3A). After 24 h post second transfection, cells were transfected with DENV naked RNA to bypass entry step. After 24 h post transfection, cells were collected for determining intracellular viral RNA, intracellular virus and culture supernatants were harvested for examining extracellular virus in a single round of replication. The results showed that knockdown of AP2M1 increased intracellular viral RNA and virions but reduced extracellular virus (Fig. 3B-D). These results suggested that knockdown of AP2M1 affected DENV release.

Part III: Coat Protein Complex I Facilitates Dengue Virus Production

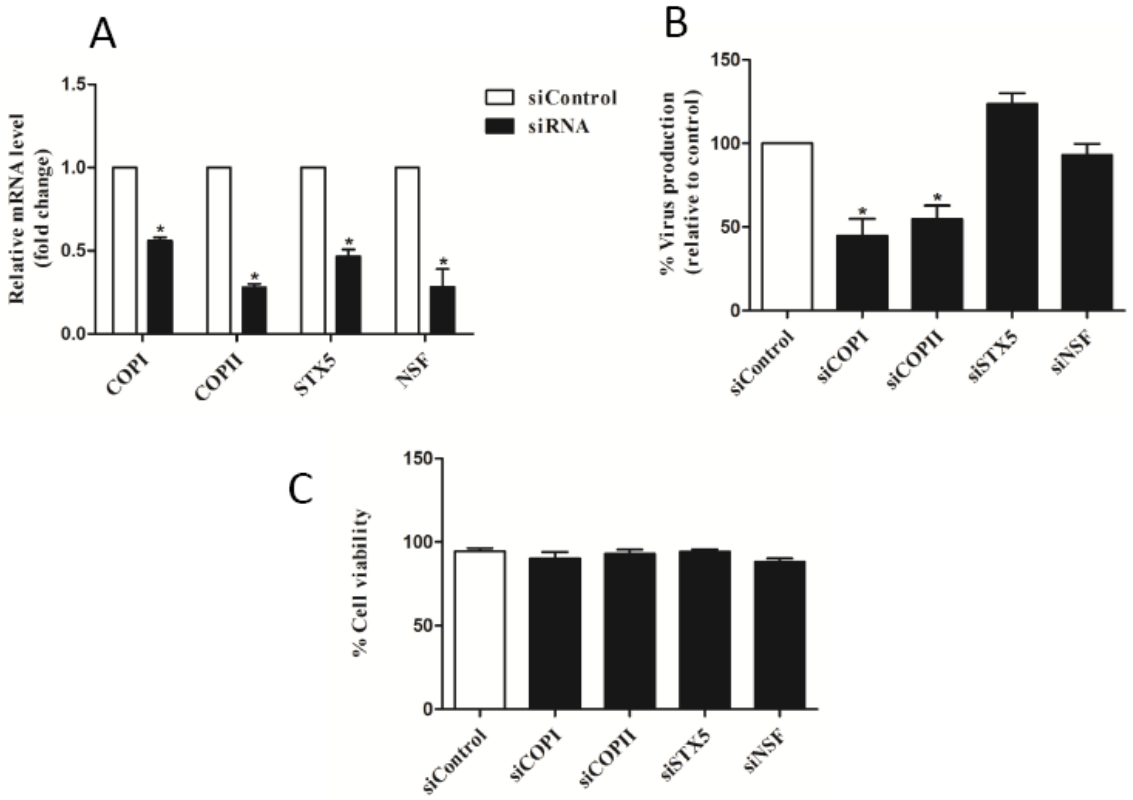

Fig. 1 RNA interference against COPI and COPII decreased DENV production in Huh7 cells. (A) Knockdown efficacy was analyzed by real-time RT-PCR and shown as relative mRNA level normalized with GAPDH. (B) At 24 hpi, infectious virus production in culture supernatants was determined by FFU assay and calculated as a percentage of virus production relative to siControl. (C) Percentage of cell viability was measured by trypan blue exclusion assay. The mean of three independent experiments was the recorded result. An asterisk indicates statistical significance between siControl and specific siRNAs ($p<0.05$).

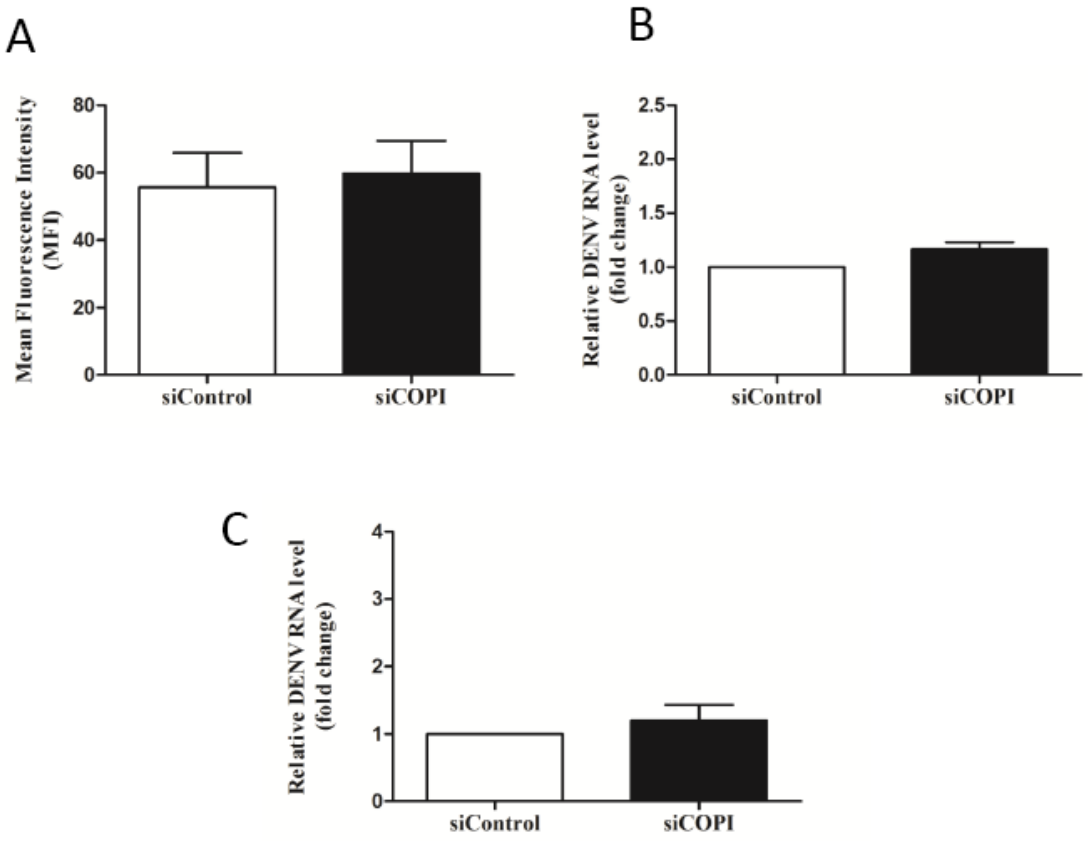

Fig. 2 COPI did not facilitate binding, entry, or RNA replication of DENV in Huh7 cells. (A) At 48 h post-transfection, knockdown cells were blocked with 1% BSA-PBS for 30 min and incubated with DENV-2 at an MOI of 1 for 30 min on ice to inhibit endocytosis. DENV binding on the cell surface was analyzed by flow cytometry, and results were described as mean fluorescence intensity (MFI) of the surface of DENV-E-positive cells. (B) Knockdown cells were infected with DENV-2 at an MOI of 1 for 2 h at 37°C to allow entry of DENV. DENV internalization was analyzed by real-time RT-PCR and shown as relative mRNA level normalized with GAPDH. (C) At 24 hpi, intracellular DENV RNA was analyzed by real-time RT-PCR. The mean of three independent experiments was the recorded result. An asterisk indicates statistical significance between siControl and specific siRNAs ($p<0.05$).

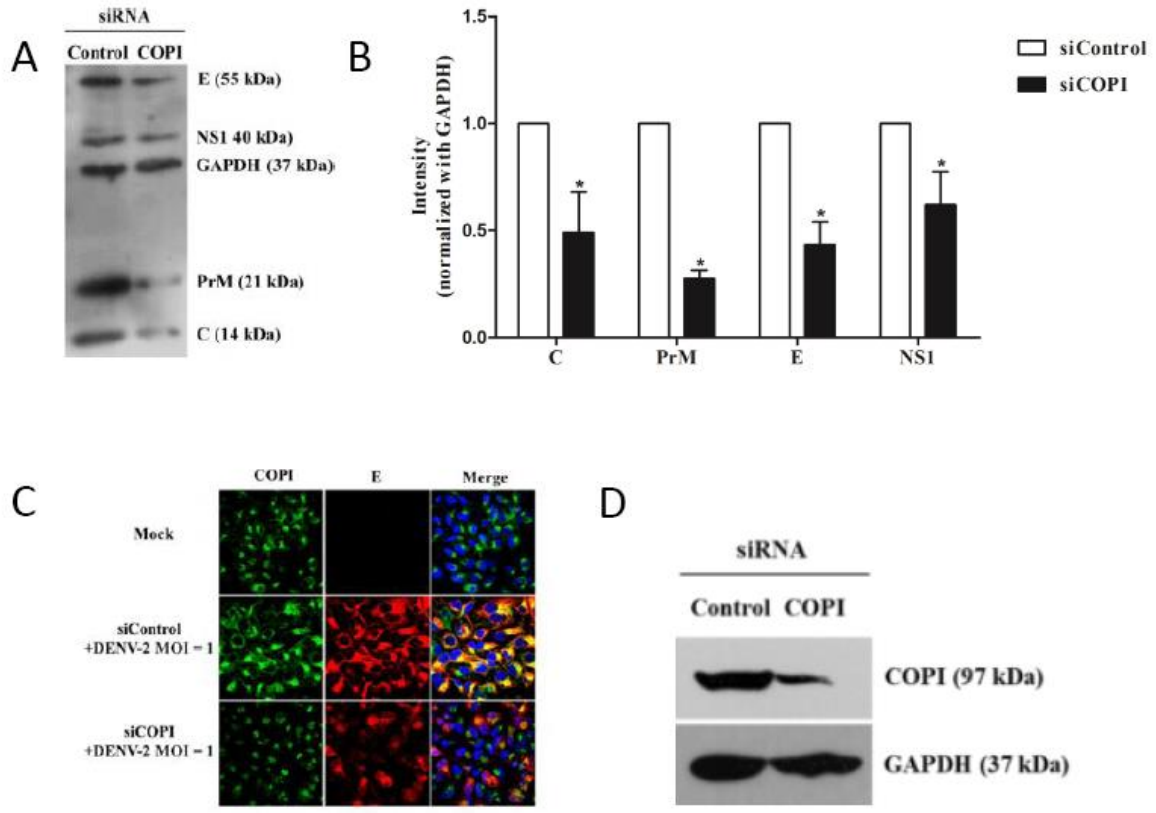

Fig. 3 Depletion of COPI decreased DENV proteins. Huh7 cells were transfected with siCOPI or siControl twice at 24 h intervals. At 48 h post-transfection, knockdown cells were infected with DENV-2 at an MOI of 1. (A) At 24 hpi, DENV proteins were analyzed by Western blot analysis, and shown as (B) intensity normalized with GAPDH. The mean of three independent experiments was the recorded result. An asterisk indicates statistical significance between siControl and specific siRNAs ($p<0.05$). (C) Huh7 cells on coverslips were transfected with siCOPI or siControl twice and infected with DENV-2 at an MOI of 1 [as performed in (A)], and double immunofluorescence staining was performed and analyzed by laser scanning confocal microscope to compare between siControl and siCOPI at 24 hpi. (D) Knockdown efficacy of COPI was analyzed by Western blot analysis.

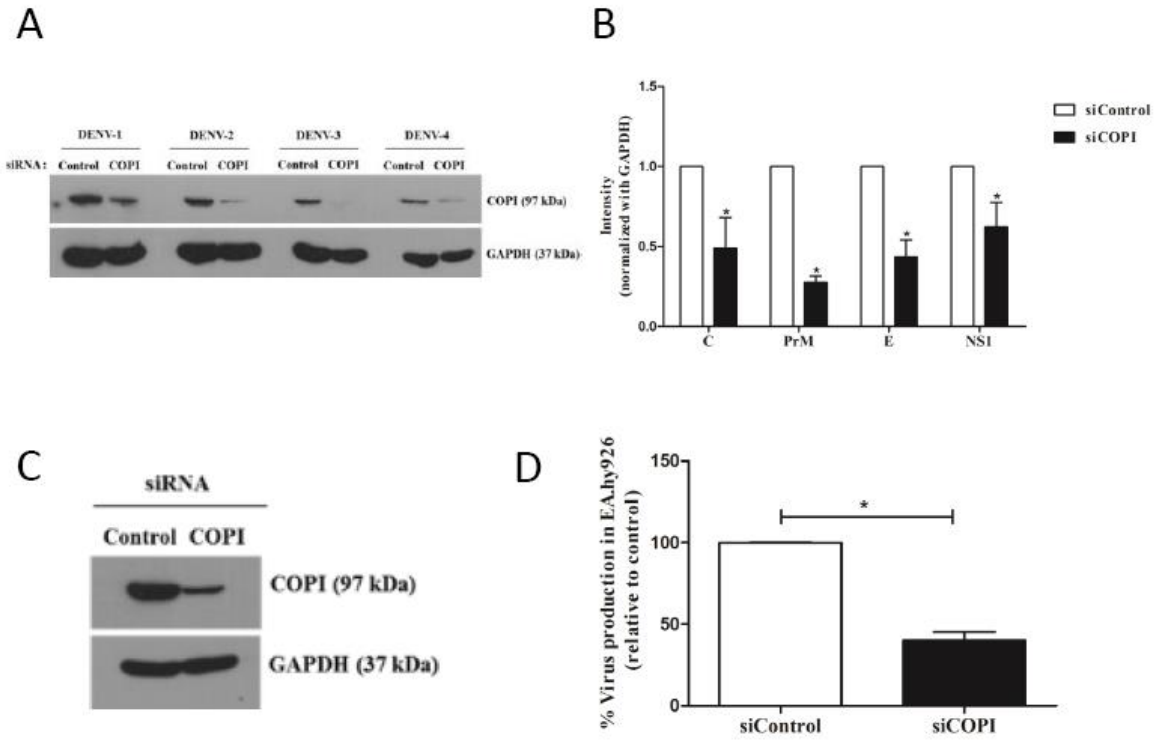

Fig. 4 COPI facilitated virion production in all serotypes of DENV and in other cell line.

(A) At 24 hpi, knockdown efficacy of COPI was analyzed in Huh7 cells infected with all four DENV serotypes by Western blot analysis. (B) Infectious virus production from Huh7 culture supernatants following infection with all four DENV serotypes was determined by FFU assay, and calculated as a percentage of virus production relative to siControl. (C) EA.hy926 cells were used as another target cell. At 24 hpi, knockdown efficacy of COPI was analyzed by Western blot analysis. (D) Infectious virus production from EA.hy926 culture supernatants was determined by FFU assay and calculated as a percentage of virus production relative to siControl. The mean of three independent experiments was the recorded result. An asterisk indicates statistical significance between siControl and siCOPI ($p<0.05$).

Discussion

Part I: Adaptor Protein 1A Facilitates Dengue Virus Replication

Using a human-genome-wide RNAi screen, clathrin and its adaptor proteins were shown to decrease DENV infection [52]. A pathway-specific siRNA library further revealed the role of clathrin and its adaptor proteins in mediating DENV entry [4] and secretion of subviral particles [53]. Furthermore, the role of AP-1A in DENV production was shown to play a role at the egress stage from the TGN to plasma membrane [54]. In the present study, we showed that treatment with AP-1-dependent traffic inhibitor (A5), or transfection with AP-1A siRNA decreased replication of DENV, thereby reducing viral protein expression and production. Thus, AP-1 may have an additional role besides aiding egression of DENV, as shown previously [54]. This hypothesis was supported by RNAi, which showed that DENV RNA was significantly reduced in DENV-infected Huh7 cells transfected with AP-1A siRNA compared with control siRNA. Naked DENV RNA transfection, which bypassed the process of viral fusion and uncoating, demonstrated decreased production of viral RNA and infectious virions in cells transfected with AP-1A siRNA compared with control siRNA-transfected cells. This was indicative of an essential function of AP-1A in the step of DENV RNA replication. Vesicular packets, which are a proposed replication site for DENV, were fewer in number in Huh7 cells transfected with AP-1A siRNA compared with control siRNA.

AP-1, GTPase ADP-ribosylation factor 1(ARF)-1 and phosphatidylinositol-4-phosphate (PI4P) are the components, which are essential for reorganization of donor membrane for clathrin-coated vesicle[55]. AP-1A and AP-3A are required for transport between endosomal/lysosomal systems and the secretory pathway [56, 57]. AP-3A was previously shown to be involved in replication of DENV [54], therefore, we proposed here that AP-1A may act in concert with AP-3A to facilitate replication of DENV. AP-1A and AP-3A coat assembly are controlled by GTPase ARF-1 [58, 59]. ARF-1 plays a key role in

trafficking through the Golgi apparatus, where it is involved in the formation of vesicular packets, and ARF family siRNAs have an inhibitory effect on DENV recombinant subviral particle secretion [53, 60]. Rab18, a GTPase involved in vesicular trafficking, also regulates DENV replication by targeting enzymes required for cellular fatty acid synthesis to the replication site [61]. Enhanced fatty acid synthesis is required for efficient membrane proliferation and rearrangement in DENV replication [62-64]. Recruitment of PI4P is also required for membrane reorganization [65]. DENV may use AP-1A to recruit enzymes (PI4K-IIIβ) for synthesis of PI4P to help its own replication. Purified AP-1 binds to PI4P, and anti-PI4P inhibits recruitment of cytosolic AP-1 to normal cellular membranes [66]; therefore, disruption of AP-1A by RNAi in the present study may have affected synthesis of PI4P and membrane organization required for DENV replication. The role of phosphatidylinositol-4-kinases, including PI4K-IIIα, as a modulator of hepatitis C virus (HCV), was demonstrated by co-localization of PI4K-IIIα and HCV NS5A in lipid rafts. Inhibition of web formation by siRNA against PI4K-IIIα correlates with the decrease in HCV replication and infectious virion production. PI4K-IIIα is proposed to produce pools of PI4P for HCV replication [67]. In addition, DENV can activate autophagic machinery for viral replication both *in vitro* and *in vivo* [68, 69]. DENV infection can induce an autophagy-dependent processing of lipid droplets and triglycerides to release free fatty acids for replication [63], linking of DENV replication through autophagolysosome was demonstrated [70], and dysfunction of the AP-1A-dependent clathrin coating at the TGN can prevent autophagosome formation [71]. AP-1A may be a host component, which can recruit enzymes required for fatty acid synthesis and dysfunction of AP-1A may affect membrane organization, thereby decreasing replication of virus in infected cells.

Part II: Exocytosis Role of Adaptor Protein 2 in Dengue Virus Infection

Intracellular vesicular trafficking is a pathway which is hijacked by DENV. Clathrin-mediated transport plays an important role in cargo sorting by coordinating with clathrin adaptor protein complexes. The well-characterized clathrin adaptor protein complexes are AP-1 and AP-2 which mediates vesicular transport in secretory and endocytic pathway, respectively. Adaptor protein complexes are hijacked by several viruses for their own replication. It has been reported that AP-1 plays role in DENV secretion [54]. AP-1 is involved in retroviral budding at plasma membrane by interacting with Gag and mediating Gag trafficking [72]. Our previous study has been demonstrated that AP-1 plays an additional role in DENV RNA replication by involving in replication site biogenesis [51]. Based on the classical role of AP-2 in receptor-mediated endocytosis, AP-2-dependent clathrin-mediated endocytosis is characterized as a pathway for viral entry. In hepatitis C virus (HCV), AP-2 plays role in HCV entry. AP-2 activity is regulated by host kinases including AAK1 and GAK. Phosphorylation of the μ subunit of AP-2 mediated cargo sorting. Knockdown of the μ subunit of AP-2 and inhibition of AAK1 and GAK by two FDA drug approved, sunitinib and erlotinib which is AAK1 and GAK inhibitor, respectively decreases HCV entry [73]. Moreover, AP-2 plays an alternative role in HCV assembly. AP-2 interacts with core proteins and mediates core trafficking to assembly site [74]. Two FDA drug approved, sunitinib and erlotinib also inhibit HCV assembly. In SIV, AP-2 interacts with SIV Nef and down-regulates host tethering protein, BST-2 resulting in SIV release [75]. These evidences demonstrate that AP-2 plays several roles in viral entry, assembly and egress. These studies revealed that host proteins are subverted by viruses in both the classical and non-classical functions. Recently, inhibition effect of sunitinib and erlotinib in DENV entry has been reported. Phosphorylation of T156 in the mu subunit of AP-2 is inhibited by sunitinib and

erlotinib in DENV-infected cells [76]. However, an alternative role of AP-2 in DENV life cycle is not investigated. In this study, role of AP-2 in DENV replication cycle was determined by inhibiting AP-2 activity using sunitinib and depleting of the μ subunit of AP-2 (AP2M1) by siRNA. Time-of-addition studies of sunitinib including pre-, co- and post-treatment were performed to verify which step is AP-2 involved. Virus titer was examined at 24 h post infection to determine the effect of sunitinib in a single round of DENV replication cycle. The results showed that virus titer was reduced in all time of addition. Because sunitinib targets AAK1 which regulates AP2M1 phosphorylation by competitive binding, reduction of DENV production in pre-treatment and co-treatment assay confirmed the action of sunitinib against host protein and suggested the role of AP-2 in DENV entry. Interestingly, sunitinib reduced virus production in post-treatment assay. To confirm the role of AP-2 in DENV production, DENV RNA and virus titer were investigated in AP2M1 knockdown cells at 8 and 24 h post infection. The reduction of intracellular RNA at 8 h post infection suggested the role of AP-2 in DENV entry resulting in the reduction of virus titer. At 24 h post infection, knockdown of AP2M1 decreased extracellular virus without affecting intracellular DENV RNA. From these results, it is possible that AP-2 may affect viral release at that time. This evidence was further characterized by observing intracellular DENV RNA, intracellular virions and extracellular virions which were produced in DENV-naked RNA transfected cells. Transfection of DENV-naked RNA can bypass the entry step. Interestingly, knockdown of AP2M1 increased intracellular DENV RNA and intracellular virions but decreased extracellular virions. After assembly, immature DENV is transported through endoplasmic reticulum (ER), Golgi apparatus and trans-Golgi network (TGN). At TGN, prM is cleaved by furin to form mature virion before release. Mature virus will infect target cells for next round of replication. From this reason, we hypothesized that AP-2 play role in post assembly step. Immunofluorescence staining of DENV envelope protein showed the pattern

of dot-like structure at cell periphery. It has been reported that DENV release is restricted by interferon-stimulated protein, BST-2 by tethering viral particles at plasma membrane [77]. However, mechanisms how BST-2 mediated DENV egress is unknown. AP-2 may play role in DENV release by removing host proteins which trap DENV particles from plasma membrane. Taken together, this study provides an additional role of AP-2 in DENV replication cycle.

Part III: Coat Protein Complex I Facilitates Dengue Virus Production

The role of coat protein complex and SNARE proteins were studied in DENV-infected Huh7 cells. SNARE proteins, including STX5 and NSF, were previously shown to be required for the efficient production of infectious virions in other viruses [39, 78]; however, STX5 and NSF were not involved in DENV production in Huh7 cells. As different SNARE members can be formed into various SNARE complexes to facilitate different transport events [79, 80], other SNARE members, such as SNAP and VAMP, should be tested to determine if they facilitate DENV production. In contrast, coat proteins, including COPI and COPII, facilitated DENV production in Huh7 cells.

COPI does not help DENV relative to binding, internalization, or replication. This finding contrasts the effect of COPI in other virus infections, whereby COPI can facilitate the entry of viruses, including influenza [81], vesicular stomatitis virus (VSV) [82], and Semliki Forest virus [83]. High-throughput screening from siRNA targeting of 779 kinase-related genes in DENV infection also identified COPB2 and ARCN1, which are subunits of the cellular coat protein complex, for their role in reducing infection [38]. The level of DENV RNA was decreased in inhibitor (golgicide A)-treated compared to that of untreated DENV-infected cells [84]. The differences between two studies may be due to the specificity of

golgicide A (GCA), given that GCA also targets other host proteins in addition to COPI. Another target of GCA is GBF1, a guanine nucleotide exchange factor that has several downstream effectors, including adaptor protein 1 (AP1) complex [85, 86], which was previously shown to be involved in the replication of DENV RNA [51]. Recently, the GBF1-Arf-COPI system was shown to be essential for the delivery of viral capsid to lipid droplets of DENV [87].

DENV C, PrM, E, and NS1 proteins were significantly decreased in COPI-silenced DENV-infected Huh7 cells, when compared to those of control siRNA-transfected DENV-infected Huh7 cells. This may be due to either defective translation of viral proteins or decreased stability of viral proteins in COPI-silenced DENV-infected Huh7 cells. Moreover, depletion of COPI decreased DENV production in DENV-infected Huh7 cells. This may be due to defective interactions between COPI and several ER chaperones, such as glucose-regulated protein-78 (GRP78) and calreticulin [88, 89], which were previously shown to be essential for DENV production [90, 91]. These ER chaperones were also shown to facilitate viral protein folding, assembly, and maturation of hepatitis C virus (HCV) and human immunodeficiency virus (HIV-1) [92-94]. Potential impairment of retrograde recycling of these chaperones to the ER compartment following COPI knockdown may affect DENV protein folding, potentially leading to increased viral protein degradation thereby reducing virion production. However, the molecular mechanisms that dictate how interactions between this complex and viral and host proteins contributes to the pathogenesis of DENV disease merit further investigations.

References

[1] D.J. Gubler, Dengue and dengue hemorrhagic fever, Clin Microbiol Rev, 11 (1998) 480-496.

[2] S.B. Halstead, Pathogenesis of dengue: challenges to molecular biology, Science, 239 (1988) 476-481.

[3] S.B. Halstead, Dengue, Lancet, 370 (2007) 1644-1652.

[4] F. Ang, A.P. Wong, M.M. Ng, J.J. Chu, Small interference RNA profiling reveals the essential role of human membrane trafficking genes in mediating the infectious entry of dengue virus, Virol J, 7 (2010) 24.

[5] T. Peng, J.L. Wang, W. Chen, J.L. Zhang, N. Gao, Z.T. Chen, X.F. Xu, D.Y. Fan, J. An, Entry of dengue virus serotype 2 into ECV304 cells depends on clathrin-dependent endocytosis, but not on caveolae-dependent endocytosis, Can J Microbiol, 55 (2009) 139-145.

[6] J.P. Chen, H.L. Lu, S.L. Lai, G.S. Campanella, J.M. Sung, M.Y. Lu, B.A. Wu-Hsieh, Y.L. Lin, T.E. Lane, A.D. Luster, F. Liao, Dengue virus induces expression of CXC chemokine ligand 10/IFN-gamma-inducible protein 10, which competitively inhibits viral binding to cell surface heparan sulfate, J Immunol, 177 (2006) 3185-3192.

[7] Y.L. Lin, H.Y. Lei, Y.S. Lin, T.M. Yeh, S.H. Chen, H.S. Liu, Heparin inhibits dengue-2 virus infection of five human liver cell lines, Antiviral Res, 56 (2002) 93-96.

[8] S.L. Hung, P.L. Lee, H.W. Chen, L.K. Chen, C.L. Kao, C.C. King, Analysis of the steps involved in Dengue virus entry into host cells, Virology, 257 (1999) 156-167.

[9] Y. Chen, T. Maguire, R.E. Hileman, J.R. Fromm, J.D. Esko, R.J. Linhardt, R.M. Marks, Dengue virus infectivity depends on envelope protein binding to target cell heparan sulfate, Nat Med, 3 (1997) 866-871.

[10] R. Germi, J.M. Crance, D. Garin, J. Guimet, H. Lortat-Jacob, R.W. Ruigrok, J.P. Zarski, E. Drouet, Heparan sulfate-mediated binding of infectious dengue virus type 2 and yellow fever virus, Virology, 292 (2002) 162-168.

[11] J. Reyes-Del Valle, S. Chavez-Salinas, F. Medina, R.M. Del Angel, Heat shock protein 90 and heat shock protein 70 are components of dengue virus receptor complex in human cells, J Virol, 79 (2005) 4557-4567.

[12] S. Jindadamrongwech, C. Thepparit, D.R. Smith, Identification of GRP 78 (BiP) as a liver cell expressed receptor element for dengue virus serotype 2, Arch Virol, 149 (2004) 915-927.

[13] P.Y. Lozach, L. Burleigh, I. Staropoli, E. Navarro-Sanchez, J. Harriague, J.L. Virelizier, F.A. Rey, P. Despres, F. Arenzana-Seisdedos, A. Amara, Dendritic cell-specific intercellular adhesion molecule 3-grabbing non-integrin (DC-SIGN)-mediated enhancement of dengue virus infection is independent of DC-SIGN internalization signals, J Biol Chem, 280 (2005) 23698-23708.

[14] E. Navarro-Sanchez, R. Altmeyer, A. Amara, O. Schwartz, F. Fieschi, J.L. Virelizier, F. Arenzana-Seisdedos, P. Despres, Dendritic-cell-specific ICAM3-grabbing non-integrin is essential for the productive infection of human dendritic cells by mosquito-cell-derived dengue viruses, EMBO Rep, 4 (2003) 723-728.

[15] B. Tassaneetrithep, T.H. Burgess, A. Granelli-Piperno, C. Trumpfheller, J. Finke, W. Sun, M.A. Eller, K. Pattanapanyasat, S. Sarasombath, D.L. Birx, R.M. Steinman, S. Schlesinger, M.A. Marovich, DC-SIGN (CD209) mediates dengue virus infection of human dendritic cells, J Exp Med, 197 (2003) 823-829.

[16] H.M. van der Schaar, M.J. Rust, C. Chen, H. van der Ende-Metselaar, J. Wilschut, X. Zhuang, J.M. Smit, Dissecting the cell entry pathway of dengue virus by single-particle tracking in living cells, PLoS Pathog, 4 (2008) e1000244.

[17] Y. Modis, S. Ogata, D. Clements, S.C. Harrison, Structure of the dengue virus envelope protein after membrane fusion, Nature, 427 (2004) 313-319.

[18] S. Welsch, S. Miller, I. Romero-Brey, A. Merz, C.K. Bleck, P. Walther, S.D. Fuller, C. Antony, J. Krijnse-Locker, R. Bartenschlager, Composition and three-dimensional architecture of the dengue virus replication and assembly sites, Cell Host Microbe, 5 (2009) 365-375.

[19] J. Junjhon, J.G. Pennington, T.J. Edwards, R. Perera, J. Lanman, R.J. Kuhn, Ultrastructural characterization and three-dimensional architecture of replication sites in dengue virus-infected mosquito cells, J Virol, 88 (2014) 4687-4697.

[20] S. Apte-Sengupta, D. Sirohi, R.J. Kuhn, Coupling of replication and assembly in flaviviruses, Curr Opin Virol, 9C (2014) 134-142.

[21] S. Mukhopadhyay, R.J. Kuhn, M.G. Rossmann, A structural perspective of the flavivirus life cycle, Nat Rev Microbiol, 3 (2005) 13-22.

[22] T. Kanaseki, K. Kadota, The "vesicle in a basket". A morphological study of the coated vesicle isolated from the nerve endings of the guinea pig brain, with special reference to the mechanism of membrane movements, J Cell Biol, 42 (1969) 202-220.

[23] F. Nakatsu, K. Hase, H. Ohno, The Role of the Clathrin Adaptor AP-1: Polarized Sorting and Beyond, Membranes (Basel), 4 (2014) 747-763.

[24] H. Ohno, M.C. Fournier, G. Poy, J.S. Bonifacino, Structural determinants of interaction of tyrosine-based sorting signals with the adaptor medium chains, J Biol Chem, 271 (1996) 29009-29015.

[25] H. Ohno, J. Stewart, M.C. Fournier, H. Bosshart, I. Rhee, S. Miyatake, T. Saito, A. Gallusser, T. Kirchhausen, J.S. Bonifacino, Interaction of tyrosine-based sorting signals with clathrin-associated proteins, Science, 269 (1995) 1872-1875.

[26] D.J. Owen, P.R. Evans, A structural explanation for the recognition of tyrosine-based endocytotic signals, Science, 282 (1998) 1327-1332.

[27] J.F. Roeth, M. Williams, M.R. Kasper, T.M. Filzen, K.L. Collins, HIV-1 Nef disrupts MHC-I trafficking by recruiting AP-1 to the MHC-I cytoplasmic tail, J Cell Biol, 167 (2004) 903-913.

[28] H. Folsch, M. Pypaert, S. Maday, L. Pelletier, I. Mellman, The AP-1A and AP-1B clathrin adaptor complexes define biochemically and functionally distinct membrane domains, J Cell Biol, 163 (2003) 351-362.

[29] A.L. Ang, H. Folsch, U.M. Koivisto, M. Pypaert, I. Mellman, The Rab8 GTPase selectively regulates AP-1B-dependent basolateral transport in polarized Madin-Darby canine kidney cells, J Cell Biol, 163 (2003) 339-350.

[30] H. Folsch, M. Pypaert, P. Schu, I. Mellman, Distribution and function of AP-1 clathrin adaptor complexes in polarized epithelial cells, J Cell Biol, 152 (2001) 595-606.

[31] F. Brandizzi, C. Barlowe, Organization of the ER-Golgi interface for membrane traffic control, Nat Rev Mol Cell Biol, 14 (2013) 382-392.

[32] M.C. Lee, E.A. Miller, J. Goldberg, L. Orci, R. Schekman, Bi-directional protein transport between the ER and Golgi, Annu Rev Cell Dev Biol, 20 (2004) 87-123.

[33] D. Brandhorst, D. Zwilling, S.O. Rizzoli, U. Lippert, T. Lang, R. Jahn, Homotypic fusion of early endosomes: SNAREs do not determine fusion specificity, Proc Natl Acad Sci U S A, 103 (2006) 2701-2706.

[34] Y.A. Chen, R.H. Scheller, SNARE-mediated membrane fusion, Nat Rev Mol Cell Biol, 2 (2001) 98-106.

[35] S. Cherry, A. Kunte, H. Wang, C. Coyne, R.B. Rawson, N. Perrimon, COPI activity coupled with fatty acid biosynthesis is required for viral replication, PLoS Pathog, 2 (2006) e102.

[36] R.C. Rust, L. Landmann, R. Gosert, B.L. Tang, W. Hong, H.P. Hauri, D. Egger, K. Bienz, Cellular COPII proteins are involved in production of the vesicles that form the poliovirus replication complex, J Virol, 75 (2001) 9808-9818.

[37] J. Wang, Z. Wu, Q. Jin, COPI is required for enterovirus 71 replication, PLoS One, 7 (2012) e38035.

[38] Y.S. Ooi, K.M. Stiles, C.Y. Liu, G.M. Taylor, M. Kielian, Genome-wide RNAi screen identifies novel host proteins required for alphavirus entry, PLoS Pathog, 9 (2013) e1003835.

[39] A. Joshi, H. Garg, S.D. Ablan, E.O. Freed, Evidence of a role for soluble N-ethylmaleimide-sensitive factor attachment protein receptor (SNARE) machinery in HIV-1 assembly and release, J Biol Chem, 286 (2011) 29861-29871.

[40] Y.S. Lim, H.T. Ngo, J. Lee, K. Son, E.M. Park, S.B. Hwang, ADP-ribosylation Factor-related Protein 1 Interacts with NS5A and Regulates Hepatitis C Virus Propagation, Sci Rep, 6 (2016) 31211.

[41] Y.J. Kwon, J. Heo, H.E. Wong, D.J. Cruz, S. Velumani, C.T. da Silva, A.L. Mosimann, C.N. Duarte Dos Santos, L.H. Freitas-Junior, K. Fink, Kinome siRNA screen identifies novel cell-type specific dengue host target genes, Antiviral Res, 110 (2014) 20-30.

[42] C. Puttikhunt, W. Kasinrerk, S. Srisa-ad, T. Duangchinda, W. Silakate, S. Moonsom, N. Sittisombut, P. Malasit, Production of anti-dengue NS1 monoclonal antibodies by DNA immunization, J Virol Methods, 109 (2003) 55-61.

[43] E.A. Henchal, J.M. McCown, D.S. Burke, M.C. Seguin, W.E. Brandt, Epitopic analysis of antigenic determinants on the surface of dengue-2 virions using monoclonal antibodies, Am J Trop Med Hyg, 34 (1985) 162-169.

[44] E.A. Henchal, M.K. Gentry, J.M. McCown, W.E. Brandt, Dengue virus-specific and flavivirus group determinants identified with monoclonal antibodies by indirect

immunofluorescence, The American journal of tropical medicine and hygiene, 31 (1982) 830-836.

[45] M.C. Duncan, D.G. Ho, J. Huang, M.E. Jung, G.S. Payne, Composite synthetic lethal identification of membrane traffic inhibitors, Proc Natl Acad Sci U S A, 104 (2007) 6235-6240.

[46] N. Jirakanjanakit, T. Sanohsomneing, S. Yoksan, N. Bhamarapravati, The micro-focus reduction neutralization test for determining dengue and Japanese encephalitis neutralizing antibodies in volunteers vaccinated against dengue, Transactions of the Royal Society of Tropical Medicine and Hygiene, 91 (1997) 614-617.

[47] H. Towbin, T. Staehelin, J. Gordon, Electrophoretic transfer of proteins from polyacrylamide gels to nitrocellulose sheets: procedure and some applications, Proceedings of the National Academy of Sciences of the United States of America, 76 (1979) 4350-4354.

[48] W. Strober, Trypan blue exclusion test of cell viability, Curr Protoc Immunol, Appendix 3 (2001) Appendix 3B.

[49] K.J. Livak, T.D. Schmittgen, Analysis of relative gene expression data using real-time quantitative PCR and the 2(-Delta Delta C(T)) Method, Methods, 25 (2001) 402-408.

[50] S. Noisakran, S. Sengsai, V. Thongboonkerd, R. Kanlaya, S. Sinchaikul, S.T. Chen, C. Puttikhunt, W. Kasinrerk, T. Limjindaporn, W. Wongwiwat, P. Malasit, P.T. Yenchitsomanus, Identification of human hnRNP C1/C2 as a dengue virus NS1-interacting protein, Biochem Biophys Res Commun, 372 (2008) 67-72.

[51] U. Yasamut, N. Tongmuang, P.T. Yenchitsomanus, M. Junking, S. Noisakran, C. Puttikhunt, J.J. Chu, T. Limjindaporn, Adaptor Protein 1A Facilitates Dengue Virus Replication, PLoS One, 10 (2015) e0130065.

[52] M.N. Krishnan, A. Ng, B. Sukumaran, F.D. Gilfoy, P.D. Uchil, H. Sultana, A.L. Brass, R. Adametz, M. Tsui, F. Qian, R.R. Montgomery, S. Lev, P.W. Mason, R.A. Koski, S.J.

Elledge, R.J. Xavier, H. Agaisse, E. Fikrig, RNA interference screen for human genes associated with West Nile virus infection, Nature, 455 (2008) 242-245.

[53] P.G. Wang, M. Kudelko, J. Lo, L.Y. Siu, K.T. Kwok, M. Sachse, J.M. Nicholls, R. Bruzzone, R.M. Altmeyer, B. Nal, Efficient assembly and secretion of recombinant subviral particles of the four dengue serotypes using native prM and E proteins, PLoS One, 4 (2009) e8325.

[54] T. Agrawal, P. Schu, G.R. Medigeshi, Adaptor protein complexes-1 and 3 are involved at distinct stages of flavivirus life-cycle, Scientific reports, 3 (2013) 1813.

[55] T. Baust, C. Czupalla, E. Krause, L. Bourel-Bonnet, B. Hoflack, Proteomic analysis of adaptor protein 1A coats selectively assembled on liposomes, Proc Natl Acad Sci U S A, 103 (2006) 3159-3164.

[56] J.S. Bonifacino, L.M. Traub, Signals for sorting of transmembrane proteins to endosomes and lysosomes, Annu Rev Biochem, 72 (2003) 395-447.

[57] M.S. Robinson, Adaptable adaptors for coated vesicles, Trends Cell Biol, 14 (2004) 167-174.

[58] E.C. Dell'Angelica, R. Puertollano, C. Mullins, R.C. Aguilar, J.D. Vargas, L.M. Hartnell, J.S. Bonifacino, GGAs: a family of ADP ribosylation factor-binding proteins related to adaptors and associated with the Golgi complex, J Cell Biol, 149 (2000) 81-94.

[59] C.E. Ooi, E.C. Dell'Angelica, J.S. Bonifacino, ADP-Ribosylation factor 1 (ARF1) regulates recruitment of the AP-3 adaptor complex to membranes, J Cell Biol, 142 (1998) 391-402.

[60] M. Kudelko, J.B. Brault, K. Kwok, M.Y. Li, N. Pardigon, J.S. Peiris, R. Bruzzone, P. Despres, B. Nal, P.G. Wang, Class II ADP-ribosylation factors are required for efficient secretion of dengue viruses, J Biol Chem, 287 (2012) 767-777.

[61] W.C. Tang, R.J. Lin, C.L. Liao, Y.L. Lin, Rab18 facilitates dengue virus infection by targeting fatty acid synthase to sites of viral replication, J Virol, 88 (2014) 6793-6804.

[62] M.M. Samsa, J.A. Mondotte, N.G. Iglesias, I. Assuncao-Miranda, G. Barbosa-Lima, A.T. Da Poian, P.T. Bozza, A.V. Gamarnik, Dengue virus capsid protein usurps lipid droplets for viral particle formation, PLoS Pathog, 5 (2009) e1000632.

[63] N.S. Heaton, G. Randall, Dengue virus-induced autophagy regulates lipid metabolism, Cell Host Microbe, 8 (2011) 422-432.

[64] N.S. Heaton, R. Perera, K.L. Berger, S. Khadka, D.J. Lacount, R.J. Kuhn, G. Randall, Dengue virus nonstructural protein 3 redistributes fatty acid synthase to sites of viral replication and increases cellular fatty acid synthesis, Proc Natl Acad Sci U S A, 107 (2010) 17345-17350.

[65] N.Y. Hsu, O. Ilnytska, G. Belov, M. Santiana, Y.H. Chen, P.M. Takvorian, C. Pau, H. van der Schaar, N. Kaushik-Basu, T. Balla, C.E. Cameron, E. Ehrenfeld, F.J. van Kuppeveld, N. Altan-Bonnet, Viral reorganization of the secretory pathway generates distinct organelles for RNA replication, Cell, 141 (2010) 799-811.

[66] Y.J. Wang, J. Wang, H.Q. Sun, M. Martinez, Y.X. Sun, E. Macia, T. Kirchhausen, J.P. Albanesi, M.G. Roth, H.L. Yin, Phosphatidylinositol 4 phosphate regulates targeting of clathrin adaptor AP-1 complexes to the Golgi, Cell, 114 (2003) 299-310.

[67] K.L. Berger, J.D. Cooper, N.S. Heaton, R. Yoon, T.E. Oakland, T.X. Jordan, G. Mateu, A. Grakoui, G. Randall, Roles for endocytic trafficking and phosphatidylinositol 4-kinase III alpha in hepatitis C virus replication, Proc Natl Acad Sci U S A, 106 (2009) 7577-7582.

[68] Y.R. Lee, H.Y. Lei, M.T. Liu, J.R. Wang, S.H. Chen, Y.F. Jiang-Shieh, Y.S. Lin, T.M. Yeh, C.C. Liu, H.S. Liu, Autophagic machinery activated by dengue virus enhances virus replication, Virology, 374 (2008) 240-248.

[69] Y.R. Lee, H.Y. Hu, S.H. Kuo, H.Y. Lei, Y.S. Lin, T.M. Yeh, C.C. Liu, H.S. Liu, Dengue virus infection induces autophagy: an in vivo study, J Biomed Sci, 20 (2013) 65.

[70] A. Khakpoor, M. Panyasrivanit, N. Wikan, D.R. Smith, A role for autophagolysosomes in dengue virus 3 production in HepG2 cells, The Journal of general virology, 90 (2009) 1093-1103.

[71] Y. Guo, C. Chang, R. Huang, B. Liu, L. Bao, W. Liu, AP1 is essential for generation of autophagosomes from the trans-Golgi network, J Cell Sci, 125 (2012) 1706-1715.

[72] G. Camus, C. Segura-Morales, D. Molle, S. Lopez-Verges, C. Begon-Pescia, C. Cazevieille, P. Schu, E. Bertrand, C. Berlioz-Torrent, E. Basyuk, The clathrin adaptor complex AP-1 binds HIV-1 and MLV Gag and facilitates their budding, Molecular biology of the cell, 18 (2007) 3193-3203.

[73] G. Neveu, A. Ziv-Av, R. Barouch-Bentov, E. Berkerman, J. Mulholland, S. Einav, J.H.J. Ou, AP-2-Associated Protein Kinase 1 and Cyclin G-Associated Kinase Regulate Hepatitis C Virus Entry and Are Potential Drug Targets, Journal of Virology, 89 (2015) 4387-4404.

[74] G. Neveu, R. Barouch-Bentov, A. Ziv-Av, D. Gerber, Y. Jacob, S. Einav, Identification and targeting of an interaction between a tyrosine motif within hepatitis C virus core protein and AP2M1 essential for viral assembly, PLoS pathogens, 8 (2012) e1002845.

[75] F. Zhang, W.N. Landford, M. Ng, M.W. McNatt, P.D. Bieniasz, T. Hatziioannou, SIV Nef proteins recruit the AP-2 complex to antagonize Tetherin and facilitate virion release, PLoS pathogens, 7 (2011) e1002039.

[76] E. Bekerman, G. Neveu, A. Shulla, J. Brannan, S.Y. Pu, S. Wang, F. Xiao, R. Barouch-Bentov, R.R. Bakken, R. Mateo, J. Govero, C.M. Nagamine, M.S. Diamond, S. De Jonghe, P. Herdewijn, J.M. Dye, G. Randall, S. Einav, Anticancer kinase inhibitors impair intracellular viral trafficking and exert broad-spectrum antiviral effects, The Journal of clinical investigation, 127 (2017) 1338-1352.

[77] X.B. Pan, J.C. Han, X. Cong, L. Wei, BST2/tetherin inhibits dengue virus release from human hepatoma cells, PloS one, 7 (2012) e51033.

[78] L. Cruz, N.T. Streck, K. Ferguson, T. Desai, D.H. Desai, S.G. Amin, N.J. Buchkovich, Potent Inhibition of Human Cytomegalovirus by Modulation of Cellular SNARE Syntaxin 5, J Virol, 91 (2017).

[79] R. Jahn, R.H. Scheller, SNAREs--engines for membrane fusion, Nat Rev Mol Cell Biol, 7 (2006) 631-643.

[80] W. Hong, SNAREs and traffic, Biochim Biophys Acta, 1744 (2005) 493-517.

[81] R. Konig, S. Stertz, Y. Zhou, A. Inoue, H.H. Hoffmann, S. Bhattacharyya, J.G. Alamares, D.M. Tscherne, M.B. Ortigoza, Y. Liang, Q. Gao, S.E. Andrews, S. Bandyopadhyay, P. De Jesus, B.P. Tu, L. Pache, C. Shih, A. Orth, G. Bonamy, L. Miraglia, T. Ideker, A. Garcia-Sastre, J.A. Young, P. Palese, M.L. Shaw, S.K. Chanda, Human host factors required for influenza virus replication, Nature, 463 (2010) 813-817.

[82] D.K. Cureton, R. Burdeinick-Kerr, S.P. Whelan, Genetic inactivation of COPI coatomer separately inhibits vesicular stomatitis virus entry and gene expression, J Virol, 86 (2012) 655-666.

[83] E. Daro, D. Sheff, M. Gomez, T. Kreis, I. Mellman, Inhibition of endosome function in CHO cells bearing a temperature-sensitive defect in the coatomer (COPI) component epsilon-COP, J Cell Biol, 139 (1997) 1747-1759.

[84] L.N. Carpp, R.S. Rogers, R.L. Moritz, J.D. Aitchison, Quantitative proteomic analysis of host-virus interactions reveals a role for Golgi brefeldin A resistance factor 1 (GBF1) in dengue infection, Mol Cell Proteomics, 13 (2014) 2836-2854.

[85] K. Dumaresq-Doiron, M.F. Savard, S. Akam, S. Costantino, S. Lefrancois, The phosphatidylinositol 4-kinase PI4KIIIalpha is required for the recruitment of GBF1 to Golgi membranes, J Cell Sci, 123 (2010) 2273-2280.

[86] J. Lowery, T. Szul, M. Styers, Z. Holloway, V. Oorschot, J. Klumperman, E. Sztul, The Sec7 guanine nucleotide exchange factor GBF1 regulates membrane recruitment of BIG1 and BIG2 guanine nucleotide exchange factors to the trans-Golgi network (TGN), J Biol Chem, 288 (2013) 11532-11545.

[87] N.G. Iglesias, J.A. Mondotte, L.A. Byk, F.A. De Maio, M.M. Samsa, C. Alvarez, A.V. Gamarnik, Dengue Virus Uses a Non-Canonical Function of the Host GBF1-Arf-COPI System for Capsid Protein Accumulation on Lipid Droplets, Traffic, 16 (2015) 962-977.

[88] P. Pimpl, J.P. Taylor, C. Snowden, S. Hillmer, D.G. Robinson, J. Denecke, Golgi-mediated vacuolar sorting of the endoplasmic reticulum chaperone BiP may play an active role in quality control within the secretory pathway, Plant Cell, 18 (2006) 198-211.

[89] C. Howe, M. Garstka, M. Al-Balushi, E. Ghanem, A.N. Antoniou, S. Fritzsche, G. Jankevicius, N. Kontouli, C. Schneeweiss, A. Williams, T. Elliott, S. Springer, Calreticulin-dependent recycling in the early secretory pathway mediates optimal peptide loading of MHC class I molecules, EMBO J, 28 (2009) 3730-3744.

[90] T. Limjindaporn, W. Wongwiwat, S. Noisakran, C. Srisawat, J. Netsawang, C. Puttikhunt, W. Kasinrerk, P. Avirutnan, S. Thiemmeca, R. Sriburi, N. Sittisombut, P. Malasit, P.T. Yenchitsomanus, Interaction of dengue virus envelope protein with endoplasmic reticulum-resident chaperones facilitates dengue virus production, Biochem Biophys Res Commun, 379 (2009) 196-200.

[91] D. Mairiang, H. Zhang, A. Sodja, T. Murali, P. Suriyaphol, P. Malasit, T. Limjindaporn, R.L. Finley, Jr., Identification of new protein interactions between dengue fever virus and its hosts, human and mosquito, PLoS One, 8 (2013) e53535.

[92] A. Choukhi, S. Ung, C. Wychowski, J. Dubuisson, Involvement of endoplasmic reticulum chaperones in the folding of hepatitis C virus glycoproteins, J Virol, 72 (1998) 3851-3858.

[93] P.L. Earl, B. Moss, R.W. Doms, Folding, interaction with GRP78-BiP, assembly, and transport of the human immunodeficiency virus type 1 envelope protein, J Virol, 65 (1991) 2047-2055.

[94] A. Otteken, B. Moss, Calreticulin interacts with newly synthesized human immunodeficiency virus type 1 envelope glycoprotein, suggesting a chaperone function similar to that of calnexin, J Biol Chem, 271 (1996) 97-103.

Output

1. Publications

1. Yasamut U, Tongmuang N, Yenchitsomanus PT, Junking M, Noisakran S, Puttikhunt C, Chu JJ, Limjindaporn T. Adaptor Protein 1A Facilitates Dengue Virus Replication. PLoS One. 2015 Jun 19;10(6):e0130065.
2. Rattanaburee T, Junking M, Panya A, Sawasdee N, Songprakhon P, Suttitheptumrong A, Limjindaporn T, Haegeman G, Yenchitsomanus PT. Inhibition of dengue virus production and cytokine/chemokine expression by ribavirin and compound A. Antiviral Res. 2015 Dec;124:83-92
3. Sreekanth GP, Chuncharunee A, Sirimontaporn A, Panaampon J, Noisakran S, Yenchitsomanus PT, Limjindaporn T. SB203580 Modulates p38 MAPK Signaling and Dengue Virus-Induced Liver Injury by Reducing MAPKAPK2, HSP27, and ATF2 Phosphorylation. PLoS One. 2016 Feb 22;11(2):e0149486.
4. Dechtawewat T, Paemanee A, Roytrakul S, Songprakhon P, Limjindaporn T, Yenchitsomanus PT, Saitornuang S, Puttikhunt C, Kasinrerk W, Malasit P, Noisakran S. Mass spectrometric analysis of host cell proteins interacting with

dengue virus nonstructural protein 1 in dengue virus-infected HepG2 cells. Biochim Biophys Acta. 2016 Sep;1864(9):1270-1280

5. Leela SL, Srisawat C, Sreekanth GP, Noisakran S, Yenchitsomanus PT, Limjindaporn T. Drug repurposing of minocycline against dengue virus infection. Biochem Biophys Res Commun. 2016 Sep 9;478(1):410-416.
6. Limjindaporn T, Panaampon J, Malakar S, Noisakran S, Yenchitsomanus PT. Tyrosine kinase/phosphatase inhibitors decrease dengue virus production in HepG2 cells. Biochem Biophys Res Commun. 2017 Jan 29;483(1):58-63.
7. Sreekanth GP, Chuncharunee A, Cheunsuchon B, Noisakran S, Yenchitsomanus PT, Limjindaporn T. JNK1/2 inhibitor reduces dengue virus-induced liver injury. Antiviral Res. 2017 May;141:7-18.
8. Morchang A, Lee RCH, Yenchitsomanus PT, Sreekanth GP, Noisakran S, Chu JJH, Limjindaporn T. RNAi screen reveals a role of SPHK2 in dengue virus-mediated apoptosis in hepatic cell lines. PLoS One. 2017 Nov 16;12(11):e0188121.
9. Tongmuang N, Yasamut U, Noisakran S, Yenchitsomanus PT, Limjindaporn T. Coat protein complex I facilitates dengue virus production. Virus Research 2018 (submitted).
10. Yasamut U, Tongmuang N, Noisakran S, Yenchitsomanus PT, Limjindaporn T. Exocytosis Role of Adaptor Protein 2 in Dengue Virus Infection. Biochem Biophys Res Commun. 2018 (Manuscript in preparation).

2. Presentations

1. การนำเสนอผลงานแบบบรรยาย เรื่อง “Adaptor Protein 1A Facilitates Dengue Virus Replication” .ในงานประชุมวิชาการระดับนานาชาติ. The First Year PhD Student’s Symposium, University of Salford, Manchester, UK. 7th July, 2015
2. การนำเสนอผลงานแบบโปสเตอร์ เรื่อง “Minocyline decreases dengue virus infection in HepG2 cell line”. ในงานประชุมวิชาการระดับนานาชาติ siCMPH 2016. 13th-15th June 2016.
3. การนำเสนอผลงานแบบบรรยายเรื่อง “Antiviral effect of quinine sulfate on dengue virus-infected HepG2 cell line ” ในงานประชุมวิชาการระดับ Graduate Research Forum, Thailand. 26th May, 2017
4. การนำเสนอผลงานแบบแบบโปสเตอร์เรื่อง “Antiviral activity of 4-(2-Aminoethyl) benzenesulfonyl fluoride hydrochloride against dengue virus Infection” ในงานประชุมวิชาการระดับ Graduate Research Forum, Thailand. 26th May, 2017

3. Graduate students

ชื่อนักศึกษา/ระดับปริญญา (สำเร็จการศึกษา)

1. Sreekanth Gopinathan Pillai, Ph.D. in Medical Biochemistry and Molecular Biology, Mahidol University.
2. Shilpa Lekshmi Leela, Ph.D. in Medical Biochemistry and Molecular Biology, Mahidol University.
3. Umpa Yasamut, Ph.D. in Immunology , Mahidol University.
4. Atthapan Morchang, Ph.D. in Immunology, Mahidol University.

ชื่อนักศึกษา/ระดับปริญญา (กำลังศึกษา)

5. Nopparat thongmuang, Ph.D. student in Molecular Medicine, Mahidol University.
6. Shilu Malakar, Ph.D. student in Immunology, Mahidol University.
7. Liji S Unnithan, Ph.D. student in Medical Biochemistry and Molecular Biology, Mahidol University.

PLOS ONE

RESEARCH ARTICLE

Adaptor Protein 1A Facilitates Dengue Virus Replication

Umpa Yasamut[1,2], Nopprarat Tongmuang[1], Pa-thai Yenchitsomanus[1], Mutita Junking[1], Sansanee Noisakran[3], Chunya Puttikhunt[3], Justin Jang Hann Chu[4], Thawornchai Limjindaporn[5]*

1 Division of Molecular Medicine, Department of Research and Development, Faculty of Medicine Siriraj Hospital, Mahidol University, Bangkok, Thailand, **2** Graduate Program in Immunology, Department of Immunology, Faculty of Medicine Siriraj Hospital, Mahidol University, Bangkok, Thailand, **3** Medical Biotechnology Unit, National Center for Genetic Engineering and Biotechnology, National Science and Technology Development Agency, Bangkok, Thailand, **4** Laboratory of Molecular RNA Virology and Antiviral Strategies, Department of Microbiology, Yong Loo Lin School of Medicine, National University Health System, National University of Singapore, Singapore, **5** Department of Anatomy, Faculty of Medicine Siriraj Hospital, Mahidol University, Bangkok, Thailand

* thawornchai.lim@mahidol.ac.th

OPEN ACCESS

Citation: Yasamut U, Tongmuang N, Yenchitsomanus P-t, Junking M, Noisakran S, Puttikhunt C, et al. (2015) Adaptor Protein 1A Facilitates Dengue Virus Replication. PLoS ONE 10 (6): e0130065. doi:10.1371/journal.pone.0130065

Academic Editor: Xia Jin, University of Rochester, UNITED STATES

Received: February 9, 2015

Accepted: May 15, 2015

Published: June 19, 2015

Data Availability Statement: All relevant data are within the paper and its Supporting Information files.

Funding: This work is supported by Thailand Research Fund (RSA5780012) to TL. UY is the RGJ-Ph.D. student (PHD/0259/2552). The funders had no role in study design, data collection and analysis, decision to publish, or preparation of the manuscript.

Competing Interests: The authors have declared that no competing interests exist.

Abstract

Rearrangement of membrane structure induced by dengue virus (DENV) is essential for replication, and requires host cellular machinery. Adaptor protein complex (AP)-1 is a host component, which can be recruited to components required for membrane rearrangement. Therefore, dysfunction of AP-1 may affect membrane organization, thereby decreasing replication of virus in infected cells. In the present study, AP-1-dependent traffic inhibitor inhibited DENV protein expression and virion production. We further clarified the role of AP-1A in the life cycle of DENV by RNA interference. AP-1A was not involved in DENV entry into cells. However, it facilitated DENV RNA replication. Viral RNA level was reduced significantly in Huh7 cells transfected with AP-1A small interfering RNA (siRNA) compared with control siRNA. Transfection of naked DENV viral RNA into Huh7 cells transfected with AP-1A siRNA resulted in less viral RNA and virion production than transfection into Huh7 cells transfected with control siRNA. Huh7 cells transfected with AP-1A siRNA showed greater modification of membrane structures and fewer vesicular packets compared with cells transfected with control siRNA. Therefore, AP-1A may partly control DENV-induced rearrangement of membrane structures required for viral replication.

Introduction

Dengue virus (DENV) is a positive-stranded RNA virus in the *Flaviviridae* family, which is transmitted by mosquito vectors. The genome of DENV has sequences encoding structural proteins including capsid (C), pre-membrane protein (prM), and envelope (E), and non-structural proteins (NS) including NS1, NS2A, NS2B, NS3, NS4A, NS4B and NS5 [1]. DENV consists of four serotypes, and secondary infection by different serotypes of DENV contributes to

severe dengue [2]. Patients with dengue hemorrhagic fever often present with plasma leakage, hemoconcentration, thrombocytopenia, and hemorrhagic tendencies. Additionally, serious complications of dengue hemorrhagic fever, such as organ failure, may lead to dengue shock syndrome [1–3]. Currently, there are no effective vaccines or antiviral drugs available; therefore, a better understanding of dengue pathogenesis is required.

DENV needs host cellular machinery for its replication. It binds to receptors and enters host cells by clathrin-mediated endocytosis [4–16]. Reduced pH in the endosomes induces fusion of viral and host cell membranes, thereby releasing DENV RNA into the cytoplasm [17]. Viral replication occurs on the network of modified endoplasmic reticulum (ER) membranes, including vesicular packets, virus-induced vesicles, and convoluted membranes [18–20]. Immature viral particles are transported through the trans-Golgi network (TGN) and mature virions are generated after cleavage of prM protein by host furin. Mature viruses are finally released from the host cells by exocytosis [21].

Host genes are important for the viral life cycle, including endocytosis, virus-induced membrane rearrangement, viral RNA replication and translation, and virion assembly and production. RNA interference (RNAi) is commonly used as a tool to identify the role of host proteins during DENV infection [4, 20, 22–28]. One of the host protein complexes identified is adaptor protein complex [4, 22, 24].

Adaptor protein complex (AP) was originally identified as a component of the clathrin-coated vesicles in the brain [29, 30]. Each member of AP has two large subunits (γ/β1, α/β2, δ/β3, ε/β4 or ζ/β5), one medium subunit (μ1–β5), and one small subunit (σ1–σ5). AP-1A consists of one medium subunit (μ1A), two large subunits (β1 and γ), and one small subunit (σ1). AP-1B consists of one medium subunit (μ1B), two large subunits (β1 and δ), and one small subunit (σ1). The μ subunit mediates a selection of cargo proteins via its binding with tyrosine-based sorting motif on the cargo protein [31–33]. AP-1A is expressed ubiquitously and regulates the TGN-basolateral plasma membrane transport. AP-1B is expressed in epithelial cells and regulates the basolateral transport of proteins from the recycling endosomes [34–36]. AP-1A can be recruited to components required for membrane rearrangement. In addition, interactions between AP-1A and viral proteins are reported [37, 38]. Therefore, dysfunction of AP-1A may affect membrane organization, thereby decreasing viral replication in DENV-infected cells.

Materials and Methods

Cell lines, virus, and antibodies

Human hepatocellular carcinoma (Huh7) cells were obtained from the JCRB Cell Bank (Osaka, Japan) and cultured in RPMI 1640 (Gibco, Carlsbad, CA, USA) supplemented with 10% heat-inactivated fetal bovine serum (FBS; Gibco), 1% non-essential amino acid (Gibco), 37 μg/ml penicillin (Sigma, St Louis, MO, USA) and 60 μg/ml streptomycin (Sigma) at 37°C in a 5% CO_2 incubator with a humidified atmosphere. Human lung carcinoma (A549) cells were obtained from ATCC and cultured in DMEM (Gibco, Carlsbad, CA, USA) supplemented with 10% heat-inactivated fetal bovine serum (FBS; Gibco), 1% non-essential amino acid (Gibco), 1mM sodium pyruvate (Gibco), 37 μg/ml penicillin (Sigma, St Louis, MO, USA) and 60 μg/ml streptomycin (Sigma) at 37°C in a 5% CO_2 incubator with a humidified atmosphere. Propagation of DENV-1 (Hawaii), DENV-2 strain 16681, DENV-3 (H87), and DENV-4 (H241) was performed in C6/36 mosquito cells (ATCC). DENV-2 was used in all experiments. Mouse monoclonal antibodies specific for DENV E (clones 3H5 and 4G2), DENV prM (clone 1C3), and DENV NS1 (clone NS1-3F.1) were produced from previously established hybridoma cells [39–41]. Mouse polyclonal antibody specific for AP-1A (μ1A subunit) was purchased from

Abnova (Taipei, Taiwan). Mouse monoclonal antibody specific for β-actin and goat polyclonal antibody specific for GRP78 were purchased from Santa Cruz Biotechnology (Santa Cruz, CA, USA).

AP-1-dependent traffic inhibitor and DENV infection

Huh7 cells or A549 cells were infected with DENV-2 at a multiplicity of infection (MOI) of 1 for 2 h. Excess viruses were removed and cells were washed three times with PBS. DENV-infected or mock-infected cells were incubated with AP-1-dependent traffic inhibitor (A5) (Merck KGaA, Darmstadt, Germany) [42] at a final concentration of 0, 25, 50, 100 or 200 μM in 2% FBS–RPMI 1640 for 24 h. DENV-infected Huh7 cells were harvested for measuring viral protein expression by western blotting using antibody to DENV E (4G2). The culture supernatants were also collected to measure the amount of DENV production by a focus forming unit (FFU) assay, as described previously [43]. Cell viability was determined by PrestoBlue cell viability assay (Invitrogen, Carlsbad, CA, USA). To test the effect of A5 to ER stress pathway, DENV-infected or mock-infected cells were incubated with A5 at a final concentration of 0, 100 or 200 μM in 2% FBS–RPMI 1640 for 48 h. Clear lysates were subjected to western blot analysis using antibody to GRP78, which is a maker for ER stress (S1 Fig). To establish whether AP-1-mediated traffic was involved in production of four serotypes of DENV, Huh7 cells were infected with DENV-1, -2, -3 or -4 at a MOI of 1 for 2 h. Unbound virus was removed by washing with PBS. DENV-infected Huh7 cells were incubated with A5 (200 μM) or culture medium (control) for 24 h. Virus titer in culture supernatants was measured by FFU assay [43].

Knockdown of AP-1A

Huh7 cells were seeded onto a 24-well plate in culture medium without antibiotics at a concentration of 8×10^4 cells/well. Twenty-four hours later, the medium was replaced with fresh RPMI 1640 medium and the cells were transfected with duplex AP-1A-specific siRNA (AP1M1 (μ1A) siRNA: 5-CCGAAGGCAUCAAGUAUCGGAAGAA-3, Invitrogen) or control siRNA (Cat.No. 12935–300; Invitrogen) using LipofectamineRNAi Max (Invitrogen). After incubation with siRNA (100 nM) for 6 h, the cells were supplemented with maintenance medium and incubated for a further 24 h. The second round of siRNA transfection was performed. mRNA and protein expression of AP-1A and β-actin was subsequently verified by real-time reverse transcription polymerase chain reaction (RT-PCR) (Lightcycler RNA Amplification Kit; Roche, Basel, Switzerland) and western blot analysis [44] using AP-1A and β-actin antibodies, respectively. Cell viability was measured by trypan blue exclusion, as described previously [45].

Binding assay

Huh7 cells transfected with AP-1A siRNA or control siRNA were detached by trypsinization. After washing three times with PBS, cells were blocked with 1% bovine serum albumin (BSA)–PBS for 30 min and incubated with DENV-2 at a MOI of 1 or MOI of 10 for 30 min on ice to prevent endocytosis. Cells were washed twice with 1% BSA–PBS and incubated with anti-DENV E antibody (3H5) for 30 min on ice. After washing, rabbit anti-mouse IgG conjugated with fluorescein isothiocyanate (dilution 1:50) was added and incubated for 30 min on ice. Cells were washed three times with 1% BSA–PBS and resuspended in 350 μl of 1% paraformaldehyde–PBS. Virus binding was finally counted by the mean fluorescence intensity of surface DENV-E-positive cells analyzed by flow cytometry.

Internalization assay

Huh7 cells transfected with AP-1A siRNA or control siRNA were incubated with DENV-2 at a MOI of 1 or MOI of 10 for 2 h at 37°C to allow penetration of DENV. To remove excess virus, cells were washed three times with PBS. RNA was extracted from DENV-infected Huh7 cells using the High Pure RNA isolation kit (Roche) and 0.5 μg RNA was reverse transcribed by random hexamer primers from the Superscript III cDNA synthesis kit (Invitrogen). cDNA was amplified by PCR using SYBR Green I Master Mix and primers specific to DENV E. Real-time RT-PCR was performed by LightCycler 480 II (Roche) with: (i) 40 amplification cycles of denaturation at 95°C for 10 s, annealing at 60°C for 10 s, and extension at 72°C for 10 s; and (ii) melting curve and cooling steps as recommended by the manufacturer. Relative levels of human AP-1A mRNA and viral RNA expression were determined by normalization to the expression levels of human β-actin according to the $2^{-\Delta\Delta Ct}$ method [46].

Real-time RT-PCR

RNA was extracted from DENV-infected Huh7 cells, which were transfected with AP-1A-specific siRNA or control siRNA using the High Pure RNA isolation kit (Roche). Reverse transcription was performed using total RNA (1 μg) and SuperScript III reverse transcriptase (Invitrogen). Oligo(dT) 20 primer or random hexamer primers were used for synthesis of cDNA template for determination of human AP-1A, AP-2, AP-3A and β-actin mRNA, as well as DENV RNA. Real-time RT-PCR was performed using primers (S1 Table) by LightCycler 480 II (Roche) with: (i) 40 amplification cycles of denaturation at 95°C for 10 s, annealing at 60°C for 10 s, and extension at 72°C for 10 s; and (ii) melting curve and cooling steps as recommended by the manufacturer's instructions. Relative levels of human AP-1A, AP-2, AP-3A mRNA and viral RNA expression were determined by normalization to the expression levels of human β-actin according to the $2^{-\Delta\Delta Ct}$ method [46].

Viral RNA transfection

DENV RNA was isolated from culture supernatant of DENV-infected C6/36 cells using the High Pure RNA isolation kit (Roche). In a 24-well plate, cells transfected with AP-1A siRNA or control siRNA were transfected with DENV RNA (0.5 μg) using Lipofectamine 2000. At 4 h post-transfection, transfection reagent was removed and replaced with complete RPMI 1640 medium. Cells were harvested at 6, 12 and 24 h post-transfection for detection of viral RNA by real-time RT-PCR. The culture supernatant was collected at 24 h and 48 h post-transfection for FFU assay [43].

Indirect immunofluorescence staining

Huh7 cells were plated on coverslips, transfected with a plasmid containing AP-1A [47]and infected with DENV for 24 h. The cells were fixed with 4% paraformaldehyde-PBS (Sigma-Aldrich) and 0.2% Triton X-100-PBS (Sigma) for 10 min at room temperature. The cells were incubated with mouse monoclonal anti-double-stranded RNA (anti-dsRNA) antibody (English & Scientific Consulting), rabbit polyclonal anti-GFP antibody (Abcam) for 1 h at room temperature. Upon removal of primary antibodies, cells were incubated with secondary antibodies (Alexa Fluor 488-conjugated donkey anti-rabbit IgG (Invitrogen), Alexa Fluor 594-conjugated donkey anti-mouse IgG (Invitrogen) for 30 min at room temperature. Hoechst 33342 (Molecular Probe) was used to stain cell nuclei. The stained cells were visualized by a confocal laser-scanning microscope (LSM 510 Meta).

Translation assay

pRL-SV40 vector (Promega), which contains *Renilla* luciferase gene, was linearized with *Xba*I. One μg of purified DNA was subjected to *in vitro* transcription using the RiboMAX Large Scale RNA Production System-T7 (Promega) in the presence of 20 mM $m^7G(5')ppp(5')G$ RNA cap structure analog (New England BioLabs, Ipswich, MA, USA) and resultant RNA product was purified using RNeasy Mini Kit (QIAGEN, Hilden, Germany). To determine the effect of AP-1A knockdown on translation, Huh7 cells were transfected twice with AP-1A-specific siRNA or control siRNA in a 96-well plate within a 24-h interval using Lipofectamine 2000 (Invitrogen) according to the manufacturer's instructions. After the second round of siRNA transfection, cells were transfected with 2.5 nM reporter RNA using Lipofectamine 2000 (Invitrogen) followed by replacement with fresh culture medium at 4 h later. Following 8 h after transfection with reporter RNA, cells were harvested and determined for *Renilla* luciferase expression using Luciferase Reporter Assay System (Promega). *Renilla* luciferase signal was measured by Synergy H1 Hybrid multi-mode microplate reader (BioTek, Winooski, VT, USA).

Western blotting

Clear lysates prepared from Huh7 cells transfected with AP-1A siRNA or control siRNA were mixed with 4× loading buffer [50 mMTris–HCl (pH 6.8), 2% SDS, 0.1% bromophenol blue and 10% glycerol] and heated at 95°C for 5 min. Proteins in the samples were subjected to 10% SDS-PAGE and transferred to nitrocellulose membranes (GE Healthcare Life Sciences,Freiburg, Germany) as described previously [28]. The membranes were incubated with 5% skimmed milk in PBS or in Tris-buffered saline with 0.1% Tween 20 (TBST) for 1 h to block non-specific binding and with mouse monoclonal antibodies specific for DENV E (clones 4G2), DENV PrM (clone 1C3), and DENV NS1 (clone NS1-3F.1) or human β-actin at 4°C overnight. The membranes were washed three times with PBS or TBST and incubated with horseradish peroxidase (HRP)-conjugated rabbit anti-mouse immunoglobulin antibody (DAKO, Santa Clara, CA, USA) at a dilution of 1:1000 for 1 h at room temperature, followed by three further washes. Proteins were visualized using an enhanced chemiluminescence detection kit (SuperSignal West Pico Chemiluminescent Substrate; Thermo Scientific, Waltham, MA, USA). Relative expression levels of human AP-1A, and DENV proteins were assessed by normalization of their protein band intensities to human β-actin intensity using ImageJ software (National Institutes of Health, Bethesda, MD, USA).

Transmission electron microscopy (TEM)

Huh7 cells transfected with AP-1A siRNA or control siRNA were infected with DENV-2 at a MOI of 10 for 2 h. Cells were washed three times with PBS and incubated in maintenance medium (2% FBS–RPMI 1640) for 24 h. Cells were fixed with 2% paraformaldehyde/2% glutaraldehyde in PBS for 24 h at 4°C, post-fixed with 1% osmium tetroxide and 1% potassium ferrocyanide for 1 h at room temperature, followed by dehydration in a graded series of ethanol (25%, 50%, 75%, 95% and 100%) for 20 min. Cells were embedded in LRW resin and incubated at 60°C for polymerization for 48 h. Sections were obtained with a Reichert–Jung Ultracut E Ultramicrotome and diamond knife, counterstained with uranyl acetate and lead citrate for 10 min each, and examined with a JEOL-1010 transmission electron microscope (JEOL USA, Peabody, MA, USA).

Lipid complementation assay

Huh7 cells were infected with DENV-2 at MOI of 1 for 2 h. Excess viruses were removed and cells were washed three times with PBS. DENV-infected were incubated with A5 (200 μM) in

the presence of oleic acid-BSA (Sigma) or fatty acid free-BSA (Sigma) for 24 h. The culture supernatants were collected to measure the amount of DENV production by a focus forming unit (FFU) assay, as described previously [43].

FFU assay

Supernatants collected from DENV-infected Huh7 cells transfected with AP-1A siRNA or control siRNA were assessed for DENV production. Vero cells were seeded onto a 96-well plate (Sigma) at 3×10^4 cells/well in minimal essential medium (MEM) supplemented with 10% FBS, 2 mM L-glutamine, 36 μg/ml penicillin and 60 μg/ml streptomycin, and cultured at 37°C in a 5% CO_2 incubator for 24 h. The medium was removed from each well. DENV was serially diluted 10-fold in MEM containing 3% FBS, 2 mML-glutamine, 36 μg/ml penicillin and 60 μg/ml streptomycin, added to each well (100 μl/well), and incubated at 37°C in a 5% CO_2 incubator for 2 h. Overlay medium (MEM containing 3% FBS, 2 mML-glutamine, 2% carboxy methyl cellulose, 10% tryptose phosphate broth, 37 μg/ml penicillin and 60 μg/ml streptomycin was added to each well (100 μl/well), and the culture was incubated for 3 days. The medium was discarded from DENV-infected cells. The adherent cells were washed three times with PBS (pH 7.4), fixed with 3.7% formaldehyde (BDH Laboratory Supplies, Poole, UK) in PBS at room temperature for 10 min, followed by an additional 10 min permeabilization with 1% Triton X-100 (Fluka, Steinheim, Switzerland). The cells were incubated sequentially with mouse anti-DENV E monoclonal antibody (clone 4G2) at 37°C for 1 h and HRP-conjugated rabbit anti-mouse immunoglobulins (DAKO) at a dilution of 1:1000 in PBS containing 2% FBS and 0.05% Tween-20 in the dark at 37°C for 30 min. To develop an enzymatic reaction, the cells were incubated with a substrate solution containing 0.6 mg/ml diaminobenzidine, 0.03% H_2O_2 and 0.08% $NiCl_2$ in PBS at room temperature in the dark for 5 min. After washing three times with PBS, dark brown foci of the DENV-infected cells were counted under a light microscope. Virus titers were reported as FFU/ml.

Statistical analysis

Data were statistically analyzed by unpaired *t* test, with the use of GraphPad Prism version 5.0 (San Diego, CA, USA). Results were expressed as mean and standard error of the mean (SEM) and $P<0.05$ was considered significant.

Results

Inhibition of DENV production by AP-1-dependent traffic inhibitor

AP-1-dependent traffic inhibitor (A5) was previously shown to inhibit transport between TGN and Golgi in yeast [42]. We first determined whether A5 can inhibit DENV infection. DENV-infected Huh7 cells were incubated with different concentrations of A5. DENV viral protein synthesis was determined by western blotting and DENV production was measured by FFU assay. Although the viability of the cells was comparable (Fig 1C), A5 inhibited DENV protein synthesis (Fig 1A) and DENV production (Fig 1B) in a dose-dependent manner. Whether this effect was occurred in different cell line, DENV-infected A549 cells were tested in the presence or absence of A5. The result shows that A5 inhibited DENV protein synthesis (Fig 2A) and DENV production (Fig 2B) without affecting cell viability (Fig 2C). Data suggest that AP-1 is involved in DENV protein synthesis and production of dengue infectious virions.

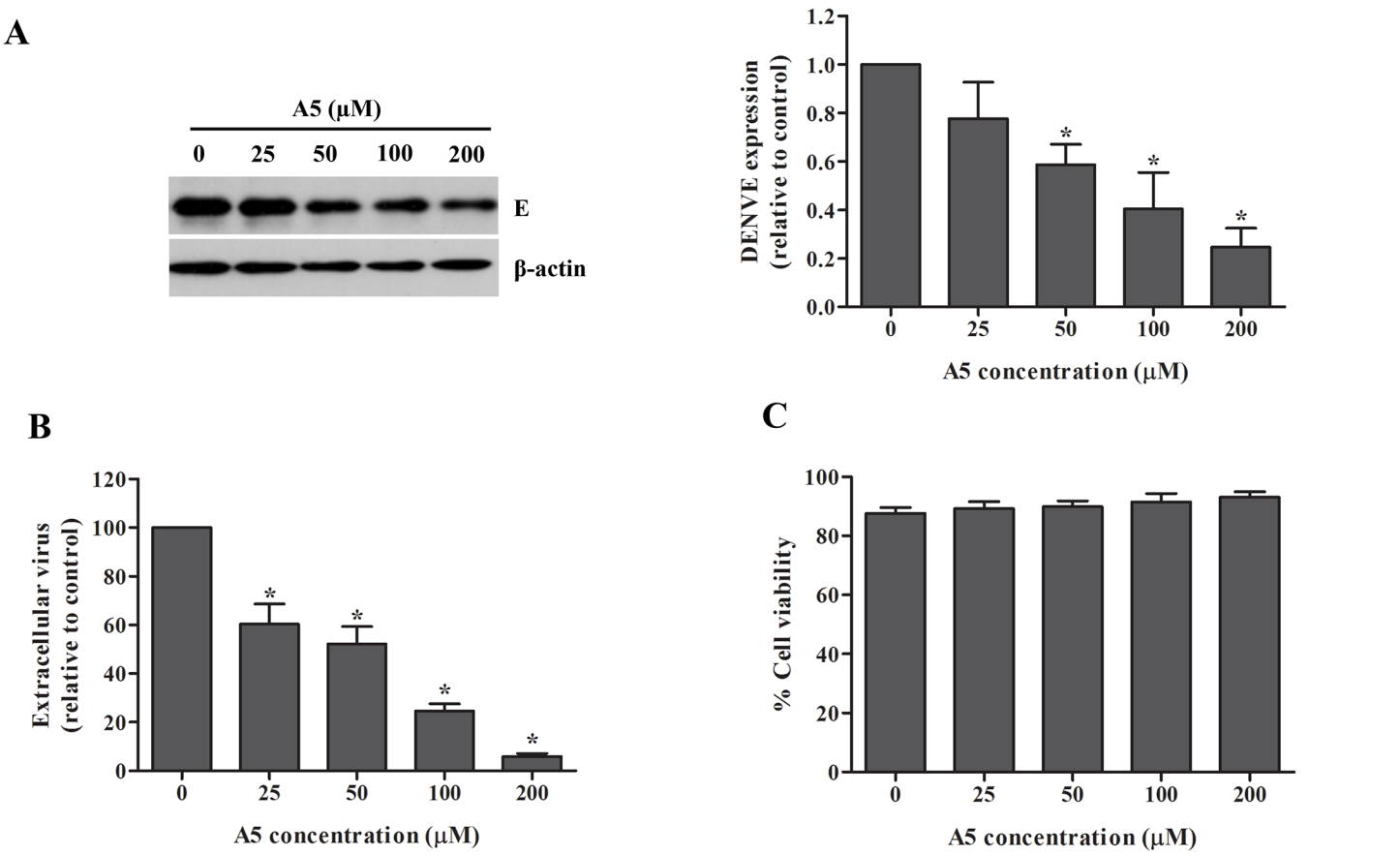

Fig 1. AP-1-dependent traffic inhibitor, A5, inhibited DENV production in Huh7 cells. Huh7 cells were infected with DENV-2 at a MOI of 1 for 2 h. Unbound virus was removed by washing with PBS. Mock- or DENV-infected cells were incubated with A5 at 0, 25, 50, 100 and 200 μM for 24 h. (A) DENV envelope protein in cell lysates was examined at 24 h post-treatment with A5 by western blotting. Band intensity of DENV envelope protein was quantified using Image J software. (B) Virus titer in culture supernatants was measured by FFU assay. (C) Viability of DENV-infected cells was measured using PrestoBlue cell viability reagent. Statistical significance was analyzed using the unpaired *t* test. *P<0.05. Error bars represent SEM from three independent experiments.

doi:10.1371/journal.pone.0130065.g001

AP-1A is not involved in steps of binding and internalization

For the AP-1A knockdown experiment, Huh7 cells were transfected twice with duplex AP-1A-specific siRNA or control siRNA for 24 h. After the second transfection, expression of AP-1A and β-actin mRNA was measured by real-time RT-PCR. Expression of AP-1A and β-actin protein was determined by western blotting using anti-AP-1A and anti-β-actin, respectively. Cell viability was determined by trypan blue exclusion assay. AP-1A mRNA expression and protein expression were reduced in Huh7 cells transfected with AP-1A siRNA compared with control siRNA (Fig 3A and 3B).

For the binding assay, Huh7 cells transfected with AP-1A siRNA or control siRNA were incubated with DENV at a MOI of 1 or at a MOI of 10 at 4°C to prevent viral internalization. Viral binding was determined by DENV E surface staining and analyzed by flow cytometry. The intensity of DENV-E-positive cells in Huh7 cells transfected with AP-1A siRNA or control siRNA was similar (Fig 3C). Therefore, AP-1A may not be involved in the binding of DENV E to Huh7 cells.

For the internalization assay, Huh7 cells transfected with AP-1A siRNA or control siRNA were incubated with DENV at a MOI of 1 or at a MOI of 10 at 37°C for 2 h to allow

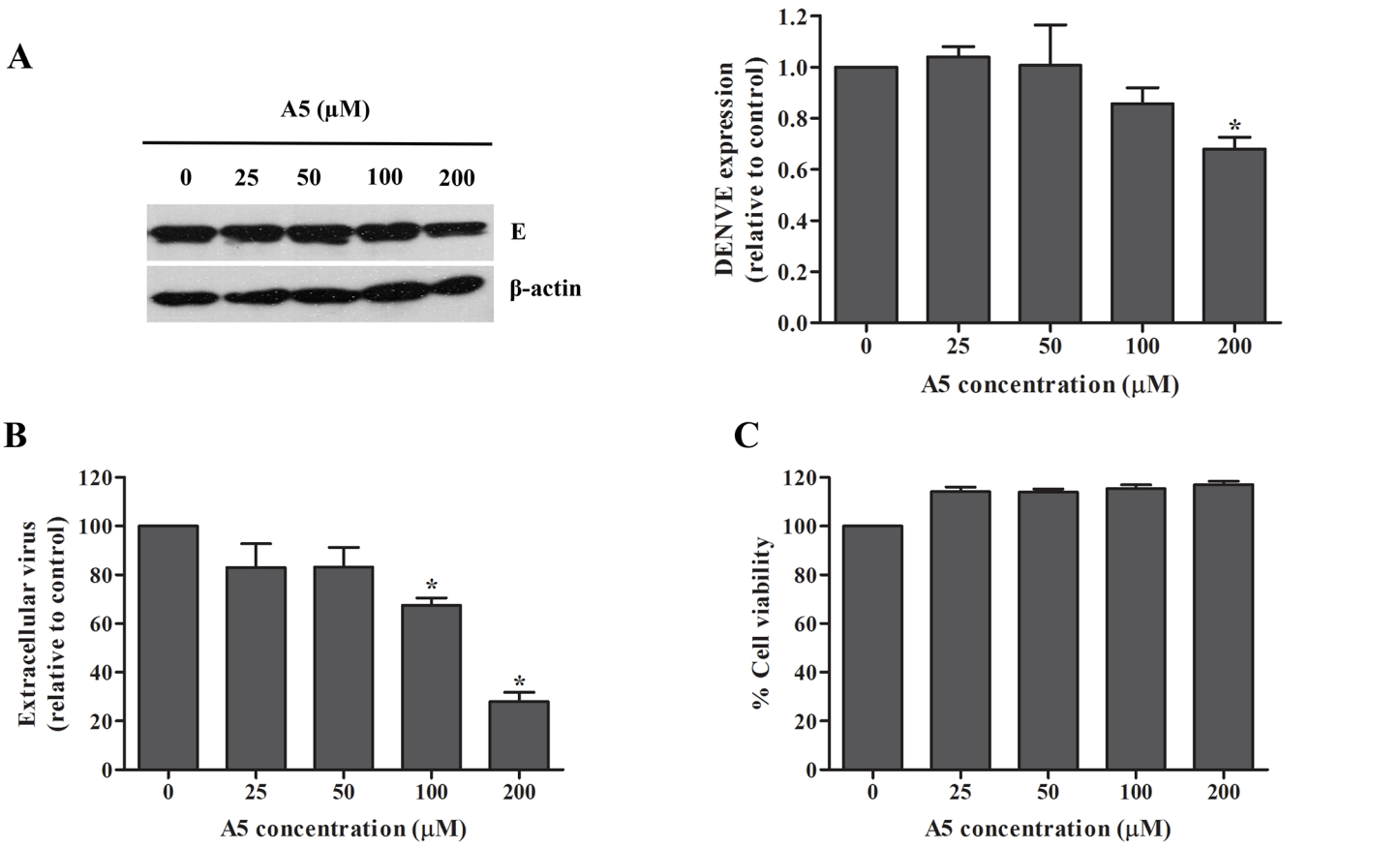

Fig 2. AP-1-dependent traffic inhibitor, A5, inhibited DENV production in A549 cells. A549 cells were infected with DENV-2 at a MOI of 1 for 2 h. Unbound virus was removed by washing with PBS. Mock- or DENV-infected cells were incubated with A5 at 0, 25, 50, 100 and 200 μM for 24 h. (A) DENV envelope protein in cell lysates was examined at 24 h post-treatment with A5 by western blotting. Band intensity of DENV envelope protein was quantified using Image J software. (B) Virus titer in culture supernatants was measured by FFU assay. (C) Viability of DENV-infected cells was measured using PrestoBlue cell viability reagent. Statistical significance was analyzed using the unpaired *t* test. *P<0.05. Error bars represent SEM from three independent experiments.

doi:10.1371/journal.pone.0130065.g002

endocytosis. Viral RNA was determined by real-time RT-PCR. The results indicated that the viral RNA in AP-1A siRNA-transfected Huh7 cells or in control siRNA-transfected Huh7 cells was not significantly altered (Fig 3D). Therefore, AP-1A may not be involved in the internalization of DENV into Huh7 cells.

AP-1A facilitates DENV RNA replication

We compared viral RNA in Huh7 cells transfected with AP-1A siRNA or control siRNA at 24 h post-infection. Viral RNA level in Huh7 cells transfected with AP-1A siRNA was reduced by ~80% compared with that in cells transfected with control siRNA (Fig 4A), implying a role of AP-1A in DENV replication. We next determined how early AP-1A became involved in DENV replication. Huh7 cells transfected with AP-1A siRNA or control siRNA were infected with DENV-2 at a MOI of 1 for 2 h. Cells were harvested to measure DENV RNA by real-time RT-PCR at 0, 4, 8 and 12 h. Relative to the Huh7 cells transfected with control siRNA, DENV RNA level was lower in cells transfected with AP-1A siRNA at 8 and 12 h post-infection (Fig 4B), suggesting early involvement of AP-1A in DENV replication. Expression of AP-1A post-

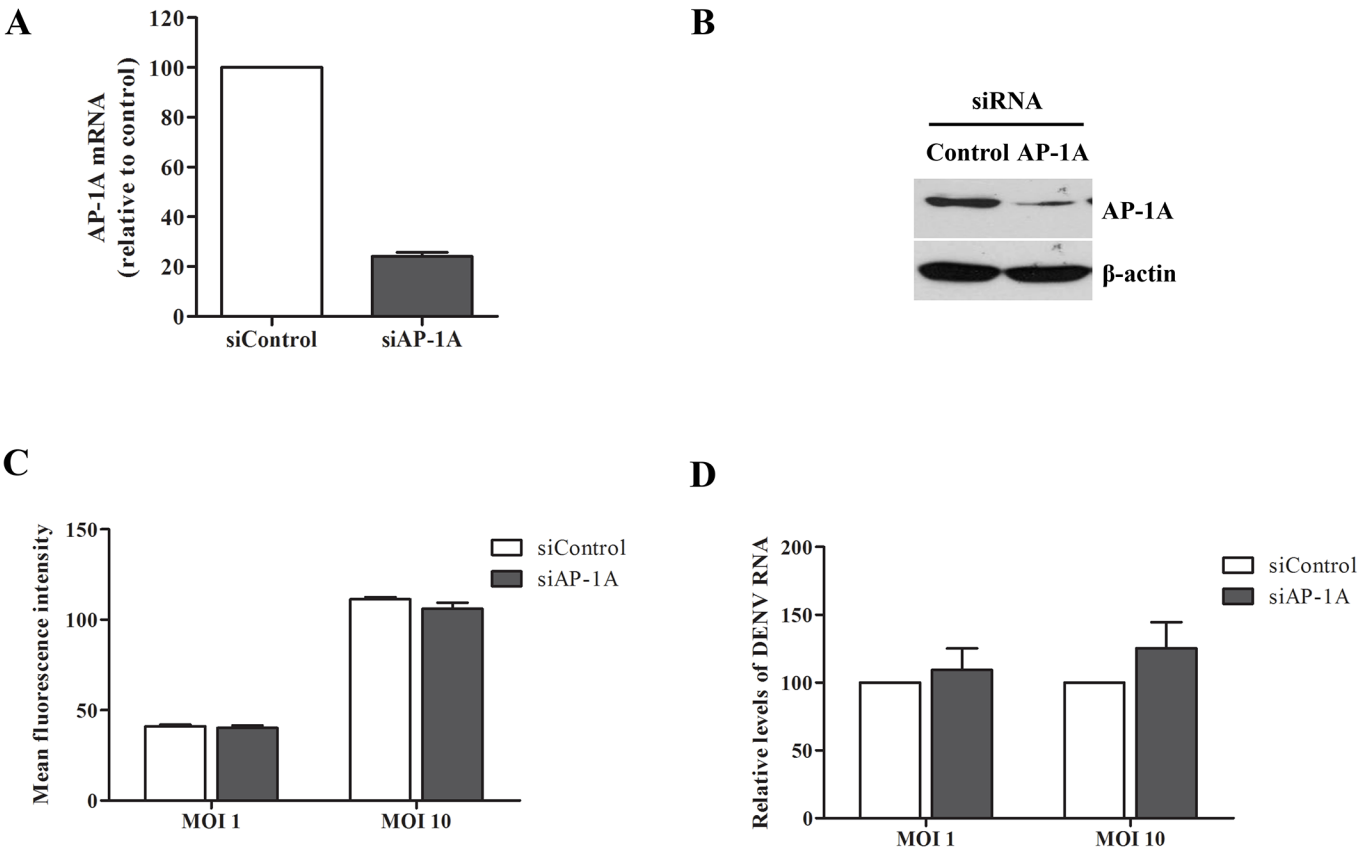

Fig 3. AP-1A was not involved in DENV binding and internalization. (A) Knockdown efficiency of AP-1A siRNA in Huh7 cells was examined by real-time RT-PCR at 48 h after second transfection. (B) AP-1A protein was measured by western blotting. (C) Quantification of DENV binding on Huh7 cells transfected with AP-1A siRNA. Cells transfected with control siRNA and AP-1A siRNA were incubated with DENV-2 at a MOI of 1 for 30 min on ice. Cells were surface stained with antibody to DENV E, followed by staining with the rabbit anti-mouse IgG conjugated with fluorescein isothiocyanate. The surface E-positive cells were analyzed by flow cytometry. (D) Viral internalization was determined by detecting DENV RNA at 2 h post-infection using real-time RT-PCR. Statistical significance was analyzed using unpaired *t* test (*P<0.05). Error bars represent SEM from three independent experiments.

doi:10.1371/journal.pone.0130065.g003

infection is shown in Fig 4C, which confirms that AP-1A was knocked down at each time point.

Immunofluoresence assay was subsequently performed to determine whether AP-1A is co-localizaed with viral RNA at the replication site during DENV infection. The result shows that AP-1A was partially co-localized with dsRNA near the perinuclear region of DENV-infected Huh7 cells (Fig 5) suggesting that AP-1A may be recruited into the replication site during DENV infection.

Naked DENV RNA was directly transfected into Huh7 cells transfected with AP-1A siRNA or control siRNA to exclude the role of AP-1A in viral fusion and uncoating. Viral RNA was measured by real-time RT-PCR at 6, 12 and 24 h post-transfection. DENV RNA was significantly decreased in Huh7 cells transfected with AP-1A siRNA compared with control siRNA at 24 h post-transfection, suggesting that naked DENV RNA replicates in Huh7 cells, but DENV RNA replication was decreased in the absence of AP-1A (Fig 6A). FFU assay was subsequently performed. Naked DENV RNA produced infectious virions in Huh7 cells transfected with control siRNA, but production was significantly decreased in the absence of AP-1A (Fig 6B).

TEM was performed to determine the morphology of Huh7 cells transfected with AP-1A siRNA or control siRNA and infected with DENV at a MOI of 10. Compared with mock-

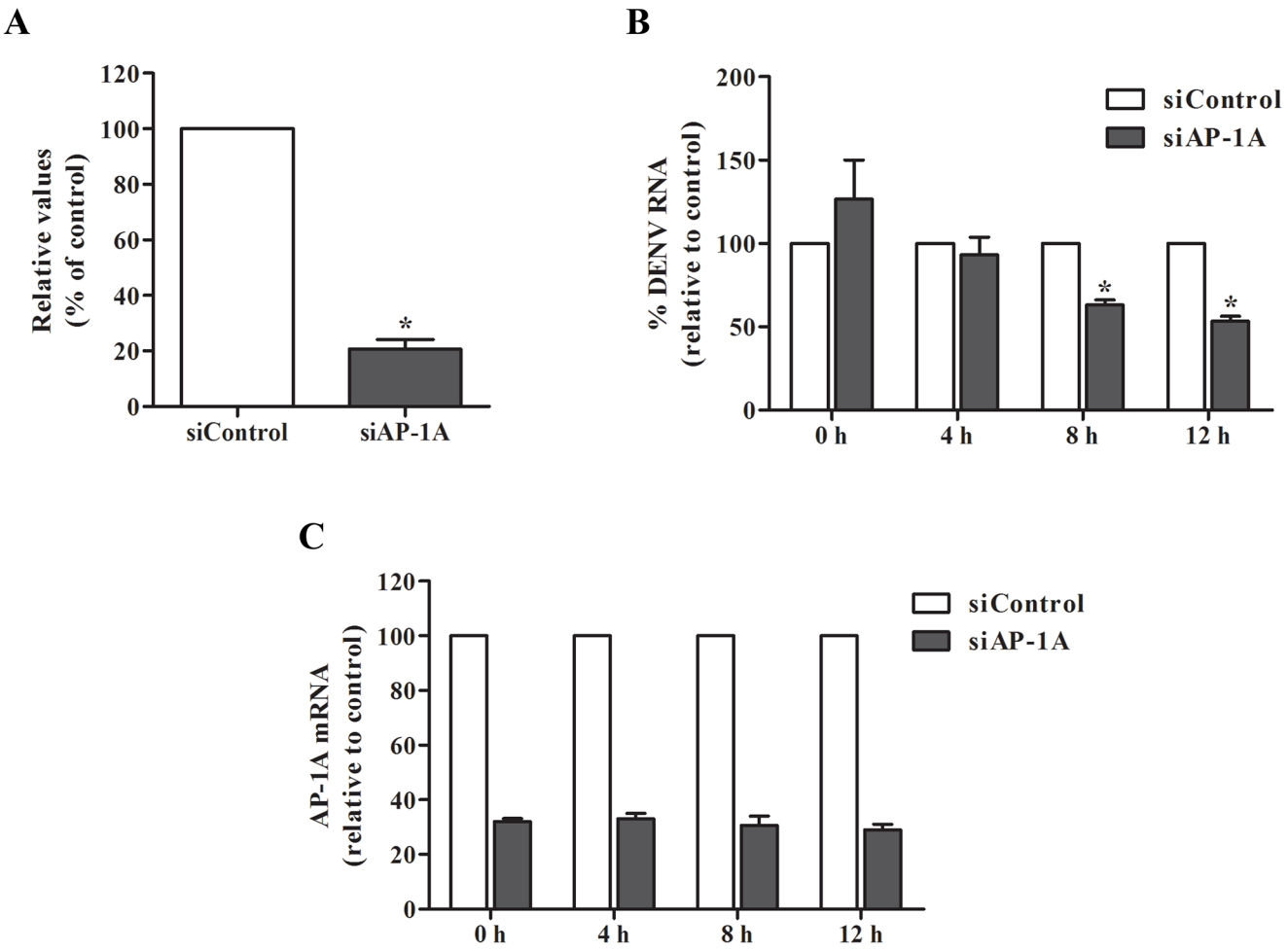

Fig 4. Silencing of AP-1A reduced DENV RNA level. (A) DENV RNA level was measured by real-time RT-PCR at 24 h post-infection. (B) Kinetics of DENV RNA expression were determined by real-time RT-PCR. Relative expression of DENV RNA in AP-1A knockdown cells was compared with control cells. (C) Knockdown efficiency of AP-1A siRNA was examined by real-time RT-PCR. The results were plotted relative to cells transfected with control siRNA. Statistical significance was analyzed using the unpaired *t* test (*P<0.05). Error bars represent SEM from three independent experiments.

doi:10.1371/journal.pone.0130065.g004

infected cells (Fig 7A), DENV-infected Huh7 cells at 24 h post-infection had virus particles, and modification of ER membranes including vesicular packets (Fig 7B). However, these packets were reduced in number in Huh7 cells transfected with AP-1A siRNA (Fig 7C). Modification of ER membranes was conserved in Huh7 cells transfected with AP-2 siRNA (Fig 7D). Our data indicated the role of AP-1A in replication of DENV.

We verified whether DENV protein expression was affected after DENV RNA replication. Western blotting was performed using lysates prepared from DENV-infected or mock-infected Huh7 cells in the presence or absence of AP-1A. Expression of DENV prM, DENV E and DENV NS1 in Huh7 cells transfected with AP-1A siRNA was decreased compared with that in cells transfected with control siRNA (Fig 8A). We further tested whether host transcription and translation were compromised by AP-1A disruption by real-time RT-PCR using primers specific to AP-2, and AP-3A and by translation assay, respectively. The result in Fig 8B demonstrated that the mRNA expression of AP-2, and AP-3A was not compromised by AP-1A disruption. Furthermore, host translation machinery was not compromised by AP-1A disruption as luminescence intensity of *Renilla* luciferase activities between Huh7 cells transfected with

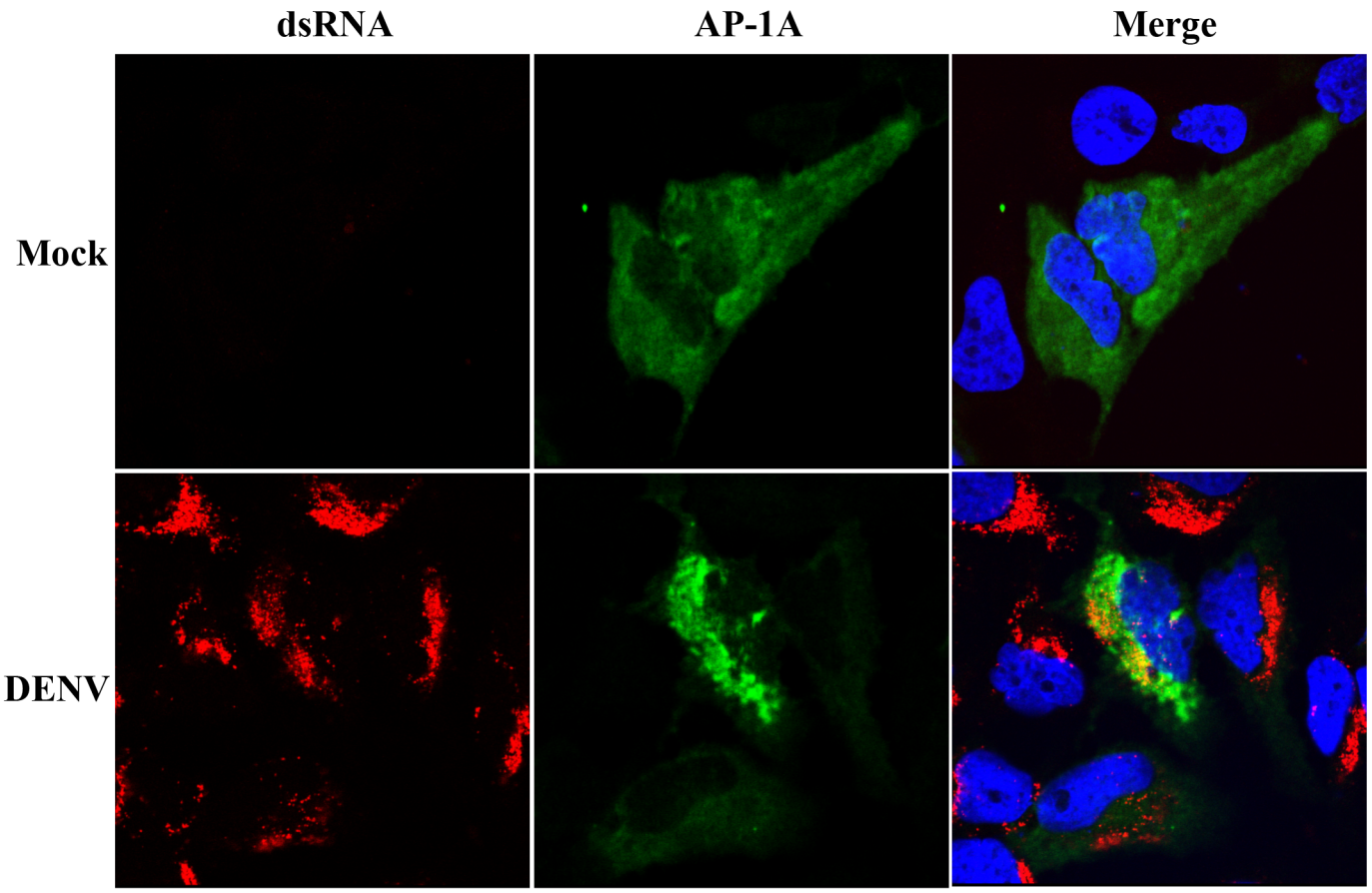

Fig 5. AP-1A was partially co-localized with dsRNA in DENV-infected cells. Huh7 cells were plated on coverslips, transfected with a plasmid containing AP-1A [47] and infected with DENV for 24 h. The cells were fixed and incubated with anti-dsRNA antibody and anti-GFP antibody, Upon removal of primary antibodies, cells were incubated with Alexa Fluor 488-conjugated donkey anti-rabbit IgG and Alexa Fluor 594-conjugated donkey anti-mouse IgG Hoechst 33342 was used to stain nuclei of the cells. The cells were visualized by a confocal laser-scanning microscope (LSM 510 Meta).

doi:10.1371/journal.pone.0130065.g005

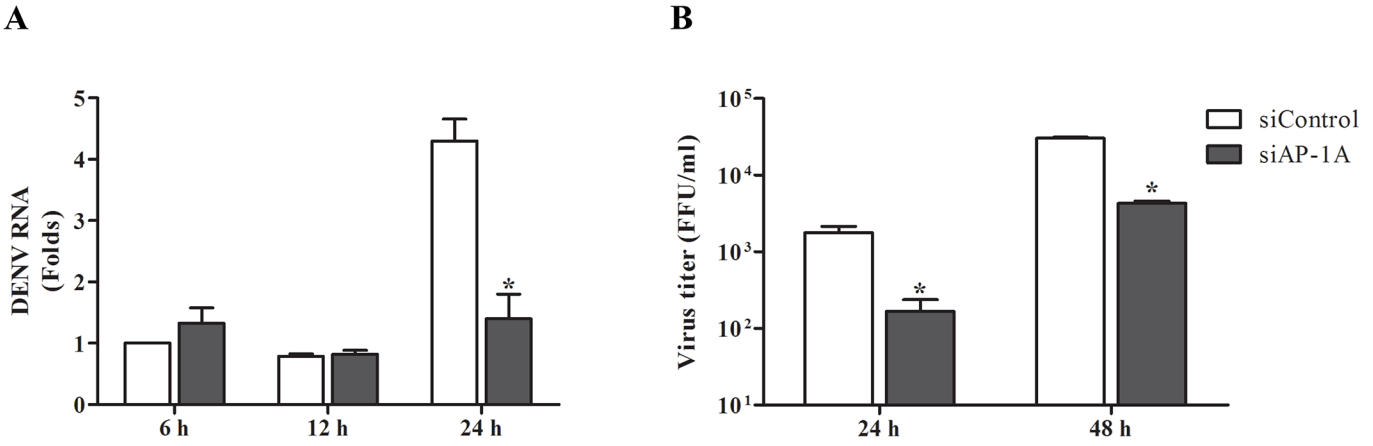

Fig 6. Depletion of AP-1A impaired DENV genome replication. (A) Effect of AP-1A siRNA on DENV RNA synthesis. Cells transfected with control and AP-1A siRNA were transfected with 0.5 μg DENV RNA using Lipofectamine 2000. Viral RNA level was determined by real-time RT-PCR at 6, 12 and 24 h post-transfection. (B) Quantification of virions released from cells transfected with DENV RNA. At 24 h and 48 h post-transfection, culture supernatants were collected for titration by FFU assay. The results were plotted relative to cells transfected with control siRNA. Statistical significance was analyzed using unpaired *t* test (*P<0.05). Error bars represent SEM from three independent experiments.

doi:10.1371/journal.pone.0130065.g006

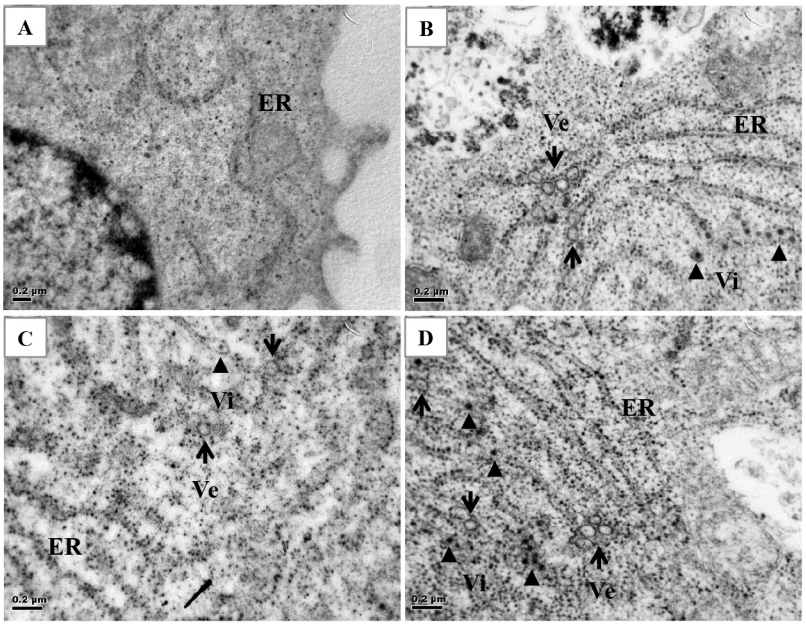

Fig 7. AP-1A knockdown affected the DENV replication site. (A) Ultrastructural analysis of Huh7 cells transfected with control siRNA was observed by TEM at 48 h after second transfection. (B) Cells transfected with control siRNA. (C) Cells transfected with AP-1A siRNA. (D) Cells transfected with AP-2 siRNA were infected with DENV-2 at a MOI of 10 for 24 h. Cells were fixed, processed and analyzed by TEM. Ve, virus-induced vesicles (arrow); Vi, virus particles (arrowhead).

doi:10.1371/journal.pone.0130065.g007

AP-1A siRNA or with control siRNA were relatively similar (Fig 8C). As ER stress may be activated during AP-1A disruption thereby leading to translation inhibition, which could reduce expression of viral proteins, western blot analysis was performed using lysates form DENV-infected Huh7 cells in the presence or absence of AP-1-dependent traffic inhibitor (A5), the result shows that GRP78 protein expression was relatively similar (S1 Fig); therefore, AP-1A disruption may not lead to translation inhibition to reduce viral protein expression. All data suggest that DENV protein expression was reduced after DENV RNA replication in Huh7 cells transfected with AP-1A siRNA.

Enhanced fatty acid synthesis is required for efficient membrane proliferation and rearrangement. Rearrangement of membrane structure induced by dengue virus (DENV) is essential for replication, and requires host cellular machinery [25, 48, 49]. We next asked whether disturbance of AP-1 by A5 affect fatty acid synthesis, which is essential for dengue viral replication. Lipid complementation assay was performed. DENV-infected Huh7 cells were incubated with A5 in the presence of oleic acid-BSA or fatty acid free-BSA for 24 h. The culture supernatants were collected for FFU assay. Oleic acid-BSA could increase DENV production compared to fatty acid free-BSA (Fig 9) suggesting that AP-1 may involve in lipid synthesis required for DENV replication.

The final step was to verify DENV production in Huh7 cells transfected with AP-1A siRNA compared with control siRNA. Although the number of viable cells was similar, AP-1A siRNA decreased the yield of viral progeny compared with that of control siRNA (Fig 10A and 10B).

AP-1 is involved in virion production for all serotypes

To determine whether AP-1-dependent traffic plays a role in four serotypes of DENV, Huh7 cells were infected with each DENV serotype, followed by treatment with AP-1-dependent

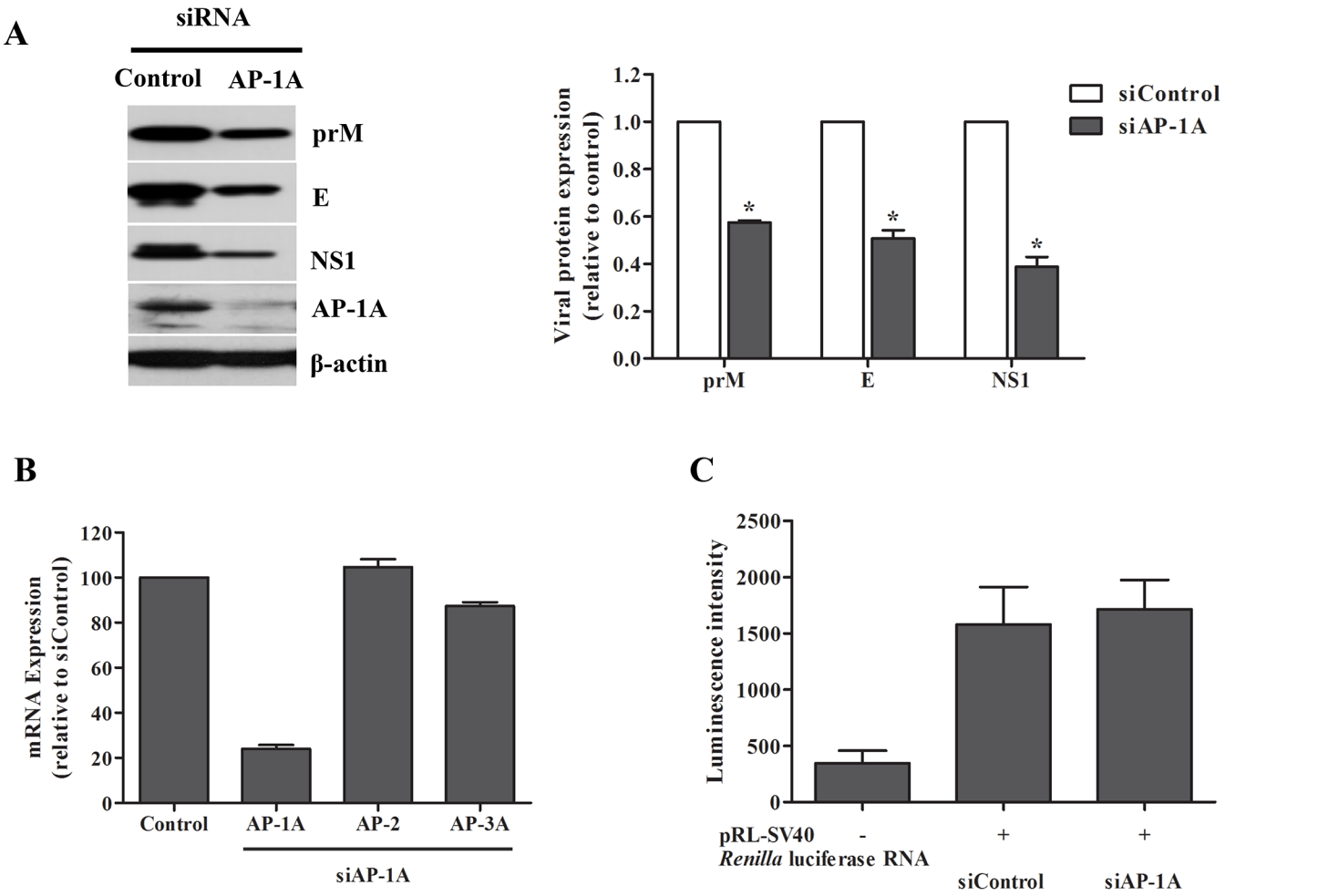

Fig 8. Expression of DENV protein was decreased in Huh7 cells transfected with AP-1A siRNA. (A) Huh7 cells were transfected with control siRNA and AP-1A siRNA and infected with DENV-2 for 24 h. DENV proteins were examined at 24 h post-infection by western blotting. Band intensity of DENV proteins was quantified using Image J software. (B) Expression of AP-1A, AP-2 or AP-3A in Huh7 cells was examined by real-time RT-PCR at 48 h after second transfection. (C) pRL-SV40 vector, which contains *Renilla* luciferase gene, was subjected to *in vitro* transcription. To determine the effect of AP-1A knockdown on translation, Huh7 cells were transfected twice with AP-1A-specific siRNA or control siRNA. After the second round of siRNA transfection, cells were transfected with 2.5 nM reporter RNA followed by replacement with fresh culture medium at 4 h later. Following 8 h after transfection with reporter RNA, cells were harvested and determined for *Renilla* luciferase expression using Luciferase Reporter Assay System (Promega).

doi:10.1371/journal.pone.0130065.g008

traffic inhibitor (A5).The titer of DENV was measured in culture supernatant by FFU assay. A5 had an inhibitory effect on all serotypes of DENV (Fig 11A–11D). However, the reduction for DENV-2 was greater than for the other serotypes.

Discussion

Using a human-genome-wide RNAi screen, clathrin and its adaptor proteins were shown to decrease DENV infection [22]. A pathway-specific siRNA library further revealed the role of clathrin and its adaptor proteins in mediating DENV entry [4] and secretion of subviral particles [24]. Furthermore, the role of AP-1A in DENV production was shown to play a role at the egress stage from the TGN to plasma membrane [38]. In the present study, we showed that treatment with AP-1-dependent traffic inhibitor (A5), or transfection with AP-1A siRNA decreased replication of DENV, thereby reducing viral protein expression and production. Thus, AP-1 may have an additional role besides aiding egression of DENV, as shown previously [38].

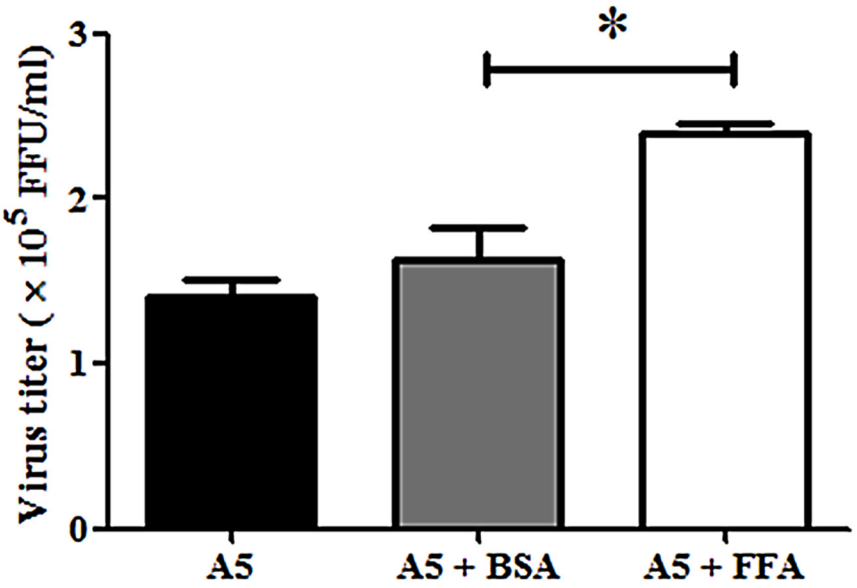

Fig 9. Exogenous fatty acid increased DENV production after A5 treatment. DENV-infected Huh7 cells were incubated with A5 in the presence of oleic acid-BSA or fatty acid free-BSA for 24 h. The culture supernatants were collected for FFU assay. Statistical significance was analyzed using the unpaired *t* test. *P<0.05. Error bars represent SEM from three independent experiments.

doi:10.1371/journal.pone.0130065.g009

This hypothesis was supported by RNAi, which showed that DENV RNA was significantly reduced in DENV-infected Huh7 cells transfected with AP-1A siRNA compared with control siRNA. Naked DENV RNA transfection, which bypassed the process of viral fusion and uncoating, demonstrated decreased production of viral RNA and infectious virions in cells transfected with AP-1A siRNA compared with control siRNA-transfected cells. This was indicative of an essential function of AP-1A in the step of DENV RNA replication. Vesicular packets, which are a proposed replication site for DENV, were fewer in number in Huh7 cells transfected with AP-1A siRNA compared with control siRNA.

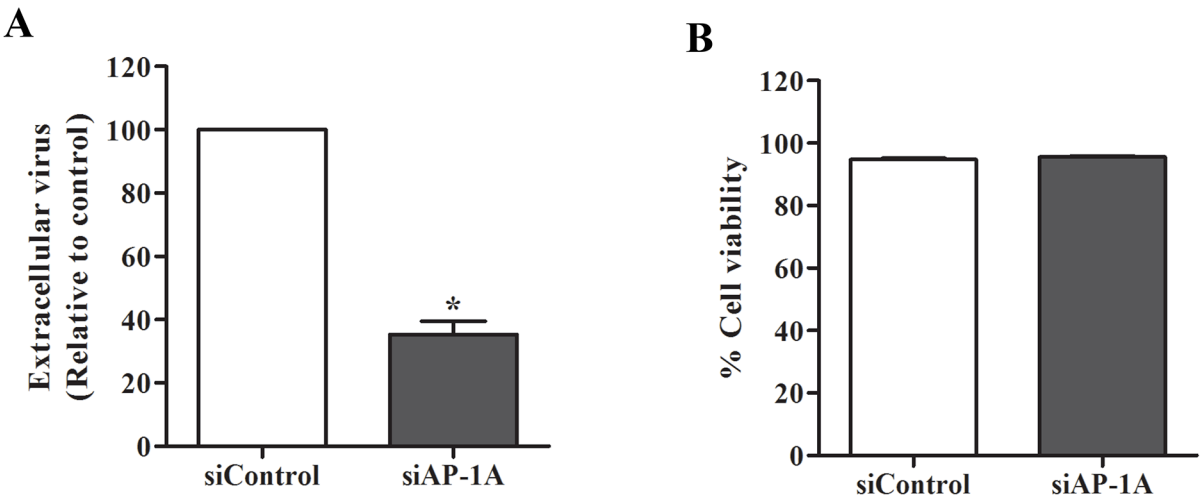

Fig 10. Silencing of AP-1A reduced virus production. Huh7 cells were transfected with control siRNA and AP-1A siRNA and infected with DENV-2 for 24 h. (A) Virus titer in culture supernatants was measured by FFU assay. (B) Cell viability was measured by trypan blue exclusion. Statistical significance was analyzed using unpaired *t* test. *P<0.05. Error bars represent SEM from three independent experiments.

doi:10.1371/journal.pone.0130065.g010

AP-1, GTPase ADP-ribosylation factor 1 (ARF)-1 and phosphatidylinositol-4-phosphate (PI4P) are the components, which are essential for reorganization of donor membrane for clathrin-coated vesicle [50]. AP-1A and AP-3A are required for transport between endosomal/lysosomal systems and the secretory pathway [51, 52]. AP-3A was previously shown to be involved in replication of DENV [38], therefore, we proposed here that AP-1A may act in concert with AP-3A to facilitate replication of DENV. AP-1A and AP-3A coat assembly are controlled by GTPase ARF-1 [53, 54]. ARF-1 plays a key role in trafficking through the Golgi apparatus, where it is involved in the formation of vesicular packets, and ARF family siRNAs have an inhibitory effect on DENV recombinant subviral particle secretion [24, 55]. Rab18, a GTPase involved in vesicular trafficking, also regulates DENV replication by targeting enzymes required for cellular fatty acid synthesis to the replication site [56]. Enhanced fatty acid synthesis

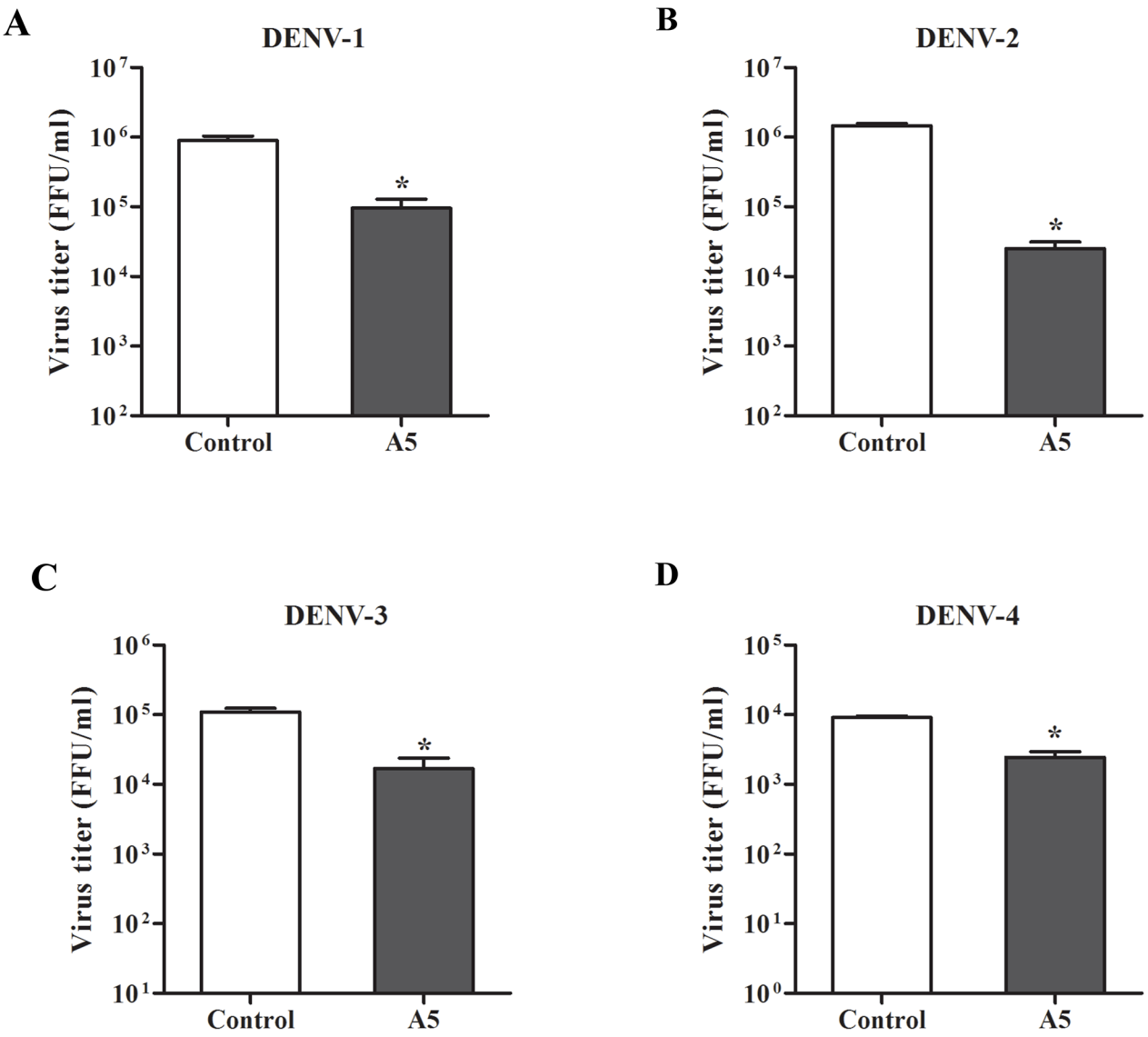

Fig 11. AP-1 was involved in production of four serotypes of DENV. Inhibitory effect of A5 on virus replication was determined in all four serotypes of DENV. Huh7 cells were infected with DENV-1, -2, -3 and -4 at a MOI of 1 for 2 h. Unbound virus was removed by washing with PBS. DENV-infected cells were incubated with A5 (200 μM) or culture medium (control) for 24 h. Virus titer in culture supernatants was measured by FFU assay. (A) Titer of DENV-1; (B) titer of DENV-2; (C) titer of DENV-3; (D) titer of DENV-4. Statistical significance was analyzed using unpaired *t* test (*P<0.05). Error bars represent SEM from three independent experiments.

doi:10.1371/journal.pone.0130065.g011

is required for efficient membrane proliferation and rearrangement in DENV replication [25, 26, 57]. Recruitment of PI4P is also required for membrane reorganization [58]. DENV may use AP-1A to recruit enzymes (PI4K-IIIβ) for synthesis of PI4P to help its own replication. Purified AP-1 binds to PI4P, and anti-PI4P inhibits recruitment of cytosolic AP-1 to normal cellular membranes [59]; therefore, disruption of AP-1A by RNAi in the present study may have affected synthesis of PI4P and membrane organization required for DENV replication. The role of phosphatidylinositol-4-kinases, including PI4K-IIIα, as a modulator of hepatitis C virus (HCV), was demonstrated by co-localization of PI4K-IIIα and HCV NS5A in lipid rafts. Inhibition of web formation by siRNA against PI4K-IIIα correlates with the decrease in HCV replication and infectious virion production. PI4K-IIIα is proposed to produce pools of PI4P for HCV replication [60]. In addition, DENV can activate autophagic machinery for viral replication both *in vitro* and *in vivo* [61, 62]. DENV infection can induce an autophagy-dependent processing of lipid droplets and triglycerides to release free fatty acids for replication [26], linking of DENV replication through autophagolysosome was demonstrated [63], and dysfunction of the AP-1A-dependent clathrin coating at the TGN can prevent autophagosome formation [64]. AP-1A may be a host component, which can recruit enzymes required for fatty acid synthesis and dysfunction of AP-1A may affect membrane organization, thereby decreasing replication of virus in infected cells.

Conclusion

AP-1A was characterized to establish its role during the DENV life cycle, using an inhibitor and RNAi. RNAi specific to AP-1A decreased viral RNA and protein levels, and virion production in Huh7 cells.

Supporting Information

S1 Fig. AP-1-dependent traffic inhibitor, A5, did not induce ER stress. Huh7 cells were infected with DENV-2 at a MOI of 1 for 2 h. Unbound virus was removed by washing with PBS. Mock- or DENV-infected Huh7 cells were incubated with A5 at different concentrations (0, 100 or 200 μM) for 48 h. The cells were lysed and subjected to western blot analysis using antibodies specific to human GRP78 and β-actin.
(TIF)

S1 Table. Primers used for real-time RT-PCR analysis. RNA was extracted from DENV-infected Huh7 cells, which were transfected with AP-1A-specific siRNA or control siRNA. After cDNA synthesis, Real-time RT-PCR was performed using primers listed in S1 Table. Relative levels of human AP-1A, AP-2, AP-3A mRNA and viral RNA expression were determined by normalization to the expression levels of human β-actin.
(PDF)

Acknowledgments

This work is supported by Thailand Research Fund (RSA5780012) to TL. UY is the RGJ-Ph.D. student (PHD/0259/2552). The funders had no role in study design, data collection and analysis, decision to publish, or preparation of the manuscript.

Author Contributions

Conceived and designed the experiments: TL PY JC. Performed the experiments: UY NT. Analyzed the data: MJ SN. Contributed reagents/materials/analysis tools: CP. Wrote the paper: UY SN MJ TL.

References

1. Gubler DJ. Dengue and dengue hemorrhagic fever. Clin Microbiol Rev. 1998; 11(3):480–96. Epub 1998/07/17. PMID: 9665979.
2. Halstead SB. Pathogenesis of dengue: challenges to molecular biology. Science. 1988; 239 (4839):476–81. Epub 1988/01/29. PMID: 3277268.
3. Halstead SB. Dengue. Lancet. 2007; 370(9599):1644–52. Epub 2007/11/13. doi: S0140-6736(07) 61687-0 [pii] doi: 10.1016/S0140-6736(07)61687-0 PMID: 17993365.
4. Ang F, Wong AP, Ng MM, Chu JJ. Small interference RNA profiling reveals the essential role of human membrane trafficking genes in mediating the infectious entry of dengue virus. Virol J. 2010; 7:24. Epub 2010/02/04. doi: 1743-422X-7-24 [pii] doi: 10.1186/1743-422X-7-24 PMID: 20122152.
5. Peng T, Wang JL, Chen W, Zhang JL, Gao N, Chen ZT, et al. Entry of dengue virus serotype 2 into ECV304 cells depends on clathrin-dependent endocytosis, but not on caveolae-dependent endocytosis. Can J Microbiol. 2009; 55(2):139–45. Epub 2009/03/20. doi: w08-107 [pii] doi: 10.1139/w08-107 PMID: 19295646.
6. Chen JP, Lu HL, Lai SL, Campanella GS, Sung JM, Lu MY, et al. Dengue virus induces expression of CXC chemokine ligand 10/IFN-gamma-inducible protein 10, which competitively inhibits viral binding to cell surface heparan sulfate. J Immunol. 2006; 177(5):3185–92. Epub 2006/08/22. doi: 177/5/3185 [pii]. PMID: 16920957.
7. Lin YL, Lei HY, Lin YS, Yeh TM, Chen SH, Liu HS. Heparin inhibits dengue-2 virus infection of five human liver cell lines. Antiviral Res. 2002; 56(1):93–6. Epub 2002/09/27. doi: S0166354202000955 [pii]. PMID: 12323403.
8. Hung SL, Lee PL, Chen HW, Chen LK, Kao CL, King CC. Analysis of the steps involved in Dengue virus entry into host cells. Virology. 1999; 257(1):156–67. Epub 1999/04/20. doi: S0042-6822(99) 99633-2 [pii] doi: 10.1006/viro.1999.9633 PMID: 10208929.
9. Chen Y, Maguire T, Hileman RE, Fromm JR, Esko JD, Linhardt RJ, et al. Dengue virus infectivity depends on envelope protein binding to target cell heparan sulfate. Nat Med. 1997; 3(8):866–71. Epub 1997/08/01. PMID: 9256277.
10. Germi R, Crance JM, Garin D, Guimet J, Lortat-Jacob H, Ruigrok RW, et al. Heparan sulfate-mediated binding of infectious dengue virus type 2 and yellow fever virus. Virology. 2002; 292(1):162–8. Epub 2002/03/07. doi: 10.1006/viro.2001.1232 S0042682201912322 [pii]. PMID: 11878919.
11. Reyes-Del Valle J, Chavez-Salinas S, Medina F, Del Angel RM. Heat shock protein 90 and heat shock protein 70 are components of dengue virus receptor complex in human cells. J Virol. 2005; 79(8):4557–67. Epub 2005/03/30. doi: 79/8/4557 [pii] doi: 10.1128/JVI.79.8.4557–4567.2005 PMID: 15795242.
12. Jindadamrongwech S, Thepparit C, Smith DR. Identification of GRP 78 (BiP) as a liver cell expressed receptor element for dengue virus serotype 2. Arch Virol. 2004; 149(5):915–27. Epub 2004/04/21. doi: 10.1007/s00705-003-0263-x PMID: 15098107.
13. Lozach PY, Burleigh L, Staropoli I, Navarro-Sanchez E, Harriague J, Virelizier JL, et al. Dendritic cell-specific intercellular adhesion molecule 3-grabbing non-integrin (DC-SIGN)-mediated enhancement of dengue virus infection is independent of DC-SIGN internalization signals. J Biol Chem. 2005; 280 (25):23698–708. Epub 2005/04/28. doi: M504337200 [pii] doi: 10.1074/jbc.M504337200 PMID: 15855154.
14. Navarro-Sanchez E, Altmeyer R, Amara A, Schwartz O, Fieschi F, Virelizier JL, et al. Dendritic-cell-specific ICAM3-grabbing non-integrin is essential for the productive infection of human dendritic cells by mosquito-cell-derived dengue viruses. EMBO Rep. 2003; 4(7):723–8. Epub 2003/06/05. doi: 10.1038/sj.embor.embor866 embor866 [pii]. PMID: 12783086.
15. Tassaneetrithep B, Burgess TH, Granelli-Piperno A, Trumpfheller C, Finke J, Sun W, et al. DC-SIGN (CD209) mediates dengue virus infection of human dendritic cells. J Exp Med. 2003; 197(7):823–9. Epub 2003/04/12. doi: 10.1084/jem.20021840 jem.20021840 [pii]. PMID: 12682107.
16. van der Schaar HM, Rust MJ, Chen C, van der Ende-Metselaar H, Wilschut J, Zhuang X, et al. Dissecting the cell entry pathway of dengue virus by single-particle tracking in living cells. PLoS Pathog. 2008; 4(12):e1000244. Epub 2008/12/20. doi: 10.1371/journal.ppat.1000244 PMID: 19096510.
17. Modis Y, Ogata S, Clements D, Harrison SC. Structure of the dengue virus envelope protein after membrane fusion. Nature. 2004; 427(6972):313–9. Epub 2004/01/23. doi: 10.1038/nature02165 nature02165 [pii]. PMID: 14737159.
18. Welsch S, Miller S, Romero-Brey I, Merz A, Bleck CK, Walther P, et al. Composition and three-dimensional architecture of the dengue virus replication and assembly sites. Cell Host Microbe. 2009; 5 (4):365–75. Epub 2009/04/22. doi: S1931-3128(09)00098-5 [pii] doi: 10.1016/j.chom.2009.03.007 PMID: 19380115.

19. Junjhon J, Pennington JG, Edwards TJ, Perera R, Lanman J, Kuhn RJ. Ultrastructural characterization and three-dimensional architecture of replication sites in dengue virus-infected mosquito cells. J Virol. 2014; 88(9):4687–97. Epub 2014/02/14. doi: JVI.00118-14 [pii] doi: 10.1128/JVI.00118-14 PMID: 24522909.

20. Apte-Sengupta S, Sirohi D, Kuhn RJ. Coupling of replication and assembly in flaviviruses. Curr Opin Virol. 2014; 9C:134–42. Epub 2014/12/03. doi: S1879-6257(14)00202-8 [pii] doi: 10.1016/j.coviro.2014.09.020 PMID: 25462445.

21. Mukhopadhyay S, Kuhn RJ, Rossmann MG. A structural perspective of the flavivirus life cycle. Nat Rev Microbiol. 2005; 3(1):13–22. Epub 2004/12/21. doi: nrmicro1067 [pii] doi: 10.1038/nrmicro1067 PMID: 15608696.

22. Krishnan MN, Ng A, Sukumaran B, Gilfoy FD, Uchil PD, Sultana H, et al. RNA interference screen for human genes associated with West Nile virus infection. Nature. 2008; 455(7210):242–5. Epub 2008/08/12. doi: nature07207 [pii] doi: 10.1038/nature07207 PMID: 18690214.

23. Sessions OM, Barrows NJ, Souza-Neto JA, Robinson TJ, Hershey CL, Rodgers MA, et al. Discovery of insect and human dengue virus host factors. Nature. 2009; 458(7241):1047–50. Epub 2009/04/28. doi: nature07967 [pii] doi: 10.1038/nature07967 PMID: 19396146.

24. Wang PG, Kudelko M, Lo J, Siu LY, Kwok KT, Sachse M, et al. Efficient assembly and secretion of recombinant subviral particles of the four dengue serotypes using native prM and E proteins. PLoS One. 2009; 4(12):e8325. Epub 2009/12/18. doi: 10.1371/journal.pone.0008325 PMID: 20016834.

25. Heaton NS, Perera R, Berger KL, Khadka S, Lacount DJ, Kuhn RJ, et al. Dengue virus nonstructural protein 3 redistributes fatty acid synthase to sites of viral replication and increases cellular fatty acid synthesis. Proc Natl Acad Sci U S A. 2010; 107(40):17345–50. Epub 2010/09/22. doi: 1010811107 [pii] doi: 10.1073/pnas.1010811107 PMID: 20855599.

26. Heaton NS, Randall G. Dengue virus-induced autophagy regulates lipid metabolism. Cell Host Microbe. 2011; 8(5):422–32. Epub 2010/11/16. doi: S1931-3128(10)00343-4 [pii] doi: 10.1016/j.chom.2010.10.006 PMID: 21075353.

27. Limjindaporn T, Wongwiwat W, Noisakran S, Srisawat C, Netsawang J, Puttikhunt C, et al. Interaction of dengue virus envelope protein with endoplasmic reticulum-resident chaperones facilitates dengue virus production. Biochem Biophys Res Commun. 2009; 379(2):196–200. Epub 2008/12/25. doi: S0006-291X(08)02402-9 [pii] doi: 10.1016/j.bbrc.2008.12.070 PMID: 19105951.

28. Noisakran S, Sengsai S, Thongboonkerd V, Kanlaya R, Sinchaikul S, Chen ST, et al. Identification of human hnRNP C1/C2 as a dengue virus NS1-interacting protein. Biochem Biophys Res Commun. 2008; 372(1):67–72. Epub 2008/05/13. doi: S0006-291X(08)00858-9 [pii] doi: 10.1016/j.bbrc.2008.04.165 PMID: 18471994.

29. Kanaseki T, Kadota K. The "vesicle in a basket". A morphological study of the coated vesicle isolated from the nerve endings of the guinea pig brain, with special reference to the mechanism of membrane movements. J Cell Biol. 1969; 42(1):202–20. Epub 1969/07/01. PMID: 4182372.

30. Nakatsu F, Hase K, Ohno H. The Role of the Clathrin Adaptor AP-1: Polarized Sorting and Beyond. Membranes (Basel). 2014; 4(4):747–63. Epub 2014/11/12. doi: membranes4040747 [pii] doi: 10.3390/membranes4040747 PMID: 25387275.

31. Ohno H, Fournier MC, Poy G, Bonifacino JS. Structural determinants of interaction of tyrosine-based sorting signals with the adaptor medium chains. J Biol Chem. 1996; 271(46):29009–15. Epub 1996/11/15. PMID: 8910552.

32. Ohno H, Stewart J, Fournier MC, Bosshart H, Rhee I, Miyatake S, et al. Interaction of tyrosine-based sorting signals with clathrin-associated proteins. Science. 1995; 269(5232):1872–5. Epub 1995/09/29. PMID: 7569928.

33. Owen DJ, Evans PR. A structural explanation for the recognition of tyrosine-based endocytotic signals. Science. 1998; 282(5392):1327–32. Epub 1998/11/13. PMID: 9812899.

34. Folsch H, Pypaert M, Maday S, Pelletier L, Mellman I. The AP-1A and AP-1B clathrin adaptor complexes define biochemically and functionally distinct membrane domains. J Cell Biol. 2003; 163(2):351–62. Epub 2003/10/29. doi: 10.1083/jcb.200309020 jcb.200309020 [pii]. PMID: 14581457.

35. Folsch H, Pypaert M, Schu P, Mellman I. Distribution and function of AP-1 clathrin adaptor complexes in polarized epithelial cells. J Cell Biol. 2001; 152(3):595–606. Epub 2001/02/07. PMID: 11157985.

36. Gan Y, McGraw TE, Rodriguez-Boulan E. The epithelial-specific adaptor AP1B mediates post-endocytic recycling to the basolateral membrane. Nat Cell Biol. 2002; 4(8):605–9. Epub 2002/07/10. doi: 10.1038/ncb827 ncb827 [pii]. PMID: 12105417.

37. Roeth JF, Williams M, Kasper MR, Filzen TM, Collins KL. HIV-1 Nef disrupts MHC-I trafficking by recruiting AP-1 to the MHC-I cytoplasmic tail. J Cell Biol. 2004; 167(5):903–13. Epub 2004/12/01. doi: jcb.200407031 [pii] doi: 10.1083/jcb.200407031 PMID: 15569716.

38. Agrawal T, Schu P, Medigeshi GR. Adaptor protein complexes-1 and 3 are involved at distinct stages of flavivirus life-cycle. Sci Rep. 2013; 3:1813. Epub 2013/05/10. doi: srep01813 [pii] doi: 10.1038/srep01813 PMID: 23657274.

39. Puttikhunt C, Kasinrerk W, Srisa-ad S, Duangchinda T, Silakate W, Moonsom S, et al. Production of anti-dengue NS1 monoclonal antibodies by DNA immunization. J Virol Methods. 2003; 109(1):55–61. Epub 2003/04/02. doi: S0166093403000454 [pii]. PMID: 12668268.

40. Henchal EA, McCown JM, Burke DS, Seguin MC, Brandt WE. Epitopic analysis of antigenic determinants on the surface of dengue-2 virions using monoclonal antibodies. Am J Trop Med Hyg. 1985; 34 (1):162–9. PMID: 2578750.

41. Henchal EA, Gentry MK, McCown JM, Brandt WE. Dengue virus-specific and flavivirus group determinants identified with monoclonal antibodies by indirect immunofluorescence. Am J Trop Med Hyg. 1982; 31(4):830–6. PMID: 6285749.

42. Duncan MC, Ho DG, Huang J, Jung ME, Payne GS. Composite synthetic lethal identification of membrane traffic inhibitors. Proc Natl Acad Sci U S A. 2007; 104(15):6235–40. Epub 2007/04/04. doi: 0607773104 [pii] doi: 10.1073/pnas.0607773104 PMID: 17404221.

43. Jirakanjanakit N, Sanohsomneing T, Yoksan S, Bhamarapravati N. The micro-focus reduction neutralization test for determining dengue and Japanese encephalitis neutralizing antibodies in volunteers vaccinated against dengue. Transactions of the Royal Society of Tropical Medicine and Hygiene. 1997; 91 (5):614–7. PMID: 9463684.

44. Towbin H, Staehelin T, Gordon J. Electrophoretic transfer of proteins from polyacrylamide gels to nitrocellulose sheets: procedure and some applications. Proc Natl Acad Sci U S A. 1979; 76(9):4350–4. Epub 1979/09/01. PMID: 388439.

45. Strober W. Trypan blue exclusion test of cell viability. Curr Protoc Immunol. 2001;Appendix 3:Appendix 3B. Epub 2008/04/25. doi: 10.1002/0471142735.ima03bs21 PMID: 18432654.

46. Livak KJ, Schmittgen TD. Analysis of relative gene expression data using real-time quantitative PCR and the 2(-Delta Delta C(T)) Method. Methods. 2001; 25(4):402–8. Epub 2002/02/16. doi: 10.1006/meth.2001.1262 S1046-2023(01)91262-9 [pii]. PMID: 11846609.

47. Sawasdee N, Junking M, Ngaojanlar P, Sukomon N, Ungsupravate D, Limjindaporn T, et al. Human kidney anion exchanger 1 interacts with adaptor-related protein complex 1 mu1A (AP-1 mu1A). Biochem Biophys Res Commun. 2010; 401(1):85–91. Epub 2010/09/14. doi: S0006-291X(10)01690-6 [pii] doi: 10.1016/j.bbrc.2010.09.015 PMID: 20833140.

48. Heaton NS, Randall G. Dengue virus and autophagy. Viruses. 2010; 3(8):1332–41. Epub 2011/10/14. doi: 10.3390/v3081332 viruses-03-01332 [pii]. PMID: 21994782.

49. Heaton NS, Randall G. Dengue virus-induced autophagy regulates lipid metabolism. Cell Host Microbe. 2010; 8(5):422–32. Epub 2010/11/16. doi: S1931-3128(10)00343-4 [pii] doi: 10.1016/j.chom.2010.10.006 PMID: 21075353.

50. Baust T, Czupalla C, Krause E, Bourel-Bonnet L, Hoflack B. Proteomic analysis of adaptor protein 1A coats selectively assembled on liposomes. Proc Natl Acad Sci U S A. 2006; 103(9):3159–64. Epub 2006/02/24. doi: 0511062103 [pii] doi: 10.1073/pnas.0511062103 PMID: 16492770.

51. Bonifacino JS, Traub LM. Signals for sorting of transmembrane proteins to endosomes and lysosomes. Annu Rev Biochem. 2003; 72:395–447. Epub 2003/03/26. doi: 10.1146/annurev.biochem.72.121801.161800 121801.161800 [pii]. PMID: 12651740.

52. Robinson MS. Adaptable adaptors for coated vesicles. Trends Cell Biol. 2004; 14(4):167–74. Epub 2004/04/07. doi: 10.1016/j.tcb.2004.02.002 S0962892404000492 [pii]. PMID: 15066634.

53. Dell'Angelica EC, Puertollano R, Mullins C, Aguilar RC, Vargas JD, Hartnell LM, et al. GGAs: a family of ADP ribosylation factor-binding proteins related to adaptors and associated with the Golgi complex. J Cell Biol. 2000; 149(1):81–94. Epub 2000/04/04. PMID: 10747089.

54. Ooi CE, Dell'Angelica EC, Bonifacino JS. ADP-Ribosylation factor 1 (ARF1) regulates recruitment of the AP-3 adaptor complex to membranes. J Cell Biol. 1998; 142(2):391–402. Epub 1998/07/29. PMID: 9679139.

55. Kudelko M, Brault JB, Kwok K, Li MY, Pardigon N, Peiris JS, et al. Class II ADP-ribosylation factors are required for efficient secretion of dengue viruses. J Biol Chem. 2012; 287(1):767–77. Epub 2011/11/23. doi: M111.270579 [pii] doi: 10.1074/jbc.M111.270579 PMID: 22105072.

56. Tang WC, Lin RJ, Liao CL, Lin YL. Rab18 facilitates dengue virus infection by targeting fatty acid synthase to sites of viral replication. J Virol. 2014; 88(12):6793–804. Epub 2014/04/04. doi: JVI.00045-14 [pii] doi: 10.1128/JVI.00045-14 PMID: 24696471.

57. Samsa MM, Mondotte JA, Iglesias NG, Assuncao-Miranda I, Barbosa-Lima G, Da Poian AT, et al. Dengue virus capsid protein usurps lipid droplets for viral particle formation. PLoS Pathog. 2009; 5(10): e1000632. Epub 2009/10/24. doi: 10.1371/journal.ppat.1000632 PMID: 19851456.

58. Hsu NY, Ilnytska O, Belov G, Santiana M, Chen YH, Takvorian PM, et al. Viral reorganization of the secretory pathway generates distinct organelles for RNA replication. Cell. 2010; 141(5):799–811. Epub 2010/06/01. doi: S0092-8674(10)00369-7 [pii] doi: 10.1016/j.cell.2010.03.050 PMID: 20510927.

59. Wang YJ, Wang J, Sun HQ, Martinez M, Sun YX, Macia E, et al. Phosphatidylinositol 4 phosphate regulates targeting of clathrin adaptor AP-1 complexes to the Golgi. Cell. 2003; 114(3):299–310. Epub 2003/08/14. doi: S0092867403006032 [pii]. PMID: 12914695.

60. Berger KL, Cooper JD, Heaton NS, Yoon R, Oakland TE, Jordan TX, et al. Roles for endocytic trafficking and phosphatidylinositol 4-kinase III alpha in hepatitis C virus replication. Proc Natl Acad Sci U S A. 2009; 106(18):7577–82. Epub 2009/04/21. doi: 0902693106 [pii] doi: 10.1073/pnas.0902693106 PMID: 19376974.

61. Lee YR, Lei HY, Liu MT, Wang JR, Chen SH, Jiang-Shieh YF, et al. Autophagic machinery activated by dengue virus enhances virus replication. Virology. 2008; 374(2):240–8. Epub 2008/03/21. doi: S0042-6822(08)00112-8 [pii] doi: 10.1016/j.virol.2008.02.016 PMID: 18353420.

62. Lee YR, Hu HY, Kuo SH, Lei HY, Lin YS, Yeh TM, et al. Dengue virus infection induces autophagy: an in vivo study. J Biomed Sci. 2013; 20:65. Epub 2013/09/10. doi: 1423-0127-20-65 [pii] doi: 10.1186/1423-0127-20-65 PMID: 24011333.

63. Khakpoor A, Panyasrivanit M, Wikan N, Smith DR. A role for autophagolysosomes in dengue virus 3 production in HepG2 cells. J Gen Virol. 2009; 90(Pt 5):1093–103. Epub 2009/03/07. doi: vir.0.007914–0 [pii] doi: 10.1099/vir.0.007914–0 PMID: 19264601.

64. Guo Y, Chang C, Huang R, Liu B, Bao L, Liu W. AP1 is essential for generation of autophagosomes from the trans-Golgi network. J Cell Sci. 2012; 125(Pt 7):1706–15. Epub 2012/02/14. doi: jcs.093203 [pii] doi: 10.1242/jcs.093203 PMID: 22328508.

Antiviral Research 124 (2015) 83–92

Contents lists available at ScienceDirect

Antiviral Research

journal homepage: www.elsevier.com/locate/antiviral

Inhibition of dengue virus production and cytokine/chemokine expression by ribavirin and compound A

Thidarath Rattanaburee [a, b], Mutita Junking [a], Aussara Panya [a, c], Nunghathai Sawasdee [a], Pucharee Songprakhon [a], Aroonroong Suttitheptumrong [a], Thawornchai Limjindaporn [d], Guy Haegeman [a], Pa-thai Yenchitsomanus [a, *]

[a] Division of Molecular Medicine, Department of Research and Development, Faculty of Medicine Siriraj Hospital, Mahidol University, Bangkok 10700, Thailand
[b] Graduate Program in Immunology, Department of Immunology, Faculty of Medicine Siriraj Hospital, Mahidol University, Bangkok 10700, Thailand
[c] Graduate Program in Biochemistry, Department of Biochemistry, Faculty of Medicine Siriraj Hospital, Mahidol University, Bangkok 10700, Thailand
[d] Department of Anatomy, Faculty of Medicine Siriraj Hospital, Mahidol University, Bangkok 10700, Thailand

ARTICLE INFO

Article history:
Received 6 July 2015
Received in revised form
3 October 2015
Accepted 5 October 2015
Available online 2 November 2015

Keywords:
Dengue virus
Compound A
Ribavirin
Cytokine
Chemokine

ABSTRACT

Dengue virus (DENV) infection is a worldwide public health problem with an increasing magnitude. The severity of disease in the patients with DENV infection correlates with high viral load and massive cytokine production – the condition referred to as "cytokine storm". Thus, concurrent inhibition of DENV and cytokine production should be more effective for treatment of DENV infection. In this study, we investigated the effects of the antiviral agent – ribavirin (RV), and the anti-inflammatory compound – compound A (CpdA), individually or in combination, on DENV production and cytokine/chemokine transcription in human lung epithelial carcinoma (A549) cells infected with DENV. Initially, the cells infected with DENV serotype 2 (DENV2) was studied. The results showed that treatment of DENV-infected cells with RV could significantly reduce both DENV production and cytokine (IL-6 and TNF-α) and chemokine (IP-10 and RANTES) transcription while treatment of DENV-infected cells with CpdA could significantly reduce cytokine (IL-6 and TNF-α) and chemokine (RANTES) transcription. Combined RV and CpdA treatment of the infected cells showed greater reduction of DENV production and cytokine/chemokine transcription. Similar results of this combined treatment were observed for infection with any one of the four DENV (DENV1, 2, 3, and 4) serotypes. These results indicate that combination of the antiviral agent and the anti-inflammatory compound offers a greater efficiency in reduction of DENV and cytokine/chemokine production, providing a new therapeutic approach for DENV infection.

1. Introduction

Dengue virus (DENV) infection, a mosquito-borne viral disease, is a major public health problem worldwide (Gubler, 2011; Halstead, 2007). DENV is transmitted by *Aedes aegypti* and *Aedes albopictus* mosquitoes, which are widespread in the tropical and subtropical regions (Bhatt et al., 2013; Kyle and Harris, 2008). Approximately 390 million people worldwide are at risk for DENV infection (Bhatt et al., 2013) with 500,000 dengue hemorrhagic fever (DHF) cases and more than 22,000 deaths each year (Gubler, 2002; Murray et al., 2013; Shepard et al., 2011). DENV is a member of *Flaviviridae* family and *Flavivirus* genus; its genome is a single positive-strand RNA with approximately 10.6 kilobases (Qi et al., 2008). It consists of four antigenically related serotypes, DENV 1, DENV 2, DENV 3, and DENV 4 (Blok, 1985).

The clinical manifestations of DENV infection range from asymptomatic or undifferentiated febrile illness, dengue fever (DF), dengue haemorrhagic fever (DHF), to dengue shock syndrome (DSS) (Simmons et al., 2012). Currently, there is neither licensed vaccine for prevention nor specific antiviral drug for treatment of DENV infection. Several studies have shown that severity of disease in the patients with DENV infection correlates with high viral load and host immune response, especially elevation of cytokines (Green and Rothman, 2006; Guilarde et al., 2008; Tricou et al., 2011; Vaughn et al., 2000, 1997). In the severe forms of DENV infection,

* Corresponding author.
E-mail addresses: pathai.yen@mahidol.ac.th, ptyench@gmail.com (P.-t. Yenchitsomanus).

http://dx.doi.org/10.1016/j.antiviral.2015.10.005
0166-3542/

DHF/DSS, there are marked increases of pro-inflammatory cytokines, immunosuppressive cytokines, and chemokines such as IL-6, IP-10, RANTES, TNF-α, and IFN-γ (Castro et al., 2011; Malavige et al., 2012; Nguyen et al., 2004; Rathakrishnan et al., 2012; Restrepo et al., 2008; Suharti et al., 2003). The correlation between severity of DENV infection and high viral titer as well as extreme cytokine production – the condition referred to as "cytokine storm" prompts us to hypothesize that concurrent inhibition of DENV and cytokine production should be more effective for treatment of DENV infection. Thus, the use of combined antiviral and anti-inflammation drugs or a single drug with both effects is a promising therapeutic strategy for DENV infection.

An antiviral drug, ribavirin (RV), has been used for treatment of hepatitis C virus (HCV) infection (Abdel-Hady et al., 2014; Bansal et al., 2015) and in experimental studies with flaviviruses including DENV (Diamond et al., 2002; Lee et al., 2012; Takhampunya et al., 2006), suggesting potential for use in combinations against other flaviviruses such as DENV. Combination of RV with α-glucosidase inhibitor efficiently inhibited DENV infection of cultured human cells (Chang et al., 2011). As anti-inflammatory drug, dexamethasone (DEX) – a synthetic glucocorticoid, was tested for its modulation in DENV infection, showing optimistic results in both decreasing cell infection rates and inhibiting TNF-α, IFN-α and IL-10 production (Reis et al., 2007). However, the use of the glucocorticoid for treatment of DENV infection is controversial because of its efficacy and side effects (Halvorsen et al., 2003; Heimdal et al., 1992; Vardy et al., 2006). Our group has recently reported the results of *in vitro* studies using compound A (CpdA) as anti-inflammatory compound in DENV infection (Khunchai et al., 2015; Suttitheptumrong et al., 2013). CpdA is a plant-derived phenyl aziridine precursor extracted from *Salsola tuberculatiformis* Botschantzev, a Namibian shrub (De Bosscher et al., 2005; Louw and Swart, 1999; Louw et al., 1997), that contains an anti-inflammatory effect and acts as a dissociated non-steroidal glucocorticoid receptor modulator. CpdA has been studied in inflammatory diseases such as rheumatoid arthritis (Dewint et al., 2008; Gossye et al., 2009; Rauch et al., 2011) and multiple sclerosis (Wust et al., 2009). Our recent study showed that CpdA reduced DENV-induced cytokine secretion and DENV production in the infected human hepatocellular carcinoma (HepG2) cell line (Suttitheptumrong et al., 2013). CpdA reduced inflammatory cytokines via inhibition of NF-κB transcriptional factors (Gossye et al., 2009; Rauch et al., 2011; Reber et al., 2012). We also demonstrated that CpdA, which acts as an NF-κB inhibitor, could suppress RANTES in DENV-infected human embryonic kidney cells (Khunchai et al., 2015).

In this study, we investigated the effects of the antiviral drug (RV) and the anti-inflammatory compound (CpdA), individually and in combination, on DENV production and cytokine transcription in human lung epithelial carcinoma (A549) cells, which were primarily infected with DENV2. The effects of combined treatment were then observed for the infection with either DENV1, 2, 3 or 4. The results of our study indicate that combination of RV and CpdA offers greater effects on reduction of DENV and cytokine production, paving a new way for treatment of DENV infection.

2. Materials and methods

2.1. DENV propagation

DENV serotype 1 (DENV1) strain Hawaii, DENV serotype 2 (DENV2) strains 16681, DENV serotype 3 (DENV3) strains H87, and DENV serotype 4 (DENV4) strains H241 were propagated in C6/36 cells. The C6/36 cells were separately infected with each DENV serotype at a multiplicity of infection (MOI) of 0.1 in maintenance medium and incubated for 3 h at room temperature on a shaker. Subsequently, unbound viruses were removed and fresh maintenance medium was added. Then, the infected cells were incubated at 28 °C for 5–7 days or until cells showed cytopathic effect (CPE). The culture supernatant containing DENV was collected and stored at −70 °C until used.

2.2. Foci-forming unit assay (FFU)

The Vero cells were cultured with ten-fold dilutions of DENV and incubated at 37 °C, 5% CO_2 for 2 h. After virus absorption, overlay medium was added and incubated for 3 days. The overlay media was removed and the infected cells were saved. Cells were fixed with formaldehyde/PBS and permeabilized with 0.2% Triton-X100/PBS for 15 min. Infected cells containing DENV antigen were identified by incubation with mouse monoclonal anti-DENV-E protein (4G2) antibody followed by HRP-conjugated rabbit anti-mouse IgG for 60 min (Dako, Denmark) and then stained with DAB (3,3′-diaminobenzidine) substrate solution. The foci-forming units were counted under light microscope.

2.3. A549 cell culture

The A549 cells were maintained in Dulbecco's modified Eagle's medium (DMEM) (GIBCO BRL, USA), supplemented with 10% fetal bovine serum (FBS, GIBCO, USA), 36 μg/ml penicillin G (Sigma, USA), 60 μg/ml streptomycin (Sigma, USA), 2 mM L-glutamine (Sigma, USA), 1 mM non-essential amino acids (GIBCO BRL, Invitrogen, USA), and 1 mM sodium pyruvate (Sigma, USA), at 37 °C on a humidified atmosphere with 5% CO_2.

2.4. DENV infection and compound treatment

DENV1-4 serotypes were prepared in 2% DMEM and then taken to infect in A549 cells at MOI 5. The A549 cells without DENV infection were used as mock control. After absorption onto the cells, unbound DENV was removed. After 24 h post-infection, the infected cells were treated individually or in combination with RV (Sigma, USA) dissolved in PBS, CpdA [Laboratory of Eukaryotic Gene Expression & Signal Transduction (LEGEST), Department of Physiology, Ghent University, Belgium] dissolved in PBS, or DEX (Sigma, USA) dissolved in DMSO at concentrations as indicated in the experiments, which was then added into 2% DMEM for 24 h. The supernatant were then collected to determine DENV production by the FFU assay. The treated A549 cells were collected to measure cytokine transcription by real-time PCR method.

2.5. Real time reverse transcription-polymerase chain reaction (RT-PCR)

To examine cytokine/chemokine transcription, total RNA was prepared from mock and DENV-infected cells, with or without treatment as indicated, by using Trizol™ reagent (Invitrogen, New Zealand), following the manufacturer's procedure. Cytokine/chemokine mRNA was quantified by real-time RT-PCR technique using specific primers (Table 1). cDNA was synthesized using Superscript®III reverse transcriptase (Invitrogen, New Zealand). The cDNA synthesis was performed by following the manufacturer's guidelines. Amplification of cDNA by real-time PCR was carried out in a reaction mixture (Roche, Germany). The real-time PCR profile

Table 1
Sequences of primers for cytokine transcription study.

Primer	Orientation	Sequence (5′-3′)
IP-10_F	Forward	GAATCGAAGGCCATCAAGAA
IP-10_R	Reverse	AAGCAGGGTCAGAACATCCA
RANTES_F	Forward	TCCTGCAGAGGATCAAGACA
RANTES_R	Reverse	TCCTGCAGAGGATCAAGACA
IL-6_F	Forward	GTACATCCTCGACGGCATC
IL-6_R	Reverse	AGCCACTGGTTCTGTGCCT
TNF-α_F	Forward	TGCTTGTTCCTCAGCCTCTT
TNF-α_R	Reverse	ATGGGCTACAGGCTTGTCACT
GAPDH_F	Forward	CGACCACTTTGTCAAGCTCA
GAPDH_R	Reverse	AGGGGTCTACATGGCAACTG

was set for: (i) pre-incubation at 95 °C for 5 min; (ii) PCR for 35 cycles (consisting of 95 °C for 10 s, 60 °C for 10, and 72 °C for 20 s, per cycle); (iii) melting curve analysis. The relative mRNA expression was normalized against GAPDH mRNA level by using a comparative Ct (delta delta Ct) method.

2.6. Calculation of additive and synergistic effects

The combinatory effects of RV and CpdA on DENV production and cytokine transcription were calculated by comparing theoretically additive effect with combinatory effect of two agents according to the fractional product method (Webb, 1961). The formula is as follows:

$$\text{Theoretically additive (or predicted) effect} = (\text{fu})_{\text{RV}} \times (\text{fu})_{\text{CpdA}}$$

$(\text{fu})_{\text{RV}}$ = fractional unaffected or the result from experiment with RV treatment alone.
$(\text{fu})_{\text{CpdA}}$ = fractional unaffected or the result from experiment with CpdA treatment alone.

Combinatory (or actual) effect = fractional unaffected or the result from experiment with combined treatment.

The result of theoretically additive effect and combinatory effect were plotted to compare and evaluate the combined effect. Additive effect was assigned when the theoretically additive effect was found to be equal to the combinatory effect. Synergistic effect was assigned when the combinatory reduction was found to be greater than the theoretically additive reduction.

2.7. Enzyme-linked immunosorbent assay (ELISA)

The level of IP-10 and RANTES production were measured in the supernatant collected from RV and CpdA treated DENV2 infected A549 cells by ELISA (R&D Systems) by following the manufacturer's instruction.

2.8. Statistical analysis

Statistical analyses were conducted by using Graph-Pad Prism 6 Software (GraphPad Software, Inc.). Mean and standard error of mean (SEM) from three independent experiments were calculated. The difference in experimental results was analyzed by one-way ANOVA, followed by Tukey's *pos hoc* test. A p-value less than 0.05 were considered statistically significant.

3. Results

3.1. RV and CpdA reduced DENV production and cytokine/chemokine transcription in DENV2-infected A549 cells

Initially, the experiments were conducted by using DENV2. Cell viability in each condition was more than 90% (Fig. 1A) and the infection efficiency was examined by flow cytometry (Fig. 1S). The supernatant was collected to determine DENV production by the FFU assay. The mRNA levels of IL-6, TNF-α, IP-10, and RANTES were determined by real-time RT-PCR method.

The anti-viral drug (RV) reduced DENV2 production in dose dependent manner (Fig. 1B) when compared to untreated, PBS-treated or DMSO-treated controls, while DENV2 production was not significantly reduced by treatment with either CpdA at 5, 10, or 20 μM ($p > 0.99$, $p = 0.98$, and $p = 0.52$, respectively) or DEX at 50 μM ($p = 0.90$). Treatment of DENV2-infected cells with RV decreased the transcription of IL-6 (Fig. 1C), TNF-α (Fig. 1D), IP-10 (Fig. 1E) and RANTES (Fig. 1F), when compared to that of PBS-treated. CpdA at 20 μM reduced cytokine/chemokine transcription in DENV2-infected cells (Fig. 1C, D, and F), although IP-10 (Fig. 1E) mRNA level reduction was not statistically significant ($p = 0.06$). DEX at 50 μM also reduced cytokine/chemokine transcription in DENV2-infected cells (Fig. 1C, D, and E), although RANTES (Fig. 1F) mRNA level reduction was not statistically significant ($p = 0.19$). Thus, individual treatment of DENV2-infected cells with RV reduced DENV production, and IL-6, TNF-α, IP-10, and RANTES transcription while CpdA reduced IL-6, TNF-α, and RANTES transcription but did not reduce DENV production and IP-10 transcription.

3.2. Combined treatments of RV and CpdA on DENV production and cytokine/chemokine transcription in DENV2-infected A549 cells

To investigate combined effects of RV and CpdA on DENV2 production and cytokine/chemokine transcription, RV and CpdA were tested with DENV2-infected A549 cells. The combined RV (at 50 and 100 μM) and CpdA (at 5, 10, and 20 μM) treatments to DENV2-infected A549 cells showed significant reduction of DENV2 production (Fig. 2B) when compared with that of individual treatments, with cell viability greater than 90% (Fig. 2A). The infection efficiency of DENV2-infected cells was examined by flow cytometry (Fig. 2S). Similarly, the combined RV and CpdA treatments also showed significant reduction of cytokine/chemokine transcription, including IL-6 (Fig. 2C), TNF-α (Fig. 2D), IP-10 (Fig. 2E), and RANTES (Fig. 2F), in the DENV2-infected A549 cells. The effect of combined RV and CpdA treatments on the reduction of DENV2 production and cytokine/chemokine transcription was greater than that of the individual treatments.

3.3. Individual and combined treatments of RV and CpdA reduced DENV production and cytokine/chemokine transcription in A549 cells infected with DENV1, DENV2, DENV3, or DENV4

To examine whether or not individual or combined RV and CpdA treatment could reduce virus production and cytokine/chemokine transcription in A549 cells infected with other DENV serotypes, A549 cells were infected with DENV1, DENV2, DENV3 or DENV4 at MOI 5. Then, the infected cells were incubated, individually or in combination, with RV at 50 μM and CpdA at 20 μM. The cell viabilities were more than 90% (Fig. 3A). The infection efficiency of DENV-infected were observed by flow cytometry (Fig. 3S).

The results showed that treatments of A549 cells infected

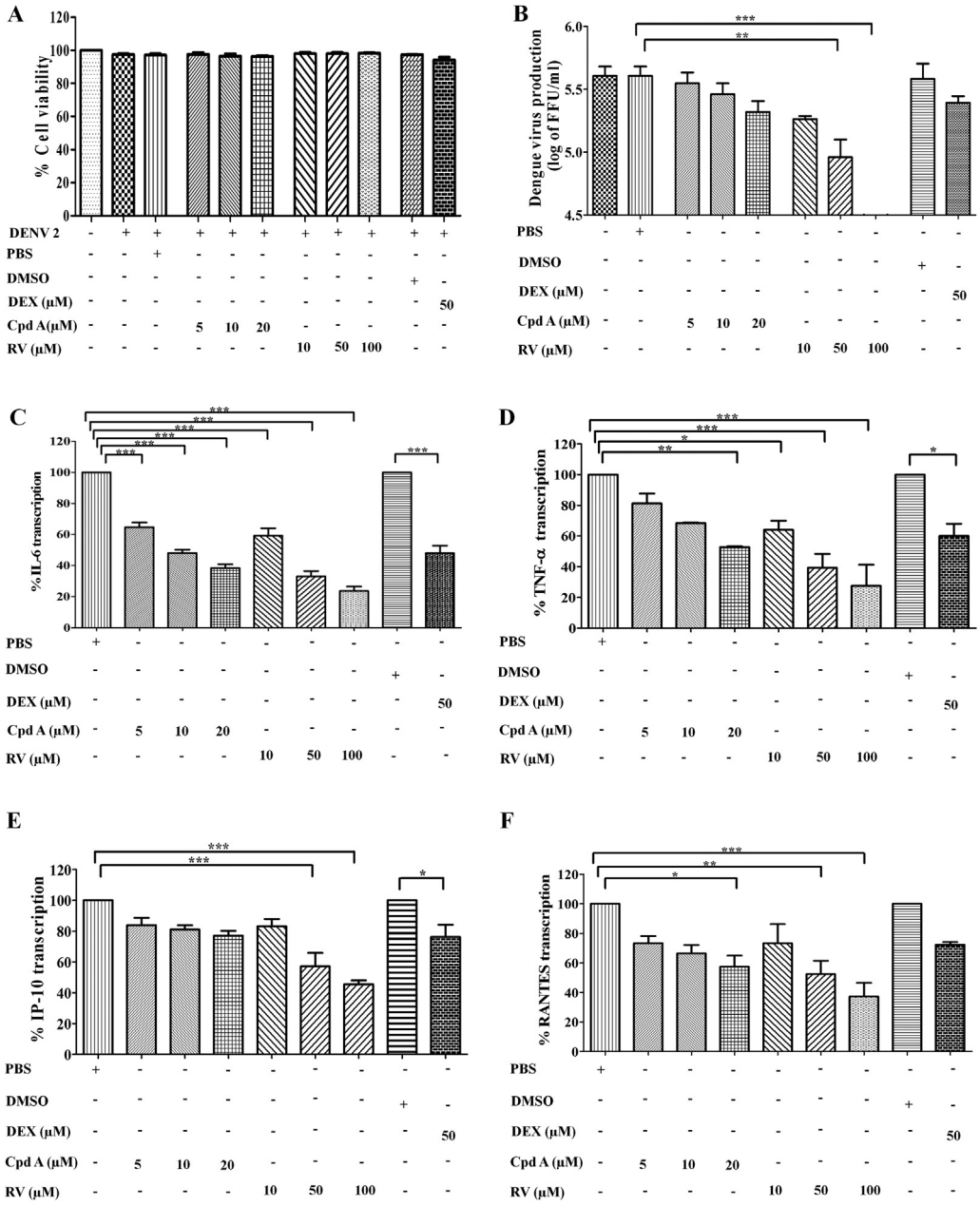

Fig. 1. Effects of ribavirin (RV) and compound A (CpdA) on DENV production and cytokine transcription. A549 cells were infected with DENV2 at MOI 5 and then individually treated with RV or CpdA. **(A)** Cell viability (presented as percentage) was determined by trypan blue exclusion assay of DENV2-infected A549 cells that were individually incubated with RV or CpdA at the indicated concentrations. **(B)** DENV production in cell culture supernatant analyzed by the foci-forming unit (FFU) assay. **(C–F)** Transcription of IL-6, TNF-α, IP-10, and RANTES in DENV2-infected A549 cells determined by real-time RT-PCR technique. The results were conducted in five independent experiments and mean ± SEM were calculated and plotted (* = $p < 0.05$, ** = $p < 0.01$, *** = $p < 0.001$).

with either DENV1, DENV2, DENV3 or DENV4 with combined RV at 50 μM and CpdA at 20 μM could significantly reduce DENV production for all DENV serotypes (Fig. 3B). Treatment of A549 cells infected with either DENV1, DENV2, DENV3 or DENV4 with combined RV at 50 μM and CpdA at 20 μM could also significantly reduce IL-6 (Fig. 3C), TNF-α (Fig. 3D), IP-10 (Fig. 3E), and RANTES (Fig. 3F) transcription.

The effects of combined RV and CpdA treatments on the reduction of DENV1, DENV2, DENV3, and DENV4 productions and cytokine/chemokine transcription were generally greater than that of individual treatments with RV at 50 μM.

3.4. Calculation of additive and synergistic effects of RV and CpdA

The combinatory effects of RV and CpdA on DENV production and cytokine/chemokine transcription were calculated by comparing the theoretically additive (or predicted) effects of RV and CpdA with the combinatory (or actual) effects of the two agents from the experiments by using fractional product method. The results of theoretically additive effect and combinatory effect were plotted (Fig. 4) to evaluate their combined effects. The effects of combined RV and CpdA treatments on DENV2 production and cytokine/chemokine transcription obtained from the

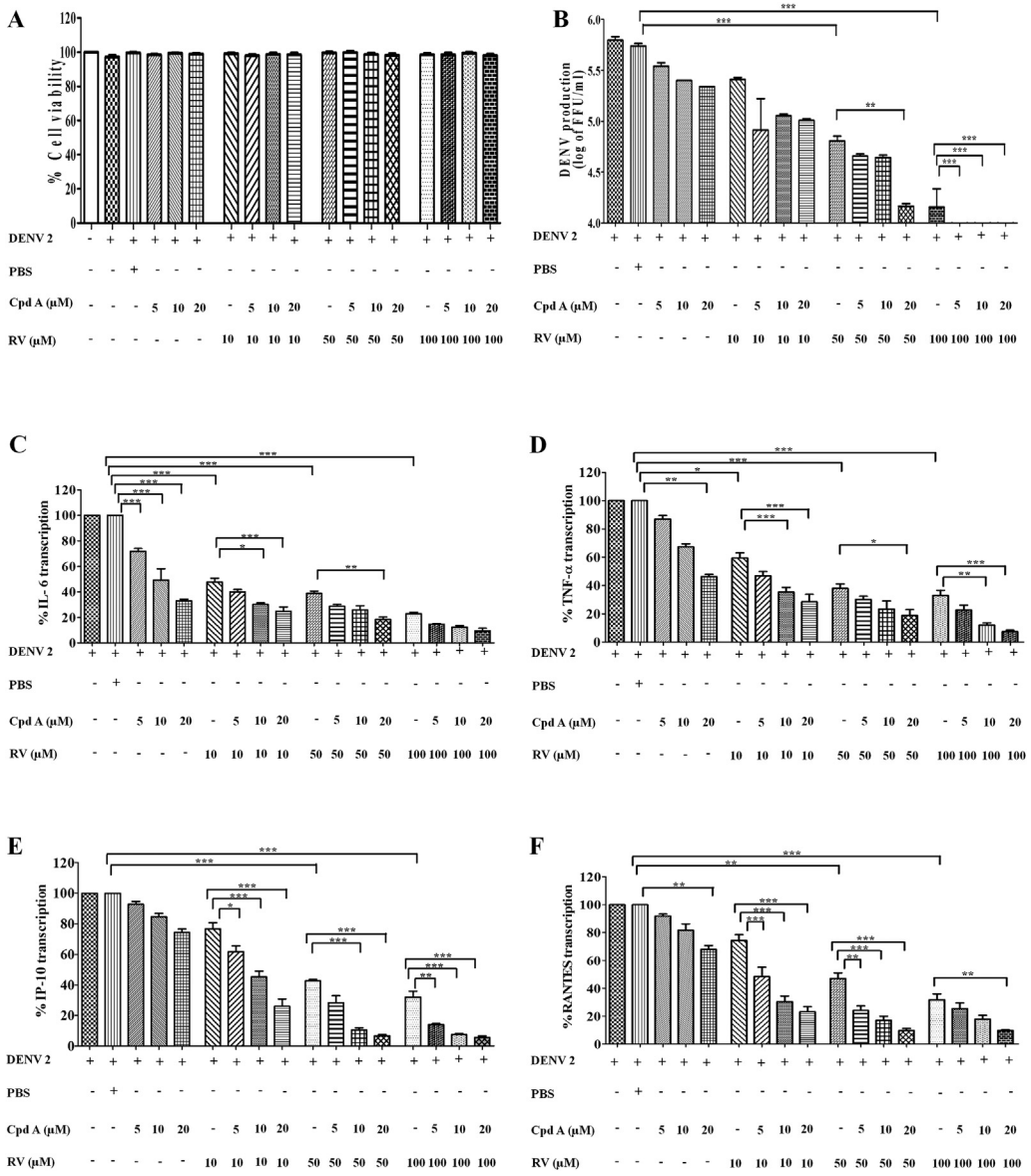

Fig. 2. Combined effects of ribavirin (RV) and compound A (CpdA) on DENV2 production and cytokine transcription. A549 cells were infected with DENV2 at a MOI 5 and subjected to individual or combined treatment with RV and CpdA. **(A)** Cell viability (presented as percentage) determined by the trypan blue exclusion assay of DENV2-infected A549 cells that were incubated with RV alone or in combination with CpdA at the indicated concentrations. **(B)** DENV production in cell culture supernatants analyzed by the foci forming unit (FFU) assay. **(C–F)** Transcription of IL-6, TNF-α, IP-10, and RANTES in DENV2-infected A549 cells determined by real-time RT-PCR technique. The results were conducted in five independent experiments and mean ± SEM were calculated and plotted (* = $p < 0.05$, ** = $p < 0.01$, *** = $p < 0.001$).

calculation for theoretically additive effect and combinatory effect were compared (Fig. 4A–E). It was found that combined RV and CpdA treatments on the DENV2-infected A549 cells resulted in the reduction of DENV2 production and cytokine (IL-6, and TNF-α) transcription in additive effect model, since the theoretical additive effects were equal to the combinatory effects (Fig. 4A–C). An effect in which two substances or actions used in combination produced a total effect on the DENV2-infected A549 cells led to the reduction of chemokine (IP-10 and RANTES) transcription in synergistic effect model, since synergistic effect was assigned when the combinatory effect was significantly more than expected for a theoretically additive effect (Fig. 4D and E).

The additive or synergistic effect model of combined treatments was then evaluated by using fractional product method for four DENV serotypes. The results supported the previous finding that the combined RV and CpdA treatments of the A549 cells infected with either DENV1, DENV2, DENV3 or DENV4 resulted in the reduction of virus production (Fig. 5A) in additive model because the combinatory effects were not greater than the theoretically additive effect ($p = 0.34$, $p = 0.46$, $p = 0.85$, and $p = 0.17$, respectively). The additive effect was also observed with cytokine (IL-6 and TNF-α) transcription (Fig. 5B and C). In contrast, the combined RV and CpdA treatment of the A549 cells-infected with either DENV1, DENV2, DENV3 or DENV4 led to the reduction of chemokine (IP-10 and RANTES) transcription in the synergistic effect model (Fig. 5D and E). Thus, combined RV and CpdA treatment reduced virus production and cytokine/chemokine transcription in the A549 cells infected with any one of the 4 DENV serotypes. The combined treatment showed an additive effect on virus production

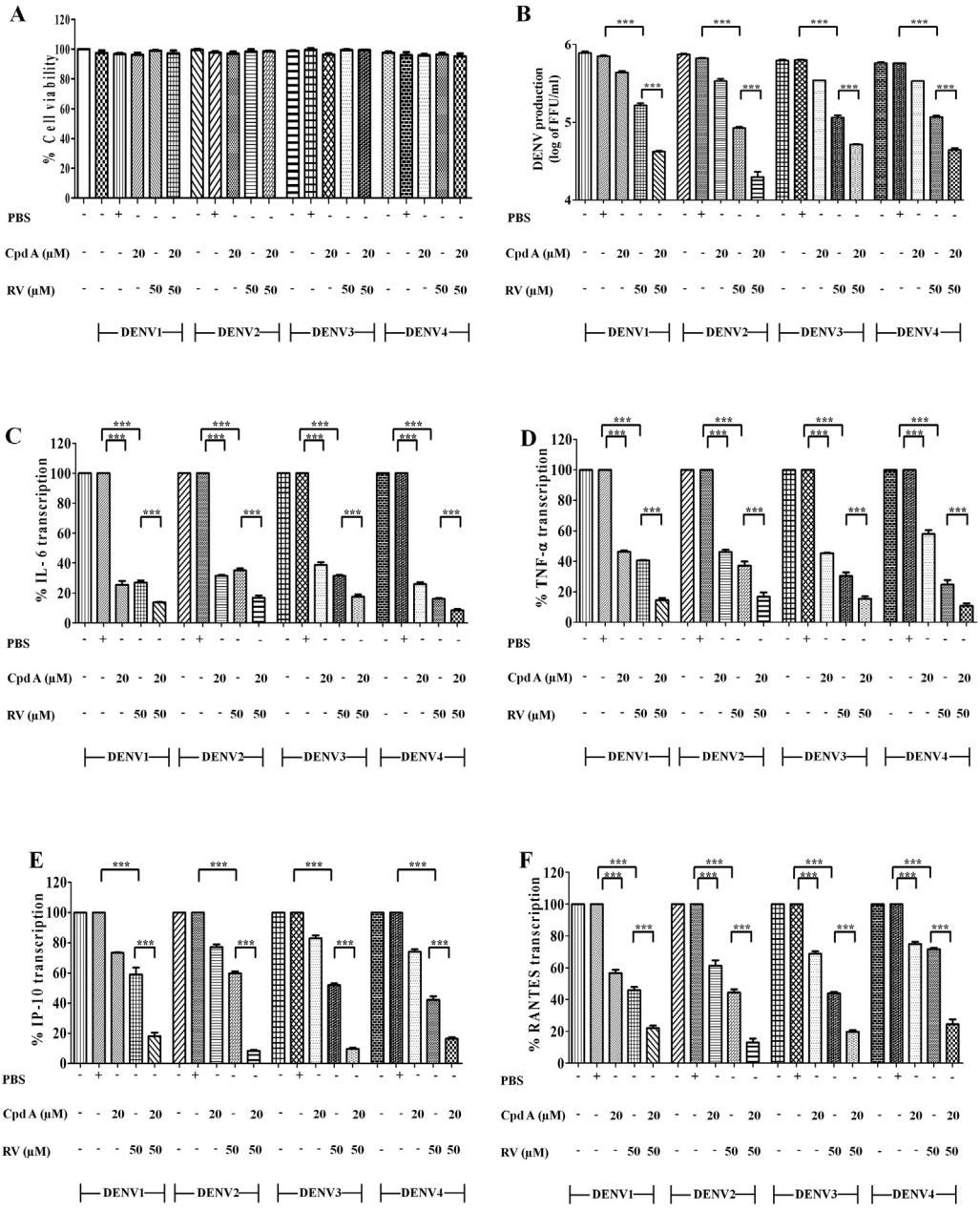

Fig. 3. Combined effects of ribavirin (RV) and compound A (CpdA) on DENV production and cytokine transcription in A549 cells infected with DENV serotypes 1, 2, 3, and 4. A549 cells were infected with each serotype of DENV at MOI 5 and then incubated with RV at 50 μM or CpdA at 20 μM or their combination. **(A)** Cell viability (presented as percentage) determined by the trypan blue exclusion assay of DENV-infected A549 cells that were incubated with RV or CpdA alone or their combination. **(B)** DENV production in cell culture supernatants analyzed by the foci-forming unit (FFU) assay. **(C–F)** Transcription of IL-6, TNF-α, IP-10, and RANTES in DENV-infected A549 cells determined by the real-time RT-PCR technique. The results were conducted in five independent experiments and mean ± SEM were calculated and plotted (* = $p < 0.05$, *** = $p < 0.001$).

and cytokine transcription but a synergistic effect on chemokine transcription.

Since the synergistic effect of the combined RV (50 μM) and CpdA (20 μM) on the DENV-infected A549 cells in the reduction of IP-10 and RANTES transcription was observed, the protein levels of IP-10 and RANTES in the supernatants of DENV2-infected A549 cells were determined by ELISA. As shown in Fig. 6, the protein levels of IP-10 (Fig. 6A) was reduced when treated with RV alone. The protein levels of RANTES (Fig. 6B) were not significantly reduced by RV alone ($p = 0.07$). Individual treatment of CpdA reduced IP-10 and RANTES proteins but did not reach significant levels ($p = 0.74$ and $p = 0.47$, respectively). The combined treatment of RV and CpdA significantly reduced IP-10 and RANTES protein levels, when compared with the result of either RV or CpdA treatment alone.

4. Discussion

We conducted the *in vitro* study by infecting A549 cells with DENV and treating the infected cells with the antiviral drug – ribavirin (RV) and anti-inflammatory compound – compound A (CpdA) for inhibition of DENV production and the cytokine/chemokine expression, respectively. The A549 cells were used in this study because they are susceptible to DENV infection and showed

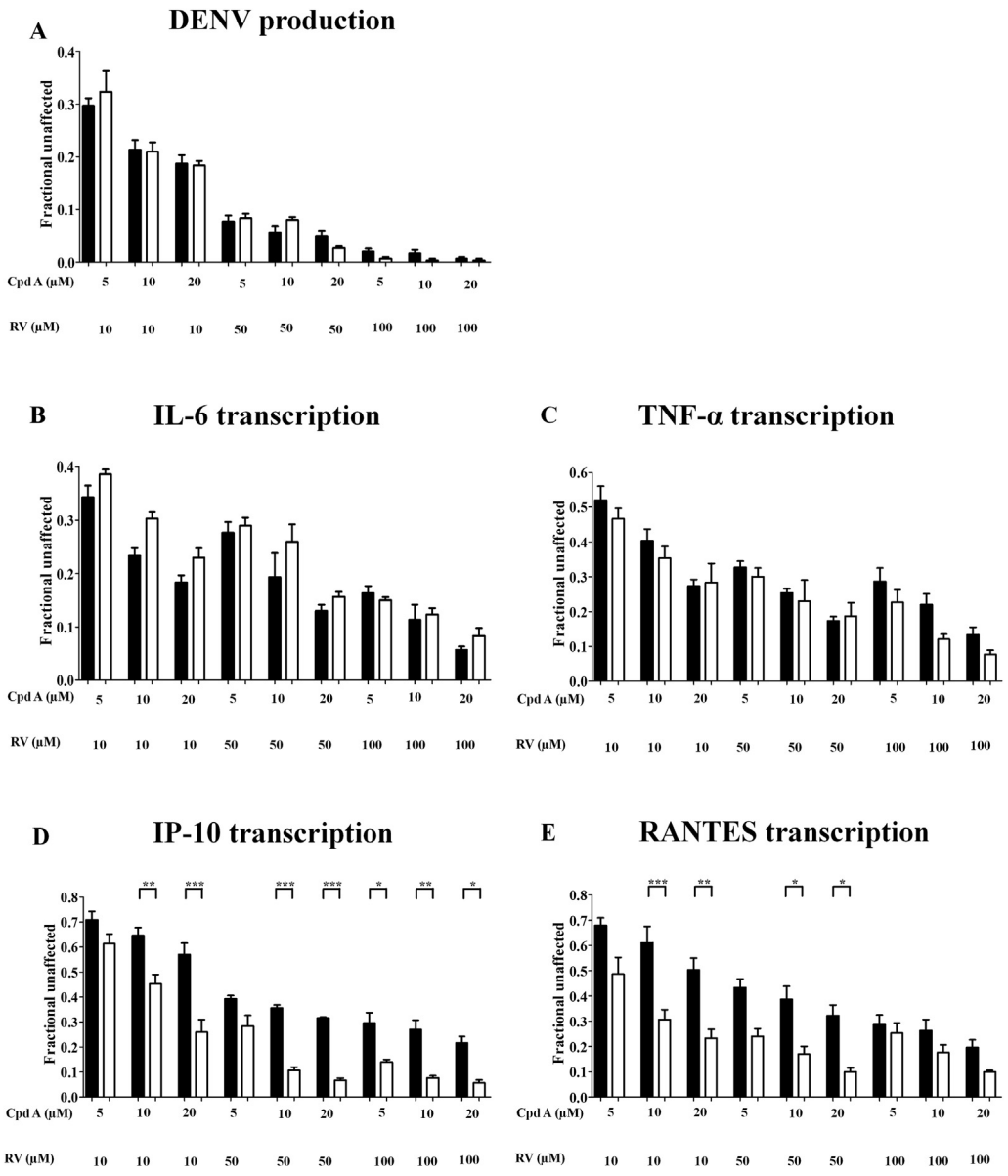

Fig. 4. Calculation of combinatorial effects of ribavirin (RV) and compound A (CpdA) together on DENV production and cytokine transcription. A549 cells were infected with DENV2 at MOI 5 and incubated with RV and CpdA as shown in Fig. 2. **(A)** DENV production, and **(B–E)** transcription of IL-6, TNF-α, IP-10, and RANTES, calculated by fractional product method. Black and white bars represented theoretical additive (or predicted) effects and combinatory (or actual) effects, respectively. The results were conducted in five independent experiments and plotted (* = $p < 0.05$, ** = $p < 0.01$, *** = $p < 0.001$).

the highest virus replication rate when compared to other cells (Yohan et al., 2014). Moreover, lung is a human organ affected by DENV infection (Povoa et al., 2014; Rodrigues et al., 2014). The antiviral drug, RV, is a broad antiviral agent that is currently used for treatment of HCV infection and has previously been reported to reduce DENV production in hepatoma cell lines (Diamond et al., 2002). Although it failed to inhibit DENV infection in AG129 mouse model (Schul et al., 2007), the combination between RV and glucosidase inhibitor enhanced the antiviral activity in this animal model in synergistic manner (Chang et al., 2011). The anti-inflammatory compound, CpdA, has recently been tested with DENV-infected HepG2 cells by our group (Suttitheptumrong et al., 2013), in which it was found to reduce cytokine (CXCL10 and TNFα) secretion and also DENV production. CpdA also suppressed RANTES production in DENV-infected HEK293 cells (Khunchai et al., 2015).

By using DENV2 at the beginning, we have shown in the present study that at the concentrations that did not affect A549 cell viability, RV could significantly reduce both DENV2 production and cytokine/chemokine (IL-6, TNF-α, IP-10 and RANTES) transcription (Fig. 1) while CpdA could significantly reduce cytokine/chemokine (IL-6, TNF-α, and RANTES) transcription but did not reduce DENV production and IP-10 transcription. Since RV could significantly reduce DENV production, which may subsequently lead to the reduction of cytokine/chemokine transcription in DENV infected cells. In addition to anti-DENV, RV may also have immune modification mechanisms. However, when it was combined with CpdA, DENV production could be greatly reduced. This indicates that, possibly in the initial phase of its infection, DENV may require cytokine/chemokine for activation of the cells to promote DENV replication.

The combination of RV and CpdA could even more

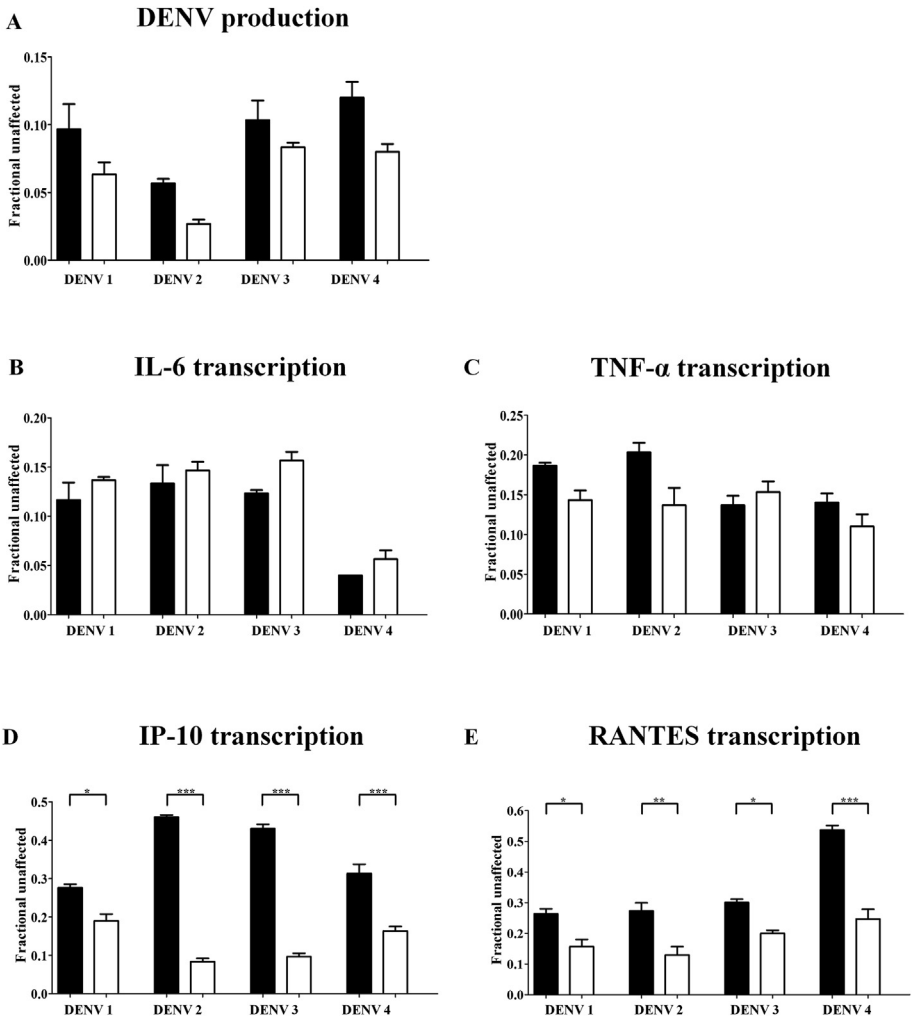

Fig. 5. Calculation of combinatorial effects of ribavirin (RV) and compound A (CpdA) together on DENV production and cytokine transcription in A549 cells infected by DENV serotype 1, 2, 3, and 4. A549 cells were infected with DENV serotypes 1, 2, 3, and 4 at MOI of 5 and incubated with combined of RV and CpdA as shown in Fig. 3. **(A)** DENV production, and **(B–E)** transcription of IL-6, TNF-α, IP-10, and RANTES, calculated by the fractional product method. Black and white bar represented theoretical additive (or predicted) effects and combinatory (or actual) effects respectively. The results were conducted in five independent experiments and plotted (* = $p < 0.05$, ** = $p < 0.01$, *** = $p < 0.001$).

significantly reduce DENV2 production and cytokine/chemokine transcription in dose-dependent manner, when it was compared with that of individual treatments to the DENV2-infected A549 cells (Fig. 2). This combined effect of RV and CpdA on the reduction of both virus production and cytokine/chemokine transcription in the infected A549 cells was not only observed for the infection with DENV2 but also for that with all four DENV serotypes (Fig. 3). Interestingly, the combined RV and CpdA treatment on the DENV2-infected A549 cells resulted in the reduction of viral production and cytokine (IL-6, and TNF-α) transcription in an additive effect model (Fig. 4A–C), whereas the same treatments caused the reduction of chemokine (IP-10 and RANTES) transcription in a synergistic effect model (Fig. 4D–4E). Additionally, similar findings were observed for the infection with all four DENV serotypes (Fig. 5). It has been known that TNF-α and IL-6 are pro-inflammatory cytokines, that promote systemic inflammatory response (Hernandez-Rodriguez et al., 2004), while IP-10 and RANTEs are chemokines that have the action to recruit immune cells to the site of infection, resulting in tissue damage (Agostini et al., 1998; Rathakrishnan et al., 2012; Sundstrom et al., 2001). These cytokines/chemokines were frequently investigated in the patients with severe DENV infection (Castro et al., 2011; Nguyen et al., 2004; Rathakrishnan et al., 2012; Restrepo et al., 2008; Suharti et al., 2003; Vennemann et al., 2012). The additive effect model of the combined RV and CpdA treatment on the reduction of DENV production and cytokine (IL-6, and TNF-α) transcription might result from the collective direct-inhibitory effects of RV and CpdA on the DENV-infected cells. However, the synergistic effect model of the combined RV and CpdA treatment on the reduction of chemokine (IP-10 and RANTES) transcription, and also resulting in the reduction of their protein levels, may be explained by the inhibition in two fold, from both direct-inhibitory effects of RV and CpdA, and also from the indirect inhibitory effect on the reduction of cytokine (IL-6, and TNF-α) expression that might in turn affect the reduction of chemokine. The transcription of chemokines (IP-10 and RANTES) is regulated by TNF-α (Ammit et al., 2002; Yeruva et al., 2008), which was also reduced by combined treatment of RV and CpdA. Taken together, the result of this study indicates that the combined treatment by anti-viral

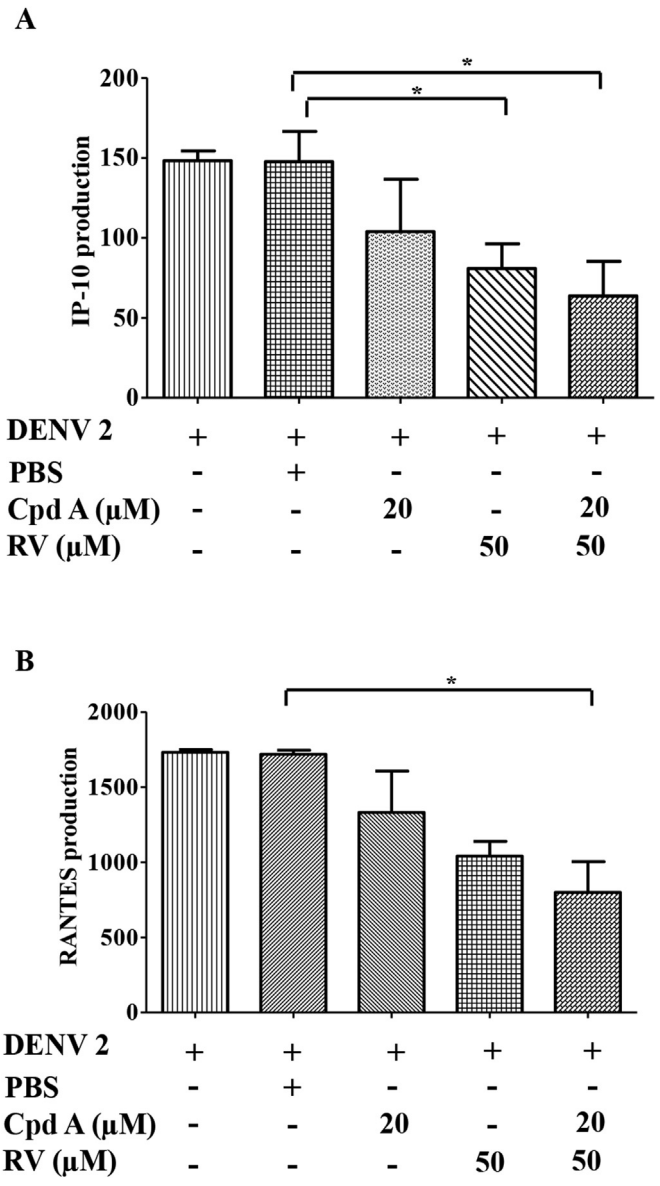

Fig. 6. Combined effects of RV and CpdA on IP-10 and RANTES protein production on DENV2 infected cells. A549 cells were infected with DENV2 at a MOI of 5 and incubated with RV at 50 μM, CpdA at 20 μM, and combinations of RV and CpdA for 24 h. Supernatants were collected and analyzed for **(A)** IP-10 and **(B)** RANTES protein production by ELISA (* = $p < 0.05$, ** = $p < 0.01$).

(RV) and anti-inflammatory (CpdA) agents offers a greater inhibitory effect on DENV production and host cytokine/chemokine transcription than the treatment by individual compound. Thus, the therapeutic approach using combined anti-viral and anti-inflammatory drugs for treatment of DENV infection is proposed, which merits further studies.

Conflict of interest

The authors declare that they have no conflict of interest.

Acknowledgments

This work was financially supported by Thailand Research Fund (TRF). TR was supported by Siriraj Graduate Scholarship, AP by TRF-Royal Golden Jubilee (RGJ) Ph.D. Scholarship, MJ, TL, and PY by Mahidol University and TRF, and GH by Faculty of Medicine Siriraj Hospital.

Appendix A. Supplementary data

Supplementary data related to this article can be found at http://dx.doi.org/10.1016/j.antiviral.2015.10.005.

References

Abdel-Hady, M., Bansal, S., Davison, S.M., Brown, M., Tizzard, S.A., Mulla, S., Barnes, E., Davies, P., Mieli-Vergani, G., Kelly, D.A., 2014. Treatment of chronic viral hepatitis C in children and adolescents: UK experience. Arch. Dis. Child. 99, 505–510.

Agostini, C., Cassatella, M., Zambello, R., Trentin, L., Gasperini, S., Perin, A., Piazza, F., Siviero, M., Facco, M., Dziejman, M., Chilosi, M., Qin, S., Luster, A.D., Semenzato, G., 1998. Involvement of the IP-10 chemokine in sarcoid granulomatous reactions. J. Immunol. 161, 6413–6420.

Ammit, A.J., Lazaar, A.L., Irani, C., O'Neill, G.M., Gordon, N.D., Amrani, Y., Penn, R.B., Panettieri Jr., R.A., 2002. Tumor necrosis factor-alpha-induced secretion of RANTES and interleukin-6 from human airway smooth muscle cells: modulation by glucocorticoids and beta-agonists. Am. J. Respir. Cell Mol. Biol. 26, 465–474.

Bansal, S., Singal, A.K., McGuire, B.M., Anand, B.S., 2015. Impact of all oral anti-hepatitis C virus therapy: a meta-analysis. World J. Hepatol. 7, 806–813.

Bhatt, S., Gething, P.W., Brady, O.J., Messina, J.P., Farlow, A.W., Moyes, C.L., Drake, J.M., Brownstein, J.S., Hoen, A.G., Sankoh, O., Myers, M.F., George, D.B., Jaenisch, T., Wint, G.R., Simmons, C.P., Scott, T.W., Farrar, J.J., Hay, S.I., 2013. The global distribution and burden of dengue. Nature 496, 504–507.

Blok, J., 1985. Genetic relationships of the dengue virus serotypes. J. Gen. Virol. 66 (Pt 6), 1323–1325.

Castro, J.E., Vado-Solis, I., Perez-Osorio, C., Fredeking, T.M., 2011. Modulation of cytokine and cytokine receptor/antagonist by treatment with doxycycline and tetracycline in patients with dengue fever. Clin. Dev. Immunol. 2011, 370872.

Chang, J., Schul, W., Butters, T.D., Yip, A., Liu, B., Goh, A., Lakshminarayana, S.B., Alonzi, D., Reinkensmeier, G., Pan, X., Qu, X., Weidner, J.M., Wang, L., Yu, W., Borune, N., Kinch, M.A., Rayahin, J.E., Moriarty, R., Xu, X., Shi, P.Y., Guo, J.T., Block, T.M., 2011. Combination of alpha-glucosidase inhibitor and ribavirin for the treatment of dengue virus infection in vitro and in vivo. Antivir. Res. 89, 26–34.

De Bosscher, K., Vanden Berghe, W., Beck, I.M., Van Molle, W., Hennuyer, N., Hapgood, J., Libert, C., Staels, B., Louw, A., Haegeman, G., 2005. A fully dissociated compound of plant origin for inflammatory gene repression. Proc. Natl. Acad. Sci. U. S. A. 102, 15827–15832.

Dewint, P., Gossye, V., De Bosscher, K., Vanden Berghe, W., Van Beneden, K., Deforce, D., Van Calenbergh, S., Muller-Ladner, U., Vander Cruyssen, B., Verbruggen, G., Haegeman, G., Elewaut, D., 2008. A plant-derived ligand favoring monomeric glucocorticoid receptor conformation with impaired transactivation potential attenuates collagen-induced arthritis. J. Immunol. 180, 2608–2615.

Diamond, M.S., Zachariah, M., Harris, E., 2002. Mycophenolic acid inhibits dengue virus infection by preventing replication of viral RNA. Virology 304, 211–221.

Gossye, V., Elewaut, D., Bougarne, N., Bracke, D., Van Calenbergh, S., Haegeman, G., De Bosscher, K., 2009. Differential mechanism of NF-kappaB inhibition by two glucocorticoid receptor modulators in rheumatoid arthritis synovial fibroblasts. Arthritis Rheum. 60, 3241–3250.

Green, S., Rothman, A., 2006. Immunopathological mechanisms in dengue and dengue hemorrhagic fever. Curr. Opin. Infect. Dis. 19, 429–436.

Gubler, D.J., 2002. The global emergence/resurgence of arboviral diseases as public health problems. Arch. Med. Res. 33, 330–342.

Gubler, D.J., 2011. Dengue, urbanization and globalization: the unholy trinity of the 21(st) Century. Trop. Med. Health 39, 3–11.

Guilarde, A.O., Turchi, M.D., Siqueira Jr., J.B., Feres, V.C., Rocha, B., Levi, J.E., Souza, V.A., Boas, L.S., Pannuti, C.S., Martelli, C.M., 2008. Dengue and dengue hemorrhagic fever among adults: clinical outcomes related to viremia, serotypes, and antibody response. J. Infect. Dis. 197, 817–824.

Halstead, S.B., 2007. Dengue. Lancet 370, 1644–1652.

Halvorsen, P., Raeder, J., White, P.F., Almdahl, S.M., Nordstrand, K., Saatvedt, K., Veel, T., 2003. The effect of dexamethasone on side effects after coronary revascularization procedures. Anesth. Analg. 96, 1578–1583 (table of contents).

Heimdal, K., Hirschberg, H., Slettebo, H., Watne, K., Nome, O., 1992. High incidence of serious side effects of high-dose dexamethasone treatment in patients with epidural spinal cord compression. J. Neurooncol. 12, 141–144.

Hernandez-Rodriguez, J., Segarra, M., Vilardell, C., Sanchez, M., Garcia-Martinez, A., Esteban, M.J., Queralt, C., Grau, J.M., Urbano-Marquez, A., Palacin, A., Colomer, D., Cid, M.C., 2004. Tissue production of pro-inflammatory cytokines (IL-1beta, TNFalpha and IL-6) correlates with the intensity of the systemic inflammatory response and with corticosteroid requirements in giant-cell arteritis. Rheumatol. Oxf. 43, 294–301.

Khunchai, S., Junking, M., Suttitheptumrong, A., Kooptiwut, S., Haegeman, G., Limjindaporn, T., Yenchitsomanus, P.T., 2015. NF-kappaB is required for dengue virus NS5-induced RANTES expression. Virus Res. 197, 92–100.

Kyle, J.L., Harris, E., 2008. Global spread and persistence of dengue. Annu. Rev. Microbiol. 62, 71–92.
Lee, H.L., Phong, T.V., Rohani, A., 2012. Effects of ribavirin and hydroxyurea on oral infection of Aedes aegypti (L.) with dengue virus. Southeast Asian J. Trop. Med. Public Health 43, 1358–1364.
Louw, A., Swart, P., 1999. Salsola tuberculatiformis Botschantzev and an aziridine precursor analog mediate the in vivo increase in free corticosterone and decrease in corticosteroid-binding globulin in female Wistar rats. Endocrinology 140, 2044–2053.
Louw, A., Swart, P., de Kock, S.S., van der Merwe, K.J., 1997. Mechanism for the stabilization in vivo of the aziridine precursor –(4-acetoxyphenyl)-2-chloro-N-methyl-ethylammonium chloride by serum proteins. Biochem. Pharmacol. 53, 189–197.
Malavige, G.N., Huang, L.C., Salimi, M., Gomes, L., Jayaratne, S.D., Ogg, G.S., 2012. Cellular and cytokine correlates of severe dengue infection. PLoS One 7, e50387.
Murray, N.E., Quam, M.B., Wilder-Smith, A., 2013. Epidemiology of dengue: past, present and future prospects. Clin. Epidemiol. 5, 299–309.
Nguyen, T.H., Lei, H.Y., Nguyen, T.L., Lin, Y.S., Huang, K.J., Le, B.L., Lin, C.F., Yeh, T.M., Do, Q.H., Vu, T.Q., Chen, L.C., Huang, J.H., Lam, T.M., Liu, C.C., Halstead, S.B., 2004. Dengue hemorrhagic fever in infants: a study of clinical and cytokine profiles. J. Infect. Dis. 189, 221–232.
Povoa, T.F., Alves, A.M., Oliveira, C.A., Nuovo, G.J., Chagas, V.L., Paes, M.V., 2014. The pathology of severe dengue in multiple organs of human fatal cases: histopathology, ultrastructure and virus replication. PLoS One 9, e83386.
Qi, R.F., Zhang, L., Chi, C.W., 2008. Biological characteristics of dengue virus and potential targets for drug design. Acta Biochim. Biophys. Sin. Shanghai 40, 91–101.
Rathakrishnan, A., Wang, S.M., Hu, Y., Khan, A.M., Ponnampalavanar, S., Lum, L.C., Manikam, R., Sekaran, S.D., 2012. Cytokine expression profile of dengue patients at different phases of illness. PLoS One 7, e52215.
Rauch, A., Gossye, V., Bracke, D., Gevaert, E., Jacques, P., Van Beneden, K., Vandooren, B., Rauner, M., Hofbauer, L.C., Haegeman, G., Elewaut, D., Tuckermann, J.P., De Bosscher, K., 2011. An anti-inflammatory selective glucocorticoid receptor modulator preserves osteoblast differentiation. FASEB J. 25, 1323–1332.
Reber, L.L., Daubeuf, F., Plantinga, M., De Cauwer, L., Gerlo, S., Waelput, W., Van Calenbergh, S., Tavernier, J., Haegeman, G., Lambrecht, B.N., Frossard, N., De Bosscher, K., 2012. A dissociated glucocorticoid receptor modulator reduces airway hyperresponsiveness and inflammation in a mouse model of asthma. J. Immunol. 188, 3478–3487.
Reis, S.R., Sampaio, A.L., Henriques, M., Gandini, M., Azeredo, E.L., Kubelka, C.F., 2007. An in vitro model for dengue virus infection that exhibits human monocyte infection, multiple cytokine production and dexamethasone immunomodulation. Mem. Inst. Oswaldo Cruz 102, 983–990.
Restrepo, B.N., Isaza, D.M., Salazar, C.L., Ramirez, R., Ospina, M., Alvarez, L.G., 2008. Serum levels of interleukin-6, tumor necrosis factor-alpha and interferon-gamma in infants with and without dengue. Rev. Soc. Bras. Med. Trop. 41, 6–10.
Rodrigues, R.S., Brum, A.L., Paes, M.V., Povoa, T.F., Basilio-de-Oliveira, C.A., Marchiori, E., Borghi, D.P., Ramos, G.V., Bozza, F.A., 2014. Lung in dengue: computed tomography findings. PLoS One 9, e96313.
Schul, W., Liu, W., Xu, H.Y., Flamand, M., Vasudevan, S.G., 2007. A dengue fever viremia model in mice shows reduction in viral replication and suppression of the inflammatory response after treatment with antiviral drugs. J. Infect. Dis. 195, 665–674.
Shepard, D.S., Coudeville, L., Halasa, Y.A., Zambrano, B., Dayan, G.H., 2011. Economic impact of dengue illness in the Americas. Am. J. Trop. Med. Hyg. 84, 200–207.
Simmons, C.P., Farrar, J.J., Nguyen, V.V., Wills, B., 2012. Dengue. N. Engl. J. Med. 366, 1423–1432.
Suharti, C., van Gorp, E.C., Dolmans, W.M., Setiati, T.E., Hack, C.E., Djokomoeljanto, R., van der Meer, J.W., 2003. Cytokine patterns during dengue shock syndrome. Eur. Cytokine Netw. 14, 172–177.
Sundstrom, J.B., McMullan, L.K., Spiropoulou, C.F., Hooper, W.C., Ansari, A.A., Peters, C.J., Rollin, P.E., 2001. Hantavirus infection induces the expression of RANTES and IP-10 without causing increased permeability in human lung microvascular endothelial cells. J. Virol. 75, 6070–6085.
Suttitheptumrong, A., Khunchai, S., Panaampon, J., Yasamut, U., Morchang, A., Puttikhunt, C., Noisakran, S., Haegeman, G., Yenchitsomanus, P.T., Limjindaporn, T., 2013. Compound A, a dissociated glucocorticoid receptor modulator, reduces dengue virus-induced cytokine secretion and dengue virus production. Biochem. Biophys. Res. Commun. 436, 283–288.
Takhampunya, R., Ubol, S., Houng, H.S., Cameron, C.E., Padmanabhan, R., 2006. Inhibition of dengue virus replication by mycophenolic acid and ribavirin. J. Gen. Virol. 87, 1947–1952.
Tricou, V., Minh, N.N., Farrar, J., Tran, H.T., Simmons, C.P., 2011. Kinetics of viremia and NS1 antigenemia are shaped by immune status and virus serotype in adults with dengue. PLoS Negl. Trop. Dis. 5, e1309.
Vardy, J., Chiew, K.S., Galica, J., Pond, G.R., Tannock, I.F., 2006. Side effects associated with the use of dexamethasone for prophylaxis of delayed emesis after moderately emetogenic chemotherapy. Br. J. Cancer 94, 1011–1015.
Vaughn, D.W., Green, S., Kalayanarooj, S., Innis, B.L., Nimmannitya, S., Suntayakorn, S., Endy, T.P., Raengsakulrach, B., Rothman, A.L., Ennis, F.A., Nisalak, A., 2000. Dengue viremia titer, antibody response pattern, and virus serotype correlate with disease severity. J. Infect. Dis. 181, 2–9.
Vaughn, D.W., Green, S., Kalayanarooj, S., Innis, B.L., Nimmannitya, S., Suntayakorn, S., Rothman, A.L., Ennis, F.A., Nisalak, A., 1997. Dengue in the early febrile phase: viremia and antibody responses. J. Infect. Dis. 176, 322–330.
Vennemann, M.M., Loddenkotter, B., Fracasso, T., Mitchell, E.A., Debertin, A.S., Larsch, K.P., Sperhake, J.P., Brinkmann, B., Sauerland, C., Lindemann, M., Bajanowski, T., 2012. Cytokines and sudden infant death. Int. J. Legal Med. 126, 279–284.
Webb, J.L., 1961. Effect of more than one inhibitor. In: Enzyme and Metabolic Inhibitors. Academic Press, New York.
Wust, S., Tischner, D., John, M., Tuckermann, J.P., Menzfeld, C., Hanisch, U.K., van den Brandt, J., Luhder, F., Reichardt, H.M., 2009. Therapeutic and adverse effects of a non-steroidal glucocorticoid receptor ligand in a mouse model of multiple sclerosis. PLoS One 4, e8202.
Yeruva, S., Ramadori, G., Raddatz, D., 2008. NF-kappaB-dependent synergistic regulation of CXCL10 gene expression by IL-1beta and IFN-gamma in human intestinal epithelial cell lines. Int. J. Colorectal Dis. 23, 305–317.
Yohan, B., Kendarsari, R.I., Mutia, K., Bowolaksono, A., Harahap, A.R., Sasmono, R.T., 2014. Growth characteristics and cytokine/chemokine induction profiles of dengue viruses in various cell lines. Acta Virol. 58, 20–27.

Biochimica et Biophysica Acta 1864 (2016) 1270–1280

Contents lists available at ScienceDirect

Biochimica et Biophysica Acta

journal homepage: www.elsevier.com/locate/bbapap

Mass spectrometric analysis of host cell proteins interacting with dengue virus nonstructural protein 1 in dengue virus-infected HepG2 cells

Thanyaporn Dechtawewat [a], Atchara Paemanee [b], Sittiruk Roytrakul [b], Pucharee Songprakhon [a], Thawornchai Limjindaporn [c], Pa-thai Yenchitsomanus [a], Sawanan Saitornuang [d,e], Chunya Puttikhunt [d,e], Watchara Kasinrerk [f,g], Prida Malasit [d,e], Sansanee Noisakran [d,e,*]

[a] Division of Molecular Medicine, Department of Research and Development, Faculty of Medicine Siriraj Hospital, Mahidol University, Bangkok 10700, Thailand
[b] Proteomics Research Unit, National Center for Genetic Engineering and Biotechnology, National Science and Technology Development Agency, Pathum Thani 12120, Thailand
[c] Department of Anatomy, Faculty of Medicine Siriraj Hospital, Mahidol University, Bangkok 10700, Thailand
[d] Division of Dengue Hemorrhagic Fever Unit, Department of Research and Development, Faculty of Medicine Siriraj Hospital, Mahidol University, Bangkok 10700, Thailand
[e] Medical Biotechnology Research Unit, National Center for Genetic Engineering and Biotechnology, National Science and Technology Development Agency, Bangkok 10700, Thailand
[f] Biomedical Technology Research Center, National Center for Genetic Engineering and Biotechnology, National Science and Technology Development Agency, Chiang Mai 50200, Thailand
[g] Division of Clinical Immunology, Department of Medical Technology, Faculty of Associated Medical Sciences, Chiang Mai University, Chiang Mai 50200, Thailand

ARTICLE INFO

Article history:
Received 9 October 2015
Received in revised form 26 March 2016
Accepted 19 April 2016
Available online 21 April 2016

Keywords:
Dengue virus
Nonstructural protein 1
Virus–host interaction
Virus replication

ABSTRACT

Dengue virus (DENV) infection is a leading cause of the mosquito-borne infectious diseases that affect humans worldwide. Virus–host interactions appear to play significant roles in DENV replication and the pathogenesis of DENV infection. Nonstructural protein 1 (NS1) of DENV is likely involved in these processes; however, its associations with host cell proteins in DENV infection remain unclear. In this study, we used a combination of techniques (immunoprecipitation, in-solution trypsin digestion, and LC–MS/MS) to identify the host cell proteins that interact with cell-associated NS1 in an *in vitro* model of DENV infection in the human hepatocyte HepG2 cell line. Thirty-six novel host cell proteins were identified as potential DENV NS1-interacting partners. A large number of these proteins had characteristic binding or catalytic activities, and were involved in cellular metabolism. Coimmunoprecipitation and colocalization assays confirmed the interactions of DENV NS1 and human NIMA-related kinase 2 (NEK2), thousand and one amino acid protein kinase 1 (TAO1), and component of oligomeric Golgi complex 1 (COG1) proteins in virus-infected cells. This study reports a novel set of DENV NS1-interacting host cell proteins in the HepG2 cell line and proposes possible roles for human NEK2, TAO1, and COG1 in DENV infection.

1. Introduction

Dengue virus (DENV) is the causative agent of dengue hemorrhagic fever and dengue shock syndrome, potentially life-threatening diseases affecting the human population globally. Approximately 390 million people acquire DENV infection through mosquito bites each year, and 96 million of them present varying degrees of clinical manifestations [1]. Nevertheless, the underlying mechanisms of these severe dengue diseases remain unclear and neither a dengue vaccine nor a specific antiviral drug is commercially available.

DENV is a positive-sense, single-stranded, enveloped RNA virus of the family Flaviviridae, which produces three structural proteins (capsid, C; premembrane, prM; envelope, E) and seven nonstructural proteins (NS1, NS2A, NS2B, NS3, NS4A, NS4B, and NS5) in virus-infected cells. The nonstructural protein NS1 is an essential viral product implicated in DENV replication [2–7] and the pathogenesis of dengue hemorrhagic fever and dengue shock syndrome [8–11]. DENV NS1 exists in multiple forms, which are found inside and on the surfaces of virus-infected cells and in the extracellular milieu [12–17]. Intracellular NS1 can be detected in the same localities as double-stranded viral RNA in virus-induced membrane structures, which are possible sites of viral replication [2,18], and interacts with NS4A and NS4B as part of the viral replication complex [6,19–21]. Complementation of NS1 in *trans* restored viral RNA synthesis and replication in defective flaviviruses (yellow fever virus and West Nile virus) [5,22]. These lines of evidence suggest that NS1 is a cofactor in flavivirus replication. The level of secreted NS1 in the circulation also appears to correlate with viremia and the severity of dengue diseases [23–25]. This soluble NS1 protein participates in the formation of the immune complex, complement activation [9,26–30], and the immune evasion of DENV [31–33]. It also activates immune cells via toll-like receptors and triggers the release of

* Corresponding author at: Medical Biotechnology Research Unit, National Center for Genetic Engineering and Biotechnology, National Science and Technology Development Agency, Bangkok 10700, Thailand.
E-mail address: sansanee@biotec.or.th (S. Noisakran).

http://dx.doi.org/10.1016/j.bbapap.2016.04.008
1570-9639/

proinflammatory cytokines, endothelial permeability, and vascular leak, which may contribute to the pathogenesis of dengue diseases [34–36].

Interactions between DENV NS1 and host cell proteins have been demonstrated previously using *in vitro* binding assays and yeast two-hybrid systems with human bone-marrow and liver cDNA libraries [32,33,37–39]. These interactions include those between DENV NS1 and the complement regulatory protein clusterin [39], complement components C1s, C4, and C1q, C4-binding protein [32,33,38], and signal transducer and activator of transcription 3β (STAT3β) [37] and may contribute to viral immune escape and the immune-mediated pathogenesis of dengue diseases. In our previous study using immunoprecipitation and two-dimensional (2D) gel electrophoresis, heterogeneous ribonucleoprotein (hnRNP) C1/C2 is a DENV NS1-interacting partner in virus-infected HEK293T cells [40]. Because the sensitivity of 2D gel electrophoresis in protein detection is limited, we used a similar immunoprecipitation technique combined with in-solution trypsin digestion and subsequent liquid chromatography–tandem mass spectrometry (LC–MS/MS) in this study to identify the host cell proteins that interact with DENV NS1 in DENV-infected human hepatocyte HepG2 cells, which represent relevant target cells for DENV infection *in vitro* [41–45]. Thirty-six novel host cell proteins were identified as DENV-NS1-interacting proteins in this model of DENV-infected human hepatocyte cells.

2. Materials and methods

2.1. Cell lines, virus, and antibodies

Human hepatocellular carcinoma (HepG2) cells were cultured in DMEM (Invitrogen, Carlsbad, CA, USA) supplemented with 10% heat-inactivated FBS (Invitrogen), 0.1 mM nonessential amino acids (Merck, Darmstadt, Germany), 1 mM sodium pyruvate (Merck), 2 mM L-glutamine (Sigma, St. Louis, MO, USA), 36 μg/ml penicillin (Sigma), and 60 μg/ml streptomycin (Sigma) at 37 °C in a 5% CO_2 incubator with a humidified atmosphere. A DENV serotype 2 (strain 16681) stock was propagated in C6/36 mosquito cells. Mouse monoclonal antibodies specific for DENV NS1 (clones NS1-3F.1 and 1A4) and DENV E (clone 3H5) were produced from previously established hybridoma cells [46–48]. Mouse monoclonal antibodies specific for human never in mitosis A-related kinase 2 (NEK2) and human thousand and one amino acid protein kinase 1 (TAO1) were purchased from Santa Cruz Biotechnology (Santa Cruz, CA, USA). A rabbit anti-human TAO1 antibody was purchased from Assay Biotechnology (Sunnyvale, CA, USA). Goat and rabbit polyclonal antibodies specific for human component of oligomeric Golgi complex 1 (COG1) were purchased from Everest Biotech (Oxfordshire, UK) and Bioss USA (Woburn, MA, USA), respectively. Mouse isotype-matched control IgG1 and IgG2a antibodies (clones MOPC 21 and UPC 10) and a mouse anti-FLAG monoclonal antibody were purchased from Sigma. A goat IgG antibody was purified from normal goat serum (Vector Laboratories, Burlingame, CA, USA) by protein G affinity chromatography [49].

2.2. DENV infection

HepG2 cells were seeded and cultured in tissue culture flasks (Costar, Cambridge, MA, USA) for 24 h. The adherent cells were incubated in culture medium with DENV-2 at a multiplicity of infection (MOI) of 5 or with culture medium alone (uninfected control) at 37 °C in a 5% CO_2 incubator for 2 h. After the supernatant was discarded, the culture was maintained in fresh medium under the same conditions. At 48 h postinfection, the uninfected and DENV-infected HepG2 cells were harvested and assessed for viability with a Trypan blue dye exclusion assay and for percentage DENV infection with an immunofluorescent staining assay for DENV E and NS1 proteins, as previously described [50]. The immunofluorescently stained cells (10,000 events) were analyzed with flow cytometry to determine the percentages of DENV E- and DENV NS1-expressing cells, which represented the efficiency of DENV infection. Six independent experiments were performed to analyze the percentages of cell viability and DENV E-and DENV NS1-expressing cells.

2.3. Immunoprecipitation of DENV NS1 protein

At 48 h postinfection, the uninfected and DENV-infected cells (10^7) were washed with PBS by centrifugation at 470 ×*g* for 5 min. The cell pellets were resuspended in RIPA buffer containing 20 mM Tris–HCl (pH 7.5), 5 mM EDTA, 150 mM NaCl, 1% NP-40, 0.1% SDS, and 0.5% deoxycholate, with a protease inhibitor cocktail (Roche, Mannheim, Germany), incubated on ice for 30 min, and centrifuged at 9100 ×*g* at 4 °C for 5 min. The clear lysates were subjected to immunoprecipitation by incubating them at 4 °C overnight with a 50% slurry of protein-G-conjugated Sepharose 4B beads (GE Healthcare, Uppsala, Sweden) that had been coated with 20 μg of mouse isotype-matched control IgG2a antibody or mouse anti-DENV NS1 monoclonal antibodies (clones NS1-3F.1 and 1A4, recognizing different DENV NS1 epitopes), followed by centrifugation at 15,300 ×*g* at 4 °C for 5 min. The immunoprecipitated samples were washed three times with RIPA and then three times with 10 mM Tris–HCl (pH 7.5). One set of the immunoprecipitated samples was resuspended in loading buffer (50 mM Tris–HCl [pH 6.8], 2% SDS, 0.1% bromophenol blue, 10% glycerol) and subjected to an immunoblotting analysis to confirm the presence of the DENV NS1 protein, as previously described [50]. The other set was resuspended in 0.1% RapiGest SF surfactant (Waters Corporation, Milford, MA, USA) in 50 mM ammonium bicarbonate to be further processed for the proteomic analysis of the DENV NS1-interacting host cell proteins.

2.4. Preparation of immunoprecipitated samples for LC–MS/MS

Three samples were prepared for one set of experiments: DENV-infected cell lysate immunoprecipitated with an anti-NS1 antibody (test sample), uninfected cell lysate immunoprecipitated with an anti-NS1 antibody (control sample), and DENV-infected cell lysate immunoprecipitated with an isotype-matched control antibody (control sample). The latter two samples were used as background controls for the immunoprecipitation process. All three immunoprecipitated samples on the Sepharose 4B beads were resuspended in 0.1% RapiGest in 50 mM ammonium bicarbonate, and then heated at 100 °C for 5 min, incubated with 5 mM dithiothreitol at 60 °C for 30 min, and cooled to room temperature. The samples were then incubated with 15 mM iodoacetamide at room temperature for 30 min in the dark and centrifuged at 15,300 ×*g* for 5 min. The clear supernatants were harvested and incubated with 80 ng of trypsin (sequencing grade; Promega, Madison, WI, USA) at 37 °C for 1 h and then with 0.5% trifluoroacetic acid at 37 °C for 45 min, followed by centrifugation at 15,300 ×*g* for 10 min to precipitate the RapiGest SF. The clear supernatants were collected and dried with a speed vacuum concentrator. The dried peptides were resuspended in 10 μl 0.1% formic acid and subjected to LC–MS/MS analysis. Three independent sets of experiments were performed. Each set of the resultant peptides was injected three times into LC–MS/MS.

2.5. LC–MS/MS analysis

Protonated peptides in 0.1% formic acid were injected into a NanoAcquity system (Waters Corporation) equipped with a Symmetry C18 5 μm, 180 μm × 20 mm Trap column and a BEH130 C18 1.7 μm, 100 μm × 100 mm analytical reversed-phase column (Waters Corporation). The samples were initially passed through the trap column at a flow rate of 15 μl/min for 1 min. Mobile phase A was 0.1% formic acid in water and mobile phase B was 0.1% formic acid in acetonitrile. The peptides were separated with a gradient of 15%–50% mobile phase B over 15 min at a flow rate of 600 nl/min, followed by a 3 min rinse with 80% mobile phase B. The column temperature was maintained at

35 °C. For all measurements, a SYNAPT HDMS mass spectrometer (Waters Corporation) was operated in V-mode with a resolution (full-width half-maximum) of at least 10,000. All analyses were performed in nano-electrospray positive-ion mode. Accurate mass LC–MS data were acquired in the direct data acquisition mode. The trap was set at collision energy of 6 V. In the transfer collision energy control, low energy was set at 4 V. The quadrupole mass analyzer was adjusted to allow the efficient transmission of ions in an *m/z* range of 300–1800. The MS/MS survey was in the range of 50–1990 Da and the scan time was 0.5 s. The DeCyder MS Differential Analysis Software version 2.0 (GE Healthcare Life Sciences, Pittsburgh, PA, USA) was used for the differential quantitation of the peptides based on the MS signal intensities at different retention times. The peptide ion signal intensities in the range of retention times of 7–18 min were quantified using the PepDetect module for the automated detection of peptides and the assignment of charge states with the following parameters: typical peak width, 0.25 min; TOF resolution, 5000; charge states, 1–3; *m/z* shift tolerance, 0.1 U. Peptides with low-quality LC peaks were removed from the analysis. Different peptide ion signal intensity maps of the test and control groups were evaluated to establish an average abundance ratio for each peptide using the PepMatch module, with a retention time tolerance of 1 min and *m/z* tolerance of 0.5 Da. The NCBInr database (taxonomy: *Homo sapiens*) was searched with the LC–MS/MS data from the DeCyder MS analysis and the proteins were identified with the MASCOT search engine (Matrix Science, London, UK), with the following parameters: enzyme, trypsin; allowance of missed cleavages, 3; fixed modification, carbamidomethylation of cysteine residues; variable modification, oxidation of methionine residues; mass values, monoisotopic; peptide mass tolerance, 1.2 Da; MS/MS tolerance, 0.6 Da; peptide charge states, 1+, 2+, 3+; data format, Mascot generic; instrument, ESI-Q-TOF mass spectrometer. The GI numbers of identified peptides were mapped to the UniProt database (http://www.uniprot.org/uploadlists/) to obtain the protein accession numbers. The identified proteins were classified based on their molecular functions and biological processes using the PANTHER Classification System version 9.0 (http://go.pantherdb.org/).

One-way ANOVA and Benjamini and Hochberg multiple testing correction with a threshold of 5% false discovery rate [51] were applied to analyze statistically significant differences in average peptide ion intensities between the test sample and two control samples from three independent experiments. Human host proteins that had Benjamini and Hochberg adjusted p value between sample groups < 0.05 and an average (peptide ion intensity of test sample)/(peptide ion intensity of either control sample) ratio > 1.5 were considered candidate DENV NS1-interacting proteins.

2.6. Coimmunoprecipitation of DENV NS1 and host cell proteins

Uninfected and DENV-infected cells were processed for immunoprecipitation with an isotype-matched control antibody or anti-DENV NS1 monoclonal antibodies, as described above. The immunoprecipitated complexes were eluted with loading buffer in the presence or the absence of 5% β-mercaptoethanol, and subjected to an immunoblotting analysis to determine the presence of human NEK2, TAO1, or COG1 and DENV NS1 using the specific antibodies described above. Reciprocal immunoprecipitation was performed with anti-NEK2, anti-TAO1 and anti-COG1 antibodies, or their respective control antibodies using the similar methods described above with minor modifications. The immunoprecipitated samples were assessed for the presence of corresponding host proteins and DENV NS1 by immunoblotting analysis.

2.7. Colocalization of DENV NS1 and host cell proteins

HepG2 cells were grown in a poly-D-lysine-coated chamber slide or a 96-well plate for 24 h. The adherent cells were infected with DENV-2 at an MOI of 2.5 or left uninfected (uninfected control) for 8 h, and then transfected with 1.0–2.5 μg of empty pcDNA Hygro vector (vector control) or pcDNA Hygro encoding the human NEK2A, NEK2B, TAO1, or COG1 protein fused to the FLAG tag at the N-terminus using Lipofectamine 3000 (Invitrogen), according to the manufacturer's instructions, with minor modifications. At 48 h postinfection, the cells were processed for double immunofluorescent staining for DENV NS1 and host cell proteins using a previously described method [50]. Briefly, the cells were fixed with 4% paraformaldehyde in PBS for 20 min and permeabilized with 0.2% Triton X-100 in PBS for 10 min. The nonspecific binding sites on the cells were blocked with 10% human AB serum for 30 min at room temperature. The cells were then incubated successively with 1 μg/ml mouse anti-FLAG monoclonal antibody (Sigma) for 1 h and Cy3-conjugated goat anti-mouse IgG antibody (Jackson ImmunoResearch Laboratories, West Grove, PA, USA), diluted 1:2000, for 30 min at room temperature. Following three washes with PBS, the stained cells were incubated with 10% normal mouse serum in PBS for 30 min and with a mixture of 3.75 μg/ml mouse anti-NS1 monoclonal antibody (clone 1A4) conjugated with Alexa Fluor 488 and 10 μg/ml Hoechst 33342 (Molecular Probes, Eugene, OR, USA) for 30 min. The stained cells were postfixed with 1% paraformaldehyde in PBS for 30 min and visualized with the EVOS FL Cell Imaging System (Invitrogen) or under a confocal laser-scanning microscope (LSM 510 Meta; Carl Zeiss, Jena, Germany). Captured cell images were analyzed for pixel intensities of the fluorescent signals to generate histogram profiles by LSM Software version 3.2 (Carl Zeiss).

2.8. Statistical analysis

Differences in peptide ion intensities between the samples in the test group (DENV-infected cell lysate immunoprecipitated with anti-NS1 antibody) and the samples in the two control groups (uninfected cell lysate immunoprecipitated with anti-NS1 antibody or DENV-infected cell lysate immunoprecipitated with isotype-matched control antibody) were analyzed statistically with one-way ANOVA using GraphPad Prism version 6.0 and Benjamini and Hochberg multiple testing correction at a false discovery rate of 5% [51]. The peptide ion intensities for all three sample groups were compared. Differences in the peptide ion intensities of the sample groups were considered significant at $p < 0.05$.

3. Results

To identify potential host cell proteins that interact with DENV NS1, HepG2 cells were infected with DENV at MOI 5 or left uninfected (uninfected control), and harvested at 48 h postinfection to analyze the percentage DENV infection and cell viability. In immunofluorescent staining for the expression of viral antigen which reflects the efficiency of viral infection, the percentages of DENV E- and DENV NS1-expressing cells among the DENV-infected cells were 81.7 ± 3.5% and 80.0 ± 5.2%, whereas the background staining levels were 2.9 ± 0.9% and 4.7 ± 1.1%, respectively, in the uninfected control (Fig. 1A). In the analysis of cell viability with a Trypan blue dye exclusion assay, the majority of DENV-infected cells (75.5 ± 3.6%) were viable under these infection conditions, compared with 95.2 ± 0.7% viability of the uninfected control cells (Fig. 1B). Uninfected and DENV-infected HepG2 cells prepared under the same conditions were then immunoprecipitated with DENV NS1-specific antibodies or an isotype-matched control antibody. The presence of DENV NS1 in the immunoprecipitated samples was verified with an immunoblotting analysis, and the samples were subsequently processed for a proteomic analysis with LC–MS/MS. Three independent sets of uninfected and DENV-infected samples were prepared for the proteomic analysis. A schematic diagram of the experimental strategy is shown in Supplementary Fig. 1.

In the immunoblotting analysis, DENV NS1 was detected specifically in the DENV-infected sample immunoprecipitated with the anti-NS1 antibody (Fig. 2, lane DENV–αNS1 Ab), but not in the DENV-infected sample immunoprecipitated with the isotype-matched control antibody (Fig. 2,

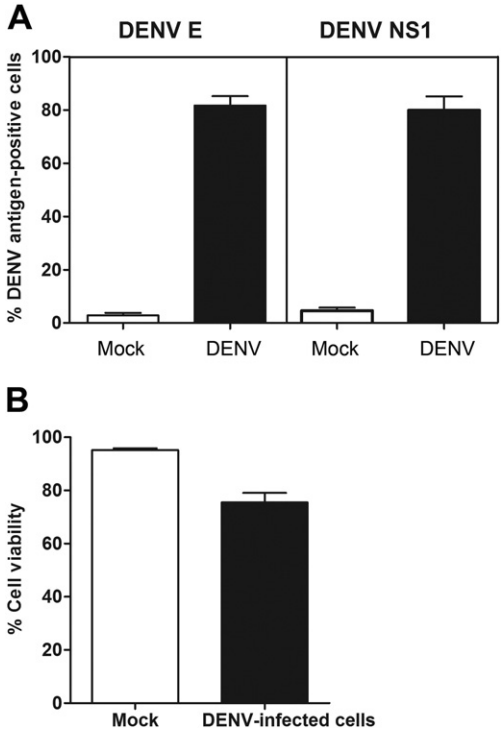

Fig. 1. DENV infection rate of HepG2 cells. HepG2 cells were infected with DENV at MOI 5 or left uninfected (uninfected control), and harvested at 48 h postinfection. The percentage DENV infection was determined with immunofluorescent staining for DENV E and NS1 antigens with a subsequent flow-cytometric analysis (A), and cell viability with a Trypan blue dye exclusion assay (B).

lane DENV–control Ab) or the uninfected samples immunoprecipitated with either antibody (Fig. 2, lanes mock–control Ab and mock–αNS1 Ab). The three independent sets of prepared samples showed similar outcomes. The immunoprecipitated samples containing DENV NS1 were then subjected to in-solution digestion with trypsin and processed for LC–MS/MS. The DeCyder MS Differential Analysis Software was used to align and quantify the primary MS protein data based on the ion intensities of the tryptic peptides from the DENV-infected sample immunoprecipitated with the anti-NS1 antibody (test sample, DENV–αNS1), the DENV-infected sample immunoprecipitated with

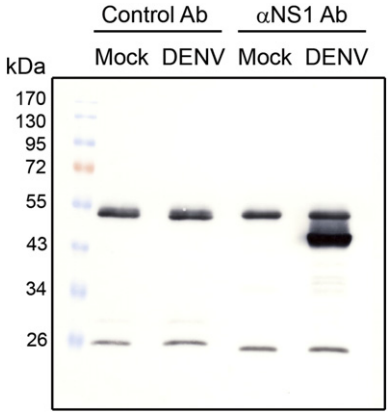

Fig. 2. Immunoprecipitation of DENV NS1 from DENV-infected cells. Uninfected (Mock) and DENV-infected (DENV) cells were immunoprecipitated with anti-DENV NS1 monoclonal antibodies (αNS1 Ab) or an isotype-matched control antibody (Control Ab). The immunoprecipitated samples were subjected to an immunoblotting analysis using mouse anti-DENV NS1 monoclonal antibody and rabbit anti-mouse IgG conjugated with HRP as primary and secondary antibodies. A specific band of DENV NS1 (about 46 kDa) was detected under reducing and heated conditions. Approximately 50-kDa and 25-kDa protein bands observed in all samples tested are heavy and light chains of mouse IgG used for immunoprecipitation.

the isotype-matched control antibody (control sample, DENV–IgG2a), and the uninfected sample immunoprecipitated with the anti-NS1 antibody (control sample, mock–αNS1). After the peptide ion intensity maps of the test and control samples were aligned, the NCBInr database (*Homo sapiens*) was searched for all the matched peptides using the MASCOT search engine to identify the proteins. The peptides with the highest ID scores were determined for their average peptide ion intensities from three independent experiments. All the peptide ion intensities of 392 identified proteins were compared between the test sample and two control samples using one-way ANOVA and Benjamini and Hochberg multiple testing correction with a threshold of 5% false discovery rate. The peptide ion intensities of these proteins in the test sample were normalized against that of each control sample and any protein with an average (peptide ion intensity in test sample)/(peptide ion intensity in either control sample) ratio > 1.5 was selected from the overall data.

When the criteria described above were used, 36 host cell proteins were identified as potential DENV NS1-interacting host proteins in the DENV-infected cells (Table 1, Fig. 3, and Supplementary Table 1). These protein identifications were based on single peptide assignments and the sequences of identified peptides were presented in Supplementary Table 1. The average peptide ion intensity ratios between the test sample (DENV–αNS1) and the control samples (DENV–IgG2a and mock–αNS1) for the 36 identified proteins, derived from three independent experiments (three LC–MS/MS injections of each sample in each experiment), are shown in Table 1. Statistically significant differences in the peptide ion intensities were evident between the test sample and both control samples for 19 proteins (protein IDs 1–13 and 17–22) and between the test sample and single control samples for 17 proteins (protein IDs 14–16 and 23–36) (Fig. 3).

In further analysis of the 36 identified host proteins, the majority of these proteins could be mapped to the UniProt database, either with previously reported functions (24/36 proteins, 67%) or with uncharacterized functions (3/36 proteins, 8%), whereas 9/36 proteins (25%) could not be mapped to this database (Fig. 4A). The peptide ion intensities, peptide sequences, and molecular masses of the unmapped host proteins (protein IDs 1, 10, 16, 18, 19, 30, 33, 35, and 36) are shown in Table 1, Fig. 3, and Supplementary Table 2. The mapped human proteins were further categorized with the PANTHER classification system based on their molecular functions and biological processes. Approximately 39% and 34% of the human proteins identified had binding activities (i.e., ATP, ion, nucleic acid, lipid, and protein binding) and enzymatic activities (i.e., transferase, hydrolase, kinase, phosphatase, isomerase, ligase, lyase, and oxidoreductase), respectively (Fig. 4B, left panel). Other molecular functions of the identified proteins included structural molecule (11%), enzyme regulator (5%), receptor (5%), transporter (4%), and transcription factor/transcription regulator (2%) activities (Fig. 4B, left panel). A major group of the identified human proteins (about 26%) were involved in biological processes associated with cellular metabolism, including protein metabolism and modification, carbohydrate metabolism, nucleic acid metabolism, and lipid and fatty acid metabolism (Fig. 4B, right panel). Other biological processes in which the identified proteins were involved included transport (11%), cell structure and motility (10%), signal transduction (8%), immunity and defense (8%), cell communication (8%), cell cycle (7%), response to stimulus (5%), cell adhesion (4%), apoptosis (3%), cell proliferation and differentiation (3%), developmental process (3%), homeostasis (1%), sensory perception (1%), and protein targeting and localization (1%) (Fig. 4B, right panel). The molecular functions and biological processes of all the DENV NS1-interacting proteins identified are shown in Supplementary Tables 3 and 4, respectively.

To confirm that the identified host proteins interact with DENV NS1 in virus-infected cells, the three mapped human proteins with the highest significant differences (>2.5-fold) in the peptide ion intensities between the test sample and the two control samples (Table 1 and Fig. 3) were assessed for their association with DENV

Table 1
DENV NS1-interacting host proteins identified in DENV-infected HepG2 cells.

ID	Protein name	GI number	UniProt accession number	UniProt entry name	Intensity ratio of DENV–αNS1 to DENV–IgG2a	Intensity ratio of DENV–αNS1 to mock–αNS1
1	Chromosome 21 open reading frame 70	gi|119629776	–	–	8.67	3.80
2	Serine/threonine-protein kinase Nek2	gi|4505373	P51955	NEK2_HUMAN	4.94	UD
3	Serine/threonine-protein kinase TAO1	gi|45439370	Q7L7X3	TAOK1_HUMAN	3.52	4.68
4	Conserved oligomeric Golgi complex subunit 1	gi|71052081	Q4G0L8	Q4G0L8_HUMAN	2.75	3.69
5	Protein phosphatase 1 M	gi|34526234	Q96MI6	PPM1M_HUMAN	2.80	1.99
6	Folylpolyglutamate synthetase mitochondrial isoform	gi|15911844	Q96LE4	Q96LE4_HUMAN	2.40	2.46
7	Protein AHNAK2	gi|156766050	Q8IVF2	AHNK2_HUMAN	2.25	2.01
8	Melanin-concentrating hormone receptor 1	gi|12804625	Q99705	MCHR1_HUMAN	2.18	2.09
9	WD repeat-containing protein 78	gi|55665586	Q5VTH9	WDR78_HUMAN	14.47	1.57
10	hCG2040936	gi|119620382	–	–	2.30	1.71
11	Transmembrane and coiled-coil domain-containing protein 3	gi|15214846	Q6UWJ1	TMCO3_HUMAN	1.91	1.54
12	Actin-related protein 10	gi|10433978	Q9NZ32	ARP10_HUMAN	10.59	1.61
13	Trifunctional enzyme subunit alpha, mitochondrial	gi|20127408	P40939	ECHA_HUMAN	1.75	3.54
14	Serpin A9	gi|28207593	Q86WD7	SPA9_HUMAN	8.54	1.72
15	Zinc finger protein 1 homolog	gi|119226229	Q6P2D0	ZFP1_HUMAN	3.00	1.53
16	hCG1777996	gi|119615085	–	–	2.29	1.65
17	Centrin-3	gi|2246401	O15182	CETN3_HUMAN	1.59	1.41
18	Hypothetical protein LOC85007, isoform 2	gi|119574225	–	–	1.81	1.43
19	hCG1995002	gi|119602612	–	–	6.75	1.24
20	Golgin subfamily A member 5	gi|30260188	Q8TBA6	GOGA5_HUMAN	2.84	1.39
21	Receptor-type tyrosine-protein phosphatase epsilon	gi|15866730	P23469	PTPRE_HUMAN	1.64	1.26
22	TBC1 domain family member 31	gi|119612424	Q96DN5	TBC31_HUMAN	1.64	1.34
23	Tctex1 domain-containing protein 3	gi|28372535	Q8IZS6	TC1D3_HUMAN	1.77	1.19
24	Complement C1q tumor necrosis factor-related protein 5	gi|20810469	Q9BXJ0	C1QT5_HUMAN	2.68	1.15
25	Spectrin beta chain, non-erythrocytic 1	gi|338443	Q01082	SPTB2_HUMAN	2.26	1.32
26	Ubiquitin-protein ligase E3B	gi|35493952	Q7Z3V4	UBE3B_HUMAN	1.55	1.19
27	Neurolysin, mitochondrial precursor	gi|14149738	Q9BYT8	NEUL_HUMAN	2.03	1.31
28	LIM domain only protein 7	gi|122889104	Q8WWI1	LMO7_HUMAN	1.91	1.26
29	GTPase-activating Rap/Ran-GAP domain-like protein 3	gi|207448705	Q5VVW2	GARL3_HUMAN	1.73	1.35
30	hCG2041987	gi|119609347	–	–	2.08	1.34
31	PH domain leucine-rich repeat-containing protein phosphatase 1	gi|291219891	O60346	PHLP1_HUMAN	1.63	1.18
32	Histone H2A.V	gi|62087582	Q71UI9	H2AV_HUMAN	1.75	1.20
33	hCG1654831	gi|119587008	–	–	1.58	1.13
34	Collagen alpha-2(V) chain	gi|27696688	P05997	CO5A2_HUMAN	1.76	1.13
35	hCG2041166	gi|119627144	–	–	1.64	1.29
36	Unnamed protein	gi|56462555	–	–	1.38	7.65

UD, unable to determine the peptide ion intensity ratio: DENV–αNS1/mock–αNS1 (intensity of DENV–αNS1 = 6.22; intensity of mock–αNS1 = 0).

NS1 using coimmunoprecipitation and colocalization assays with specific antibodies. Anti-NS1 monoclonal antibodies immunoprecipitated DENV NS1, together with never in mitosis A (NIMA)-related kinase 2 (NEK2), thousand and one amino acid protein kinase 1 (TAO1), and component of oligomeric Golgi complex 1 (COG1), from DENV-infected HepG2 cell lysate, but not from uninfected control (Fig. 5A, B, and C, anti-NS1 Ab). Reciprocal immunoprecipitation with antibodies specific against human NEK2, TAO1 and COG1 also confirmed coimmunoprecipitation of the corresponding host proteins with DENV NS1 in DENV-infected cells (Fig. 5A, B, and C, anti-NEK2 Ab, anti-TAO1 Ab and anti-COG1 Ab). Immunoprecipitation with control antibodies did not yield any specific bands of human NEK2, TAO1, and COG1 in uninfected and DENV-infected samples, but relatively low background of non-specific DENV NS1 binding could be observed under certain control conditions (Fig. 5A, B and C, Control Ab). Consistent with the results of coimmunoprecipitation, TAO1, COG1, and two isoforms of NEK2 (NEK2A and NEK2B) partially colocalized with DENV NS1 in the cytoplasmic region of virus-infected cells (Fig. 6A and B and Supplementary Fig. 2). No cross-reactions of DENV NS1- and FLAG-specific antibodies with other host proteins were observed in the colocalization assay (Fig. 6A and B, anti-FLAG–pcDNA Hygro and Supplementary Fig. 3, anti-NS1). These findings indicate the interactions between the identified human host proteins and DENV NS1 during DENV infection.

4. Discussion

Investigation of the interplay between viral and host cell proteins is of particular importance in understanding the mechanisms of DENV infection and the host cellular response. In this study, we used a combination of techniques, coimmunoprecipitation, in-solution trypsin digestion, and LC–MS/MS, to investigate the human host cell proteins that interact with DENV NS1 during DENV infection. Thirty-six host proteins were identified as potential DENV NS1-interacting partners in DENV-infected HepG2 cells. The majority of these proteins had characteristic binding or enzymatic activities and were involved in several cellular metabolic processes.

Several attempts have been made in previous studies to screen for host cell proteins that interact with DENV proteins [52]. However, only limited success has been reported in identifying DENV NS1-interacting partners. When a GAL4 yeast two-hybrid system was used to screen a human bone-marrow cDNA library, STAT3β protein was identified as an interacting partner of DENV NS1 and this interaction is probably inducing the production of tumor necrosis factor α and interleukin 6, which may take part in dengue pathogenesis [37]. In other two studies using a similar GAL4 yeast two-hybrid system to screen a human liver cDNA library, completely different sets of host cell proteins interacted with DENV NS1. Specifically, one study used full-length NS1 and different NS1 fragments as baits and identified 12 host cell proteins as their interacting partners: EIF4G2, FAM123B, FGB, LAMB1, MAP3K7IP2, PAIP1, PTBP1, SERPIND1, SPTBN2, SRFBP1, TCF7L2, and WWC1. However, these interactions were not confirmed in DENV-infected cells [53]. Using the same technique, the other study identified 50 potential DENV NS1-interacting host proteins, most of which are secreted into the plasma and are classified as acute-phase proteins, and verified the interaction between complement C1q and DENV NS1 [38]. Unlike these previous studies, no host cell proteins that interacted

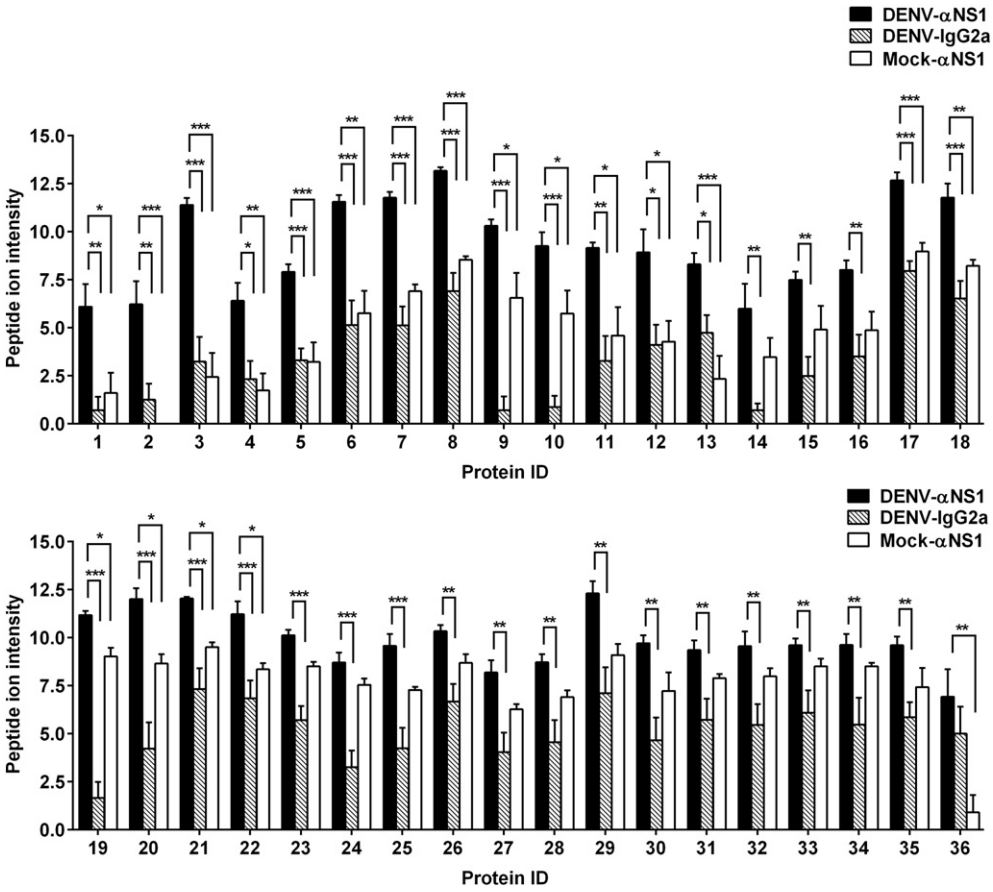

Fig. 3. Peptide ion signal intensities of immunoprecipitated samples. Uninfected and DENV-infected cells were immunoprecipitated with anti-NS1 antibodies (αNS1) or isotype-matched control antibody (IgG2a). The immunoprecipitated samples were processed and analyzed with LC–MS/MS. At a threshold of 5% false discovery rate, 36 host cell proteins, for which the peptide ion intensities in the test samples (DENV–αNS1) were 1.5-fold higher than the peptide ion intensities in either control sample (mock–αNS1 or DENV–IgG2a), were identified as potential DENV NS1-interacting host cell proteins. The protein IDs correspond to the host cell proteins listed in Table 1. Data show the peptide ion intensities (means + SEM) of the proteins identified in three independent experiments. Statistically significant differences in the peptide ion intensities between all the sample groups were analyzed with one-way ANOVA and Tukey's multiple comparison test (*$p < 0.05$; **$p < 0.01$; ***$p < 0.001$).

with DENV NS1 were detected when a LexA yeast two-hybrid system was used to screen mosquito *Aedes aegypti* and human peripheral blood leukocyte cDNA libraries [54]. A recent study using two different strategies, affinity chromatography and immunoprecipitation assays, identified 64 host cell proteins that interacted with DENV NS1 in Huh7 cells, and demonstrated the roles of 60S ribosomal protein L18 in DENV translation/replication and DENV production [55]. In a similar immunoprecipitation assay in HUVEC-C cells, DENV NS1 interacted with glyceraldehyde-3-phosphate dehydrogenase and enhanced its glycolytic activity [56]. These findings suggest that different host systems and different types of screening assays produce different outcomes in the identification of DENV NS1-interacting partners, possibly because the DENV NS1 protein conformation is highly complex in these systems.

To investigate DENV NS1-interacting proteins in an *in vitro* system closely related to natural infection, we used a coimmunoprecipitation technique to collect any host cell proteins that potentially interacted with DENV NS1 in DENV-infected cells, and then analyzed their identities with MS. Our previous work using 2D gel electrophoresis to separate the proteins before Q-TOF MS/MS identified only the hnRNP C1/C2 proteins as DENV NS1-interacting partners in virus-infected human embryonic kidney epithelial HEK293T cells [40]. The restricted number of proteins identified with that technique could be attributable to the limitations of 2D gel electrophoresis and subsequent Coomassie Blue staining, which can only detect a minimum of approximately 10–30 ng of protein [57]. To overcome this potential constraint and to better profile the DENV NS1-interacting proteins in target cells that are more relevant to DENV infection in the present study, we used DENV-infected HepG2 hepatocytes for immunoprecipitation experiments with specific antibodies, and the immunoprecipitated proteins were directly processed for in-solution trypsin digestion and LC–MS/MS analysis. Some background levels of detectable peptide ions were observed in the control samples (mock–αNS1 and DENV–IgG2a) (Fig. 3) and these were normalized to the peptide ion intensities of the test sample (DENV–αNS1). When we used a cutoff value, 36 potential DENV NS1-interacting host proteins were identified (Table 1 and Fig. 3). Of all the identified DENV NS1-interacting host proteins, NEK2, TAO1, and COG1 proteins displayed the greatest statistically significant differences (>2.5-fold) in their average peptide ion intensities between the test sample and both control samples (Table 1 and Fig. 3). Therefore, they were selected to verify their associations with DENV NS1. The coimmunoprecipitation and partial colocalization of human NEK2, TAO1, and COG1 with DENV NS1 (Fig. 5A, B and C, Fig. 6A and B, and Supplementary Fig. 2) confirmed their interactions in DENV-infected HepG2 cells.

NEK2 is a host cell protein in the NIMA-related kinase family, which has 11 member serine/threonine kinases, NEK1–NEK11 [58]. The NEK2 protein has three alternative splice variants, NEK2A, NEK2B, and NEK2C, which share an N-terminal kinase domain, a leucine zipper motif involved in dimerization, autophosphorylation, and activation processes, and a microtubule-binding site, but partly differ in their C-terminal sequences [58]. NEK2A is a 445-amino-acid protein (about 48 kDa) that contains a protein-phosphatase-1-binding site and two anaphase-promoting complex/cyclosome-dependent degradation motifs, a KEN (Lys-Glu-Asn) box, and a methionine–arginine dipeptide tail at the C-

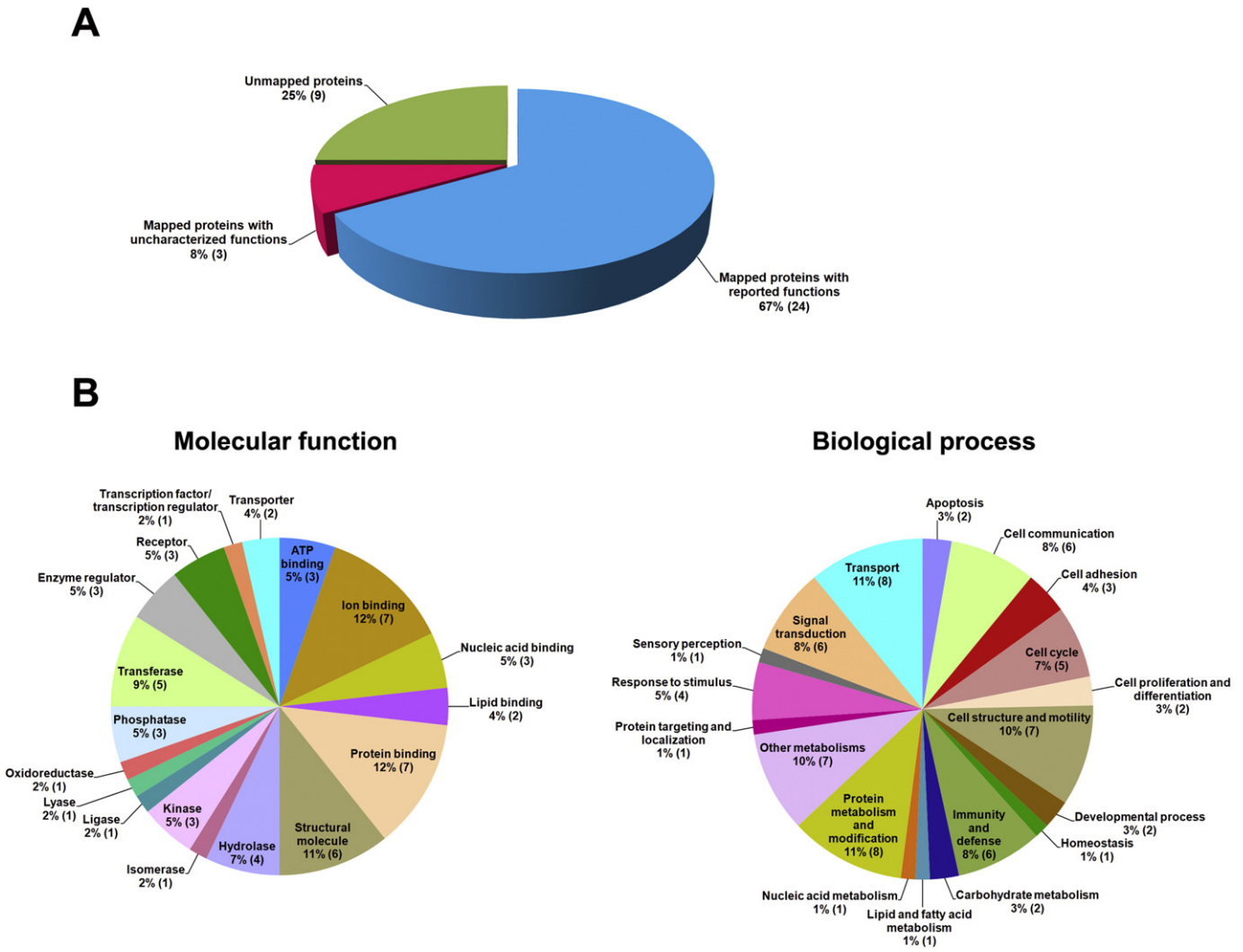

Fig. 4. Mapping and classification of DENV NS1-interacting host cell proteins. Thirty-six identified DENV NS1-interacting host cell proteins were mapped to the UniProt database. A pie chart (A) illustrates the percentages of the mapped proteins with previously reported functions or with uncharacterized functions and the unmapped proteins. All the mapped proteins with previously reported functions were further analyzed with the PANTHER classification system. Pie charts (B) illustrate the molecular functions and biological processes of these DENV NS1-interacting proteins. Numbers in parentheses represent the number of identified proteins in that particular category among the total 36 host cell proteins identified.

terminus. These specific regions are absent in NEK2B, which includes only 384 amino acids (about 44 kDa) [59]. NEK2A and NEK2C have relatively similar compositions, but an internal 8-amino-acid deletion at residues 371–378 in NEK2C generates a strong splice-site-spanning nuclear localization signal that increases NEK2C accumulation, mainly in the nucleus [60]. In our study, the specific antibody used to detect human NEK2 protein in the samples coimmunoprecipitated with the anti-DENV NS1 antibody does not distinguish between the three different isoforms of the NEK2 protein. Unlike NEK2C, NEK2A has a weak nuclear localization signal and NEK2B has no nuclear localization signal. As a result, NEK2A is distributed equally in the nucleus and cytoplasm, whereas NEK2B tends to occur predominantly in the cytoplasm [60]. However, the NEK2A and NEK2B proteins were observed in both the nucleus and cytoplasm of DENV-infected HepG2 cells in our study (Fig. 6A and B). Because previous work [2] and our results (Fig. 6A and B) have shown that intracellular DENV NS1 predominantly localizes in the perinuclear regions of DENV-infected cells, human NEK2A and NEK2B were the only isoforms chosen for further verification of their interaction with DENV NS1 in the present study, and were confirmed to partly colocalize with DENV NS1 in virus-infected cells.

NEK2 protein has important functions in centrosome splitting, mitotic spindle assembly, spindle checkpoint signaling, negative regulation of microtubule stability, cell-cycle control, and cell survival [61–66]. The expression levels, dynamic subcellular localization, and functions of the NEK2 protein probably depend on the stage of the cell cycle [67,68]. The catalytic activity and levels of NEK2 are high during the S and G2 phases, but low during the M and early G1 phases of the cell cycle [68]. Knockdown of NEK2 induced the expression of proapoptotic splice variants of BCL-X, BIN1, and MKNK2, and increased the cleavage of PARP1 and caspase 3, thus enhancing apoptosis [66]. Based on these roles of human NEK2, it is possible that the interaction between DENV NS1 and NEK2 is involved in the regulation of the cell cycle and cell survival, providing a favorable environment for DENV replication in virus-infected cells.

TAO1 is another human serine/threonine kinase identified as a DENV NS1-interacting protein in our study. TAO1, also known as PSK2, MARKK, or hKFC-B, is a member of the sterile 20 protein (Ste20p)-related kinase family and contains 1001 amino acids (about 116 kDa) [69–71]. It is one of three TAO family members (TAO1, TAO2 and TAO3), which consist of an N-terminal catalytic domain, a small serine-rich region, and a C-terminal coiled-coil regulatory domain, with different sequence homology [70,72]. Similar to NEK2, the catalytic activity of TAO1 is regulated by the cell cycle because it increases in G2/M phase and declines when the cell exits mitosis [73,74]. The cell cycle

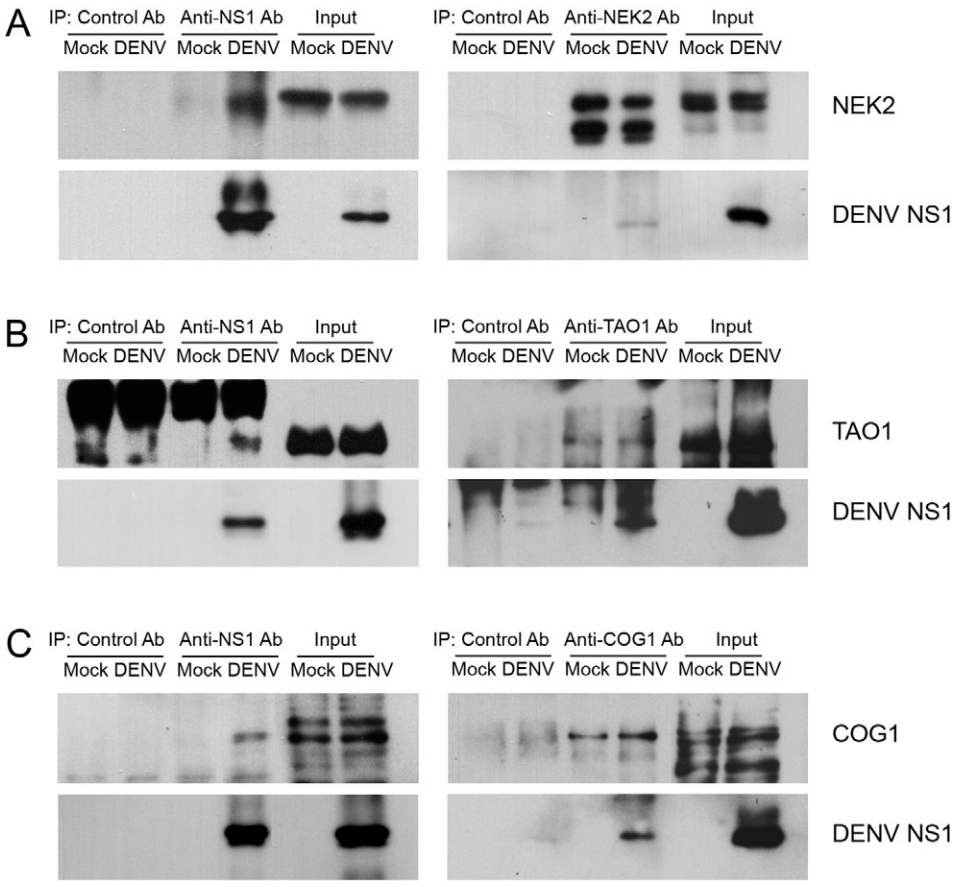

Fig. 5. Coimmunoprecipitation of DENV NS1 and human NEK2, TAO1, and COG1 proteins in DENV-infected cells. Uninfected (Mock) and DENV-infected (DENV) cells were subjected to coimmunoprecipitation assays as described in the Materials and methods. (A) Coimmunoprecipitation of DENV NS1 and human NEK2. (B) Coimmunoprecipitation of DENV NS1 and human TAO1. (C) Coimmunoprecipitation of DENV NS1 and human COG1. Uninfected and DENV-infected cell lysates without immunoprecipitation were included as the controls for the immunoblotting analysis (input).

seems to have some influence on DENV production, depending on the cell type and the DENV serotype, because cell-cycle arrest is observed in DENV-infected cells and certain stages of the cell cycle support high levels of DENV infection and the production of infectious virus [75–77]. TAO1 binds to mitogen-activated protein (MAP)/extracellular signal-regulated protein kinase (ERK) kinase 3 (MEK3), resulting in the activation of the p38 MAP kinase pathway [71]. In addition, TAO1 activates the c-Jun-N-terminal kinase (JNK) and stimulates the cleavage of Rho kinase 1 (ROCK1) and caspase 3, inducing apoptotic morphological changes [78,79]. All three subgroups of the MAPK pathway, including the ERK1/2, JNK, and p38 cascades, are activated following DENV infection and play important roles in virus production and the virus-induced inflammatory response [80,81]. These findings suggest that TAO1, in association with DENV NS1, may have a role in DENV production and the host cell responses to DENV infection, possibly by controlling the cell cycle, the MAPK pathway and apoptosis. TAO1 also acts as a microtubule affinity-regulating kinase kinase (MARKK), which regulates microtubule dynamics that can be controlled by signals from the actin cytoskeletal network to maintain microtubule stability [70,82,83]. Alterations in the actin cytoskeleton assembly have been observed in DENV-infected cells and are possibly involved in the pathogenesis of dengue diseases [84]. Therefore, it is tempting to speculate that the association between microtubule dynamics and the actin cytoskeletal network is influenced by the DENV NS1–TAO1 interaction.

COG1, previously known as LDLB, is a 109-kDa host cell protein that is a central component required for the normal assembly, processing, and stability of the conserved oligomeric Golgi (COG) complex, which comprises eight distinct subunits (COG1–COG8) [85–88]. COG1 localizes primarily in peri-Golgi vesicles, Golgi cisternal rims, and associated vesicles, and to a lesser extent, in the cytoplasm and flattened Golgi cisternal membranes [89]. The COG complex is essential for establishing and maintaining the Golgi structure and function [90], regulates the glycosylation of glycoproteins and glycolipids [91], and is involved in the retrograde vesicular transport of Golgi-resident proteins within the Golgi apparatus [86,92]. In DENV-infected cells, DENV NS1 protein is initially synthesized as a monomer, subsequently becomes a homodimer, and undergoes glycan modification while it is transported along the host secretory pathway before its release into the extracellular milieu as a hexameric lipoprotein [13–16]. It also associates with lipid rafts on the host cell membrane [17]. It is feasible that the interaction between the COG1 protein and DENV NS1 is involved in the glycosylation of viral NS1 or its associated lipid components to maintain the functions of DENV NS1 in virus-infected cells. Furthermore, the COG complex is crucial for double-membrane vesicle formation during autophagy, and the deletion of COG1 caused the strongest inhibition of nonspecific autophagosome formation when the COG subunits were deleted individually [93]. Autophagosomes have been detected in DENV-infected cells and DENV-induced autophagy promotes efficient DENV replication, possibly through the regulation of the cellular lipid metabolism [94–97]. Therefore, the interaction between COG1 and DENV NS1 may also participate in the control of autophagy and DENV production.

Using an LC–MS/MS analysis, we have identified a set of host cell proteins that interact with DENV NS1 in DENV-infected HepG2 cells, and confirmed the interactions between DENV NS1 and human NEK2, TAO1, and COG1 in virus-infected cells. Whether these host cell proteins

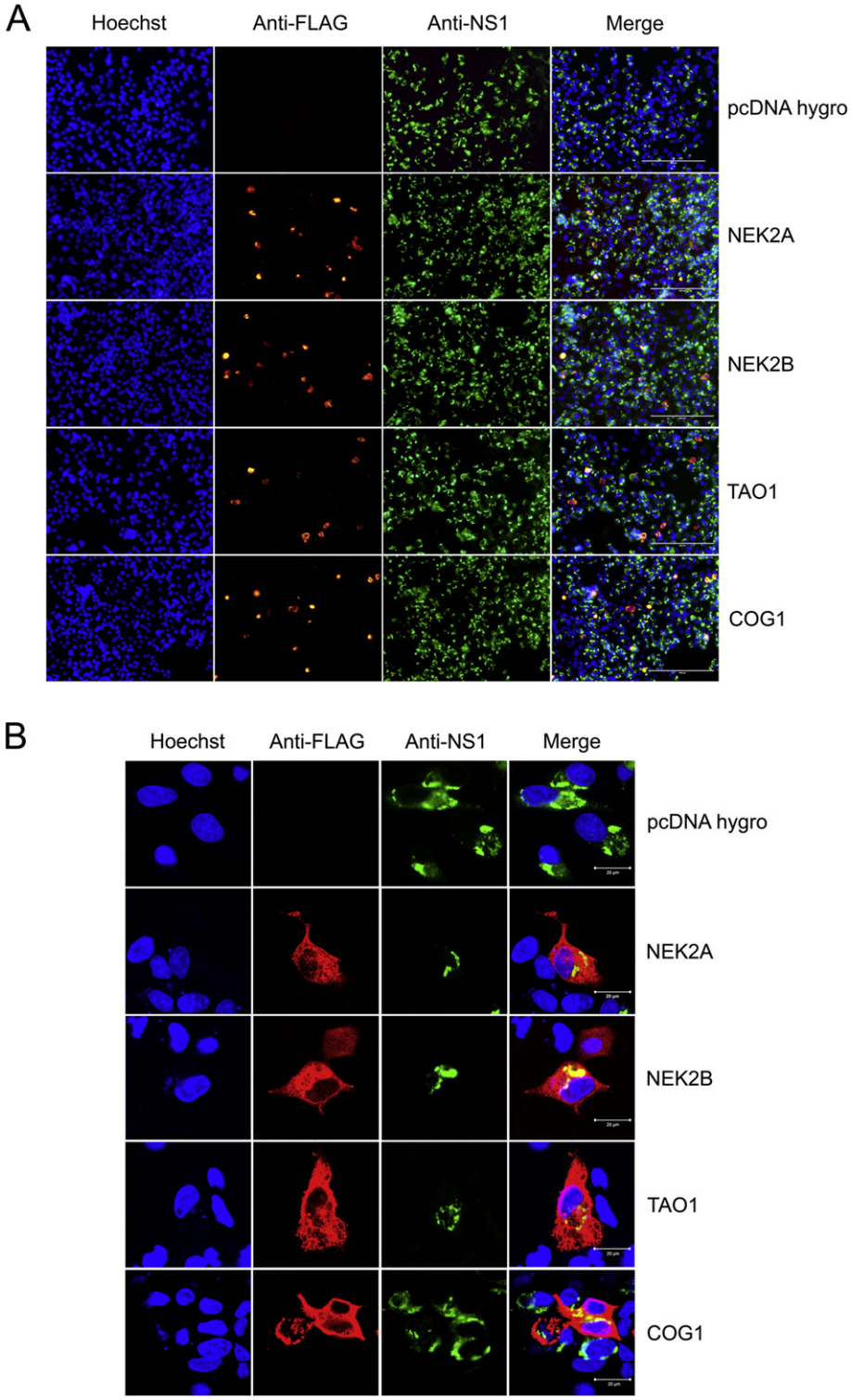

Fig. 6. Colocalization of DENV NS1 and human NEK2, TAO1, and COG1 proteins in DENV-infected cells. DENV-infected HepG2 cells were transfected with the empty pcDNA Hygro vector (vector control) or pcDNA Hygro encoding human NEK2A, NEK2B, TAO1, or COG1 fused to the FLAG tag. At 48 h postinfection, the cells were harvested and subjected to double immunofluorescent staining for human NEK2A, NEK2B, TAO1, or COG1 (red) and DENV NS1 (green), and nuclear staining (blue). Fluorescent images of the stained cells were captured with the EVOS FL Cell Imaging System with a 20× objective lens (A) and a confocal laser-scanning microscope with a 63× objective lens (B). Scale bars in (A) and (B) represent 200 μm and 20 μm, respectively.

interact with DENV NS1 directly or require the presence of other host cell components and/or other viral proteins for their associations in virus-infected cells remains to be investigated. Further studies are required to determine the detailed mechanisms of the DENV NS1-interacting host proteins identified here in the processes related to DENV production and the host cell responses.

5. Conclusions

In this study, we used a combination of techniques, immunoprecipitation, in-solution trypsin digestion, and LC–MS/MS, to investigate the host proteins that interact with DENV NS1 in DENV-infected HepG2 cells. Thirty-six host cell proteins were identified as DENV NS1-

interacting proteins, most of which are involved in binding and catalytic activities, or in cellular metabolism. Human NEK2, TAO1, and COG1 were the three host proteins identified that showed the greatest statistically significant differences (more than 2.5-fold) between the test and control samples, and were confirmed to interact with DENV NS1 in virus-infected cells. The associations between the NEK2 and TAO1 proteins and DENV NS1 may be involved in DENV production, potentially through the regulation of the cell cycle and apoptosis, whereas the interaction of COG1 with DENV NS1 probably facilitates the posttranslational modification and transport of DENV NS1 in virus-infected cells. Our findings demonstrate another novel set of DENV NS1-interacting proteins and the possible importance of NEK2, TAO1, and COG1 in DENV infection. Further research into the functional mechanisms of these host cell proteins in DENV production and the host cell responses is required.

Supplementary data to this article can be found online at http://dx.doi.org/10.1016/j.bbapap.2016.04.008.

Transparency document

The Transparency document associated with this article can be found, in the online version.

Acknowledgments

We would like to thank Dr. Dumrong Mairiang for technical advice on the data analysis. This work was supported by the Thailand Research Fund (TRF) and the National Center for Genetic Engineering and Biotechnology, National Science and Technology Development Agency, Thailand (RSA5480024 and P-11-00765 to S.N.). S.N. and T.L. were TRF Research Scholars. P.Y. was a TRF Senior Research Scholar and was supported by Chalermphrakiat Grant, Faculty of Medicine Siriraj Hospital, Mahidol University.

References

[1] S. Bhatt, P.W. Gething, O.J. Brady, J.P. Messina, A.W. Farlow, C.L. Moyes, et al., The global distribution and burden of dengue, Nature 496 (2013) 504–507.
[2] J.M. Mackenzie, M.K. Jones, P.R. Young, Immunolocalization of the dengue virus nonstructural glycoprotein NS1 suggests a role in viral RNA replication, Virology 220 (1996) 232–240.
[3] I.R. Muylaert, T.J. Chambers, R. Galler, C.M. Rice, Mutagenesis of the N-linked glycosylation sites of the yellow fever virus NS1 protein: effects on virus replication and mouse neurovirulence, Virology 222 (1996) 159–168.
[4] I.R. Muylaert, R. Galler, C.M. Rice, Genetic analysis of the yellow fever virus NS1 protein: identification of a temperature-sensitive mutation which blocks RNA accumulation, J. Virol. 71 (1997) 291–298.
[5] B.D. Lindenbach, C.M. Rice, Trans-complementation of yellow fever virus NS1 reveals a role in early RNA replication, J. Virol. 71 (1997) 9608–9617.
[6] B.D. Lindenbach, C.M. Rice, Genetic interaction of flavivirus nonstructural proteins NS1 and NS4A as a determinant of replicase function, J. Virol. 73 (1999) 4611–4621.
[7] D.A. Muller, P.R. Young, The flavivirus NS1 protein: molecular and structural biology, immunology, role in pathogenesis and application as a diagnostic biomarker, Antivir. Res. 98 (2013) 192–208.
[8] S. Alcon-LePoder, P. Sivard, M.T. Drouet, A. Talarmin, C. Rice, M. Flamand, Secretion of flaviviral non-structural protein NS1: from diagnosis to pathogenesis, Novartis Found. Symp. 277 (2006) 233–247 (discussion 47-53).
[9] P. Avirutnan, N. Punyadee, S. Noisakran, C. Komoltri, S. Thiemmeca, K. Auethavornanan, et al., Vascular leakage in severe dengue virus infections: a potential role for the nonstructural viral protein NS1 and complement, J. Infect. Dis. 193 (2006) 1078–1088.
[10] A.K. Falconar, The dengue virus nonstructural-1 protein (NS1) generates antibodies to common epitopes on human blood clotting, integrin/adhesin proteins and binds to human endothelial cells: potential implications in haemorrhagic fever pathogenesis, Arch. Virol. 142 (1997) 897–916.
[11] I.J. Liu, C.Y. Chiu, Y.C. Chen, H.C. Wu, Molecular mimicry of human endothelial cell antigen by autoantibodies to nonstructural protein 1 of dengue virus, J. Biol. Chem. 286 (2011) 9726–9736.
[12] M.G. Jacobs, P.J. Robinson, C. Bletchly, J.M. Mackenzie, P.R. Young, Dengue virus nonstructural protein 1 is expressed in a glycosyl-phosphatidylinositol-linked form that is capable of signal transduction, FASEB J. 14 (2000) 1603–1610.
[13] G. Winkler, S.E. Maxwell, C. Ruemmler, V. Stollar, Newly synthesized dengue-2 virus nonstructural protein NS1 is a soluble protein but becomes partially hydrophobic and membrane-associated after dimerization, Virology 171 (1989) 302–305.
[14] G. Winkler, V.B. Randolph, G.R. Cleaves, T.E. Ryan, V. Stollar, Evidence that the mature form of the flavivirus nonstructural protein NS1 is a dimer, Virology 162 (1988) 187–196.
[15] M. Flamand, F. Megret, M. Mathieu, J. Lepault, F.A. Rey, V. Deubel, Dengue virus type 1 nonstructural glycoprotein NS1 is secreted from mammalian cells as a soluble hexamer in a glycosylation-dependent fashion, J. Virol. 73 (1999) 6104–6110.
[16] I. Gutsche, F. Coulibaly, J.E. Voss, J. Salmon, J. d'Alayer, M. Ermonval, et al., Secreted dengue virus nonstructural protein NS1 is an atypical barrel-shaped high-density lipoprotein, Proc. Natl. Acad. Sci. U. S. A. 108 (2011) 8003–8008.
[17] S. Noisakran, T. Dechtawewat, P. Avirutnan, T. Kinoshita, U. Siripanyaphinyo, C. Puttikhunt, et al., Association of dengue virus NS1 protein with lipid rafts, J. Gen. Virol. 89 (2008) 2492–2500.
[18] E.G. Westaway, J.M. Mackenzie, M.T. Kenney, M.K. Jones, A.A. Khromykh, Ultrastructure of Kunjin virus-infected cells: colocalization of NS1 and NS3 with double-stranded RNA, and of NS2B with NS3, in virus-induced membrane structures, J. Virol. 71 (1997) 6650–6661.
[19] J.M. Mackenzie, A.A. Khromykh, M.K. Jones, E.G. Westaway, Subcellular localization and some biochemical properties of the flavivirus Kunjin nonstructural proteins NS2A and NS4A, Virology 245 (1998) 203–215.
[20] S. Welsch, S. Miller, I. Romero-Brey, A. Merz, C.K. Bleck, P. Walther, et al., Composition and three-dimensional architecture of the dengue virus replication and assembly sites, Cell Host Microbe 5 (2009) 365–375.
[21] S. Youn, T. Li, B.T. McCune, M.A. Edeling, D.H. Fremont, I.M. Cristea, et al., Evidence for a genetic and physical interaction between nonstructural proteins NS1 and NS4B that modulates replication of West Nile virus, J. Virol. 86 (2012) 7360–7371.
[22] S. Youn, R.L. Ambrose, J.M. Mackenzie, M.S. Diamond, Non-structural protein-1 is required for West Nile virus replication complex formation and viral RNA synthesis, Virol. J. 10 (2013) 339.
[23] S. Alcon, A. Talarmin, M. Debruyne, A. Falconar, V. Deubel, M. Flamand, Enzyme-linked immunosorbent assay specific to dengue virus type 1 nonstructural protein NS1 reveals circulation of the antigen in the blood during the acute phase of disease in patients experiencing primary or secondary infections, J. Clin. Microbiol. 40 (2002) 376–381.
[24] P.R. Young, P.A. Hilditch, C. Bletchly, W. Halloran, An antigen capture enzyme-linked immunosorbent assay reveals high levels of the dengue virus protein NS1 in the sera of infected patients, J. Clin. Microbiol. 38 (2000) 1053–1057.
[25] D.H. Libraty, P.R. Young, D. Pickering, T.P. Endy, S. Kalayanarooj, S. Green, et al., High circulating levels of the dengue virus nonstructural protein NS1 early in dengue illness correlate with the development of dengue hemorrhagic fever, J. Infect. Dis. 186 (2002) 1165–1168.
[26] W.E. Brandt, D. Chiewslip, D.L. Harris, P.K. Russell, Partial purification and characterization of a dengue virus soluble complement-fixing antigen, J. Immunol. 105 (1970) 1565–1568.
[27] J.J. Schlesinger, M.W. Brandriss, J.R. Putnak, E.E. Walsh, Cell surface expression of yellow fever virus non-structural glycoprotein NS1: consequences of interaction with antibody, J. Gen. Virol. 71 (Pt 3) (1990) 593–599.
[28] W. Ruangjirachuporn, S. Boonpucknavig, S. Nimmanitya, Circulating immune complexes in serum from patients with dengue haemorrhagic fever, Clin. Exp. Immunol. 36 (1979) 46–53.
[29] P. Avirutnan, P. Malasit, B. Seliger, S. Bhakdi, M. Husmann, Dengue virus infection of human endothelial cells leads to chemokine production, complement activation, and apoptosis, J. Immunol. 161 (1998) 6338–6346.
[30] P. Avirutnan, L. Zhang, N. Punyadee, A. Manuyakorn, C. Puttikhunt, W. Kasinrerk, et al., Secreted NS1 of dengue virus attaches to the surface of cells via interactions with heparan sulfate and chondroitin sulfate E, PLoS Pathog. 3 (2007) e183.
[31] P. Avirutnan, E. Mehlhop, M.S. Diamond, Complement and its role in protection and pathogenesis of flavivirus infections, Vaccine 26 (Suppl. 8) (2008) I100–I107.
[32] P. Avirutnan, A. Fuchs, R.E. Hauhart, P. Somnuke, S. Youn, M.S. Diamond, et al., Antagonism of the complement component C4 by flavivirus nonstructural protein NS1, J. Exp. Med. 207 (2010) 793–806.
[33] P. Avirutnan, R.E. Hauhart, P. Somnuke, A.M. Blom, M.S. Diamond, J.P. Atkinson, Binding of flavivirus nonstructural protein NS1 to C4b binding protein modulates complement activation, J. Immunol. 187 (2011) 424–433.
[34] J. Chen, M.M. Ng, J.J. Chu, Activation of TLR2 and TLR6 by dengue NS1 protein and its implications in the immunopathogenesis of dengue virus infection, PLoS Pathog. 11 (2015) e1005053.
[35] N. Modhiran, D. Watterson, D.A. Muller, A.K. Panetta, D.P. Sester, L. Liu, et al., Dengue virus NS1 protein activates cells via toll-like receptor 4 and disrupts endothelial cell monolayer integrity, Sci. Transl. Med. 7 (2015) 304ra142.
[36] P.R. Beatty, H. Puerta-Guardo, S.S. Killingbeck, D.R. Glasner, K. Hopkins, E. Harris, Dengue virus NS1 triggers endothelial permeability and vascular leak that is prevented by NS1 vaccination, Sci. Transl. Med. 7 (2015) 304ra141.
[37] J.J. Chua, R. Bhuvanakantham, V.T. Chow, M.L. Ng, Recombinant non-structural 1 (NS1) protein of dengue-2 virus interacts with human STAT3beta protein, Virus Res. 112 (2005) 85–94.
[38] E.M. Silva, J.N. Conde, D. Allonso, M.L. Nogueira, R. Mohana-Borges, Mapping the interactions of dengue virus NS1 protein with human liver proteins using a yeast two-hybrid system: identification of C1q as an interacting partner, PLoS ONE 8 (2013) e57514.
[39] T. Kurosu, P. Chaichana, M. Yamate, S. Anantapreecha, K. Ikuta, Secreted complement regulatory protein clusterin interacts with dengue virus nonstructural protein 1, Biochem. Biophys. Res. Commun. 362 (2007) 1051–1056.
[40] S. Noisakran, S. Sengsai, V. Thongboonkerd, R. Kanlaya, S. Sinchaikul, S.T. Chen, et al., Identification of human hnRNP C1/C2 as a dengue virus NS1-interacting protein, Biochem. Biophys. Res. Commun. 372 (2008) 67–72.

[41] L. Suksanpaisan, A. Cabrera-Hernandez, D.R. Smith, Infection of human primary hepatocytes with dengue virus serotype 2, J. Med. Virol. 79 (2007) 300–307.
[42] A. Couvelard, P. Marianneau, C. Bedel, M.T. Drouet, F. Vachon, D. Henin, et al., Report of a fatal case of dengue infection with hepatitis: demonstration of dengue antigens in hepatocytes and liver apoptosis, Hum. Pathol. 30 (1999) 1106–1110.
[43] F.C. de Macedo, A.F. Nicol, L.D. Cooper, M. Yearsley, A.R. Pires, G.J. Nuovo, Histologic, viral, and molecular correlates of dengue fever infection of the liver using highly sensitive immunohistochemistry, Diagn. Mol. Pathol. 15 (2006) 223–228.
[44] D. Kangwanpong, N. Bhamarapravati, H.L. Lucia, Diagnosing dengue virus infection in archived autopsy tissues by means of the in situ PCR method: a case report, Clin. Diagn. Virol. 3 (1995) 165–172.
[45] K.S. Aye, K. Charngkaew, N. Win, K.Z. Wai, K. Moe, N. Punyadee, et al., Pathologic highlights of dengue hemorrhagic fever in 13 autopsy cases from Myanmar, Hum. Pathol. 45 (2014) 1221–1233.
[46] C. Puttikhunt, W. Kasinrerk, S. Srisa-ad, T. Duangchinda, W. Silakate, S. Moonsom, et al., Production of anti-dengue NS1 monoclonal antibodies by DNA immunization, J. Virol. Methods 109 (2003) 55–61.
[47] E.A. Henchal, J.M. McCown, D.S. Burke, M.C. Seguin, W.E. Brandt, Epitopic analysis of antigenic determinants on the surface of dengue-2 virions using monoclonal antibodies, Am.J.Trop. Med. Hyg. 34 (1985) 162–169.
[48] E.A. Henchal, M.K. Gentry, J.M. McCown, W.E. Brandt, Dengue virus-specific and flavivirus group determinants identified with monoclonal antibodies by indirect immunofluorescence, Am.J.Trop. Med. Hyg. 31 (1982) 830–836.
[49] B. Kaboord, M. Perr, Isolation of proteins and protein complexes by immunoprecipitation, in: A. Posch (Ed.), Methods in Molecular Biology, Vol 424: 2D PAGE: Sample Preparation and Fractionation, Humana Press, New Jersey 2008, pp. 349–364.
[50] T. Dechtawewat, P. Songprakhon, T. Limjindaporn, C. Puttikhunt, W. Kasinrerk, S. Saitornueng, et al., Role of human heterogeneous nuclear ribonucleoprotein C1/C2 in dengue virus replication, Virol. J. 12 (2015) 14.
[51] Y. Benjamini, Y. Hochberg, Controlling the false discovery rate: a practical and powerful approach to multiple testing, J. R. Stat. Soc. 57 (1995) 289–300.
[52] M.I. Salazar, R.M. del Angel, H. Lanz-Mendoza, J.E. Ludert, V. Pando-Robles, The role of cell proteins in dengue virus infection, J. Proteomics 111 (2014) 6–15.
[53] S. Khadka, A.D. Vangeloff, C. Zhang, P. Siddavatam, N.S. Heaton, L. Wang, et al., A physical interaction network of dengue virus and human proteins, Mol. Cell. Proteomics 10 (2011) M111.012187.
[54] D. Mairiang, H. Zhang, A. Sodja, T. Murali, P. Suriyaphol, P. Malasit, et al., Identification of new protein interactions between dengue fever virus and its hosts, human and mosquito, PLoS ONE 8 (2013) e53535.
[55] M. Cervantes-Salazar, A.H. Angel-Ambrocio, R. Soto-Acosta, P. Bautista-Carbajal, A.M. Hurtado-Monzon, S.L. Alcaraz-Estrada, et al., Dengue virus NS1 protein interacts with the ribosomal protein RPL18: this interaction is required for viral translation and replication in Huh-7 cells, Virology 484 (2015) 113–126.
[56] D. Allonso, I.S. Andrade, J.N. Conde, D.R. Coelho, D.C. Rocha, M.L. da Silva, et al., Dengue virus NS1 protein modulates cellular energy metabolism by increasing glyceraldehyde-3-phosphate dehydrogenase activity, J. Virol. 89 (2015) 11871–11883.
[57] V.J. Gauci, E.P. Wright, J.R. Coorssen, Quantitative proteomics: assessing the spectrum of in-gel protein detection methods, J. Chem. Biol. 4 (2011) 3–29.
[58] P. Rellos, F.J. Ivins, J.E. Baxter, A. Pike, T.J. Nott, D.M. Parkinson, et al., Structure and regulation of the human Nek2 centrosomal kinase, J. Biol. Chem. 282 (2007) 6833–6842.
[59] R.S. Hames, A.M. Fry, Alternative splice variants of the human centrosome kinase Nek2 exhibit distinct patterns of expression in mitosis, Biochem. J. 361 (2002) 77–85.
[60] W. Wu, J.E. Baxter, S.L. Wattam, D.G. Hayward, M. Fardilha, A. Knebel, et al., Alternative splicing controls nuclear translocation of the cell cycle-regulated Nek2 kinase, J. Biol. Chem. 282 (2007) 26431–26440.
[61] Y. Lou, J. Yao, A. Zereshki, Z. Dou, K. Ahmed, H. Wang, et al., NEK2A interacts with MAD1 and possibly functions as a novel integrator of the spindle checkpoint signaling, J. Biol. Chem. 279 (2004) 20049–20057.
[62] A.M. Fry, P. Meraldi, E.A. Nigg, A centrosomal function for the human Nek2 protein kinase, a member of the NIMA family of cell cycle regulators, EMBO J. 17 (1998) 470–481.
[63] J. Du, X. Cai, J. Yao, X. Ding, Q. Wu, S. Pei, et al., The mitotic checkpoint kinase NEK2A regulates kinetochore microtubule attachment stability, Oncogene 27 (2008) 4107–4114.
[64] J. Park, K. Rhee, NEK2 phosphorylation antagonizes the microtubule stabilizing activity of centrobin, Biochem. Biophys. Res. Commun. 431 (2013) 302–308.
[65] Y. Chen, D.J. Riley, L. Zheng, P.L. Chen, W.H. Lee, Phosphorylation of the mitotic regulator protein Hec1 by Nek2 kinase is essential for faithful chromosome segregation, J. Biol. Chem. 277 (2002) 49408–49416.
[66] C. Naro, F. Barbagallo, P. Chieffi, C.F. Bourgeois, M.P. Paronetto, C. Sette, The centrosomal kinase NEK2 is a novel splicing factor kinase involved in cell survival, Nucleic Acids Res. 42 (2014) 3218–3227.
[67] Y. Ha Kim, J. Yeol Choi, Y. Jeong, D.J. Wolgemuth, K. Rhee, Nek2 localizes to multiple sites in mitotic cells, suggesting its involvement in multiple cellular functions during the cell cycle, Biochem. Biophys. Res. Commun. 290 (2002) 730–736.
[68] A.M. Fry, S.J. Schultz, J. Bartek, E.A. Nigg, Substrate specificity and cell cycle regulation of the Nek2 protein kinase, a potential human homolog of the mitotic regulator NIMA of *Aspergillus nidulans*, J. Biol. Chem. 270 (1995) 12899–12905.
[69] J.T. Yustein, D. Li, D. Robinson, H.J. Kung, KFC, a Ste20-like kinase with mitogenic potential and capability to activate the SAPK/JNK pathway, Oncogene 19 (2000) 710–718.
[70] T. Timm, X.Y. Li, J. Biernat, J. Jiao, E. Mandelkow, J. Vandekerckhove, et al., MARKK, a Ste20-like kinase, activates the polarity-inducing kinase MARK/PAR-1, EMBO J. 22 (2003) 5090–5101.
[71] M. Hutchison, K.S. Berman, M.H. Cobb, Isolation of TAO1, a protein kinase that activates MEKs in stress-activated protein kinase cascades, J. Biol. Chem. 273 (1998) 28625–28632.
[72] J.T. Yustein, L. Xia, J.M. Kahlenburg, D. Robinson, D. Templeton, H.J. Kung, Comparative studies of a new subfamily of human Ste20-like kinases: homodimerization, subcellular localization, and selective activation of MKK3 and p38, Oncogene 22 (2003) 6129–6141.
[73] R.L. Shrestha, N. Tamura, A. Fries, N. Levin, J. Clark, V.M. Draviam, TAO1 kinase maintains chromosomal stability by facilitating proper congression of chromosomes, Open Biol. 4 (2014) 130108.
[74] R.L. Wojtala, I.A. Tavares, P.E. Morton, F. Valderrama, N.S. Thomas, J.D. Morris, Prostate-derived sterile 20-like kinases (PSKs/TAOKs) are activated in mitosis and contribute to mitotic cell rounding and spindle positioning, J. Biol. Chem. 286 (2011) 30161–30170.
[75] H.L. Su, Y.L. Lin, H.P. Yu, C.H. Tsao, L.K. Chen, Y.T. Liu, et al., The effect of human bcl-2 and bcl-X genes on dengue virus-induced apoptosis in cultured cells, Virology 282 (2001) 141–153.
[76] S. AbuBakar, M.H. Shu, J. Johari, P.F. Wong, Senescence affects endothelial cells susceptibility to dengue virus infection, Int. J. Med. Sci. 11 (2014) 538–544.
[77] W. Phoolcharoen, D.R. Smith, Internalization of the dengue virus is cell cycle modulated in HepG2, but not Vero cells, J. Med. Virol. 74 (2004) 434–441.
[78] C. Zihni, C. Mitsopoulos, I.A. Tavares, A.J. Ridley, J.D. Morris, Prostate-derived sterile 20-like kinase 2 (PSK2) regulates apoptotic morphology via C-Jun N-terminal kinase and Rho kinase-1, J. Biol. Chem. 281 (2006) 7317–7323.
[79] M.F. Wu, S.G. Wang, Human TAO kinase 1 induces apoptosis in SH-SY5Y cells, Cell Biol. Int. 32 (2008) 151–156.
[80] I. Ceballos-Olvera, S. Chavez-Salinas, F. Medina, J.E. Ludert, R.M. del Angel, JNK phosphorylation, induced during dengue virus infection, is important for viral infection and requires the presence of cholesterol, Virology 396 (2010) 30–36.
[81] A. Huerta-Zepeda, C. Cabello-Gutierrez, J. Cime-Castillo, V. Monroy-Martinez, M.E. Manjarrez-Zavala, M. Gutierrez-Rodriguez, et al., Crosstalk between coagulation and inflammation during dengue virus infection, Thromb. Haemost. 99 (2008) 936–943.
[82] C. Johne, D. Matenia, X.Y. Li, T. Timm, K. Balusamy, E.M. Mandelkow, Spred1 and TESK1–two new interaction partners of the kinase MARKK/TAO1 that link the microtubule and actin cytoskeleton, Mol. Biol. Cell 19 (2008) 1391–1403.
[83] I. King, U. Heberlein, Tao kinases as coordinators of actin and microtubule dynamics in developing neurons, Commun. Integr. Biol. 4 (2011) 554–556.
[84] R. Kanlaya, S.N. Pattanakitsakul, S. Sinchaikul, S.T. Chen, V. Thongboonkerd, Alterations in actin cytoskeletal assembly and junctional protein complexes in human endothelial cells induced by dengue virus infection and mimicry of leukocyte transendothelial migration, J. Proteome Res. 8 (2009) 2551–2562.
[85] D.M. Kingsley, K.F. Kozarsky, M. Segal, M. Krieger, Three types of low density lipoprotein receptor-deficient mutant have pleiotropic defects in the synthesis of N-linked, O-linked, and lipid-linked carbohydrate chains, J. Cell Biol. 102 (1986) 1576–1585.
[86] D. Ungar, T. Oka, M. Krieger, F.M. Hughson, Retrograde transport on the COG railway, Trends Cell Biol. 16 (2006) 113–120.
[87] R. Quental, L. Azevedo, R. Matthiesen, A. Amorim, Comparative analyses of the Conserved Oligomeric Golgi (COG) complex in vertebrates, BMC Evol. Biol. 10 (2010) 212.
[88] J.E. Chatterton, D. Hirsch, J.J. Schwartz, P.E. Bickel, R.D. Rosenberg, H.F. Lodish, et al., Expression cloning of LDLB, a gene essential for normal Golgi function and assembly of the ldlCp complex, Proc. Natl. Acad. Sci. U. S. A. 96 (1999) 915–920.
[89] E. Vasile, T. Oka, M. Ericsson, N. Nakamura, M. Krieger, IntraGolgi distribution of the Conserved Oligomeric Golgi (COG) complex, Exp. Cell Res. 312 (2006) 3132–3141.
[90] D. Ungar, T. Oka, E.E. Brittle, E. Vasile, V.V. Lupashin, J.E. Chatterton, et al., Characterization of a mammalian Golgi-localized protein complex, COG, that is required for normal Golgi morphology and function, J. Cell Biol. 157 (2002) 405–415.
[91] I.D. Pokrovskaya, R. Willett, R.D. Smith, W. Morelle, T. Kudlyk, V.V. Lupashin, Conserved oligomeric Golgi complex specifically regulates the maintenance of Golgi glycosylation machinery, Glycobiology 21 (2011) 1554–1569.
[92] J.R. Whyte, S. Munro, Vesicle tethering complexes in membrane traffic, J. Cell Sci. 115 (2002) 2627–2637.
[93] W.L. Yen, T. Shintani, U. Nair, Y. Cao, B.C. Richardson, Z. Li, et al., The conserved oligomeric Golgi complex is involved in double-membrane vesicle formation during autophagy, J. Cell Biol. 188 (2010) 101–114.
[94] Y.R. Lee, H.Y. Lei, M.T. Liu, J.R. Wang, S.H. Chen, Y.F. Jiang-Shieh, et al., Autophagic machinery activated by dengue virus enhances virus replication, Virology 374 (2008) 240–248.
[95] N.S. Heaton, G. Randall, Dengue virus-induced autophagy regulates lipid metabolism, Cell Host Microbe 8 (2010) 422–432.
[96] A. Khakpoor, M. Panyasrivanit, N. Wikan, D.R. Smith, A role for autophagolysosomes in dengue virus 3 production in HepG2 cells, J. Gen. Virol. 90 (2009) 1093–1103.
[97] M. Panyasrivanit, A. Khakpoor, N. Wikan, D.R. Smith, Co-localization of constituents of the dengue virus translation and replication machinery with amphisomes, J. Gen. Virol. 90 (2009) 448–456.

Biochemical and Biophysical Research Communications 483 (2017) 58–63

Contents lists available at ScienceDirect

Biochemical and Biophysical Research Communications

journal homepage: www.elsevier.com/locate/ybbrc

Tyrosine kinase/phosphatase inhibitors decrease dengue virus production in HepG2 cells

Thawornchai Limjindaporn [a, *], Jutatip Panaampon [a], Shilu Malakar [b], Sansanee Noisakran [c], Pa-thai Yenchitsomanus [d]

[a] Department of Anatomy, Faculty of Medicine Siriraj Hospital, Mahidol University, Bangkok, Thailand
[b] Graduate Program in Immunology, Department of Immunology, Faculty of Medicine Siriraj Hospital, Mahidol University, Bangkok, Thailand
[c] Medical Biotechnology Unit, National Center for Genetic Engineering and Biotechnology, National Science and Technology Development Agency, Bangkok, Thailand
[d] Division of Molecular Medicine, Department of Research and Development, Faculty of Medicine Siriraj Hospital, Mahidol University, Bangkok, Thailand

ARTICLE INFO

Article history:
Received 16 December 2016
Accepted 3 January 2017
Available online 5 January 2017

Keywords:
Epidermal growth factor receptor inhibitor
Protein tyrosine phosphatase inhibitor
Antiviral activity
Dengue virus
HepG2 cells

ABSTRACT

Dengue virus is the causative agent of dengue fever, dengue hemorrhagic fever, and dengue shock syndrome. High rates of dengue virus replication and virion production are related to disease severity. To identify anti-DENV compounds, we performed cell-based ELISA testing to detect the level of DENV E protein expression. Among a total of 83 inhibitors, eight were identified as inhibitors with antiviral activity. Epidermal growth factor receptor inhibitor II (EGFR/ErbB-2/ErbB-4 inhibitor II) and protein tyrosine phosphatase inhibitor IV (PTP inhibitor IV) significantly inhibited dengue virus production and demonstrated low toxicity in hepatocyte cell lines. Our results suggest the efficacy of tyrosine kinase/phosphatase inhibitors in decreasing dengue virus production in HepG2 cells.

1. Introduction

Dengue virus (DENV), a virus that is endemic to tropical and subtropical regions, is one of the most important mosquito-borne viruses that infects humans. There are an estimated 390 million DENV infections annually [1]. Clinical manifestations of DENV infection include dengue fever, dengue hemorrhagic fever, and dengue shock syndrome. Hepatic dysfunction is an important clinical feature of DENV infection [2–5]. DENV RNA can be detected in post-mortem liver tissues by reverse transcriptase polymerase chain reaction [6]. Enhanced viral replication and viremia are suspected of causing more severe illness in DENV infection [7]. Previous studies have shown that DENV replicates in hepatic tissue, both in mouse models [8] and humans [9].

Protein kinases and phosphatases are key regulators of cellular function and they constitute one of the largest and most functionally diverse gene families. Of the 518 human protein kinases, several are involved in viral replication, such as influenza A and B viruses [10,11], measles virus [12,13], hepatitis C virus (HCV) [14], coxsackievirus [15], and hepatitis B virus [16]. Genistein, a protein tyrosine kinase inhibitor, was previously shown to inhibit replication of HIV-1 [17], herpes simplex virus-1 [18], and arenavirus [19]. Recent advances have shown that the protein tyrosine phosphatase (PTP) family of enzymes, such as PTP1B, protein tyrosine phosphatase SHP1, and protein tyrosine phosphatase SHP2, are involved in the etiology of several human diseases, including cancer [20,21], diabetes [22,23], and infection [24,25]. PTP1B was also shown to be a target for antiviral therapy [26].

In this work, we selected a tyrosine kinase/phosphatase inhibitor library containing 83 inhibitors to identify the inhibitors that can diminish DENV infection in HepG2 cells. Eight inhibitors were identified as being inhibitors of viral replication. We found that EGFR/ErbB-2/ErbB-4 inhibitor II and PTP inhibitor IV can decrease DENV production in hepatocyte cell lines.

2. Materials and methods

2.1. Cell culture and DENV infection in HepG2 cells

HepG2 cells (ATCC® HB 8065™) were cultured in Dulbecco's Modified Eagle's Medium (DMEM) (Gibco; Thermo Fisher Scientific,

* Corresponding author. Department of Anatomy, Faculty of Medicine Siriraj Hospital, Mahidol University, 2 Wanglang Road, Bangkoknoi, Bangkok 10700, Thailand.
E-mail address: thawornchai.lim@mahidol.ac.th (T. Limjindaporn).

http://dx.doi.org/10.1016/j.bbrc.2017.01.006
0006-291X/

Inc., Waltham, MA, USA), supplemented with 10% heat-inactivated fetal bovine serum (FBS), 2 mM L-glutamine, 1% non-essential amino acids, 1 mM sodium pyruvate, and 100 U/ml penicillin and streptomycin at 37 °C in a humidified atmosphere containing 5% CO_2 for 1 day before infection with DENV serotype 2 (DENV-2) strain 16681 at a multiplicity of infection (MOI) of 5. After DENV infection, HepG2 cells were grown in DMEM supplemented with 2% heat-inactivated FBS, 2 mM L-glutamine, 1% non-essential amino acids, 1 mM sodium pyruvate, and 100 U/ml penicillin and streptomycin at 37 °C in a humidified atmosphere containing 5% CO_2.

2.2. Antibodies

Supernatant from 4G2 hybridoma cell (HB-112, ATCC, USA) culture was collected for anti-DENV E antibody testing. Horseradish peroxidase (HRP)-conjugated rabbit anti-mouse antibody and HRP-conjugated swine anti-rabbit antibody were purchased from Dako (Glostrup, Denmark).

2.3. Screening of the tyrosine kinase and phosphatase inhibitor library

HepG2 cells were seeded on a 96-well plate at 20,000 cells/well and incubated at 37 °C in 5% CO_2 for 1 day. The cells were infected with DENV-2 at a MOI of 5 for 2 h. Unbound virus was removed by washing twice with 1 × DMEM. DENV-infected HepG2 cells were incubated with tyrosine kinase and phosphatase inhibitors (Calbiochem, Darmstadt, Germany) at 37 °C in 5% CO_2 for 48 h. The InhibitorSelect 96-Well Protein Tyrosine Kinase & Protein Tyrosine Phosphatase Inhibitor Library IV consists of 83 pharmacologically active and potent protein kinase and phosphatase inhibitors. An equal volume of DMSO (Sigma-Aldrich Corporation, St. Louis, MO, USA) was used as a vehicle control. All tyrosine kinase/phosphatase inhibitors were diluted 1:1000 before being added to DENV-infected HepG2 cells. After 48 h of incubation, cell viability assay and cell-based ELISA were performed.

2.4. Cell viability assay

Prestoblue cell viability assay (Invitrogen, Grand Island, NY, USA) was performed in compound treated and untreated DENV-infected HepG2 cells in a 96-well assay plate. PrestoBlue reagent was added to the HepG2 cells and incubated at 37 °C for 45 min with avoidance of light. Dual absorbance was measured at 570/595 nm. Mock-infected HepG2 cells were used as the absorbance baseline. For percentage cell viability, experiment data were compared with mock-infected HepG2 cell data (cell control) using the following formula:

$$\text{cell viability} = 100 \times \frac{(\text{OD570} - \text{OD595})\text{experiment}}{(\text{OD570} - \text{OD595})\text{cell control}}$$

[(OD) experiment = average absorbance of DENV-infected HepG2 cells; and, (OD) cell control = average absorbance of mock-infected HepG2 cells].

2.5. Cell-based ELISA

HepG2 cell monolayers were fixed with 3.6% formaldehyde and permeabilized with 1% Triton-X. Three percent (3%) H_2O_2 was then added to the wells to block endogenous peroxidase for 45 min at room temperature. Cell monolayers were incubated with 4G2 antibody (anti-DENV E protein), followed by the secondary antibody conjugated with HRP. After adding 3,3′,5,5,-tetramethylbenzidine (Invitrogen, Camarillo, CA, USA), H_2SO_4 was added to stop the reaction. The plate was read at 450 nm. For percentage of viral infection, experiment data were compared with DENV-infected HepG2 cell data (virus control) using the following formula:

$$\%\text{viral infection} = 100 \times \frac{(\text{OD of experiment} - \text{OD of cell control})}{(\text{OD of virus control} - \text{OD of cell control})}$$

[(OD) experiment = absorbance of DENV-infected HepG2 cells that were treated with tyrosine kinase and phosphatase inhibitors; (OD) virus control = absorbance of DENV-infected HepG2 cells; and, (OD) cell control = absorbance of mock-infected HepG2 cells].

2.6. Real-time reverse transcriptase polymerase chain reaction

A total of 3×10^5 HepG2 cells were seeded into a 12-well plate and incubated at 37 °C in 5% CO_2 for 1 day. Cells were infected with DENV-2 at a MOI of 5 for 2 h. Unbound virus was removed by washing twice with 1 × DMEM. DENV-infected HepG2 cells were incubated with 10 μM tyrosine kinase and phosphatase inhibitors (Calbiochem) at 37 °C in 5% CO_2 for 48 h. An equal volume of DMSO was used as a vehicle control. Total RNA from cell pellets was extracted using a High Pure RNA Isolation Kit (Roche Diagnostics, Mannheim, Germany). Total RNA was reverse-transcribed into cDNA using SuperScript III First Strand Synthesis Kit (Invitrogen). GAPDH was used as a housekeeping gene for each sample. D2L and D2R primers were used to detect the DENV genome. Amplification was monitored using SYBR Green I Reaction Mix (Roche Diagnostics) in a Roche Light Cycler 480 system (Roche Applied Science). The *Ct* of each mRNA and GAPDH control was measured. The relative expression values ($2^{-\Delta\Delta Ct}$) between untreated DENV-infected HepG2 cells and inhibitor-treated DENV-infected HepG2 cells were determined.

2.7. Immunofluorescent assay

HepG2 cell monolayers were grown on coverslips. Cells were fixed with 3.6% formaldehyde and permeabilized using 0.2% Triton-X. Ten percent (10%) FBS was then added to the wells to block nonspecific protein for 30 min at room temperature. Cell monolayers were incubated with the 4G2 antibody (anti-DENV E protein), followed by incubation with the secondary antibody (Alexa-Fluor-488-conjugated goat anti-mouse antibody). Hoechst 33342 was used to stain cell nuclei. Coverslips were mounted using 50% glycerol. The images were captured by fluorescent microscopy.

2.8. Focus forming unit (FFU) assay

A total of 3×10^4 Vero cells were seeded into a 96-well plate and incubated at 37 °C in 5% CO_2 for 1 day. Serial 10-fold dilutions of viral supernatant were added to the Vero cells. The cells were incubated for 2 h and overlaid with 1.5% gum tragacanth containing 2% FBS in minimal essential medium before further incubation at 37 °C for 72 h. Vero cell monolayers were fixed with 3.6% formaldehyde and permeabilized using 1% Triton-X. Cell monolayers were incubated with 4G2 antibody (anti-DENV E protein), followed by incubation with secondary antibody conjugated with HRP. After adding 3,3′-diaminobenzidine, the plate was incubated at room temperature for 10 min. The plate was then washed twice with PBS. Finally, stained foci were visible and counted under light microscopy to determine the number of extracellular virions.

2.9. Statistical analysis

Results are presented as mean ± standard error of the mean (SEM) using data obtained from three independent experiments.

Statistical differences between groups were tested with one-way analysis of variance (ANOVA) using Dunnett's test and GraphPad Prism version 5 (GraphPad Software, Inc., La Jolla, CA, USA). A p-value<0.05 was regarded as being statistically significant for all tests.

3. Results

3.1. Identification of tyrosine kinase/phosphatase inhibitors with anti-DENV activity

In the primary screening, percentage cell viability was assessed by PrestoBlue cell viability assay. The percentage of DENV E expression was assessed by cell-based ELISA. Viral envelope protein in DENV-infected HepG2 cells was detected using specific antibody 4G2. Eight compounds showed an inhibitory effect on DENV E expression, while percentage cell viability was not decreased compared to that of DENV-infected HepG2 cells (Fig. 1A and B). EGFR/ErbB-2/ErbB-4 inhibitor II and PTP inhibitor IV (Fig. 2A and B) were selected for further investigation, as they decreased DENV E expression by ~50% without affecting cell viability (compared with that of DENV infection). As shown in dose response curves (Fig. 2C and D), DENV E expression in HepG2 cells was inhibited in a dose-dependent manner after treatment with EGFR/ErbB-2/ErbB-4 inhibitor II and PTP inhibitor IV. The IC50 (half

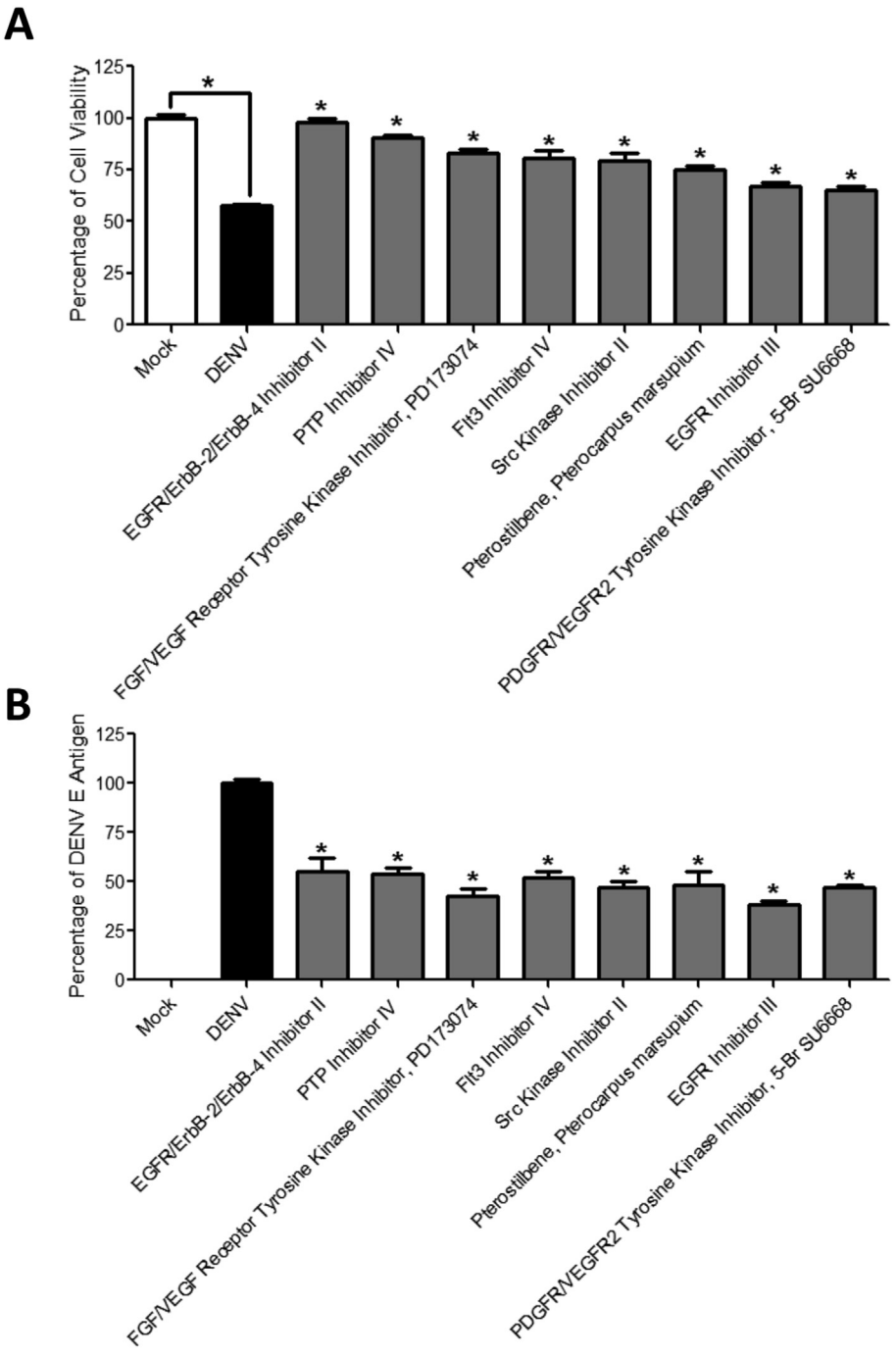

Fig. 1. Candidate antiviral compounds from primary screening. Eight inhibitors were selected from primary screening with 75% cutoff in <75% viral antigen: (A) Percentage of cell viability; and, (B) Percentage of DENV E antigen. Results were derived from data from three independent experiments.

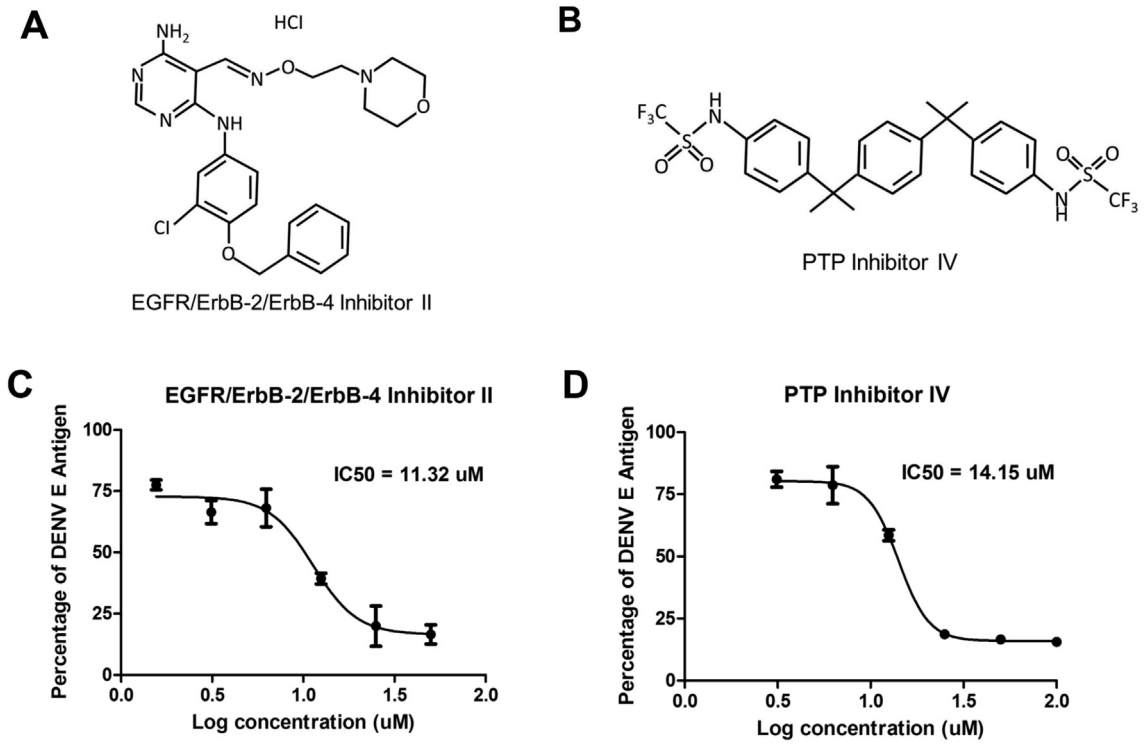

Fig. 2. Chemical structures and inhibitory effects of EGFR/ErbB-2/ErbB-4 inhibitor II and PTP inhibitor IV. (A) EGFR/ErbB-2/ErbB-4 inhibitor II; (B) Protein Tyrosine Phosphatase inhibitor IV; (C) IC50 of EGFR/ErbB-2/ErbB-4 inhibitor II; and, (D) IC50 of PTP inhibitor IV.

maximal inhibitory concentration) of EGFR/ErbB-2/ErbB-4 inhibitor II and PTP inhibitor IV was demonstrated as 11.32 μM and 14.15 μM, respectively. Synthesis of DENV proteins in HepG2 cells was then confirmed by immunofluorescent assay (IFA). As shown in Fig. 3, envelope protein of DENV-infected cells was decreased after treatment with EGFR/ErbB-2/ErbB-4 inhibitor II and PTP inhibitor IV.

3.2. EGFR/ErbB-2/ErbB-4 inhibitor II and PTP inhibitor IV inhibited DENV RNA synthesis, protein synthesis, and DENV production

DENV infection comprises several steps, including attachment and entry, fusion and uncoating, protein translation and RNA replication, and assembly and exocytosis [27]. In this study, we set

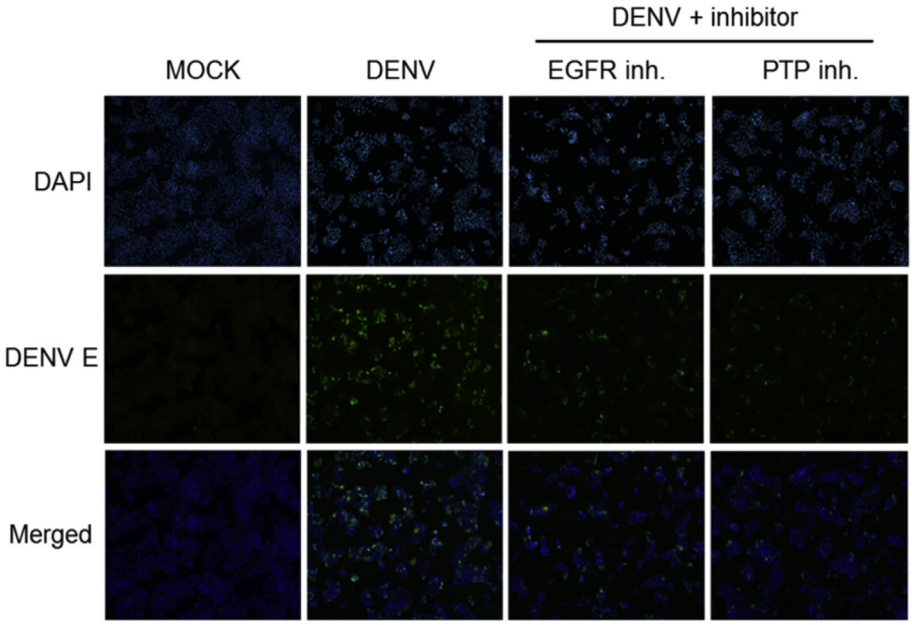

Fig. 3. Immunofluorescent staining of DENV E-expressing cells. HepG2 cells were incubated with DENV-2 strain 16681 at MOI 5 for 2 h. Unbound virus was removed by washing with serum-free medium. HepG2 cells were incubated with inhibitors. DENV E protein was detected by IFA at 48 hpi. 4G2 antibody was used to detect DENV E protein. Hoechst 33342 was used to stain cell nuclei.

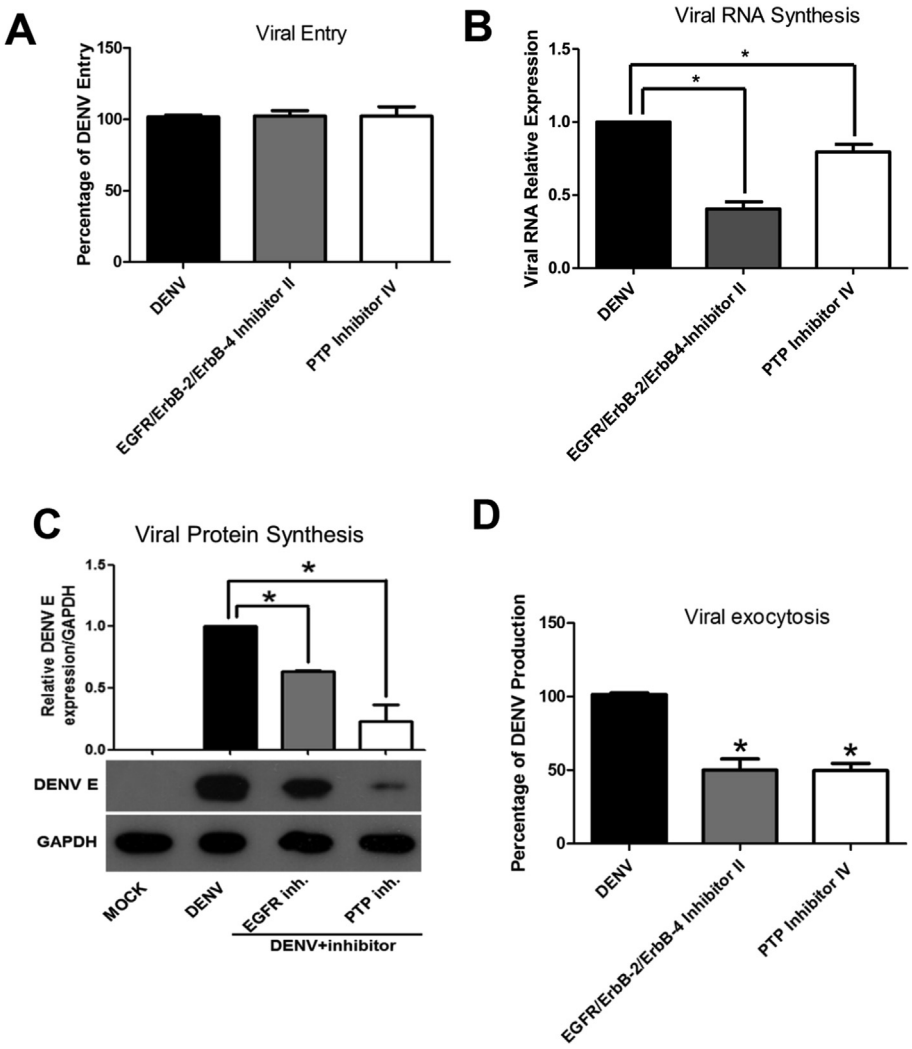

Fig. 4. EGFR/ErbB-2/ErbB-4 inhibitor II and PTP inhibitor IV reduced DENV RNA synthesis, protein synthesis, and DENV production. (A) HepG2 cells were incubated with DENV-2 strain 16681 at MOI 5 and inhibitors for 2 h. The mixture was removed by washing with serum-free medium, and maintenance medium was added. DENV E protein was detected by ELISA at 48 h post-infection (hpi). (B) HepG2 cells were incubated with DENV-2 strain 16681 at MOI 5 and inhibitors for 48 h. DENV intracellular RNA was detected at 48 hpi. (C) HepG2 cells were incubated with DENV-2 strain 16681 at MOI 5 and inhibitors for 48 h. Unbound virus was removed by washing with serum-free medium. DENV-infected HepG2 cells were incubated with inhibitors. DENV E protein was detected by Western blotting at 48 hpi. (E) Percentage of infectious virions was determined by FFU assay. Supernatant was collected from untreated and inhibitor-treated DENV-infected HepG2 cells at 48 hpi.

forth to establish whether or not EGFR/ErbB-2/ErbB-4 inhibitor II and PTP inhibitor IV affects DENV entry. We found that the percentage of DENV entry was not decreased by treatment with EGFR/ErbB-2/ErbB-4 inhibitor II or PTP inhibitor IV (Fig. 4A). Intracellular RNA was extracted from treated and untreated cells to determine the effect of EGFR/ErbB-2/ErbB-4 inhibitor II and PTP inhibitor IV on DENV RNA replication. Interestingly, we observed a statistically significant reduction in DENV RNA among inhibitor-treated cells compared with untreated cells (Fig. 4B). These results suggest that EGFR/ErbB-2/ErbB-4 inhibitor II and PTP inhibitor IV had no effect on DENV binding and entry, but they affected DENV RNA synthesis. Reduction in DENV protein level after compound treatment was shown by Western blot analysis (Fig. 4C). We also performed an FFU assay to measure the level of extracellular virus production. Serial 10-fold dilutions of supernatant from inhibitor-treated and untreated cells were incubated with Vero cells. Cells treated with EGFR/ErbB-2/ErbB-4 inhibitor II and PTP inhibitor IV had 50% and 49.7% of infectious virions, respectively, as compared to the proportion of virions observed in the untreated group (Fig. 4D).

4. Discussion

Kinase and phosphatase inhibitors were used in this study to clarify the mechanism of anti-viral activity. Epidermal growth factor receptor (EGFR) and EphA2 were previously shown to be host factors for entry of hepatitis C virus entry, which is one of the members of the Flaviviridae family [28]. Host tyrosine C-terminal Src kinase (Csk) was identified as being involved in DENV replication via regulation of Src family kinase (SFK) [29]. The assembly of dengue virions is inhibited by disatinib, a c-Src protein kinase inhibitor [30]. Inhibition of EGFR signaling impairs phosphorylated STAT3 level, which leads to enhancement of interferon response gene (IRG) expression and antiviral activity [31]. The kinase inhibitor SFV785 prevents the recruitment and assembly of nucleocapsids in the endoplasmic reticulum during DENV assembly thereby decreasing infectious virion production [32]. PTP inhibitor IV is an uncharged, 1,4-di-substituted, phenyl-linked *bis*-trifluoromethylsulfonamido phosphate mimetic that acts as a potent, reversible, competitive, and active-site-directed inhibitor of protein tyrosine phosphatases

(SHP-2, PTP1B, PTP-ε, PTP-Meg-2, PTP-ς, PTP-β, and PTP-μ). Zhang et al. published important evidence regarding the role of SHP-2 PTP in receptor-tyrosine-kinase-mediated ERK1/2 activation via Src kinases [33]. PTP1B regulates IFNAR1 endocytosis and is a target for antiviral therapy [26]. In conclusion, the results of this study suggest that EGFR/ErbB-2/ErbB-4 inhibitor II and PTP inhibitor IV demonstrate anti-DENV replication activities during the DENV RNA synthesis step, which leads to reduction in DENV protein synthesis and decrease in new DENV virion production.

Acknowledgments

This work is supported by Mahidol University Grant No. R015810002 to TL, who is a Thailand Research Fund (TRF) Scholar. The authors gratefully acknowledge Aroonroong Sutthitheptumrong and Natapol Duangtum for technical assistance.

Transparency document

Transparency document related to this article can be found online at http://dx.doi.org/10.1016/j.bbrc.2017.01.006.

References

[1] S. Bhatt, P.W. Gething, O.J. Brady, J.P. Messina, A.W. Farlow, C.L. Moyes, J.M. Drake, J.S. Brownstein, A.G. Hoen, O. Sankoh, M.F. Myers, D.B. George, T. Jaenisch, G.R. Wint, C.P. Simmons, T.W. Scott, J.J. Farrar, S.I. Hay, The global distribution and burden of dengue, Nature 496 (2013) 504–507.
[2] S.B. Halstead, Dengue, Lancet 370 (2007) 1644–1652.
[3] S.L. Seneviratne, G.N. Malavige, H.J. de Silva, Pathogenesis of liver involvement during dengue viral infections, Trans. R. Soc. Trop. Med. Hyg. 100 (2006) 608–614.
[4] A. Roy, D. Sarkar, S. Chakraborty, J. Chaudhuri, P. Ghosh, S. Chakraborty, Profile of hepatic involvement by dengue virus in dengue infected children, N. Am. J. Med. Sci. 5 (2013) 480–485.
[5] D.T. Trung, T.T. Thao le, T.T. Hien, N.T. Hung, N.N. Vinh, P.T. Hien, N.T. Chinh, C. Simmons, B. Wills, Liver involvement associated with dengue infection in adults in Vietnam, Am. J. Trop. Med. Hyg. 83 (2010) 774–780.
[6] L. Rosen, M.T. Drouet, V. Deubel, Detection of dengue virus RNA by reverse transcription-polymerase chain reaction in the liver and lymphoid organs but not in the brain in fatal human infection, Am. J. Trop. Med. Hyg. 61 (1999) 720–724.
[7] D.W. Vaughn, S. Green, S. Kalayanarooj, B.L. Innis, S. Nimmannitya, S. Suntayakorn, T.P. Endy, B. Raengsakulrach, A.L. Rothman, F.A. Ennis, A. Nisalak, Dengue viremia titer, antibody response pattern, and virus serotype correlate with disease severity, J. Infect. Dis. 181 (2000) 2–9.
[8] M.V. Paes, H.L. Lenzi, A.C. Nogueira, G.J. Nuovo, A.T. Pinhao, E.M. Mota, C.A. Basilio-de-Oliveira, H. Schatzmayr, O.M. Barth, A.M. Alves, Hepatic damage associated with dengue-2 virus replication in liver cells of BALB/c mice, Lab. Investig. 89 (2009) 1140–1151.
[9] M.R. Huerre, N.T. Lan, P. Marianneau, N.B. Hue, H. Khun, N.T. Hung, N.T. Khen, M.T. Drouet, V.T. Huong, D.Q. Ha, Y. Buisson, V. Deubel, Liver histopathology and biological correlates in five cases of fatal dengue fever in Vietnamese children, Virchows Arch. 438 (2001) 107–115.
[10] N. Kumar, N.R. Sharma, H. Ly, T.G. Parslow, Y. Liang, Receptor tyrosine kinase inhibitors that block replication of influenza a and other viruses, Antimicrob. Agents Chemother. 55 (2011) 5553–5559.
[11] N. Kumar, Y. Liang, T.G. Parslow, Y. Liang, Receptor tyrosine kinase inhibitors block multiple steps of influenza a virus replication, J. Virol. 85 (2011) 2818–2827.
[12] M. Carsillo, D. Kim, S. Niewiesk, Role of AKT kinase in measles virus replication, J. Virol. 84 (2010) 2180–2183.
[13] M. Vijayan, Y.J. Seo, C.J. Pritzl, S.A. Squires, S. Alexander, B. Hahm, Sphingosine kinase 1 regulates measles virus replication, Virol 450-451 (2014) 55–63.
[14] K. Goto, W. Lin, L. Zhang, N. Jilg, R.X. Shao, E.A. Schaefer, H. Zhao, D.N. Fusco, L.F. Peng, N. Kato, R.T. Chung, The AMPK-related kinase SNARK regulates hepatitis C virus replication and pathogenesis through enhancement of TGF-beta signaling, J. Hepatol. 59 (2013) 942–948.
[15] C.J. Lowenstein, Integrin-linked kinase plays a key role in coxsackievirus replication, Circ. Res. 99 (2006) 346–347.
[16] N.P. Klein, M.J. Bouchard, L.H. Wang, C. Kobarg, R.J. Schneider, Src kinases involved in hepatitis B virus replication, EMBO J. 18 (1999) 5019–5027.
[17] T.S. Stantchev, I. Markovic, W.G. Telford, K.A. Clouse, C.C. Broder, The tyrosine kinase inhibitor genistein blocks HIV-1 infection in primary human macrophages, Virus Res. 123 (2007) 178–189.
[18] Y. Yura, H. Yoshida, M. Sato, Inhibition of herpes simplex virus replication by genistein, an inhibitor of protein-tyrosine kinase, Arch. Virol. 132 (1993) 451–461.
[19] E.M. Vela, G.C. Bowick, N.K. Herzog, J.F. Aronson, Genistein treatment of cells inhibits arenavirus infection, Antivir. Res. 77 (2008) 153–156.
[20] M. Bentires-Alj, B.G. Neel, Protein-tyrosine phosphatase 1B is required for HER2/Neu-induced breast cancer, Cancer Res. 67 (2007) 2420–2424.
[21] G. Chan, D. Kalaitzidis, B.G. Neel, The tyrosine phosphatase Shp2 (PTPN11) in cancer, Cancer Metastasis Rev. 27 (2008) 179–192.
[22] M. Elchebly, P. Payette, E. Michaliszyn, W. Cromlish, S. Collins, A.L. Loy, D. Normandin, A. Cheng, J. Himms-Hagen, C.C. Chan, C. Ramachandran, M.J. Gresser, M.L. Tremblay, B.P. Kennedy, Increased insulin sensitivity and obesity resistance in mice lacking the protein tyrosine phosphatase-1B gene, Science 283 (1999) 1544–1548.
[23] L.D. Klaman, O. Boss, O.D. Peroni, J.K. Kim, J.L. Martino, J.M. Zabolotny, N. Moghal, M. Lubkin, Y.B. Kim, A.H. Sharpe, A. Stricker-Krongrad, G.I. Shulman, B.G. Neel, B.B. Kahn, Increased energy expenditure, decreased adiposity, and tissue-specific insulin sensitivity in protein-tyrosine phosphatase 1B-deficient mice, Mol. Cell Biol. 20 (2000) 5479–5489.
[24] P.T. Massa, S.L. Ropka, S. Saha, K.L. Fecenko, K.L. Beuler, Critical role for protein tyrosine phosphatase SHP-1 in controlling infection of central nervous system glia and demyelination by Theiler's murine encephalomyelitis virus, J. Virol. 76 (2002) 8335–8346.
[25] G. Forget, D.J. Gregory, L.A. Whitcombe, M. Olivier, Role of host protein tyrosine phosphatase SHP-1 in Leishmania donovani-induced inhibition of nitric oxide production, Infect. Immun. 74 (2006) 6272–6279.
[26] C.J. Carbone, H. Zheng, S. Bhattacharya, J.R. Lewis, A.M. Reiter, P. Henthorn, Z.Y. Zhang, D.P. Baker, R. Ukkiramapandian, K.K. Bence, S.Y. Fuchs, Protein tyrosine phosphatase 1B is a key regulator of IFNAR1 endocytosis and a target for antiviral therapies, Proc. Natl. Acad. Sci. U. S. A. 109 (2012) 19226–19231.
[27] S. Mukhopadhyay, R.J. Kuhn, M.G. Rossmann, A structural perspective of the flavivirus life cycle, Nat. Rev. Microbiol. 3 (2005) 13–22.
[28] J. Lupberger, M.B. Zeisel, F. Xiao, C. Thumann, I. Fofana, L. Zona, C. Davis, C.J. Mee, M. Turek, S. Gorke, C. Royer, B. Fischer, M.N. Zahid, D. Lavillette, J. Fresquet, F.L. Cosset, S.M. Rothenberg, T. Pietschmann, A.H. Patel, P. Pessaux, M. Doffoel, W. Raffelsberger, O. Poch, J.A. McKeating, L. Brino, T.F. Baumert, EGFR and EphA2 are host factors for hepatitis C virus entry and possible targets for antiviral therapy, Nat. Med. 17 (2011) 589–595.
[29] R. Kumar, T. Agrawal, N.A. Khan, Y. Nakayama, G.R. Medigeshi, Identification and characterization of the role of c-terminal Src kinase in dengue virus replication, Sci. Rep. 6 (2016) 30490.
[30] J.J. Chu, P.L. Yang, c-Src protein kinase inhibitors block assembly and maturation of dengue virus, Proc. Natl. Acad. Sci. U. S. A. 104 (2007) 3520–3525.
[31] J. Lupberger, F.H. Duong, I. Fofana, L. Zona, F. Xiao, C. Thumann, S.C. Durand, P. Pessaux, M.B. Zeisel, M.H. Heim, T.F. Baumert, Epidermal growth factor receptor signaling impairs the antiviral activity of interferon-alpha, Hepatology 58 (2013) 1225–1235.
[32] A. Anwar, T. Hosoya, K.M. Leong, H. Onogi, Y. Okuno, T. Hiramatsu, H. Koyama, M. Suzuki, M. Hagiwara, M.A. Garcia-Blanco, The kinase inhibitor SFV785 dislocates dengue virus envelope protein from the replication complex and blocks virus assembly, PLoS One 6 (2011) e23246.
[33] S.Q. Zhang, W. Yang, M.I. Kontaridis, T.G. Bivona, G. Wen, T. Araki, J. Luo, J.A. Thompson, B.L. Schraven, M.R. Philips, B.G. Neel, Shp2 regulates SRC family kinase activity and Ras/Erk activation by controlling Csk recruitment, Mol. Cell 13 (2004) 341–355.

PLOS ONE

RESEARCH ARTICLE

RNAi screen reveals a role of SPHK2 in dengue virus–mediated apoptosis in hepatic cell lines

Atthapan Morchang[1,2], Regina Ching Hua Lee[3], Pa-thai Yenchitsomanus[1], Gopinathan Pillai Sreekanth[1], Sansanee Noisakran[4], Justin Jang Hann Chu[3]*, Thawornchai Limjindaporn[1,5]*

1 Division of Molecular Medicine, Department of Research and Development, Faculty of Medicine Siriraj Hospital, Mahidol University, Bangkok, Thailand, **2** Graduate Program in Immunology, Department of Immunology, Faculty of Medicine Siriraj Hospital, Mahidol University, Bangkok, Thailand, **3** Laboratory of Molecular RNA Virology and Antiviral Strategies, Yong Loo Lin School of Medicine, National University Health System, National University of Singapore, Singapore, **4** Medical Biotechnology Unit, National Center for Genetic Engineering and Biotechnology, National Science and Technology Development Agency, Bangkok, Thailand, **5** Department of Anatomy, Faculty of Medicine Siriraj Hospital, Mahidol University, Bangkok, Thailand

* thawornchai.lim@mahidol.ac.th (TL); miccjh@nus.edu.sg (JJHC)

Citation: Morchang A, Lee RCH, Yenchitsomanus P-t, Sreekanth GP, Noisakran S, Chu JJH, et al. (2017) RNAi screen reveals a role of SPHK2 in dengue virus–mediated apoptosis in hepatic cell lines. PLoS ONE 12(11): e0188121. https://doi.org/10.1371/journal.pone.0188121

Editor: Xia Jin, Institut Pasteur of Shanghai Chinese Academy of Sciences, CHINA

Received: March 7, 2017

Accepted: October 31, 2017

Published: November 16, 2017

Data Availability Statement: All relevant data are within the paper and its Supporting Information files.

Funding: This study was supported by the Mahidol University Grant (R015810002) to TL and AM was supported by the Royal Golden Jubilee (RGJ) Ph.D. Scholarship (PHD/0016/2553). The funders had no role in study design, data collection and analysis, decision to publish, or preparation of the manuscript.

Abstract

Hepatic dysfunction is a feature of dengue virus (DENV) infection. Hepatic biopsy specimens obtained from fatal cases of DENV infection show apoptosis, which relates to the pathogenesis of DENV infection. However, how DENV induced liver injury is not fully understood. In this study, we aim to identify the factors that influence cell death by employing an apoptosis-related siRNA library screening. Our results show the effect of 558 gene silencing on caspase 3-mediated apoptosis in DENV-infected Huh7 cells. The majority of genes that contributed to apoptosis were the apoptosis-related kinase enzymes. Tumor necrosis factor superfamily member 12 (*TNFSF12*), and sphingosine kinase 2 (*SPHK2*), were selected as the candidate genes to further validate their influences on DENV-induced apoptosis. Transfection of siRNA targeting *SPHK2* but not *TNFSF12* genes reduced apoptosis determined by Annexin V/PI staining. Knockdown of *SPHK2* did not reduce caspase 8 activity; however, did significantly reduce caspase 9 activity, suggesting its involvement of *SPHK2* in the intrinsic pathway of apoptosis. Treatment of ABC294649, an inhibitor of *SPHK2*, reduced the caspase 3 activity, suggesting the involvement of its kinase activity in apoptosis. Knockdown of *SPHK2* significantly reduced caspase 3 activity not only in DENV-infected Huh7 cells but also in DENV-infected HepG2 cells. Our results were consistent across all of the four serotypes of DENV infection, which supports the pro-apoptotic role of *SPHK2* in DENV-infected liver cells.

Introduction

Dengue virus (DENV) infection is a mosquito-borne disease, which is characterized by symptoms that range from mild systemic illness to hemorrhagic fever and circulatory shock.

Competing interests: The authors have declared that no competing interests exist.

Abnormalities in hematologic parameters, including thrombocytopenia and leucopenia, are seen in severe DENV infection [1]. From the site of infection, the viral particles spread to multiple target organs via the circulatory system and lymphatic circulatory system [2].

Hepatic dysfunction is one of the important features of DENV infection. [3]. Liver injury due to hepatocyte apoptosis was observed in severe DENV cases [4–7]. Viral antigens were detected in hepatocytes and Kuppfer cells in patients with hepatomegaly and raising level of serum transaminases [8–12]. BALB/c mouse models of DENV infection [13–15] revealed that high levels of apoptosis were found in livers with high viral load [13, 14, 16]. World Health Organization (WHO) guideline suggested organ injury as one of the criteria for determining severity of DENV disease [17]. Viral components, including DENV membrane (DENV M) and capsid (DENV C), were found to contribute to apoptosis [18–20]. DENV induces hepatocyte apoptosis via caspase 8 and 9 suggests the involvement of both intrinsic and extrinsic pathways of apoptosis. The extrinsic pathway involves extracellular death ligands-receptors signaling such as tumor necrosis factor α (TNF-α) signaling whereas the intrinsic pathway activates the mitochondrial membrane permeabilization (MMP) event, which is triggered by intracellular stress, such as endoplasmic reticulum stress and oxidative stress [21]. Both intrinsic and extrinsic pathways contribute to caspase 3 activation both *in vitro* cultures [22, 23] and in animal models [13, 14].

Delivery of gene-specific small interfering RNA (siRNA) is a transient gene silencing tool that is widely used to investigate the biological function of a gene of interest [24]. The combination of siRNAs and a high-throughput screening platform can help to identify how multiple genes contribute to a specific molecular signaling mechanism [25]. Genome-scale knockdown experiments in flaviviral infections have been conducted by several research groups [26–28]. Two of these groups characterized a number of host factors that are mutually required for mosquito-borne flavivirus infections, including DENV, West Nile virus (WNV), and yellow fever virus (YFV) [26, 28], while the other group demonstrated the important host factors required for DENV to infect insect cells [27]. Interestingly, a pathway-focused siRNA library screening experiment explained the role of human trafficking genes in DENV entry to the host cells [29]. However, apoptosis siRNA library screening to identify genes required for DENV-induced apoptosis has never been investigated.

In this study, we employed an apoptosis pathway-focusing siRNA library, which contains a smart pool of 558 siRNAs targeting apoptotic genes to identify the genes, which were involved in apoptosis based on the level of caspase 3 activity in DENV-infected Huh7 cells. Our results show that *SPHK2* contributes to DENV-mediated apoptosis in hepatic cells.

Materials and methods

Cell culture and preparation of DENV

Huh7 cells were obtained from the Japanese Collection of Research Bioresources Cell Bank (JCRB0403). HepG2 cells and A549 cells were obtained from American Type Culture Collection (ATCC, Manassas, VA, USA). All cells were maintained in Dulbecco's Modified Eagle Medium (DMEM) (Gibco; Thermo Fisher Scientific, Inc., Waltham, MA, USA) supplemented with 10% heat inactivated fetal bovine serum (FBS) (Gibco; Thermo Fisher Scientific, Inc., Waltham, MA, USA) and 100 U/ml of penicillin and streptomycin in 37˚C, 5% CO_2 and humidified incubator. DENV serotype 1 strain Hawaii, serotype 2 strain 16881, serotype 3 strain H87, and serotype 4 strain H241 were propagated in C6/36 mosquito cell lines. Briefly, confluent monolayers of C6/36 cells were separately infected with the four serotypes of DENV at a multiplicity of infection (MOI) of 10. Six days after infection, the supernatants were collected by centrifugation at 5,000 rpm for 10 minutes. Virus titer was quantified according to

standard plaque forming unit (PFU) assay using BHK-21 cells. Supernatant containing virus was aliquoted in microcentrifuge tubes and frozen at -80˚C until use.

Assay for cell viability and caspase 3 activity

Huh7 cells were seeded at 1.5 x 10^4 cells in a 96-well white plate with a clear bottom for one day before infection. Cells were inoculated with DENV at MOI 1, 5, and 10 for 2 hours. Cells were then replenished with 100 μl of DMEM maintenance media containing 2% FBS and 100 U/ml of penicillin and streptomycin. Cells were cultured for 24, 48, 72, and 96 hours post infection (hpi). Morphological cell death was observed using phase-contrast light microscopy. Cell viability and caspase 3 activity were determined using ApoLive-Glo™ Multiplex Assay (Promega Corporation, Madison, WI, USA). This assay includes a substrate for both live-cell protease and caspase 3 protease, which are used to measure cell viability and apoptosis as a proportional fluorescent and luminescent signal, respectively. Briefly, 10 μl of viability reagent was added to cells and incubated at 37˚C for 1 hour. Fluorescent signal was measured at 400_{ex}-500_{em} nanometer using an Infinite 200 PRO microplate reader (Tecan Group Ltd., Männedorf, Switzerland). Thereafter, 100 μl of caspase 3 activity reagent was added and incubated for 1 hour at room temperature. Luminescent signals were analyzed using a GloMax®-96 Microplate Luminometer (Promega Corporation, Madison, WI, USA). Data were presented in relative fluorescent units (RFUs) and relative light units (RLUs) or percentage compared to control group.

Reverse transfection of siRNAs in Huh7 cells

Transfection was performed using DharmaFECT 4 transfection reagent (GE Dharmacon, Lafayette, CO, USA) in a 96-well white plate with a clear bottom. A smart pool of non-targeting control (NTC) siRNA (D-001206-13; GE Dharmacon) and caspase 3 siRNA (L-004307-00; GE Dharmacon) were used as negative and positive control, respectively. siRNA was diluted in DharmaFECT cell culture reagent (GE Dharmacon) and used at a final concentration of 50 nM. Transfection reagent and siRNA were mixed and incubated at 25˚C for 30 minutes to form siRNA-liposome complex. Huh7 cells at 1.5 x 10^4 cells per well were allowed to plate onto the transfection mixture and were then incubated for 24 hours. The media were then aspirated out and the transfected cells were infected with supernatant containing DENV at MOI 10 and incubated for 48 hours. Cell viability and caspase 3 activity were measured as previously described.

siRNA library

Human ON-TARGETplus® siRNA Library—Apoptosis—SMART pool (Catalogue #G-103900-E2-01) was purchased from GE Dharmacon (Lafayette, CO, USA). The library contains a smart pool of siRNAs that includes four siRNA duplexes design to target each of the 558 apoptosis-related genes. This allows specific knockdown with high efficiency, as well as prevention of gene compensation of a specific isotype. Deconvolution of this smart pool in the following experiment demonstrated the specific knockdown effect mediated by these siRNAs.

siRNA library screening

Lyophilized siRNAs in the library were resuspended in DEPC-treated water to make a stock concentration of 100 μM. Stock siRNA was diluted to working concentration of 5 μM freshly before experiments. Transfection was performed in a 384-well white plate with a clear bottom and the final concentration of each siRNA is 50 nM. For each well, 0.04 μl of transfection reagent and 0.5 μl of 5 μM working siRNA were separately diluted in 2 μl of DharmaFECT cell

culture transfection media. siNTC was used as the negative control. After separately incubation at 25˚C for 5 minutes, the reagents were combined to form siRNA-liposome complex at 25˚C for 30 minutes. At optimized conditions, 2 x 10^3 Huh7 cells in 46 μl of growth media were added directly to the transfection mixture and incubated for 24 hours to ensure knockdown efficiency. The media were then aspirated out and the transfected cells were infected with 50 μl of supernatant containing DENV at MOI 10 and further incubated for 48 hours. Cell viability and caspase 3 activity were measured, as previously described. All liquid handling steps were performed using Multidrop™ Combi Reagent Dispenser (Thermo Fisher Scientific, Inc., Waltham, MA, USA) and Embla Microplate Washer (Molecular Devices, LLC, Sunnyvale, CA, USA).

Real-time RT-PCR

Huh7 cells were transfected with either 50 nM of siNTC or 50 nM of si*TNFSF12* (5′- GC UCCUCCCUUGAGAAUUC-3′, J-010629-08; GE Dharmacon, Lafayette, CO, USA) and si*SPHK2* (5′-GAGACGGGCUGCUCCAUGA-3′, J-004831-10; GE Dharmacon, Lafayette, CO, USA). Total RNA was isolated from transfected cells using High Pure RNA Isolation Kit (Roche Applied Science, Penzberg, Germany). RNAs concentration and purity were measured using a Nano Drop ND-1000 Spectrophotometer (Thermo Fisher Scientific, Inc., Waltham, MA, USA). Equivalent concentrations of RNAs were reverse transcribed to cDNA using SuperScript® III Reverse Transcription System (Invitrogen, Carlsbad, CA, USA). cDNAs were then mixed with LightCycler® 480 SYBR Green I Master Mix (Roche Diagnostics, Basel, Switzerland) and individual primer sets for amplification. The following primers were used in this study: *TNFSF12-F*: 5′—CCT CGC AGA AGT GCA CCT AAA—3′; *TNFSF12-R*: 5′—TCA GGT AGA CAG CCT TCC CC—3′; *SPHK2-F*: 5′- CTG ACT AGC CGG GCG ATA AC—3′; *SPHK2-R*: 5′- CCT GAC CTT CAG CTC TCC AAC—3′; *ACTB-F*: 5′- AGA AAA TCT GGC ACC ACA CC—3′; and, *ACTB-R*: 5′- CTC CTT AAT GTC ACG CAC GA—3′. PCR amplification was performed on a LightCycler® 480 Real-Time PCR System (Roche Applied Science, Penzberg, Germany) with a program profile of pre-incubation at 95˚C for 10 minutes, followed by 40 cycles of denaturation at 95˚C for 10 seconds, annealing at 60˚C for 10 seconds, and extension at 72˚C for 20 seconds. Gene fold change was calculated according to $2^{-\Delta\Delta Ct}$ values compared between test and control.

Apoptosis assay using Annexin V/propidium iodide staining

Apoptosis assay was conducted using BD Pharmingen™ Annexin V-FITC Apoptosis Detection Kit I (Bectin, Dickinson and Company, Franklin Lakes, NJ, USA). Briefly, siRNA transfected and DENV-infected Huh7 cells were harvested and washed with cold 1X BD Pharmingen™ Annexin V Binding Buffer. Cells were then resuspended in 100 μl of 1X Annexin V Binding Buffer and incubated with 5 μl of Annexin V-FITC on ice in the dark for 15 minutes. Thereafter, 2.5 μl of propidium iodide (PI) was added and the final volume of reaction was adjusted to 300 μl. Stained cells were immediately subject to analysis using FACSORT™ (Bectin, Dickinson and Company). Green channel (FL-1) and red channel (FL-2) were used to detect Annexin V-FITC and PI, respectively. Annexin V-positive/PI-negative cells were considered to be apoptotic cells and were analyzed as a percentage of the entire cell population.

Assays for caspase 8 and caspase 9 activities

The cells were subjected to measure the activity of caspase 8 and caspase 9 using a specific-substrates, luminescent-based commercial kit, Caspase-Glo® 8 Assay and Caspase-Glo® 9 Assay

Systems from Promega. Briefly, the cells in 100 μl of culture medium were combined with 100 μl of Caspase-Glo® 8 or Caspase-Glo® 9 working reagents. The reagents provide lysis buffer, luminescent-conjugated substrates of caspase8 or caspase 9 and MG132. MG132 was added to lower the background signal. The reaction mix was incubated for 30 minutes at room temperature and total luminescent light was measured using Synergy H1 Multi-Mode Reader (BIOTEK, Winooski, VT, USA)

Treatment of ABC294640, a SPHK2 inhibitor

ABC294640 was purchased from Echelon Biosciences, Inc. (Salt Lake City, UT, USA) and dissolved in DMSO to create a 10 mM concentration of inhibitor stock, which was stored at -20˚C in a dark condition until use. The working solution was freshly prepared in 2.5, 5, and 10 μM concentrations before treatment. Growth media and 0.01% DMSO were used as parental and vehicle controls, respectively. For cytotoxicity testing, Huh7 cells were seeded into 96-well culture plates, treated with ABC294640 at different concentrations, and incubated for 48 hours. Cell viability was measured using PrestoBlue Assay (Invitrogen Carlsbad, CA, USA). For determination of caspase 3 activity and sub G1 cells population, Huh7 cells were pretreated with 2.5, 5, and 10 μM concentrations of ABC294640 for 2 hours. Cells were then washed with PBS and inoculated with DENV at MOI 10 for 2 hours. After washing, the cells were cultured in the presence or absence of ABC294640 for 48 hours. Caspase 3 activity was then measured as previously described. Sub G1 cells population was detected by fixing the cells in ice-cold 70% ethanol overnight, followed by treatment of 2 mg/ml of RNAse in 1% Triton X-100 for 5 minutes at room temperature. The cells were stained with 10 μg/ml of PI for 30 minutes at room temperature in the dark. The stained cells were subject to analysis using a flow cytometer. Red channel (FL-2) was used to detect DNA content, which was stained by PI.

Immunofluorescent assay (IFA)

Cells were seeded on a glass cover slip for 24 hours before experiment. HepG2 cells were infected with DENV at the MOI of 5. Huh7 cells and A549 cells were infected with DENV at the MOI of 1. After 24 hours post infection, cells were fixed by incubation with 4% paraformaldehyde at room temperature for 20 minutes. Cells were washed and permeabilized by incubation with 0.2% Triton-X (Sigma-Aldrich Corporation, St. Louis, MO, USA) at room temperature for 10 minutes. Thereafter, cells were incubated with both mouse anti-DENV E monoclonal antibody (Clone 4G2) and rabbit anti-SPHK2 (ab37977, Abcam) at a dilution of 1:50 at 37˚C for 60 minutes. Cells were washed and incubated with secondary antibodies containing goat anti-mouse IgG-Cy3 (A10521, Molecular Probes) and donkey anti-rabbit IgG-Alexa 488 (A21206, Molecular Probes) at a dilution of 1:500 at 37˚C in the dark for 1 hour. Hoechst 33342 solution (H3570, Molecular Probes) was added at a dilution of 1:1000 for nuclear detection. After the washing step, cover slips were mounted onto a glass slide using 50% glycerol, sealed, and subject to fluorescent image capture using confocal microscopy (LSM 510 Meta; Carl Zeiss Microscopy GmbH, Jena, Germany).

Statistical analysis

For the siRNA screening experiment, each siRNA reverse transfection was performed in triplicate wells and data were shown as percentage of caspase 3 activity compared to the siNTC control. The rest of the experiments were performed at least three independent experiments. Data were analyzed using GraphPad Prism Software version 5 (GraphPad Software, Inc., San Diego, CA, USA) and presented as mean ± standard deviation (SD). Statistical analysis was performed

using Student's unpaired *t*-test. A *p*-value less than 0.05 was considered to be statistically significant.

Results

DENV infection induces Huh7 cells apoptosis in a time- and dose-dependent manner

To determine the apoptosis inducing condition, Huh7 cells were infected with DENV MOI 1, 5, and 10 and were incubated for 24, 48, 72, and 96 hpi. Cell morphology, cell viability, and caspase 3 activity were determined to characterize DENV-induced cell death. No change in cell morphology was observed at 24 hpi (Fig 1A), whereas shrinking, rounding, and floating of cells were visualized at 48 hpi for MOI 5 and 10. Cell death became more obvious at 72 and 96 hpi, with commensurate increases being observed at higher MOI (Fig 1A). Decreased cell viability was consistently observed at all-time points from 48 hpi to 96 hpi (Fig 1B). As expected, increased caspase 3 activity became observable at 48 hpi for MOI 5 and 10, but it declined at 72 and 96 hpi (Fig 1C). These results suggest that DENV infection of Huh7 cells induced apoptosis in both a time-dependent and MOI-dependent manner. The apoptosis inducing condition for the screening was determined to be 48 hpi at DENV MOI 10, since the maximum increase in caspase 3 activity was observed at those parameters.

Optimization of siRNA screening platform

Optimization of a suitable siRNA screening platform according to the parameters of 48 hpi at DENV MOI of 10 was conducted. Since siRNA screening was miniaturized into a 384-well plate format, the seeding condition had to be optimized first. Huh7 cells were seeded at a density of 1000, 2000, 3000, 4000, and 5000 cells and then cultured for 72 hours. Cell morphology and confluency were then studied under a light microscope. Our results show progressive cell growth and spontaneous cell death in wells seeded with more than 2000 cells (Fig 2A). However, the seeding condition of 2000 cells per well showed an appropriate density and monolayer culture. As a result, 2000 cells per well was selected as the seeding condition for the experiments in this study.

To evaluate the accuracy and reliability of the screening, we undertook knockdown experiments with siRNA specific to caspase 3 as a positive control. Cells were reverse transfected with a non-targeted control siRNA (siNTC) or caspase 3 siRNA (si*Caspase* 3) for 24 hours and then infected with DENV MOI 10 for 48 hours. The results from 15 repeated caspase 3 knockdown wells precisely showed the reduction in caspase 3 activity upon DENV infection (Fig 2B).

siRNA library screening identifies genes, which affect caspase 3 activity in DENV-infected Huh7 cells

The SMART pool apoptosis human siRNA library comprises siRNAs that target apoptosis-related genes for the comprehensive analysis of apoptotic signaling. The siRNA targets include both cytoplasmic and membrane-bound proteins associated with programmed cell death. A SMART pool of 4 different siRNA duplexes designs for an individual gene to enhance knockdown efficiency. Complete list of the alteration of caspase 3 activity in DENV-infected Huh7 cells affected by siRNA library transfection can be found at S1 Table. Our siRNA library screening verified various genes related to apoptotic signals. Based on the highest ability to reduce caspase 3 activity in DENV-infected Huh7 cells, 20 siRNA targeted genes were reported in Table 1. Tumor necrosis factor superfamily, member 12 (*TNFSF12*), which is known as

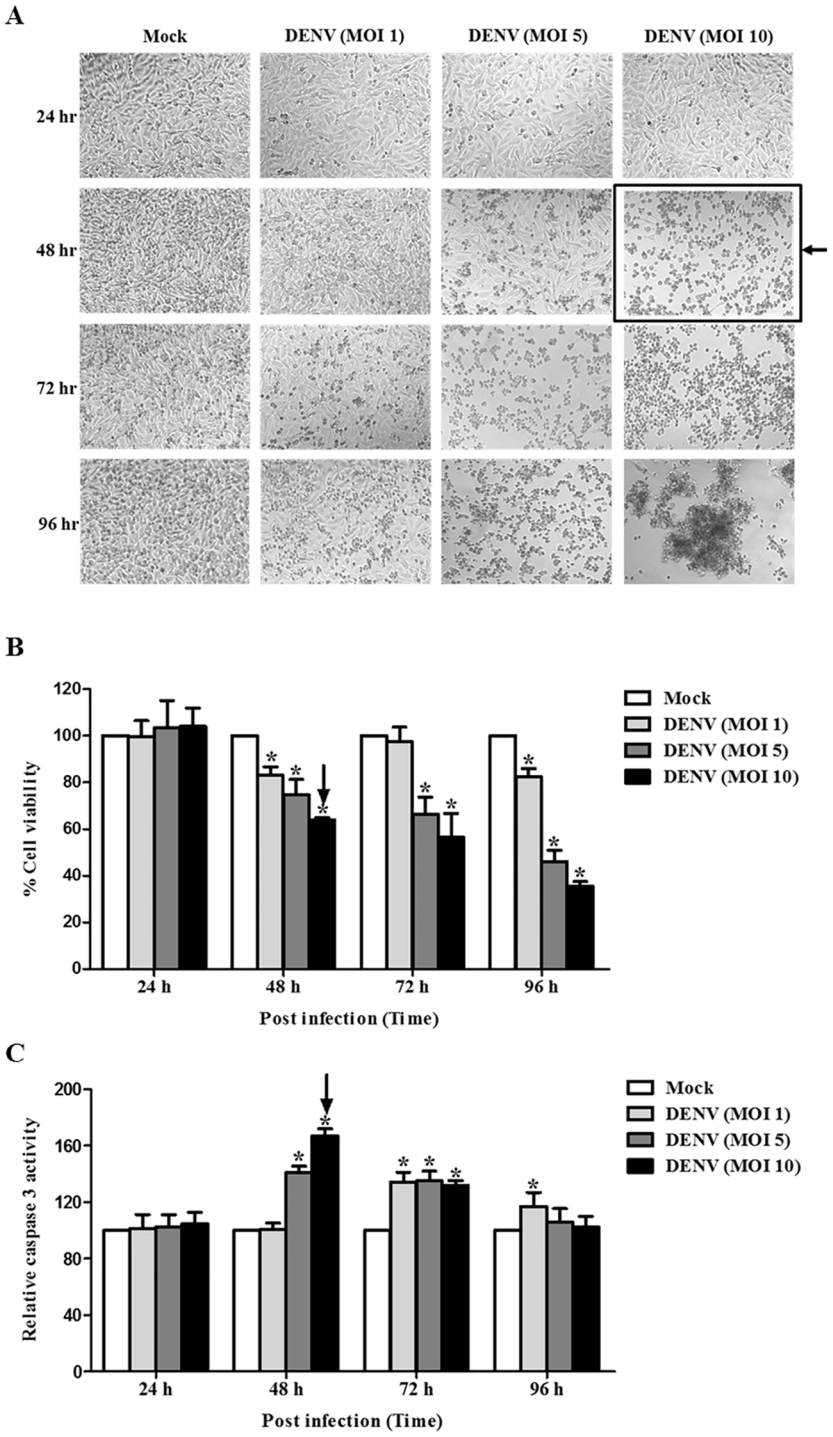

Fig 1. DENV-infected Huh7 cells undergo apoptosis in a time- and dose-dependent manner. Huh7 cells were infected with DENV at MOIs of 1, 5, and 10 and incubated at different time points of 24, 48, 72, and 96 hpi. Cell morphology was monitored using phase contrast light microscopy. Cell viability and caspase 3 activity were measured using multiplex detection kit: (A) Cell morphology; (B) Cell viability; and (C) Caspase 3 activity are shown. For (B) and (C), the results are expressed as percentage to that of mock control that obtained from the average of three independent experiments ± SD. The asterisks indicate statistically significant differences between groups ($p < 0.05$) (Student's *t* test). The arrow indicated the condition chosen for screening assay.

https://doi.org/10.1371/journal.pone.0188121.g001

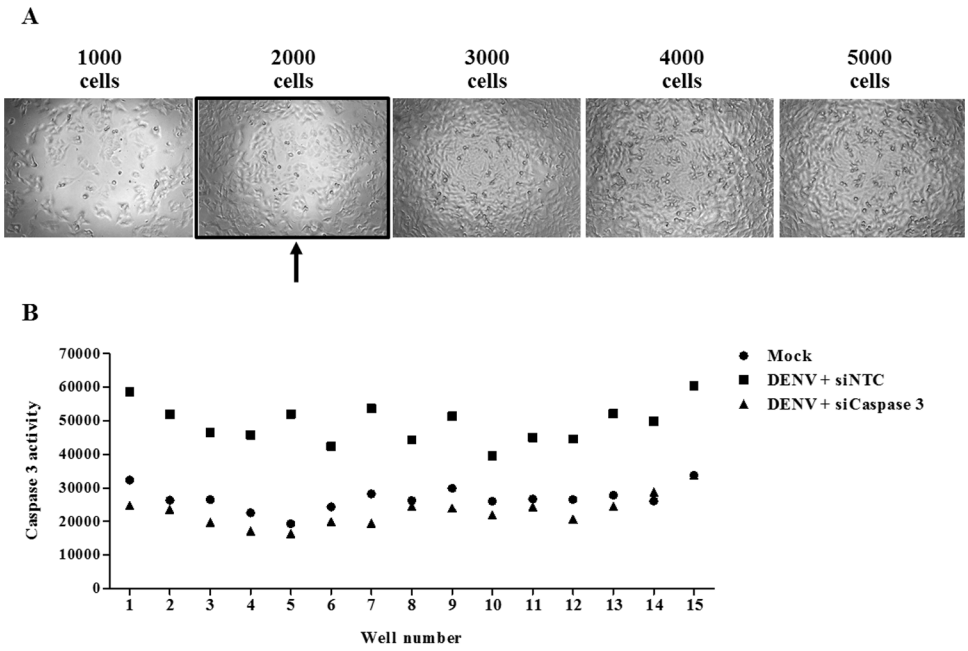

Fig 2. Optimized siRNA screening condition. (A) Huh7 cells were seeded into a 384-well plate with 1000, 2000, 3000, 4000, and 5000 cells per well. Cell morphology and confluency were observed and an image was captured 72 hours later using a phase contrast microscopy. The arrow indicates the optimized seeding condition for siRNA screening assay. (B) Huh7 cells were reverse transfected with a siNTC or si*Caspase* 3 for 24 hours before infected with DENV at MOI of 10 for 48 hpi. Conditions were replicated in 15 wells within the same plate. Caspase 3 activity was measured and plotted across the 15 wells.

https://doi.org/10.1371/journal.pone.0188121.g002

Table 1. List of top 20 genes identified from siRNA library screening.

	Gene symbol	Gene description	Percentage of caspase 3 activity (compare to siNTC)	S.D.	p-value
1	*TNFSF12*	Tumor necrosis factor ligand superfamily member 12	44.25%	6.95	0.0002
2	*RIPK2*	Receptor-interacting serine/threonine protein kinase 2	45.02%	13.36	0.0022
3	*STK17A*	Serine/threonine kinase 17a	47.46%	7.58	0.0003
4	*CARD14*	Caspase recruitment domain family member 14	48.12%	6.05	0.0001
5	*PDCD2*	Programmed cell death-2	48.51%	4.56	< 0.0001
6	*HDAC3*	Histone deacetylase 3	48.82%	7.15	0.0003
7	*PSEN2*	Presenilin 2	48.99%	6.86	0.0002
8	*PIM1*	Serine/threonine-protein kinase Pim-1	51.28%	17.36	0.0374
9	*SST*	Somatostatin	52.20%	14.23	0.0047
10	*RAD21*	RAD21 homolog (*S. pombe*)	53.45%	11.91	0.0027
11	*SPHK2*	Sphingosine kinase 2	54.68%	16.96	0.0107
12	*RASA1*	RAS P21 protein activator (GTPase activating protein) 1	54.71%	1.79	< 0.0001
13	*NME3*	NME/NM23 nucleoside diphosphate kinase 3	54.96%	8.82	0.0010
14	*CASP3*	Caspase 3, apoptosis-related cysteine peptidase	55.20%	8.89	0.0009
15	*CYCS*	Cytochrome C	55.76%	7.28	0.0005
16	*NME5*	NME/NM23 nucleoside diphosphate kinase 5	56.02%	8.31	0.0008
17	*CARD11*	Caspase recruitment domain family member 11	56.23%	2.63	< 0.0001
18	*STK17B*	Serine/threonine kinase 17b	57.00%	9.32	0.0014
19	*SIVA1*	SIVA1, Apoptosis-Inducing Factor	57.09%	8.50	0.0010
20	*CTNNAL1*	Catenin alpha-like protein	57.13%	8.03	0.0008

https://doi.org/10.1371/journal.pone.0188121.t001

TNF-related weak inducer of apoptosis (*TWEAK*), show the strongest reduction of caspase 3 activity upon silencing. Nine of the 20 genes selected by having the most reduction in caspase 3 activities were categorized as kinase enzymes, including *STK17A*, *STK17B*, *CARD11*, *CARD14*, *NME5*, *NME3*, *RIPK2*, and *SPHK2*. siRNAs targeted genes encoding caspase 3 and cytochrome C, which are the known regulators of apoptosis, were also shown to reduce caspase 3 activity.

SPHK2 knockdown reduces DENV-induced apoptosis in Huh7 cells

TNFSF12 and *SPHK2* were selected for further analysis as the contribution of these genes in DENV-mediated apoptosis has never been investigated in DENV infection. To demonstrate the knockdown efficiency, specific mRNA expression in si*TNFSF12*- and si*SPHK2*-transfected Huh7 cells were determined using real-time RT-PCR. Both mRNA expression of *TNFSF12* and *SPHK2* were more than 50% silenced in Huh7 cells after transfection with their specific siRNAs, as compared to rates observed after reverse transfection with siNTC (Fig 3A and 3B) suggesting the efficiency of the knockdown assay.

Annexin V/PI staining was performed to confirm the role of *TNFSF12* and *SPHK2* in the apoptosis of DENV-infected Huh7 cells. Our results show that DENV infection in Huh7 cells induced apoptosis, while reverse transfection with siSPHK2 significantly reduced the rate of apoptotic cell death (Annexin V+/PI-) from 32.66% to 24.87% compared to that of the siNTC transfection control (Fig 4A). However, silencing of *SPHK2* reduced the proportion of primary apoptotic cells, not that of secondary necrotic cell population. In contrast to result of *SPHK2*, reverse transfection with siTNFSF12 was not able to reduce the rate of apoptosis (32.66% to 34.15%) (Fig 4A). Statistical analysis of data from three independent experiments is shown in Fig 4B.

SPHK2 knockdown in DENV-infected Huh7 cells modulates the intrinsic pathway of apoptosis

To gain insight into how *SPHK2* modulates apoptosis in DENV-infected Huh7 cells, the activities of caspase 8 and caspase 9, which represented extrinsic and intrinsic pathways of apoptosis were investigated. Elevated caspase 8 activity (Fig 5A) and caspase 9 activity (Fig 5B) was observed in siNTC-transfected DENV-infected Huh7 cells. Knockdown of *SPHK2* in DENV-infected Huh7 cells significantly reduced caspase 9 activity without affecting caspase 8 activity (Fig 5B and 5A). These results explain the contributory role of *SPHK2* in the intrinsic pathway of apoptosis in DENV-infected Huh7 cells.

ABC294640, a selective inhibitor of SPHK2, reduces DENV-induced apoptosis in Huh7 cells

To determine whether the kinase activity of SPHK2 has any influence on the DENV-induced apoptosis of Huh7 cells, studies with ABC294640, a selective inhibitor of SPHK2, were performed. Cytotoxicity of ABC294640 was initially studied to determine the effective dose. Both ABC294640 and its solvent control (0.01% DMSO) were found to be non-toxic to Huh7 cells at the tested concentrations of 2.5, 5, and 10 μM (S1 Fig). Pre- and post-treatment with ABC294640 showed significant reduction in caspase 3 activity of DENV-infected Huh7 cells in a dose-dependent manner (Fig 6A). Measurement of sub G1 cells, a representative of the DNA fragmented apoptotic cells, consistently showed the significant reduction of apoptosis from 55.52% in untreated cell to 21.34% in ABC294640-treated DENV-infected Huh7 cells

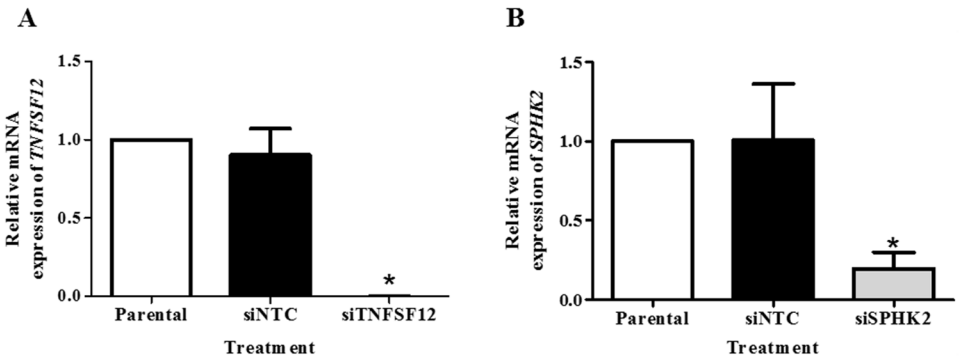

Fig 3. Knockdown efficiency of *TNFSF12* and *SPHK* in DENV-infected Huh7 cells. Huh7 cells were reverse transfected with siRNA targeted *TNFSF12* or *SPHK2* genes or the non-targeting control siRNA for 24 hours before infected with DENV for 48 hours. The mRNA expression was then analyzed using real-time RT-PCR. The mRNA expression of *TNFSF12* (A) and *SPHK2* (B) represented as fold times compared to parental control. The results are expressed as the average of three independent experiments ± SD. The asterisks indicate statistically significant differences between groups ($p < 0.05$) (Student's *t* test).

https://doi.org/10.1371/journal.pone.0188121.g003

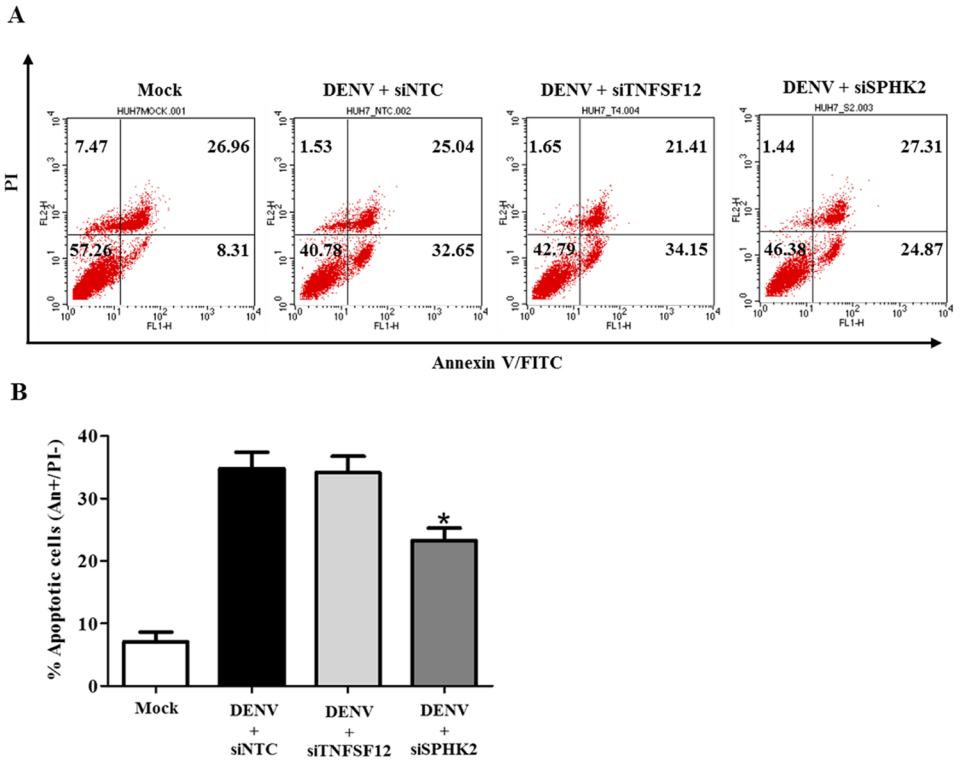

Fig 4. Knockdown of *SPHK2* but not knockdown of *TNFSF12* reduces apoptosis in DENV-infected Huh7 cells. Huh7 cells were reverse transfected with siRNA directed against *TNFSF12* or *SPHK2* genes for 24 hours before being infected with DENV for 48 hours. Apoptotic cells were determined by Annexin V/PI staining and flow cytometry analysis. (A) Dot plot indicates cell death; and, (B) Apoptotic cells (Annexin V+/PI-) were plotted and compared with percentage of cell population. The results are expressed as the average of three independent experiments ± SD. The asterisks indicate statistically significant differences between groups ($p < 0.05$) (Student's *t* test).

https://doi.org/10.1371/journal.pone.0188121.g004

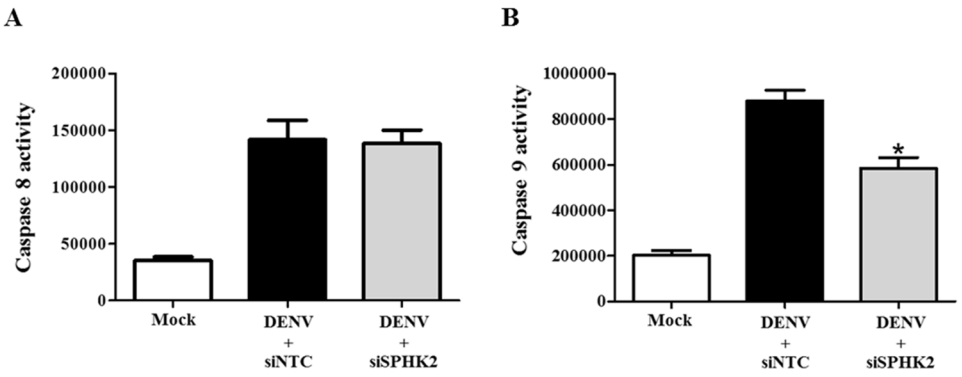

Fig 5. *SPHK2* knockdown modulates apoptosis in DENV-infected Huh7 cells via the intrinsic pathway. Huh7 cells were reverse transfected with si*SPHK2* or siNTC for 24 hours and then infected with DENV MOI 10 for 48 hours. Caspase 8 (A) and caspase 9 (B) activities were determined and measured and the values are represented in relative luminescent unit (RLU). The results are expressed as the average of three independent experiments ± SD. The asterisks indicate statistically significant differences between groups ($p < 0.05$) (Student's *t* test).

https://doi.org/10.1371/journal.pone.0188121.g005

(Fig 6B and 6C). These results suggest that the kinase activity of SPHK2 affects the DENV-induced apoptosis of Huh7 cells.

Knockdown of *SPHK2* does not affect virus production and viral protein expression

To exclude the possibility that knockdown of *SPHK2* impeded the virus infection thus indirectly affected apoptosis, the kinetic of virion production as well as the level of viral protein synthesis were determined in *SPHK2* knockdown cells. The results show that no significant difference in kinetic of virus production was observed between siNTC and si*SPHK2*-transfected cells over 0–48 hpi (Fig 7A). In consistency, DENV envelope (DENV E) expression was not affected by the transfection of siSPHK2 (Fig 7B). These results indicate that knockdown of *SPHK2* gene does not perturb the activity of DENV infection of Huh7 cells.

SPHK2 knockdown reduces apoptosis in DENV-infected hepatic cell lines

To determine whether the apoptosis role of *SPHK2* was restricted to the infected hepatic cell line, *SPHK2* knockdown and DENV infection experiments were additionally performed in HepG2 cells, another hepatic cell line and in A549, a lung cell line. Caspase 3 activity was elevated in both HepG2 cells and A549 cells upon infected with DENV suggesting the susceptibility of these cells in DENV-induced apoptosis (Fig 8A and 8B). Interestingly, knockdown of *SPHK2* significantly reduced the caspase 3 activity in infected HepG2 cells but failed to reduce that in infected-A549 cells (Fig 8A and 8B). These results suggest a role of *SPHK2* in DENV-induced apoptosis of liver cell lines. We next asked whether the expression and localization of SPHK2 in different cell lines may influence apoptosis during DENV infection. IFA double staining of SPHK2 and DENV E proteins was performed in Huh7 cells, HepG2 cells and A549 cells, respectively. Based on the fluorescent intensity, the basal level of SPHK2 protein expression was higher in Huh7 cells and HepG2 cells compared to that in A549 cells (Fig 9A, 9B and 9C). Up-regulation and altered subcellular localization of SPHK2 protein was also observed in DENV-infected liver cell lines compared to that in A549 cells (Fig 9A, 9B and 9C). Partial co-localization between DENV E and SPHK2 protein, especially in the perinuclear region, was

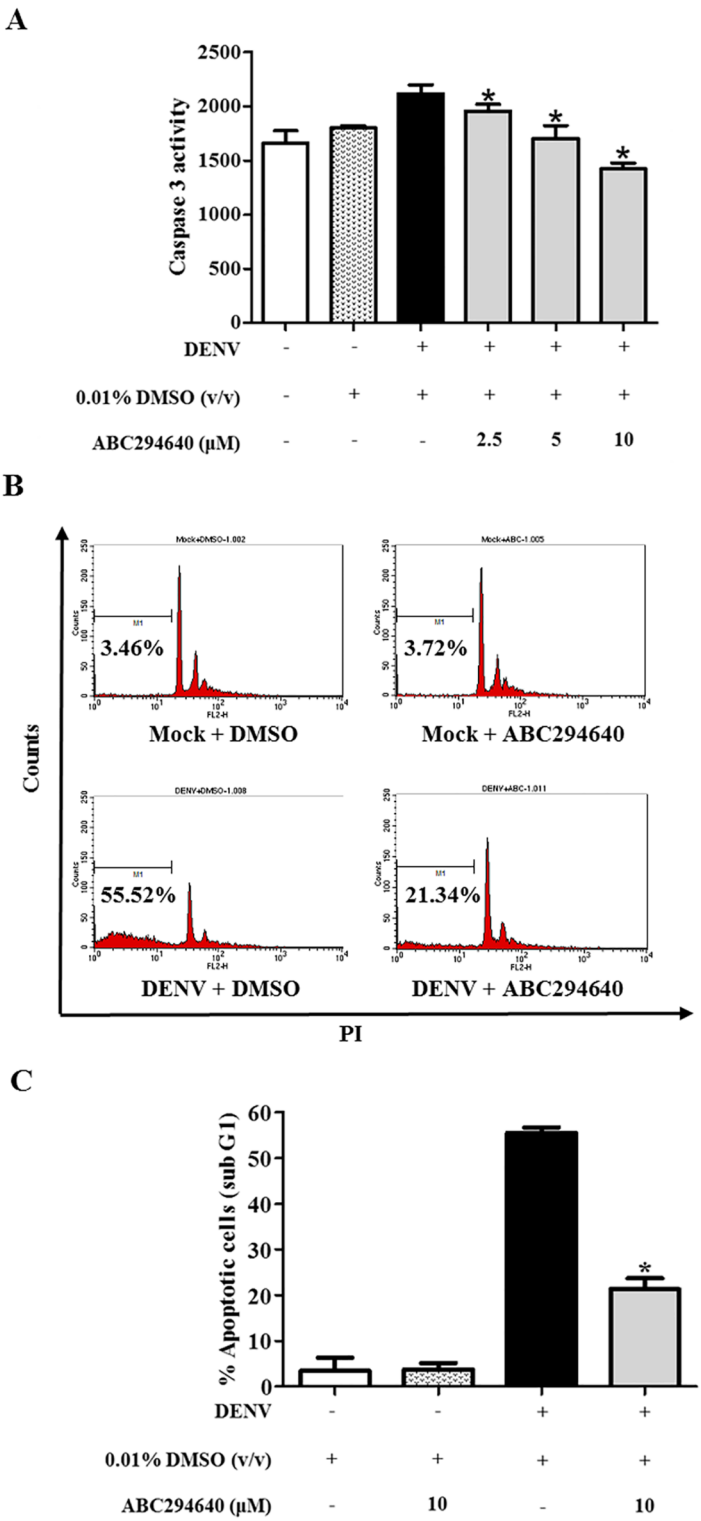

Fig 6. ABC294640 treatment reduces apoptosis in DENV-infected Huh7 cells. Huh7 cells were pre-treated with 0.01% v/v DMSO or 2.5, 5, and 10 μM concentrations of ABC294640 for 2 hours. The treated cells were infected with DENV at MOI 10 and were cultured in the presence of corresponding concentrations for 48 hours. Caspase 3 activity was measured and is represented in relative luminescent unit (RLU) (A). Huh7 cells were pre- and post-infection treated with 0.01% v/v DMSO or 10 μM concentration of ABC294640. Sub G1 cells population was detected by PI staining and flow cytometry at 48 hpi. (B) Histogram plot of sub

G1 cells and (C) bar graph represents the average percentage of three independent experiment ± SD. The asterisks indicate statistically significant differences between groups ($p < 0.05$) (Student's *t* test).

https://doi.org/10.1371/journal.pone.0188121.g006

evident in DENV-infected liver cell lines compared to that in A549 cells (Fig 9A, 9B and 9C). Data imply that expression and subcellular localization of SPHK2 may influence its role in apoptosis. The difference in expression and subcellular localization of SPHK2 between DENV-infected liver and lung cell lines may partly explain the different apoptotic phenotypes observed in this study. To conclude whether the apoptosis role of *SPHK2* was restricted to the infected liver cell lines, additional cell lines that also undergo apoptosis during DENV infection should be further tested.

SPHK2 knockdown in Huh7 cells infected with other serotypes of DENV show reduced apoptosis

To determine whether *SPHK2* is involved in the apoptosis of Huh7 cells infected with the other three serotypes of DENV (DENV1, DENV3, and DENV4), *SPHK2* knockdown

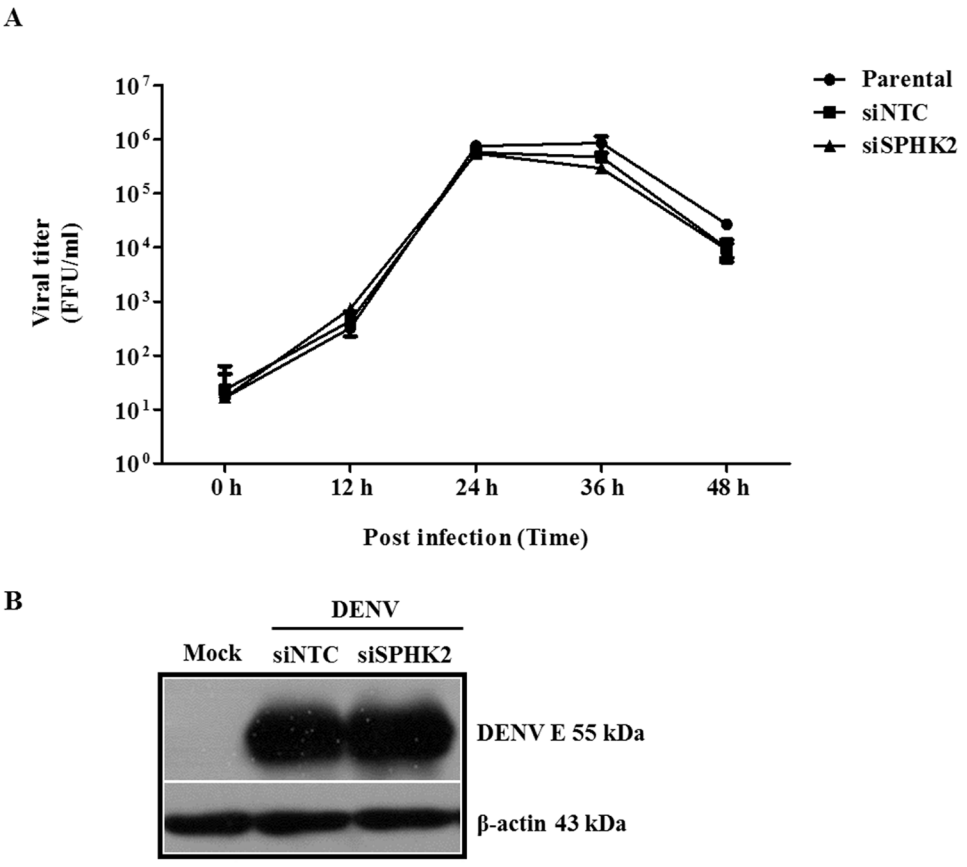

Fig 7. Knockdown of *SPHK2* does not interfere with virus production and viral protein synthesis. Huh7 cells were reverse transfected with siRNA targeted *SPHK2* gene for 24 hours before being infected with DENV for 0, 12, 24, 36 and 48 hours. (A) Virus production in supernatant was quantified by FFU assay. (B) DENV E protein expression was determined at 48 hpi using western blot analysis. The results are expressed as the average of three independent experiments ± SD. The asterisks indicate statistically significant differences between groups ($p < 0.05$) (Student's *t* test).

https://doi.org/10.1371/journal.pone.0188121.g007

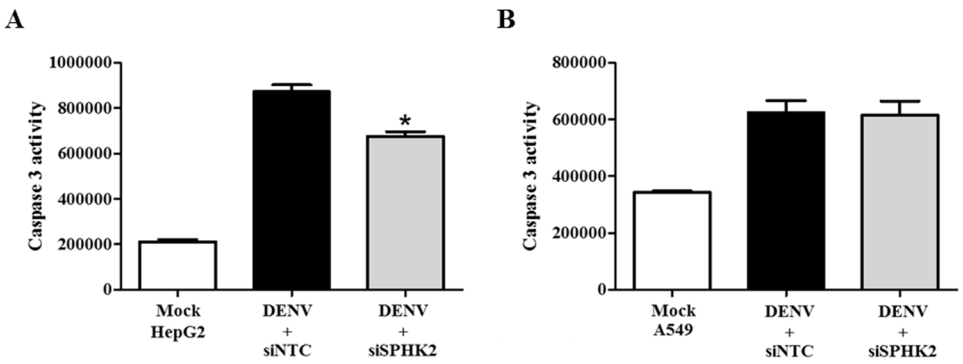

Fig 8. *SPHK2* knockdown reduces apoptosis in HepG2 cells but not in A549 cells. HepG2 cells and A549 cells were reverse transfected with si*SPHK2* or siNTC for 24 hours and then infected with DENV MOI 10 for 48 hours. Caspase 3 activity was measured and represented for (A) HepG2 cell and (B) A549 cells. The results are represented in relative luminescent unit (RLU). The results are expressed as the average of three independent experiments ± SD. The asterisks indicate statistically significant differences between groups ($p < 0.05$) (Student's *t* test).

https://doi.org/10.1371/journal.pone.0188121.g008

experiments were conducted in the other three serotypes of DENV. Caspase 3 activity was found to be elevated in Huh7 cells infected with the other three serotypes of DENV (Fig 10A, 10B and 10C). Transfection with siSPHK2 in Huh7 cells separately infected with DENV1, DENV3, and DENV4 show a significant decrease in caspase 3 activity. Data suggest that all four serotypes of DENV share the function of host protein SPHK2 to induce apoptosis at least in part of caspase-3 activity induction.

Discussion

DENV infection induces caspase 3 activity and apoptosis [22, 30]. Apoptosis-related gene expression profiling in DENV-infected HepG2 cells [31] and animal models [13, 14] was previously conducted. In this study, we set forth to screen for a list of apoptosis-related genes using siRNA library screening based on the alteration of the level of caspase 3 activity. The screening identified several genes, which involved in apoptosis of DENV-infected Huh7 cells. Knockdown of *TNFSF12* shows the strongest reduction of caspase 3 activity. *TNFSF12*, which is known as TNF-related weak inducer of apoptosis (*TWEAK*), induces apoptosis extrinsically by binding to its receptor on the cell surface [32]. *TNFSF12* was shown to be upregulated in DENV-infected HepG2 cells [33]. *TNFSF12* was also identified as the gene involved in influenza virus-induced apoptosis in lung cells [34]. However, transfection of siRNA targeting *TNFSF12* gene did not reduce DENV-induced apoptosis determined by Annexin V/PI staining (Fig 4A and 4B). The failure in reducing DENV-induced apoptosis with siRNA targeting *TNFSF12* gene could be related to the minimal presence of TNFSF12 protein after knocking down can still function to maintain apoptosis phenotype. Kinase enzymes are the majority of the identified genes in this study. Among those kinase genes, *RIPK2* was shown to be upregulated in DENV-infected HepG2 cells [33], and upregulated expression of *RIPK2* is previously shown to be essential for DENV-induced apoptosis [31]. *RIPK2* is capable of mediating apoptosis via several transduction pathways, including the NF-κB, p38, and JNK signaling pathways [35, 36]. In addition, *RIPK2* is directly activated via caspase 1 [37], which is reported to be essential for DENV-induced cell death [38]. In the present study, the apoptotic role of *RIPK2* in DENV-induced apoptosis was verified in siRNA library screening of DENV-infected Huh7 cells, suggesting its importance in DENV-mediated apoptosis of liver cells. As kinase enzymes are the majority of the identified genes in this study and *SPHK2* was shown to be

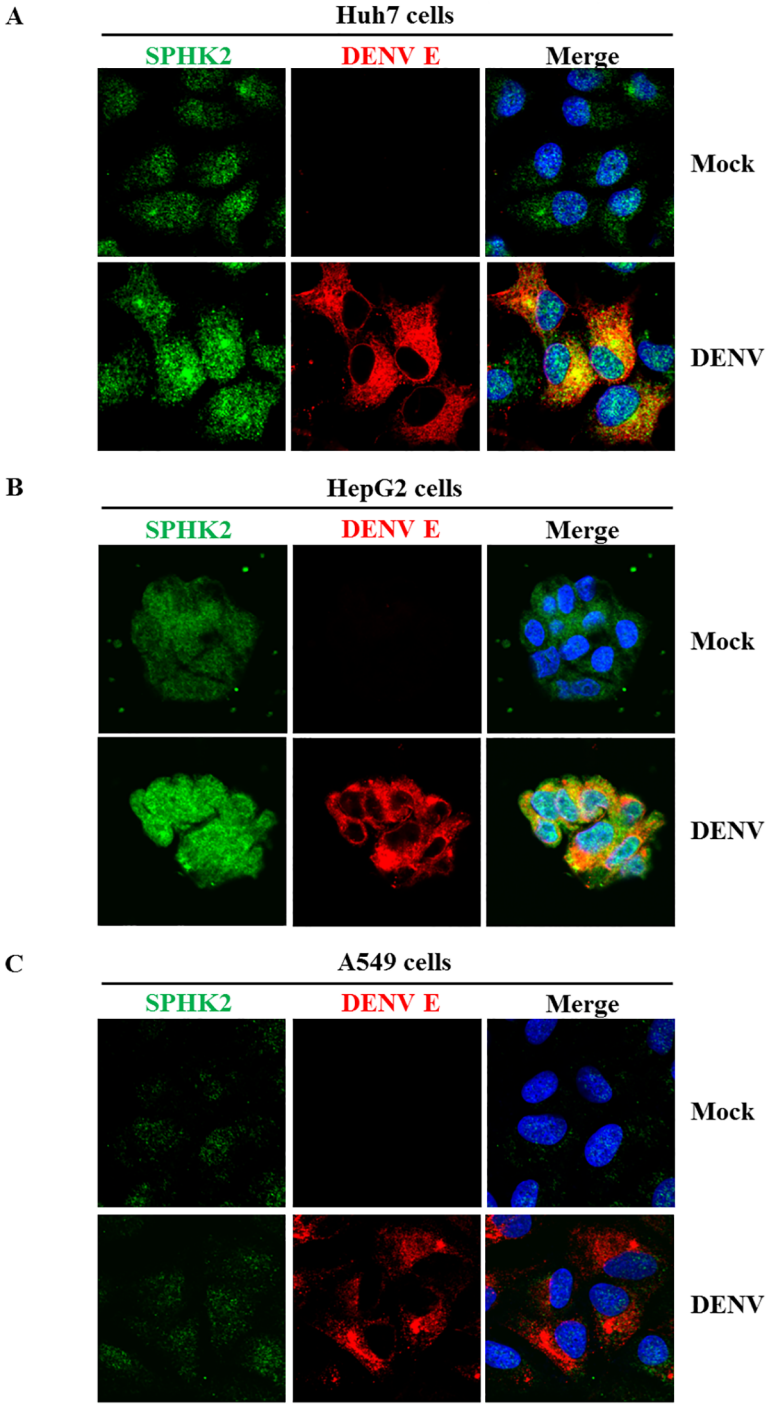

Fig 9. Alteration of SPHK2 protein expression and subcellular localization in DENV-infected Huh7 cells and HepG2 cells. Huh7 cells, HepG2 cells and A549 cells were infected with DENV at the MOI of 1, MOI of 5 and MOI of 1 for 24 hours, respectively. SPHK2 and DENV E proteins were detected by IFA and represented as green and red fluorescence, respectively. Hoechst 33342 was used to stain the nucleus. Mock cells (upper panel) and DENV-infected cells (lower panel) are (A) Huh7 cells (B) HepG2 cells and (C) A549 cells, respectively.

https://doi.org/10.1371/journal.pone.0188121.g009

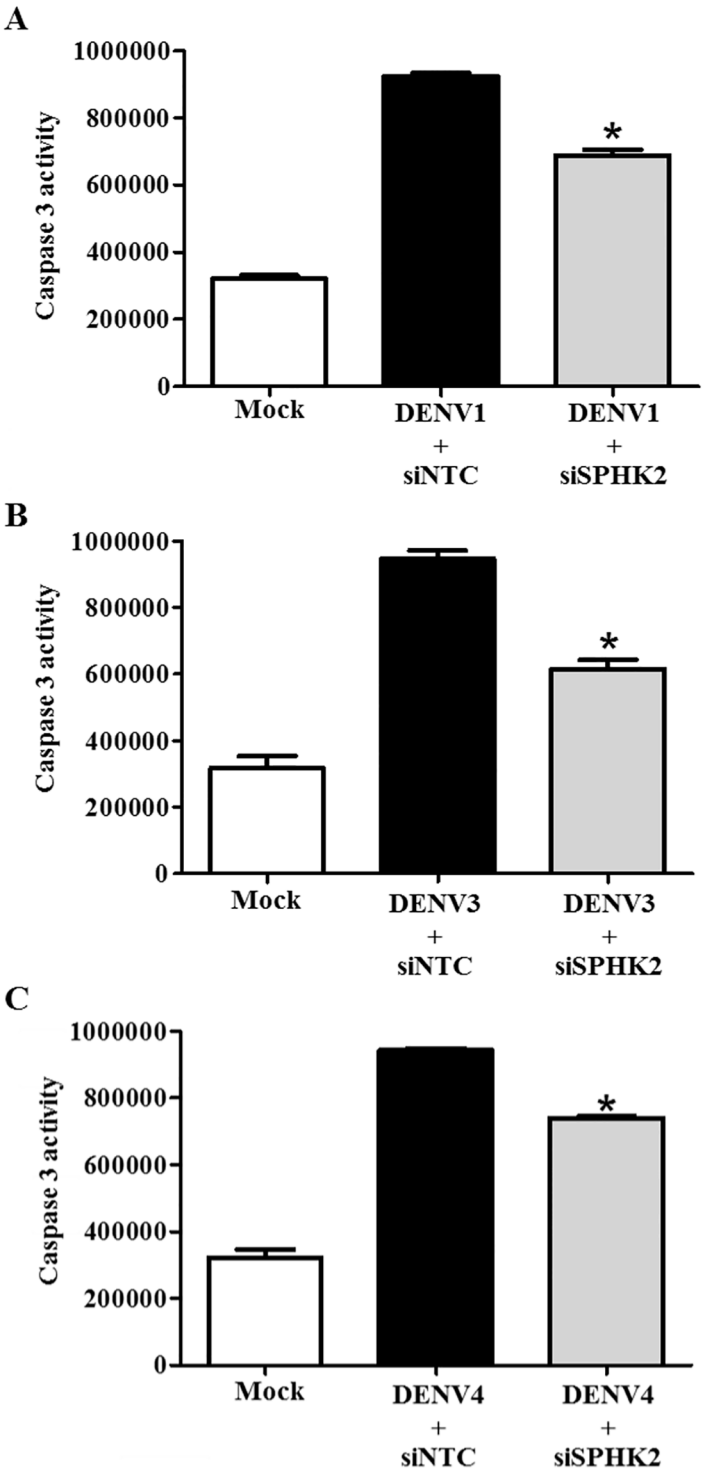

Fig 10. *SPHK2* knockdown reduces apoptosis in the other three serotypes of DENV. Huh7 cells were reverse transfected with si*SPHK2* or siNTC for 24 hours and then infected with different serotypes of DENV at MOI 10 for 48 hours. Caspase activity was measured and is represented individually for (A) DENV1-; (B) DENV3-; and, (C) DENV4-infected Huh7 cells. The results are represented in relative luminescent unit (RLU). The results are expressed as the average of three independent experiments ± SD. The asterisks indicate statistically significant differences between groups ($p < 0.05$) (Student's *t* test).

https://doi.org/10.1371/journal.pone.0188121.g010

upregulated in DENV-infected HepG2 cells [33], *SPHK2* was selected as the candidate kinase for functional analysis.

Sphingosine kinases (*SPHKs*) are sphingosine lipid metabolism enzymes, which specifically catalyze the phosphorylation of sphingosine to generate sphingosine-1-phosphate (S1P), a bioactive sphingolipid [39]. Up to date, two isoforms of *SPHKs* were characterized including *SPHK1* and *SPHK2* [40, 41]. S1P generated from *SPHK1* mediates pro-survival signals either by intracellularly activation of NF-kB [42] or extracellularly activation of the ERK1/2, PI3K/AKT, and PLC pathways [43, 44]. *SPHK1* can act as the anti-apoptotic molecule in DENV-infected HEK293 cells, where reduced *SPHK1* activity enhanced cell death [45, 46]. However, knock down of *SPHK1* in DENV-infected Huh7 cells in the present study did not affect the level of caspase 3 activity (S2 Fig). The discrepancy may be originated from the different cell types as well as the different experiment conditions used in each study. *SPHK1* was also shown to modulate DENV infection by alteration of innate responses that regulate susceptibility to DENV infection [47]. Increased plasma level of S1P was also observed in DENV-infected patients [48, 49]. Unlike *SPHK1*, roles *of SPHK2* in both anti-apoptosis and pro-apoptosis are previously reported. *SPHK2* can be one of the targets for cancer treatment as *SPHK2* functions as the pro-survival molecule in tumor growth and metastasis [50–53]. Inhibition of *SPHK2* attenuated tumor growth by induction of caspase 3-mediated cell apoptosis via enhancing the degradation of anti-apoptotic protein Mcl-1, and increasing the expression of a pro-apoptotic protein Noxa [54]. In contrast, *SPHK2* can function as the pro-apoptosis molecule. Silencing of *SPHK2* decreased TNF-α-induced apoptosis in HEK-293 cells and mouse embryonic fibroblasts [55, 56]. In addition, the mesangial cells isolated from *SPHK2*-deficient mice exhibited the resistance to staurosporine-induced apoptosis [57]. Furthermore, inhibition of *SPHK2* significantly reduced liver damage and improved the survival rate of mice suffering hepatic ischemic reperfusion. This protective effect was specifically due to the reverse of mitochondrial permeabilization event in the intrinsic pathway of apoptosis [58]. Similarly, our study also demonstrates that knockdown of *SPHK2* significantly reduced the level of caspase 3 activity in DENV-infected Huh7 cells and the reduction in caspase 3 activity was correlated with the increasing of viable cells in the *SPHK2* inhibitor-treated DENV-infected Huh7 cells at 48 and 72 hours post infection (S3 Fig). Although the role of *SPHK2* in DENV-induced apoptosis was validated by at least three assays including caspase 3 activity, subG1 staining, and Annexin V/PI staining, primary necrotic cells within Annexin V-positive/PI-negative staining phenotype should be carefully interpreted as not only apoptotic but also primary necrotic cells can have Annexin V-positive/PI-negative staining phenotype [59]. The necrotic cells (Annexin V-positive/PI-positive) was further counted and the similar level of necrotic cells was observed between siNTC- and si*SPHK2*-transfected DENV-infected Huh7 cells (S4 Fig). In this study, knockdown of *SPHK2* did not reduce caspase 8 activity; however, did reduce caspase 9 activity, suggesting its involvement of *SPHK2* in the intrinsic pathway of apoptosis. As *SPHK2* also plays roles in TNF-α-mediated extrinsic pathway of apoptosis in several apoptosis models [55, 56], the contribution of *SPHK2* in TNF-α signaling and in the extrinsic pathway of DENV-induced apoptosis needs further investigations.

Up-regulation of SPHK2, subcellular localization of SPHK2, and its co-localization with DENV proteins may influence apoptosis in DENV-infected cells. Several studies demonstrates the relationship between the pro-apoptotic function and its subcellular localization of SPHK2 [60]. S1P from ER-localized SPHK2 serves as the fuel for ceramide synthesis [41]. Ceramide can induce lysosomal membrane permeabilization (LMP) thereby affecting the cathepsin protease release [61, 62]. ER stress, which is a common feature of DENV-infected cells [63, 64], also up-regulates expression of *SPHK2* [65]. The up-regulated ER-localized SPHK2 may produce ceramide to induce LMP leading to releasing of cathepsin protease. Our group previously

reported the significance of cathepsin B, which mediates DENV-induced apoptosis via the intrinsic pathway in HepG2 cells [30]. Secondly, S1P from mitochondria-localized SPHK2 can induce Bak-dependent mitochondrial membrane permeabilization (MMP) induction and cytochrome c releasing [55, 66]. DENV infection was reported to influence the mitochondrial fission process to favor its own replication [67], whether S1P from mitochondria-localized SPHK2 contributes to DENV-induced apoptosis should be further investigated. Finally, S1P from nuclear-localized SPHK2 can bind and inhibit the function of histone deacetylase (HDAC) [68], which influences infection and apoptosis in other viruses [69]. Interactions of DENV capsid (DENV C) and Daxx was implicated in DENV-induce apoptosis [19], whether S1P from nuclear-localized SPHK2 influence apoptosis in the nucleus of infected cells via DENV C, Daxx, and HDAC merits further investigation. However, *SPHK2* may play the indirect role in DENV-induced apoptosis as proteomic study of DENV-infected Huh7 cells recently reveals several altered proteins related to apoptosis following DENV infection [33] but these proteins does not directly interact with SPHK2.

Conclusion

Based on the caspase 3 activity, siRNA library screening platform identifies *SPHK2* as one of the candidate genes involved in the apoptosis of DENV-infected hepatic cells. Functional studies demonstrate that knockdown of *SPHK2* reduces DENV-induced caspase 3 activity and caspase 9 activity in Huh7 cells suggesting its pro-apoptotic role via intrinsic pathway. In addition, *SPHK2* specifically contributes to apoptosis of DENV-infected liver cell lines. Knockdown of *SPHK2* in Huh7 cells infected with the four serotypes of DENV shows similar results, explaining the vital role of *SPHK2* in contribution to DENV-induced apoptosis.

Supporting information

S1 Fig. ABC294640 treatment does not induce toxicity in Huh7 cells at the tested concentrations. Huh7 cells were treated with doses of 2.5, 5, and 10 μM of ABC294640 or 0.01% v/v DMSO for 48 hours. Huh7 cells, which were cultured in media alone, were maintained as a parental control. Cell toxicity was determined using Presto-Blue dye assay and spectrophotometry analysis. Percentage of cell viability compared to that of parental control is shown from the average of three independent experiments. Statistical analysis was analyzed using Student's *t* test.
(TIF)

S2 Fig. Knockdown of *SPHK1* does not reduce caspase 3 activity in DENV-infected Huh7 cells. In the screening assay, Huh7 cells were reverse transfected with siRNA directed against the *SPHK1* gene for 24 hours before being infected with DENV at MOI of 10 for 48 hours. Caspase 3 activity was measured and represented as RLU. The results are expressed as the average of triplicate experiments ± SD. Statistical analysis was analyzed using Student's *t* test.
(TIF)

S3 Fig. Treatment of ABC294640 increases cellular viability of DENV-infected Huh7 cells at 48 and 72 hours post infection. Huh7 cells were pre-treated with 0.01% v/v DMSO or 10 μM concentrations of ABC294640 for 2 hours. The treated cells were infected with DENV at MOI 10 and were cultured in the presence of corresponding concentrations for 48, 72 and 96 hours. Cellular viability was determined using Presto-Blue dye assay and spectrophotometry analysis. Percentage of cell viability compared to that of mock cells-treated with DMSO control is shown from the average of three independent experiments. The asterisks indicate

statistically significant differences between groups ($p < 0.05$) (Student's *t* test).
(TIF)

S4 Fig. Comparison of necrotic cells (Annexin V+/PI+) between siNTC- and si*SPHK2*-transfected cells. Huh7 cells were reverse transfected with siRNA directed against *SPHK2* genes for 24 hours before being infected with DENV for 48 hours. Necrotic and apoptotic cells were determined by Annexin V/PI staining and flow cytometry analysis. Bar graph represented the percentage of necrotic cells (Annexin V+/PI+), which was plotted and compared between those of siNTC- and of si*SPHK2*-transfected cells. The results are expressed as the average of three independent experiments ± SD. Statistical analysis was analyzed using Student's *t* test.
(TIF)

S1 Table. List of 558 human genes targeted by apoptosis siRNA library, and the alteration level of caspase 3 activity after siRNA library screening in DENV-infected Huh7 cells. To explore the involvement of the apoptotic genes in DENV-infected Huh7 cells, human apoptosis siRNA library (Dharmacon) screening was performed in DENV-infected Huh7 cells. The full list of the alteration of caspase 3 activity upon siRNA transfection was shown in the S1 Table. The results were analyzed as the percentage of caspase 3 activity compared to siNTC-transfected cells.
(PDF)

Acknowledgments

This study was supported by the Mahidol University Grant (R015810002) to TL and AM was supported by the Royal Golden Jubilee (RGJ) Ph.D. Scholarship (PHD/0016/2553).

Author Contributions

Conceptualization: Justin Jang Hann Chu, Thawornchai Limjindaporn.

Data curation: Atthapan Morchang, Justin Jang Hann Chu.

Formal analysis: Atthapan Morchang, Justin Jang Hann Chu, Thawornchai Limjindaporn.

Funding acquisition: Atthapan Morchang, Thawornchai Limjindaporn.

Investigation: Atthapan Morchang, Regina Ching Hua Lee.

Resources: Pa-thai Yenchitsomanus, Sansanee Noisakran, Justin Jang Hann Chu, Thawornchai Limjindaporn.

Supervision: Justin Jang Hann Chu, Thawornchai Limjindaporn.

Validation: Atthapan Morchang, Thawornchai Limjindaporn.

Writing – original draft: Atthapan Morchang, Pa-thai Yenchitsomanus, Gopinathan Pillai Sreekanth, Sansanee Noisakran, Justin Jang Hann Chu, Thawornchai Limjindaporn.

Writing – review & editing: Atthapan Morchang, Pa-thai Yenchitsomanus, Gopinathan Pillai Sreekanth, Sansanee Noisakran, Justin Jang Hann Chu, Thawornchai Limjindaporn.

References

1. Guzman MG, Gubler DJ, Izquierdo A, Martinez E, Halstead SB. Dengue infection. Nat Rev Dis Primers. 2016; 2:16055. https://doi.org/10.1038/nrdp.2016.55 PMID: 27534439

2. Hapuarachchi HC, Oh HM, Thein TL, Pok KY, Lai YL, Tan LK, et al. Clinico-genetic characterisation of an encephalitic Dengue virus 4 associated with multi-organ involvement. Journal of clinical virology: the official publication of the Pan American Society for Clinical Virology. 2013; 57(1):91–4. https://doi.org/10.1016/j.jcv.2012.12.021 PMID: 23415634
3. Martina BE, Koraka P, Osterhaus AD. Dengue virus pathogenesis: an integrated view. Clin Microbiol Rev. 2009; 22(4):564–81. https://doi.org/10.1128/CMR.00035-09 PMID: 19822889
4. Bhamarapravati N. Hemostatic defects in dengue hemorrhagic fever. Rev Infect Dis. 1989; 11 Suppl 4: S826–9.
5. Burke T. Dengue haemorrhagic fever: a pathological study. Trans R Soc Trop Med Hyg. 1968; 62 (5):682–92. PMID: 5707920
6. Couvelard A, Marianneau P, Bedel C, Drouet MT, Vachon F, Henin D, et al. Report of a fatal case of dengue infection with hepatitis: demonstration of dengue antigens in hepatocytes and liver apoptosis. Hum Pathol. 1999; 30(9):1106–10. PMID: 10492047
7. Aye KS, Charngkaew K, Win N, Wai KZ, Moe K, Punyadee N, et al. Pathologic highlights of dengue hemorrhagic fever in 13 autopsy cases from Myanmar. Human pathology. 2014; 45(6):1221–33. https://doi.org/10.1016/j.humpath.2014.01.022 PMID: 24767772
8. Seneviratne SL, Malavige GN, de Silva HJ. Pathogenesis of liver involvement during dengue viral infections. Trans R Soc Trop Med Hyg. 2006; 100(7):608–14. https://doi.org/10.1016/j.trstmh.2005.10.007 PMID: 16483623
9. Kuo CH, Tai DI, Chang-Chien CS, Lan CK, Chiou SS, Liaw YF. Liver biochemical tests and dengue fever. Am J Trop Med Hyg. 1992; 47(3):265–70. PMID: 1355950
10. Wahid SF, Sanusi S, Zawawi MM, Ali RA. A comparison of the pattern of liver involvement in dengue hemorrhagic fever with classic dengue fever. Southeast Asian J Trop Med Public Health. 2000; 31 (2):259–63. PMID: 11127322
11. Mohan B, Patwari AK, Anand VK. Hepatic dysfunction in childhood dengue infection. J Trop Pediatr. 2000; 46(1):40–3. PMID: 10730040
12. Souza LJ, Alves JG, Nogueira RM, Gicovate Neto C, Bastos DA, Siqueira EW, et al. Aminotransferase changes and acute hepatitis in patients with dengue fever: analysis of 1,585 cases. Braz J Infect Dis. 2004; 8(2):156–63. /S1413-86702004000200006. PMID: 15361994
13. Sreekanth GP, Chuncharunee A, Sirimontaporn A, Panaampon J, Noisakran S, Yenchitsomanus PT, et al. SB203580 Modulates p38 MAPK Signaling and Dengue Virus-Induced Liver Injury by Reducing MAPKAPK2, HSP27, and ATF2 Phosphorylation. PloS one. 2016; 11(2):e0149486. https://doi.org/10.1371/journal.pone.0149486 PMID: 26901653
14. Sreekanth GP, Chuncharunee A, Sirimontaporn A, Panaampon J, Srisawat C, Morchang A, et al. Role of ERK1/2 signaling in dengue virus-induced liver injury. Virus research. 2014; 188:15–26. https://doi.org/10.1016/j.virusres.2014.03.025 PMID: 24704674
15. Paes MV, Lenzi HL, Nogueira AC, Nuovo GJ, Pinhao AT, Mota EM, et al. Hepatic damage associated with dengue-2 virus replication in liver cells of BALB/c mice. Laboratory investigation; a journal of technical methods and pathology. 2009; 89(10):1140–51. https://doi.org/10.1038/labinvest.2009.83 PMID: 19721415
16. Sreekanth GP, Chuncharunee A, Cheunsuchon B, Noisakran S, Yenchitsomanus PT, Limjindaporn T. JNK1/2 inhibitor reduces dengue virus-induced liver injury. Antiviral research. 2017; 141:7–18. https://doi.org/10.1016/j.antiviral.2017.02.003 PMID: 28188818
17. Dengue: Guidelines for Diagnosis, Treatment, Prevention and Control: New Edition. WHO Guidelines Approved by the Guidelines Review Committee. Geneva 2009.
18. Nasirudeen AM, Wang L, Liu DX. Induction of p53-dependent and mitochondria-mediated cell death pathway by dengue virus infection of human and animal cells. Microbes Infect. 2008; 10(10–11):1124–32. Epub 2008/07/09. https://doi.org/10.1016/j.micinf.2008.06.005 PMID: 18606243
19. Limjindaporn T, Netsawang J, Noisakran S, Thiemmeca S, Wongwiwat W, Sudsaward S, et al. Sensitization to Fas-mediated apoptosis by dengue virus capsid protein. Biochemical and biophysical research communications. 2007; 362(2):334–9. Epub 2007/08/21. https://doi.org/10.1016/j.bbrc.2007.07.194 PMID: 17707345
20. Li J, Huang R, Liao W, Chen Z, Zhang S. Dengue virus utilizes calcium modulating cyclophilin-binding ligand to subvert apoptosis. Biochemical and biophysical research communications. 2012; 418(4):622–7. Epub 2012/01/28. https://doi.org/10.1016/j.bbrc.2012.01.050 PMID: 22281498
21. Malhi H, Guicciardi ME, Gores GJ. Hepatocyte death: a clear and present danger. Physiological reviews. 2010; 90(3):1165–94. https://doi.org/10.1152/physrev.00061.2009 PMID: 20664081

22. Qi Y, Li Y, Zhang Y, Zhang L, Wang Z, Zhang X, et al. IFI6 Inhibits Apoptosis via Mitochondrial-Dependent Pathway in Dengue Virus 2 Infected Vascular Endothelial Cells. PloS one. 2015; 10(8):e0132743. https://doi.org/10.1371/journal.pone.0132743 PMID: 26244642

23. Lee CJ, Liao CL, Lin YL. Flavivirus activates phosphatidylinositol 3-kinase signaling to block caspase-dependent apoptotic cell death at the early stage of virus infection. Journal of virology. 2005; 79 (13):8388–99. https://doi.org/10.1128/JVI.79.13.8388-8399.2005 PMID: 15956583

24. Hannon GJ. RNA interference. Nature. 2002; 418(6894):244–51. https://doi.org/10.1038/418244a PMID: 12110901

25. Panda D, Cherry S. Cell-based genomic screening: elucidating virus-host interactions. Curr Opin Virol. 2012; 2(6):784–92. https://doi.org/10.1016/j.coviro.2012.10.007 PMID: 23122855

26. Krishnan MN, Ng A, Sukumaran B, Gilfoy FD, Uchil PD, Sultana H, et al. RNA interference screen for human genes associated with West Nile virus infection. Nature. 2008; 455(7210):242–5. https://doi.org/10.1038/nature07207 PMID: 18690214

27. Sessions OM, Barrows NJ, Souza-Neto JA, Robinson TJ, Hershey CL, Rodgers MA, et al. Discovery of insect and human dengue virus host factors. Nature. 2009; 458(7241):1047–50. https://doi.org/10.1038/nature07967 PMID: 19396146

28. Le Sommer C, Barrows NJ, Bradrick SS, Pearson JL, Garcia-Blanco MA. G protein-coupled receptor kinase 2 promotes flaviviridae entry and replication. PLoS Negl Trop Dis. 2012; 6(9):e1820. https://doi.org/10.1371/journal.pntd.0001820 PMID: 23029581

29. Ang F, Wong AP, Ng MM, Chu JJ. Small interference RNA profiling reveals the essential role of human membrane trafficking genes in mediating the infectious entry of dengue virus. Virol J. 2010; 7:24. https://doi.org/10.1186/1743-422X-7-24 PMID: 20122152

30. Morchang A, Panaampon J, Suttitheptumrong A, Yasamut U, Noisakran S, Yenchitsomanus PT, et al. Role of cathepsin B in dengue virus-mediated apoptosis. Biochemical and biophysical research communications. 2013; 438(1):20–5. https://doi.org/10.1016/j.bbrc.2013.07.009 PMID: 23867824

31. Morchang A, Yasamut U, Netsawang J, Noisakran S, Wongwiwat W, Songprakhon P, et al. Cell death gene expression profile: role of RIPK2 in dengue virus-mediated apoptosis. Virus Res. 2011; 156(1–2):25–34. Epub 2011/01/05. https://doi.org/10.1016/j.virusres.2010.12.012 PMID: 21195733

32. Wiley SR, Winkles JA. TWEAK, a member of the TNF superfamily, is a multifunctional cytokine that binds the TweakR/Fn14 receptor. Cytokine & growth factor reviews. 2003; 14(3–4):241–9.

33. Pando-Robles V, Oses-Prieto JA, Rodriguez-Gandarilla M, Meneses-Romero E, Burlingame AL, Batista CV. Quantitative proteomic analysis of Huh-7 cells infected with Dengue virus by label-free LC-MS. Journal of proteomics. 2014; 111:16–29. https://doi.org/10.1016/j.jprot.2014.06.029 PMID: 25009145

34. Tran AT, Rahim MN, Ranadheera C, Kroeker A, Cortens JP, Opanubi KJ, et al. Knockdown of specific host factors protects against influenza virus-induced cell death. Cell Death Dis. 2013; 4:e769. https://doi.org/10.1038/cddis.2013.296 PMID: 23949218

35. McCarthy JV, Ni J, Dixit VM. RIP2 is a novel NF-kappaB-activating and cell death-inducing kinase. The Journal of biological chemistry. 1998; 273(27):16968–75. PMID: 9642260

36. Navas TA, Baldwin DT, Stewart TA. RIP2 is a Raf1-activated mitogen-activated protein kinase kinase. The Journal of biological chemistry. 1999; 274(47):33684–90. PMID: 10559258

37. Thome M, Hofmann K, Burns K, Martinon F, Bodmer JL, Mattmann C, et al. Identification of CARDIAK, a RIP-like kinase that associates with caspase-1. Curr Biol. 1998; 8(15):885–8. PMID: 9705938

38. Nasirudeen AM, Liu DX. Gene expression profiling by microarray analysis reveals an important role for caspase-1 in dengue virus-induced p53-mediated apoptosis. J Med Virol. 2009; 81(6):1069–81. https://doi.org/10.1002/jmv.21486 PMID: 19382257

39. Santos WL, Lynch KR. Drugging sphingosine kinases. ACS chemical biology. 2015; 10(1):225–33. https://doi.org/10.1021/cb5008426 PMID: 25384187

40. Leclercq TM, Pitson SM. Cellular signalling by sphingosine kinase and sphingosine 1-phosphate. IUBMB Life. 2006; 58(8):467–72. https://doi.org/10.1080/15216540600871126 PMID: 16916784

41. Maceyka M, Sankala H, Hait NC, Le Stunff H, Liu H, Toman R, et al. SphK1 and SphK2, sphingosine kinase isoenzymes with opposing functions in sphingolipid metabolism. The Journal of biological chemistry. 2005; 280(44):37118–29. https://doi.org/10.1074/jbc.M502207200 PMID: 16118219

42. Alvarez SE, Harikumar KB, Hait NC, Allegood J, Strub GM, Kim EY, et al. Sphingosine-1-phosphate is a missing cofactor for the E3 ubiquitin ligase TRAF2. Nature. 2010; 465(7301):1084–8. https://doi.org/10.1038/nature09128 PMID: 20577214

43. Pyne NJ, Pyne S. Sphingosine 1-phosphate and cancer. Nat Rev Cancer. 2010; 10(7):489–503. https://doi.org/10.1038/nrc2875 PMID: 20555359

44. Meyer zu Heringdorf D, Jakobs KH. Lysophospholipid receptors: signalling, pharmacology and regulation by lysophospholipid metabolism. Biochim Biophys Acta. 2007; 1768(4):923–40. https://doi.org/10.1016/j.bbamem.2006.09.026 PMID: 17078925

45. Carr JM, Kua T, Clarke JN, Calvert JK, Zebol JR, Beard MR, et al. Reduced sphingosine kinase 1 activity in dengue virus type-2 infected cells can be mediated by the 3' untranslated region of dengue virus type-2 RNA. The Journal of general virology. 2013; 94(Pt 11):2437–48. https://doi.org/10.1099/vir.0.055616-0 PMID: 23939980

46. Wati S, Rawlinson SM, Ivanov RA, Dorstyn L, Beard MR, Jans DA, et al. Tumour necrosis factor alpha (TNF-alpha) stimulation of cells with established dengue virus type 2 infection induces cell death that is accompanied by a reduced ability of TNF-alpha to activate nuclear factor kappaB and reduced sphingosine kinase-1 activity. The Journal of general virology. 2011; 92(Pt 4):807–18. https://doi.org/10.1099/vir.0.028159-0 PMID: 21148274

47. Clarke JN, Davies LK, Calvert JK, Gliddon BL, Al Shujari WH, Aloia AL, et al. Reduction in sphingosine kinase 1 influences the susceptibility to dengue virus infection by altering antiviral responses. The Journal of general virology. 2016; 97(1):95–109. https://doi.org/10.1099/jgv.0.000334 PMID: 26541871

48. Michels M, Japtok L, Alisjahbana B, Wisaksana R, Sumardi U, Puspita M, et al. Decreased plasma levels of the endothelial protective sphingosine-1-phosphate are associated with dengue-induced plasma leakage. The Journal of infection. 2015; 71(4):480–7. https://doi.org/10.1016/j.jinf.2015.06.014 PMID: 26183296

49. Gomes L, Fernando S, Fernando RH, Wickramasinghe N, Shyamali NL, Ogg GS, et al. Sphingosine 1-phosphate in acute dengue infection. PloS one. 2014; 9(11):e113394. https://doi.org/10.1371/journal.pone.0113394 PMID: 25409037

50. Gao P, Smith CD. Ablation of sphingosine kinase-2 inhibits tumor cell proliferation and migration. Molecular cancer research: MCR. 2011; 9(11):1509–19. https://doi.org/10.1158/1541-7786.MCR-11-0336 PMID: 21896638

51. Chumanevich AA, Poudyal D, Cui X, Davis T, Wood PA, Smith CD, et al. Suppression of colitis-driven colon cancer in mice by a novel small molecule inhibitor of sphingosine kinase. Carcinogenesis. 2010; 31(10):1787–93. https://doi.org/10.1093/carcin/bgq158 PMID: 20688834

52. Beljanski V, Lewis CS, Smith CD. Antitumor activity of sphingosine kinase 2 inhibitor ABC294640 and sorafenib in hepatocellular carcinoma xenografts. Cancer biology & therapy. 2011; 11(5):524–34.

53. Antoon JW, White MD, Slaughter EM, Driver JL, Khalili HS, Elliott S, et al. Targeting NFkB mediated breast cancer chemoresistance through selective inhibition of sphingosine kinase-2. Cancer biology & therapy. 2011; 11(7):678–89.

54. Venkata JK, An N, Stuart R, Costa LJ, Cai H, Coker W, et al. Inhibition of sphingosine kinase 2 downregulates the expression of c-Myc and Mcl-1 and induces apoptosis in multiple myeloma. Blood. 2014; 124(12):1915–25. https://doi.org/10.1182/blood-2014-03-559385 PMID: 25122609

55. Chipuk JE, McStay GP, Bharti A, Kuwana T, Clarke CJ, Siskind LJ, et al. Sphingolipid metabolism cooperates with BAK and BAX to promote the mitochondrial pathway of apoptosis. Cell. 2012; 148(5):988–1000. https://doi.org/10.1016/j.cell.2012.01.038 PMID: 22385963

56. Okada T, Ding G, Sonoda H, Kajimoto T, Haga Y, Khosrowbeygi A, et al. Involvement of N-terminal-extended form of sphingosine kinase 2 in serum-dependent regulation of cell proliferation and apoptosis. The Journal of biological chemistry. 2005; 280(43):36318–25. https://doi.org/10.1074/jbc.M504507200 PMID: 16103110

57. Hofmann LP, Ren S, Schwalm S, Pfeilschifter J, Huwiler A. Sphingosine kinase 1 and 2 regulate the capacity of mesangial cells to resist apoptotic stimuli in an opposing manner. Biological chemistry. 2008; 389(11):1399–407. https://doi.org/10.1515/BC.2008.160 PMID: 18783337

58. Shi Y, Rehman H, Ramshesh VK, Schwartz J, Liu Q, Krishnasamy Y, et al. Sphingosine kinase-2 inhibition improves mitochondrial function and survival after hepatic ischemia-reperfusion. Journal of hepatology. 2012; 56(1):137–45. https://doi.org/10.1016/j.jhep.2011.05.025 PMID: 21756852

59. Sawai H, Domae N. Discrimination between primary necrosis and apoptosis by necrostatin-1 in Annexin V-positive/propidium iodide-negative cells. Biochemical and biophysical research communications. 2011; 411(3):569–73. https://doi.org/10.1016/j.bbrc.2011.06.186 PMID: 21763280

60. Neubauer HA, Pitson SM. Roles, regulation and inhibitors of sphingosine kinase 2. The FEBS journal. 2013; 280(21):5317–36. https://doi.org/10.1111/febs.12314 PMID: 23638983

61. Werneburg N, Guicciardi ME, Yin XM, Gores GJ. TNF-alpha-mediated lysosomal permeabilization is FAN and caspase 8/Bid dependent. American journal of physiology Gastrointestinal and liver physiology. 2004; 287(2):G436–43. https://doi.org/10.1152/ajpgi.00019.2004 PMID: 15075251

62. Ullio C, Casas J, Brunk UT, Sala G, Fabrias G, Ghidoni R, et al. Sphingosine mediates TNFalpha-induced lysosomal membrane permeabilization and ensuing programmed cell death in hepatoma cells. Journal of lipid research. 2012; 53(6):1134–43. https://doi.org/10.1194/jlr.M022384 PMID: 22454477

63. Thepparit C, Khakpoor A, Khongwichit S, Wikan N, Fongsaran C, Chingsuwanrote P, et al. Dengue 2 infection of HepG2 liver cells results in endoplasmic reticulum stress and induction of multiple pathways of cell death. BMC research notes. 2013; 6:372. https://doi.org/10.1186/1756-0500-6-372 PMID: 24034452

64. Pena J, Harris E. Dengue virus modulates the unfolded protein response in a time-dependent manner. The Journal of biological chemistry. 2011; 286(16):14226–36. https://doi.org/10.1074/jbc.M111.222703 PMID: 21385877

65. Lee SY, Hong IK, Kim BR, Shim SM, Sung Lee J, Lee HY, et al. Activation of sphingosine kinase 2 by endoplasmic reticulum stress ameliorates hepatic steatosis and insulin resistance in mice. Hepatology. 2015; 62(1):135–46. https://doi.org/10.1002/hep.27804 PMID: 25808625

66. Strub GM, Paillard M, Liang J, Gomez L, Allegood JC, Hait NC, et al. Sphingosine-1-phosphate produced by sphingosine kinase 2 in mitochondria interacts with prohibitin 2 to regulate complex IV assembly and respiration. FASEB journal: official publication of the Federation of American Societies for Experimental Biology. 2011; 25(2):600–12. https://doi.org/10.1096/fj.10-167502 PMID: 20959514

67. Barbier V, Lang D, Valois S, Rothman AL, Medin CL. Dengue virus induces mitochondrial elongation through impairment of Drp1-triggered mitochondrial fission. Virology. 2017; 500:149–60. https://doi.org/10.1016/j.virol.2016.10.022 PMID: 27816895

68. Hait NC, Allegood J, Maceyka M, Strub GM, Harikumar KB, Singh SK, et al. Regulation of histone acetylation in the nucleus by sphingosine-1-phosphate. Science. 2009; 325(5945):1254–7. https://doi.org/10.1126/science.1176709 PMID: 19729656

69. Zhou L, He X, Gao B, Xiong S. Inhibition of Histone Deacetylase Activity Aggravates Coxsackievirus B3-Induced Myocarditis by Promoting Viral Replication and Myocardial Apoptosis. J Virol. 2015; 89 (20):10512–23. https://doi.org/10.1128/JVI.01028-15 PMID: 26269170

Biochemical and Biophysical Research Communications 478 (2016) 410–416

Contents lists available at ScienceDirect

Biochemical and Biophysical Research Communications

journal homepage: www.elsevier.com/locate/ybbrc

Drug repurposing of minocycline against dengue virus infection

Shilpa Lekshmi Leela [a, b], Chatchawan Srisawat [a], Gopinathan Pillai Sreekanth [c], Sansanee Noisakran [d, e], Pa-thai Yenchitsomanus [b], Thawornchai Limjindaporn [c, *]

[a] Department of Biochemistry, Faculty of Medicine Siriraj Hospital, Mahidol University, Bangkok, Thailand
[b] Division of Molecular Medicine, Department of Research and Development, Faculty of Medicine Siriraj Hospital, Mahidol University, Bangkok, Thailand
[c] Department of Anatomy, Faculty of Medicine Siriraj Hospital, Mahidol University, Bangkok, Thailand
[d] Medical Biotechnology Unit, National Cancer Center for Genetic Engineering and Biotechnology, National Science and Technology Development Agency, Thailand
[e] Division of Dengue Hemorrhagic Fever Research, Department of Research and Development, Faculty of Medicine Siriraj Hospital, Mahidol University, Bangkok, Thailand

ARTICLE INFO

Article history:
Received 24 June 2016
Accepted 6 July 2016
Available online 7 July 2016

Keywords:
Dengue virus infection
Minocycline
ERK1/2
Antiviral activity

ABSTRACT

Dengue virus infection is one of the most common arthropod-borne viral diseases. A complex interplay between host and viral factors contributes to the severity of infection. The antiviral effects of three antibiotics, lomefloxacin, netilmicin, and minocycline, were examined in this study, and minocycline was found to be a promising drug. This antiviral effect was confirmed in all four serotypes of the virus. The effects of minocycline at various stages of the viral life cycle, such as during viral RNA synthesis, intracellular envelope protein expression, and the production of infectious virions, were examined and found to be significantly reduced by minocycline treatment. Minocycline also modulated host factors, including the phosphorylation of extracellular signal-regulated kinase1/2 (ERK1/2). The transcription of antiviral genes, including 2′-5′-oligoadenylate synthetase 1 (*OAS1*), 2′-5′-oligoadenylate synthetase 3 (*OAS3*), and interferon α (*IFNA*), was upregulated by minocycline treatment. Therefore, the antiviral activity of minocycline may have a potential clinical use against *Dengue virus* infection.

1. Introduction

Dengue virus (DENV) infection is a mosquito-borne viral disease transmitted by mosquitoes of the *Aedes* family and is mainly endemic in the tropical and subtropical regions of the world [1]. The clinical severity of DENV infection, which ranges from a mild febrile illness, dengue fever (DF), to severe forms, such as dengue hemorrhagic fever (DHF) and dengue shock syndrome (DSS), predominantly results from the existence of four distinct serotypes of DENV (DENV1–4). The serious manifestations associated with DHF include hemorrhage, thrombocytopenia, plasma leakage, and hemoconcentration, which can lead to DSS, which is associated with lethal shock [2,3]. Another serious complication of DENV infection is hepatic dysfunction, apparent as increased liver transaminase levels and hepatomegaly, and in severe cases, bleeding, hepatic cell apoptosis, and further liver damage [4,5].

Many complex factors contribute to the severity of DENV infection, including the massive activation of cytokines and the interplay between host and viral factors [2]. DENV replicates using the host machinery and therefore manipulates the innate and adaptive immune responses, resulting in uncontrolled cytokine production, which favors viral replication [6,7]. Vaccines and antiviral agents are two important ways to control viral diseases, but even after decades of research, there is no effective antiviral therapy for DENV infection.

Several antibiotics and antiviral agents have been investigated for the treatment of DENV infection. For example, an analogue of the antibiotic teicoplanin and a plant-derived alkaloid, castanospermine, were shown to reduce DENV infection [8,9]. Compounds like narasin, geneticin, and lanatoside C, have also demonstrated antiviral activity against DENV [10–12]. The antibiotics used in this study are U.S. Food and Drug Administration (FDA) approved and have been previously shown to be effective against infectious agents [13]. Lomefloxacin belongs to the fluoroquinolone group of drugs and is mainly used to treat bacterial infections, such as urinary tract infections and bronchitis. Netilmicin is an aminoglycoside family antibiotic and is mainly bacteriostatic in action.

* Corresponding author.
E-mail address: thawornchai.lim@mahidol.ac.th (T. Limjindaporn).

http://dx.doi.org/10.1016/j.bbrc.2016.07.029
0006-291X/

Minocycline is a second-generation semisynthetic tetracycline derivative with anti-inflammatory and immunomodulatory effects, and has been widely used in the treatment of rheumatoid arthritis, acne, and urinary tract infections [14,15]. The antiviral potential of minocycline against other viruses has also been reported; these include *Human immunodeficiency virus*, *Japanese encephalitis virus*, and *West Nile virus* [16–18].

In this study, we examined the effects of lomefloxacin, netilmicin, and minocycline on DENV infection. Minocycline was found to be effective in reducing DENV infection, and this antiviral effect was confirmed in all four serotypes of the virus. Minocycline reduced viral RNA synthesis, intracellular viral protein synthesis, and infectious virus production. Minocycline was then found to reduce the phosphorylation of ERK1/2, which is associated with enhanced pathogenesis and organ injury in DENV infection [19]. We also investigated whether the reduction of DENV-induced ERK1/2 phosphorylation by minocycline affects the expression of antiviral genes, because ERK signaling has been reported to downregulate the expression of antiviral genes in *Hepatitis C virus* (HCV) infection [20]. As expected, the mRNA expression of antiviral genes, such as those encoding 2′-5′-oligoadenylate synthetase 1 (*OAS1*), *OAS3*, and interferon α (*IFNA*), was upregulated after treatment with minocycline. Therefore, minocycline treatment may reduce DENV infection in HepG2 cells by reducing the phosphorylation of ERK and subsequently upregulating antiviral gene expression.

2. Materials and methods

2.1. Cell culture, virus infection and drugs treatment

The human hepatocarcinoma cell line, HepG2 (American Type Culture Collection, VA, USA) was used in this study. DENV serotype 2 (DENV2; strain 16681) was used for the major part of the study. DENV1 (strain Hawaii), DENV3 (strain H87), and DENV4 (strain H241) were also used. HepG2 cells were grown in Dulbecco's modified Eagle's medium (DMEM; Gibco-BRL, NY, USA) supplemented with 10% fetal bovine serum, 2 mM L-glutamine, 1% nonessential amino acids, 1 mM sodium pyruvate, and 100 U/ml penicillin–streptomycin, at 37 °C in a humidified chamber under 5% CO_2. The antibiotics, lomefloxacin, netilmicin, and minocycline (Sigma Aldrich, MO, USA) were dissolved in sterile water. For the study, HepG2 cells were infected with DENV2 at a multiplicity of infection (MOI) of 1 and treated with the antibiotics at doses 100, 200, and 400 μM. For studying other DENV serotypes, HepG2 cells were infected with DENV1, DENV3 and DENV4 at an MOI of 1 and treated with minocycline (100, 200, and 400 μM). All the experiments were performed 48 h after treatment.

2.2. Cytotoxicity assay

The cytotoxicity of the drugs was analyzed with the 50% cytotoxic concentration (CC_{50}, defined as the concentration at which 50% of the cells are viable). The drugs were serially diluted in maintenance DMEM and administered to HepG2 cells; untreated cells were used as the control. The plates were incubated for 48 h at 37 °C in a CO_2 incubator and then PrestoBlue Cell Viability Reagent (10 μl/well; Invitrogen, CA, USA) was added. The plates were incubated in the dark at 37 °C for 30 min and then the absorbance was measured at 570–595 nm with a Synergy microplate reader (BioTek, VT, USA). The percentage viability was calculated for each dilution of the drugs by normalizing the result to the untreated mock control (100% viability). CC_{50} was calculated and analyzed with GraphPad Prism version 5.01 (GraphPad Software, Inc.).

2.3. Real-time reverse transcription (RT)–PCR

DENV2-infected and minocycline-treated HepG2 cells were collected at 48 h after treatment, the total RNA was extracted (High Pure RNA Isolation Kit, Roche, Mannheim, Germany), and the cDNA was synthesized (GoScript™ Reverse Transcription System, Promega, WI, USA). Using specific primers, the expression of the genes of interest was measured with RT–PCR using SYBR Green I reaction mix (Roche) in the Roche Light Cycler 480. The primer sequences for each gene are shown in Table 1.

2.4. Enzyme-linked immunosorbent assay (ELISA)

DENV2-infected and minocycline-treated HepG2 cells were successively stained with a mouse monoclonal antibody against DENV E protein (4G2 clone) and horseradish peroxidase (HRP)-conjugated rabbit anti-mouse immunoglobulin antibody (diluted 1:1000; Dako, CA, USA) at 48 h after treatment. A substrate (3,3′,5,5′-tetramethylbenzidine; Invitrogen, CA, USA) was added and the absorbance was measured at 495–620 nm using a Synergy microplate reader. Cell viability was also checked by adding PrestoBlue Cell Viability Reagent (Invitrogen) and the cells were incubated for 30 min in the dark. The absorbance at 570–595 nm was measured with Synergy microplate reader and the percentage cell viability was calculated relative to that of the mock control.

2.5. Focus-forming unit (FFU) assay

The supernatants were collected 48 h after minocycline treatment and an FFU assay was performed [21]. Briefly, the collected supernatants were added to Vero cells in a 96-well plate, incubated for 2 h, and then overlain with 1.5% gum tragacanth in 2 × minimal essential medium. After incubation for 72 h, the cells were washed with PBS, fixed with 3.7% formaldehyde, and permeabilized with 1% Triton X-100. The cells were then washed and incubated with a primary antibody directed against DENV E (4G2 clone) for 1 h and with HRP-conjugated rabbit anti-mouse secondary antibody (Dako) for 30 min. The 3,3′-diaminobenzidine substrate (Sigma Aldrich) was added to develop the foci of infected cells. The foci were counted under a microscope and FFUs calculated as the number of foci/ml.

2.6. Western blotting analysis

DENV2-infected cells were collected 48 h after minocycline treatment. The cell lysates were prepared and subjected to a western blotting analysis, as previously described [22]. The protein concentrations were measured with the Bradford Protein Assay

Table 1
Primer sequences for real time RT–PCR. Primer sequences for each gene (5′ → 3′ direction; F, forward; R, reverse).

Primer name	Primer sequences (5′ → 3′)
DENV E-F	ATCCAGATGTCATCAGGAAAC
DENV E-R	CCGGCTCTACTCCTATGATG
OAS1-F	CTCAAGAGCCTCATCCG
OAS1-R	GCAGAGTTGCTGGTAGTTTA
OAS2-F	GCTTTGATGTGCTTCCTGCCTT
OAS2-R	ACCCCTTTGGCTTCAGTTTCCTT
OAS3-F	GATGGACTTGTACAGCACCCC
OAS3-R	TCACACAGCAGCCTTCACTG
IFN-α-F	TTTCTCCTGCCTGAAGGACAG
IFN-α-R	GCTCATGATTTCTGCTCTGAC
GAPDH-F	CGACCACTTTGTCAAGCTCA
GAPDH-R	AGGGGTCTACATCGCAACTG

(Bio-Rad Laboratories, CA, USA) and equal protein concentrations were loaded onto an SDS-polyacrylamide gel after denaturation at 95 °C for 5 min. The proteins in the cell lysates were separated with SDS-PAGE, and blotted onto a nitrocellulose membrane. The membrane was blocked for 1 h with 5% bovine serum albumin in Tris-buffered saline containing 0.1% Tween 20 to detect phosphorylated ERK1/2, and with 5% skim milk in PBS containing 0.1% Tween 20 to detect total ERK1/2 and glyceraldehyde 3-phosphate dehydrogenase (GAPDH). After the membrane was washed, it was incubated overnight at 4 °C with a primary antibody directed against phosphorylated ERK1/2 (rabbit anti-human; diluted 1:1000; Cell Signaling Technology, MA, USA), total ERK1/2 (mouse anti-human; diluted 1:2000; Cell Signaling), or GAPDH (mouse anti-human; diluted 1:2000; Santa Cruz Biotechnology, CA, USA). After the membrane was washed, the corresponding HRP-conjugated swine anti-rabbit or rabbit anti-mouse secondary antibody (diluted 1:2000; Dako) was added and the membrane was incubated for 1 h. SuperSignal West Pico Chemiluminescent Substrate (Thermo Fisher Scientific, MA, USA) was added and the signal was visualized by exposing the membrane to X-ray film. The band intensities from three independent experiments were quantified with the ImageJ software version 1.46r (http://imagej.nih.gov/ij).

2.7. Statistical analysis

The data obtained from three independent experiments are presented as means ± SEM. Statistical differences were analyzed with one-way ANOVA or two-way ANOVA using GraphPad Prism software. p values < 0.05 were considered significant.

3. Results and discussion

3.1. Effects of antibiotics on DENV infection

First, the cytotoxicity of each antibiotic (lomefloxacin, netilmicin, or minocycline) was analyzed as CC_{50} (Fig. 1A). Concentrations very much lower than the CC_{50} of each drug were used in subsequent experiments. The antiviral effect of each drug on DENV2 was examined. For this, DENV2-infected HepG2 cells were treated with the antibiotics. The intracellular DENV E protein level was examined with an ELISA by staining with an antibody (4G2) against the DENV E protein. Levels were expressed as the percentage of intracellular E protein relative to that in the vehicle-treated control cells (Fig. 1B). Simultaneously, the corresponding percentage cell viability was examined with the PrestoBlue Cell Viability Assay.

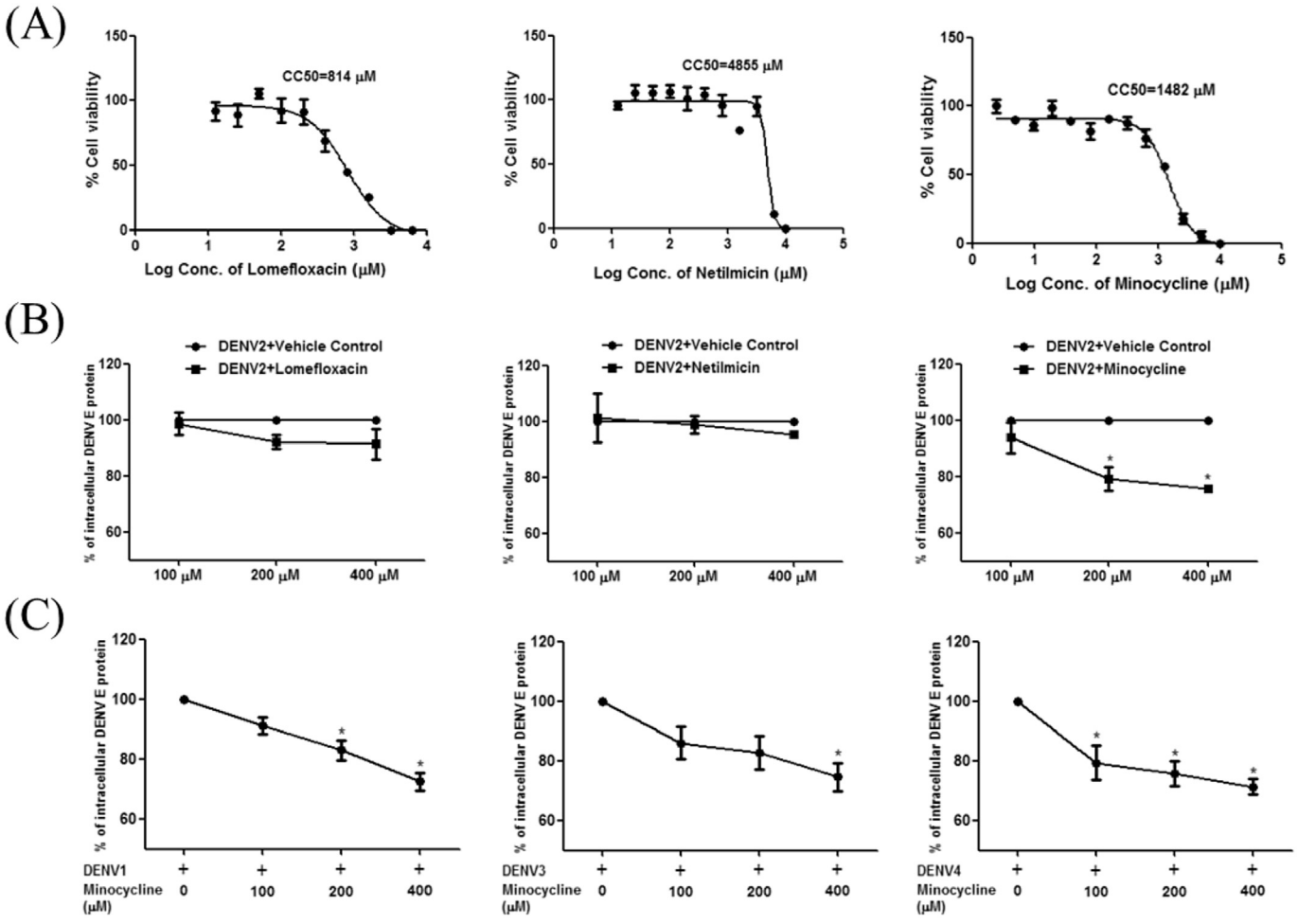

Fig. 1. Minocycline reduced DENV infection in HepG2 cells. (A) The CC_{50}s of the drugs were examined in HepG2 cells. HepG2 cell line was infected with DENV2 at an MOI of 1 and treated separately with the antibiotics lomefloxacin, netilmicin, and minocycline, at doses 100 μM, 200 μM, and 400 μM, or with vehicle. (B) At 48 h after treatment, the levels of intracellular DENV E protein were examined by staining with the 4G2 antibody directed against DENV E protein. To examine the effects of minocycline on the other DENV serotypes, the HepG2 cell line was infected separately with different DENV serotypes and treated with minocycline (100 μM, 200 μM, or 400 μM) or vehicle. (C) At 48 h after treatment, the intracellular DENV E protein levels were examined as described above. Results are the means of three independent experiments. Asterisks indicate statistically significant differences between the minocycline-treated and untreated groups ($^*p < 0.05$).

Minocycline displayed significantly greater antiviral activity against DENV infection than the other antibiotics, without being cytotoxic to the cells. Therefore, minocycline was selected for further study. To determine whether the antiviral action of minocycline is specific to all DENV serotypes, the intracellular DENV E levels in cells infected with DENV serotype 1, DENV serotype 3, or DENV serotype 4 were measured after minocycline treatment (Fig. 1C). Treatment with minocycline significantly and dose-dependently reduced the intracellular viral E protein expression, but did not induce cell cytotoxicity (Supplementary Fig. 1). Therefore, the antiviral effects of minocycline on the other serotypes of DENV (DENV1, DENV3, and DENV4) were confirmed, indicating that minocycline acts against all DENV serotypes.

3.2. Effects of minocycline on different stages of the DENV replication cycle

The antiviral effects of minocycline against DENV2 were studied at different stages of the viral life cycle. First, the expression of DENV RNA was examined with real-time RT–PCR, and was reduced dose-dependently after treatment with minocycline, suggesting that minocycline affects viral RNA synthesis (Fig. 2A). Second, intracellular DENV E protein levels were analyzed with an ELISA, and were significantly reduced by minocycline treatment, consistent with the real-time RT–PCR result, implying that minocycline interrupts the synthesis of viral proteins (Fig. 2B). Finally, the production of infectious virus was examined with an FFU assay and ~2 log reduction in virus production was observed after the minocycline treatment (Fig. 2C). Cell viability after minocycline treatment was also examined simultaneously to confirm that the observed reduction in virus was not attributable to reduced cell viability (Fig. 2D). Therefore, significant reductions in viral RNA and protein expression, and the production of infectious virus after minocycline treatment indicate the important roles of minocycline in reducing DENV infection.

3.3. Effect of minocycline on DENV-induced activation of ERK

To determine whether the effects of minocycline are exerted *via* host signaling pathways, we studied ERK1/2 signaling, which has already been shown to be involved in the pathogenesis of DENV. ERK1/2 phosphorylation was recently shown to be associated with the severity of DENV infection by increasing DENV-induced liver injury *in vivo* [19]. The inhibition of ERK1/2 phosphorylation resulted in a dose-dependent inhibition of DENV infection [23]. Minocycline was also shown to have an inhibitory effect on ERK1/2 phosphorylation in microglia [24] and neurons [25]. Therefore, in this study, to clarify the mechanism by which minocycline reduces DENV infection, the levels of phosphorylated ERK1/2 were examined after treatment with minocycline. Minocycline-treated DENV2-infected HepG2 cells were collected 48 h after treatment and a western blotting analysis was used to detect phosphorylated ERK (p-ERK) and total ERK (t-ERK) in the cell lysates. ERK phosphorylation, specifically phosphorylated ERK (p-ERK1 and p-ERK2), was significantly and dose-dependently reduced by minocycline treatment, whereas the level of t-ERK was relatively unchanged (Fig. 3A). A densitometry analysis of p-ERK1 and t-ERK1 (Fig. 3B) and p-ERK2 and t-ERK2 normalized to GAPDH (Fig. 3C) was performed in three independent experiments with the ImageJ software. We show here that the DENV-induced phosphorylation of ERK1/2 was reduced by minocycline (Fig. 3D). This demonstrates that the action of minocycline in reducing DENV infection may be mediated by the inhibition of the ERK1/2 signaling pathway.

3.4. Expression of antiviral genes after minocycline treatment

ERK1/2 activation has been reported to inhibit IFN-induced antiviral gene expression in HCV, which increases the survival of virus [20,26]. The IFN system (mainly IFN-α, IFN-β, and IFN-γ) is the major antiviral pathway that helps to block early viral replication and the associated pathogenesis, mediated by the expression of antiviral genes [27,28]. The IFN system plays an antiviral

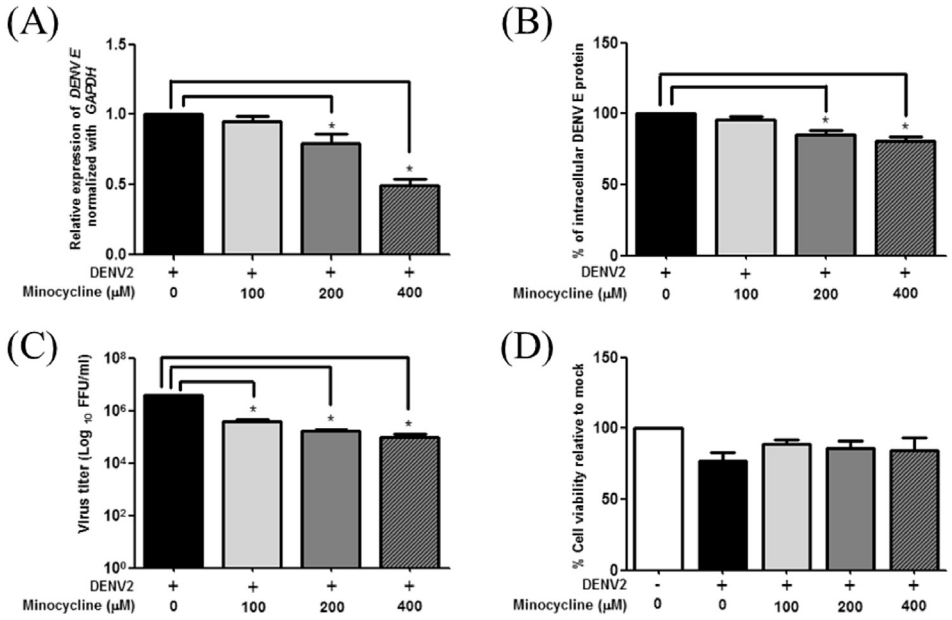

Fig. 2. Minocycline affected different stages of DENV life cycle. HepG2 cells were infected with DENV2 at an MOI of 1, treated with minocycline (100 μM, 200 μM, or 400 μM) or vehicle. After incubation for 48 h, (A) relative mRNA expression of DENV E was determined with real-time RT–PCR, and normalized to GAPDH. (B) Intracellular DENV E protein was determined with an ELISA. (C) Infectious virus production was quantified in the culture supernatants with an FFU assay. (D) Percentage cell viability was analyzed with the PrestoBlue Cell Viability Assay. Results are the averages of three independent experiments. Asterisks indicate statistically significant differences between the minocycline-treated and untreated groups ($^*p < 0.05$).

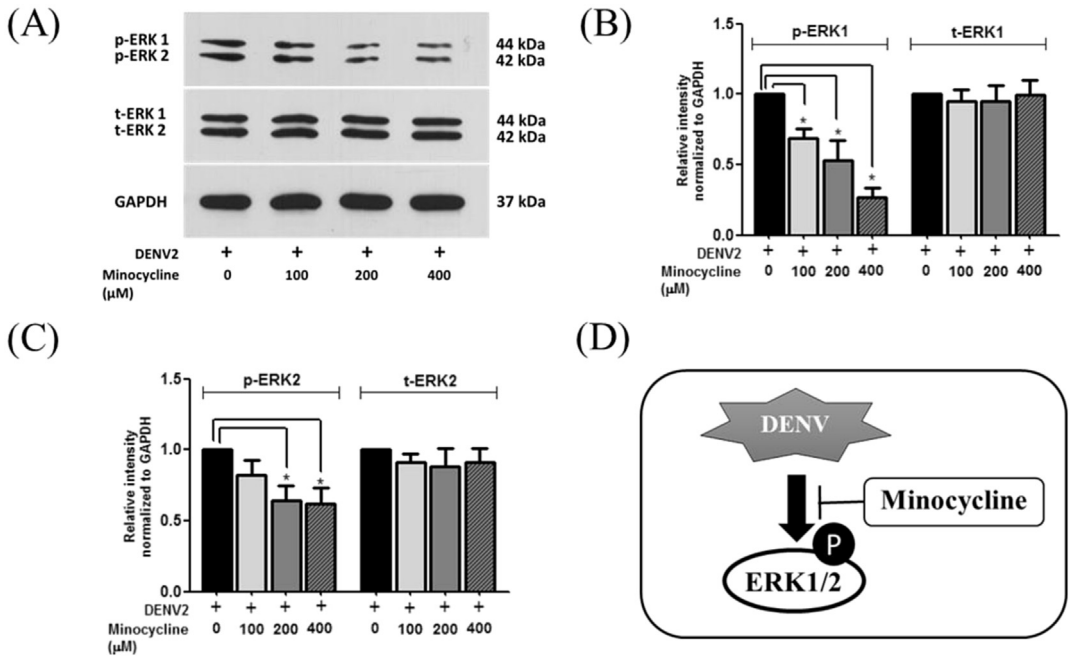

Fig. 3. Minocycline reduced DENV-induced ERK phosphorylation. HepG2 cell line was infected with DENV2 at an MOI of 1, treated with minocycline (100 μM, 200 μM, or 400 μM) or vehicle, and incubated for 48 h. (A) Western blotting analysis was performed for phosphorylated ERK, total ERK, and GAPDH. Corresponding ImageJ analyses were performed of (B) phosphorylated ERK1 and total ERK1, normalized to GAPDH; (C) phosphorylated ERK2 and total ERK2, normalized to GAPDH; (D) minocycline treatment reduced the phosphorylation of ERK1/2. Results are the means of three independent experiments. Asterisks indicate statistically significant differences between the minocycline-treated and untreated groups (*$p < 0.05$).

role in DENV infection, and DENV evades this antiviral milieu by downregulating the IFN response in different ways [29,30]. Because minocycline treatment reduced virus production and the phosphorylation of ERK, the analysis of the expression of antiviral genes is important in this context. Therefore, the transcription of some antiviral genes was examined in the minocycline-treated

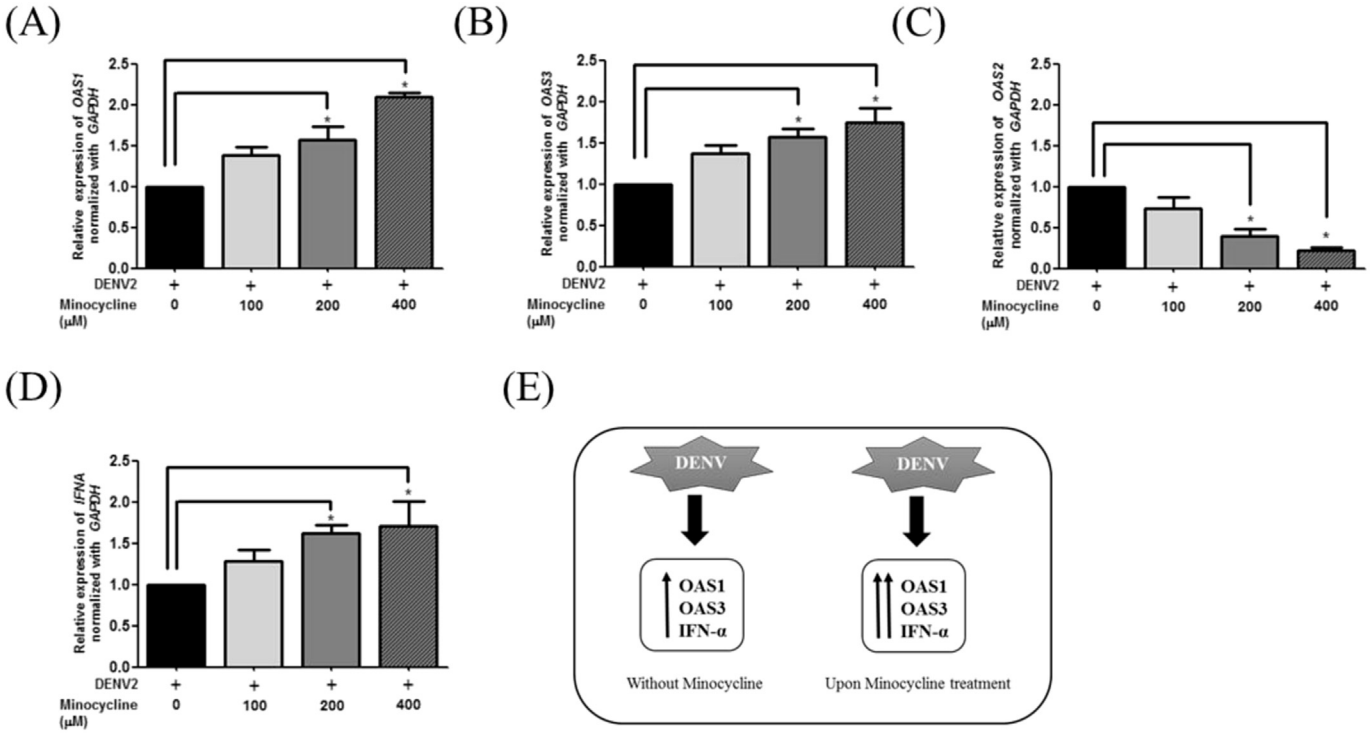

Fig. 4. Minocycline increased the expression of IFN-induced antiviral genes. HepG2 cell line was infected with DENV2 at an MOI of 1, treated with minocycline (100 μM, 200 μM, or 400 μM) or vehicle, and incubated for 48 h. Relative transcription of (A) *OAS1*, (B) *OAS3*, (C) *OAS2*, and (D) *IFNA* was measured with real-time RT–PCR. (E) Illustration of the proposed mechanism of action of minocycline against DENV infection. Results are the means of three independent experiments. Asterisks indicate statistically significant differences between the minocycline-treated and untreated groups (*$p < 0.05$).

DENV2-infected HepG2 cell line. Two isoforms of *OAS*, including *OAS1* (Fig. 4A) and *OAS3* (Fig. 4B), were significantly upregulated after minocycline treatment, whereas *OAS2* showed a decreasing trend (Fig. 4C). The expression of the *OAS* genes in humans during viral infection provides the antiviral role. Viruses counteract this antiviral effect, thus upregulating their replication [31–33]. OAS-mediated antiviral activity has been reported during DENV infection, where the OAS1 and OAS3 isoforms, but not OAS2, are upregulated by the host as an antiviral mechanism [34,35]. In this study, we also observed a significant upregulation of *OAS1* and *OAS3* expression, but not *OAS2* expression, after minocycline treatment, suggesting that OAS1 and OAS3 play major roles in antiviral activity against DENV. *IFNA* expression was also upregulated by minocycline treatment (Fig. 4D), consistent with the activation of *OAS1/3*. Thus, minocycline effectively upregulated the expression of antiviral genes, such as *OAS1* and *OAS3*, and increased *IFNA* expression in DENV2-infected HepG2 cells. The proposed mechanism of the antiviral activity of minocycline is illustrated (Fig. 4E).

In summary, DENV infection was significantly reduced after minocycline treatment, and the antiviral effect of minocycline was confirmed in all four serotypes of DENV. Reduced ERK1/2 phosphorylation and the upregulated transcription of certain antiviral genes were observed after minocycline treatment. How minocycline promotes IFN-α-mediated antiviral activity against DENV *via* the ERK1/2 pathway warrants further investigation.

Acknowledgments

We thank Dr. Mutita Junking and Dr. Vorapan Sirivatanauksorn for the supervision of SL. SL was supported by Siriraj Graduate Thesis Scholarship grant no. R015831010. This work was supported by Mahidol University grant no. R015810002 to TL.

Transparency document

Transparency document related to this article can be found online at http://dx.doi.org/10.1016/j.bbrc.2016.07.029.

Appendix A. Supplementary data

Supplementary data related to this article can be found at http://dx.doi.org/10.1016/j.bbrc.2016.07.029.

References

[1] S.B. Halstead, Dengue, Lancet 370 (2007) 1644–1652.
[2] I.A. Rodenhuis-Zybert, J. Wilschut, J.M. Smit, Dengue virus life cycle: viral and host factors modulating infectivity, Cell. Mol. Life Sci. 67 (2010) 2773–2786.
[3] H.Y. Lei, T.M. Yeh, H.S. Liu, Y.S. Lin, S.H. Chen, C.C. Liu, Immunopathogenesis of dengue virus infection, J. Biomed. Sci. 8 (2001) 377–388.
[4] S.L. Seneviratne, G.N. Malavige, H.J. de Silva, Pathogenesis of liver involvement during dengue viral infections, Trans. R. Soc. Trop. Med. Hyg. 100 (2006) 608–614.
[5] P. Marianneau, A. Cardona, L. Edelman, V. Deubel, P. Despres, Dengue virus replication in human hepatoma cells activates NF-kappaB which in turn induces apoptotic cell death, J. Virol. 71 (1997) 3244–3249.
[6] B. Pastorino, A. Nougairede, N. Wurtz, E. Gould, X. de Lamballerie, Role of host cell factors in flavivirus infection: implications for pathogenesis and development of antiviral drugs, Antivir. Res. 87 (2010) 281–294.
[7] C.F. Lin, S.C. Chiu, Y.L. Hsiao, S.W. Wan, H.Y. Lei, A.L. Shiau, H.S. Liu, T.M. Yeh, S.H. Chen, C.C. Liu, Y.S. Lin, Expression of cytokine, chemokine, and adhesion molecules during endothelial cell activation induced by antibodies against dengue virus nonstructural protein 1, J. Immunol. 174 (2005) 395–403.
[8] T. De Burghgraeve, S.J. Kaptein, N.V. Ayala-Nunez, J.A. Mondotte, B. Pastorino, S.S. Printsevskaya, X. de Lamballerie, M. Jacobs, M. Preobrazhenskaya, A.V. Gamarnik, J.M. Smit, J. Neyts, An analogue of the antibiotic teicoplanin prevents flavivirus entry in vitro, PLoS One 7 (2012) e37244.
[9] K. Whitby, T.C. Pierson, B. Geiss, K. Lane, M. Engle, Y. Zhou, R.W. Doms, M.S. Diamond, Castanospermine, a potent inhibitor of dengue virus infection in vitro and in vivo, J. Virol. 79 (2005) 8698–8706.
[10] J.S. Low, K.X. Wu, K.C. Chen, M.M. Ng, J.J. Chu, Narasin, a novel antiviral compound that blocks dengue virus protein expression, Antivir. Ther. 16 (2011) 1203–1218.
[11] X.G. Zhang, P.W. Mason, E.J. Dubovi, X. Xu, N. Bourne, R.W. Renshaw, T.M. Block, A.V. Birk, Antiviral activity of geneticin against dengue virus, Antivir. Res. 83 (2009) 21–27.
[12] Y.Y. Cheung, K.C. Chen, H. Chen, E.K. Seng, J.J. Chu, Antiviral activity of lanatoside C against dengue virus infection, Antivir. Res. 111 (2014) 93–99.
[13] P.B. Madrid, S. Chopra, I.D. Manger, L. Gilfillan, T.R. Keepers, A.C. Shurtleff, C.E. Green, L.V. Iyer, H.H. Dilks, R.A. Davey, A.A. Kolokoltsov, R. Carrion Jr., J.L. Patterson, S. Bavari, R.G. Panchal, T.K. Warren, J.B. Wells, W.H. Moos, R.L. Burke, M.J. Tanga, A systematic screen of FDA-approved drugs for inhibitors of biological threat agents, PLoS One 8 (2013) e60579.
[14] K.L. Sewell, F. Breedveld, E. Furrie, J. O'Brien, C. Brinckerhoff, R. Dynesius-Trentham, Y. Nosaka, D.E. Trentham, The effect of minocycline in rat models of inflammatory arthritis: correlation of arthritis suppression with enhanced T cell calcium flux, Cell. Immunol. 167 (1996) 195–204.
[15] M. Kloppenburg, B.A. Dijkmans, C.L. Verweij, F.C. Breedveld, Inflammatory and immunological parameters of disease activity in rheumatoid arthritis patients treated with minocycline, Immunopharmacology 31 (1996) 163–169.
[16] M. Michaelis, M.C. Kleinschmidt, H.W. Doerr, J. Cinatl Jr., Minocycline inhibits West Nile virus replication and apoptosis in human neuronal cells, J. Antimicrob. Chemother. 60 (2007) 981–986.
[17] G.L. Szeto, A.K. Brice, H.C. Yang, S.A. Barber, R.F. Siliciano, J.E. Clements, Minocycline attenuates HIV infection and reactivation by suppressing cellular activation in human CD4+ T cells, J. Infect. Dis. 201 (2010) 1132–1140.
[18] M.K. Mishra, D. Ghosh, R. Duseja, A. Basu, Antioxidant potential of Minocycline in Japanese Encephalitis Virus infection in murine neuroblastoma cells: correlation with membrane fluidity and cell death, Neurochem. Int. 54 (2009) 464–470.
[19] G.P. Sreekanth, A. Chuncharunee, A. Sirimontaporn, J. Panaampon, C. Srisawat, A. Morchang, S. Malakar, P. Thuwajit, S. Kooptiwut, A. Suttitheptumrong, P. Songprakhon, S. Noisakran, P.T. Yenchitsomanus, T. Limjindaporn, Role of ERK1/2 signaling in dengue virus-induced liver injury, Virus Res. 188 (2014) 15–26.
[20] Q. Zhang, R. Gong, J. Qu, Y. Zhou, W. Liu, M. Chen, Y. Liu, Y. Zhu, J. Wu, Activation of the Ras/Raf/MEK pathway facilitates hepatitis C virus replication via attenuation of the interferon-JAK-STAT pathway, J. Virol. 86 (2012) 1544–1554.
[21] N. Jirakanjanakit, T. Sanohsomneing, S. Yoksan, N. Bhamarapravati, The microfocus reduction neutralization test for determining dengue and Japanese encephalitis neutralizing antibodies in volunteers vaccinated against dengue, Trans. R. Soc. Trop. Med. Hyg. 91 (1997) 614–617.
[22] H. Towbin, T. Staehelin, J. Gordon, Electrophoretic transfer of proteins from polyacrylamide gels to nitrocellulose sheets: procedure and some applications, Proc. Natl. Acad. Sci. U. S. A. 76 (1979) 4350–4354.
[23] J.L. Smith, D.A. Stein, D. Shum, M.A. Fischer, C. Radu, B. Bhinder, H. Djaballah, J.A. Nelson, K. Fruh, A.J. Hirsch, Inhibition of dengue virus replication by a class of small-molecule compounds that antagonize dopamine receptor d4 and downstream mitogen-activated protein kinase signaling, J. Virol. 88 (2014) 5533–5542.
[24] M. Nikodemova, I.D. Duncan, J.J. Watters, Minocycline exerts inhibitory effects on multiple mitogen-activated protein kinases and IkappaBalpha degradation in a stimulus-specific manner in microglia, J. Neurochem. 96 (2006) 314–323.
[25] I.H. Cho, M.J. Lee, M. Jang, N.G. Gwak, K.Y. Lee, H.S. Jung, Minocycline markedly reduces acute visceral nociception via inhibiting neuronal ERK phosphorylation, Mol. Pain 8 (2012) 13.
[26] L.J. Zhao, W. Wang, W.B. Wang, H. Ren, Z.T. Qi, Involvement of ERK pathway in interferon alpha-mediated antiviral activity against hepatitis C virus, Cytokine 72 (2015) 17–24.
[27] R. Kanlaya, S.N. Pattanakitsakul, S. Sinchaikul, S.T. Chen, V. Thongboonkerd, The ubiquitin-proteasome pathway is important for dengue virus infection in primary human endothelial cells, J. Proteome Res. 9 (2010) 4960–4971.
[28] A.J. Sadler, B.R. Williams, Interferon-inducible antiviral effectors, Nat. Rev. Immunol. 8 (2008) 559–568.
[29] J.K. Calvert, K.J. Helbig, D. Dimasi, M. Cockshell, M.R. Beard, S.M. Pitson, C.S. Bonder, J.M. Carr, Dengue virus infection of primary endothelial cells induces innate immune responses, changes in endothelial cells function and is restricted by interferon-stimulated responses, J. Interferon Cytokine Res. 35 (2015) 654–665.
[30] J.A. Castillo Ramirez, S. Urcuqui-Inchima, Dengue virus control of type I IFN responses: a history of manipulation and control, J. Interferon Cytokine Res. 35 (2015) 421–430.
[31] S.V. Scherbik, J.M. Paranjape, B.M. Stockman, R.H. Silverman, M.A. Brinton, RNase L plays a role in the antiviral response to West Nile virus, J. Virol. 80 (2006) 2987–2999.
[32] R.H. Silverman, Viral encounters with 2′,5′-oligoadenylate synthetase and RNase L during the interferon antiviral response, J. Virol. 81 (2007) 12720–12729.
[33] L. Zhao, B.K. Jha, A. Wu, R. Elliott, J. Ziebuhr, A.E. Gorbalenya, R.H. Silverman, S.R. Weiss, Antagonism of the interferon-induced OAS-RNase L pathway by murine coronavirus ns2 protein is required for virus replication and liver pathology, Cell. Host Microbe 11 (2012) 607–616.
[34] E. Simon-Loriere, R.J. Lin, S.M. Kalayanarooj, A. Chuansumrit, I. Casademont,

S.Y. Lin, H.P. Yu, W. Lert-Itthiporn, W. Chaiyaratana, N. Tangthawornchaikul, K. Tangnararatchakit, S. Vasanawathana, B.L. Chang, P. Suriyaphol, S. Yoksan, P. Malasit, P. Despres, R. Paul, Y.L. Lin, A. Sakuntabhai, High anti-dengue virus activity of the OAS gene family is associated with increased severity of dengue, J. Infect. Dis. 212 (2015) 2011–2020.

[35] R.J. Lin, H.P. Yu, B.L. Chang, W.C. Tang, C.L. Liao, Y.L. Lin, Distinct antiviral roles for human 2′,5′-oligoadenylate synthetase family members against dengue virus infection, J. Immunol. 183 (2009) 8035–8043.

PLOS ONE

RESEARCH ARTICLE

SB203580 Modulates p38 MAPK Signaling and Dengue Virus-Induced Liver Injury by Reducing MAPKAPK2, HSP27, and ATF2 Phosphorylation

Gopinathan Pillai Sreekanth[1], Aporn Chuncharunee[1], Aunchalee Sirimontaporn[1], Jutatip Panaampon[1], Sansanee Noisakran[2], Pa-thai Yenchitsomanus[3], Thawornchai Limjindaporn[1]*

1 Department of Anatomy, Faculty of Medicine Siriraj Hospital, Mahidol University, Bangkok, Thailand, **2** Medical Biotechnology Unit, National Center for Genetic Engineering and Biotechnology, National Science and Technology Development Agency, Bangkok, Thailand, **3** Division of Molecular Medicine, Department of Research and Development, Faculty of Medicine Siriraj Hospital, Mahidol University, Bangkok, Thailand

* thawornchai.lim@mahidol.ac.th

OPEN ACCESS

Citation: Sreekanth GP, Chuncharunee A, Sirimontaporn A, Panaampon J, Noisakran S, Yenchitsomanus P-t, et al. (2016) SB203580 Modulates p38 MAPK Signaling and Dengue Virus-Induced Liver Injury by Reducing MAPKAPK2, HSP27, and ATF2 Phosphorylation. PLoS ONE 11(2): e0149486. doi:10.1371/journal.pone.0149486

Editor: Yi-Hsien Hsieh, Institute of Biochemistry and Biotechnology, TAIWAN

Received: November 4, 2015

Accepted: February 2, 2016

Published: February 22, 2016

Data Availability Statement: All relevant data are within the paper and its Supporting Information files.

Funding: This study was supported by Mahidol University Grant No. R015810002, Mahidol University, Thailand. TL received the funding. The funders had no role in study design, data collection and analysis, decision to publish, or preparation of the manuscript.

Competing Interests: The authors have declared that no competing interests exist.

Abstract

Dengue virus (DENV) infection causes organ injuries, and the liver is one of the most important sites of DENV infection, where viral replication generates a high viral load. The molecular mechanism of DENV-induced liver injury is still under investigation. The mitogen activated protein kinases (MAPKs), including p38 MAPK, have roles in the hepatic cell apoptosis induced by DENV. However, the *in vivo* role of p38 MAPK in DENV-induced liver injury is not fully understood. In this study, we investigated the role of SB203580, a p38 MAPK inhibitor, in a mouse model of DENV infection. Both the hematological parameters, leucopenia and thrombocytopenia, were improved by SB203580 treatment and liver transaminases and histopathology were also improved. We used a real-time PCR microarray to profile the expression of apoptosis-related genes. Tumor necrosis factor α, caspase 9, caspase 8, and caspase 3 proteins were significantly lower in the SB203580-treated DENV-infected mice than that in the infected control mice. Increased expressions of cytokines including TNF-α, IL-6 and IL-10, and chemokines including RANTES and IP-10 in DENV infection were reduced by SB203580 treatment. DENV infection induced the phosphorylation of p38MAPK, and its downstream signals including MAPKAPK2, HSP27 and ATF-2. SB203580 treatment did not decrease the phosphorylation of p38 MAPK, but it significantly reduced the phosphorylation of MAPKAPK2, HSP27, and ATF2. Therefore, SB203580 modulates the downstream signals to p38 MAPK and reduces DENV-induced liver injury.

Introduction

Dengue virus (DENV) infection is one of the most important mosquito-borne viral diseases with high incidence in tropical and subtropical regions. The clinical signs of DENV infection reflect the different levels of severity including dengue fever or dengue hemorrhagic fever, or dengue shock syndrome (DSS). Patients with more severe forms of the disease display hemorrhagic disorders, including plasma leakage, thrombocytopenia, hemoconcentration, and multi-organ failure [1–6]. Liver transaminase (alanine transaminase [ALT] and aspartate transaminase [AST]) levels increase in both DENV-infected patients [7–10] and murine models of DENV infection [11–15].

Hepatic cell apoptosis, which is related to the pathogenesis of DENV infection, has been observed both *in vitro* and *in vivo* [16–18]. DENV infection contributes to apoptosis by inducing the expression of cytokine TRAIL, observed in the hepatic cell line, HepG2 [19]. DENV infection with increased cytokine expression can proceed to liver injury. The expression of tumor necrosis factor α (TNF-α), one of the predominant pro-inflammatory cytokines, is increased in DENV infection [20–25]. The Fas receptor (FasR) is the member of the TNF death receptor family and its signaling also contributes to DENV-mediated apoptosis [26, 27]. Furthermore, DENV infection causes mitochondrial dysfunction, which contributes to hepatic cell injury [28, 29]. Activation of caspase 9 and caspase 3 is seen in DENV-infected human umbilical vascular endothelial cells (HUVECs) suggesting the involvement of mitochondrial caspase and the intrinsic pathway of apoptosis [30]. The involvement of intrinsic pathway in DENV infection is also reported in other cell types [31, 32]. Therefore, DENV infection induces both extrinsic and intrinsic pathways of apoptosis.

Mitogen-activated protein kinase (MAPK) family has been suggested to play a role in apoptosis [33]. Extracellular-signal-regulated kinase (ERK), c-Jun N-terminal kinase (JNK), and p38 MAPK represent the classical type of MAPKs and are activated during various disease conditions. Phosphorylation of MAPK signaling activates MAPKs, which then induce cytokine production [34–37]. The p38 MAPK undergoes dual phosphorylation at Thr182 and Tyr180 in the Thr–Gly–Tyr activation loop by MAP kinase kinase 6 (MKK6) [38–40]. Upon activation, p38 MAPK phosphorylates multiple substrates, including MAPK activated protein kinase 2 (MAPKAPK2) and activating transcription factor 2 (ATF-2) [41, 42]. Heat Shock Protein 27 (HSP27), which is a downstream signaling molecule to MAPKAPK2, is reported to be increased in DENV infection [43]. Upon DENV infection, phosphorylated p38 MAPK increases [20, 44–46]. In addition, DENV induces the phosphorylation of ERK and JNK, and the inhibition of ERK and JNK phosphorylation reduces the infectivity of DENV and protects the liver from injury [45, 47, 48].

SB203580 is a pyridinyl imidazole inhibitor of p38 MAPK, which controls the various inflammatory responses and cellular stresses [26, 49–52]. Interestingly, in human dendritic cells infected with *Zaire ebolavirus*, SB203580 treatment reduces cytokine stimulation [53]. In addition, SB203580 reduces the apoptosis of DENV-infected HepG2 cells by inhibiting RIPK2 expression [17]. The role of p38 MAPK in the apoptosis of DENV-infected HepG2 cells has been investigated, and the DENV-mediated apoptosis of HepG2 cell line is attributed to the increased phosphorylation of p38 MAPK [20]. In a recent study in AG129 immuno-compromised mice (deficient in Type I and II interferon receptors), SB203580 was shown to improve the clinical manifestations of DENV infection. This study shows that oral administration of SB203580 decreased the circulation of pro-inflammatory cytokines. However, the high viral load was still presented in livers of infected mice [54]. In a recent study of intra-cerebral inoculation of DENV in Balb/c mice also shows viremia and the induction of host immune response with organ damage including liver. This study shows the relationship of the elevated pro-

inflammatory cytokines in response to DENV infection in Balb/c mice [55]. However, the mechanisms by which SB203580 protects against liver injury during DENV infection *in vivo*, within the complex immune response, need further investigation. Therefore, we further investigated the role of SB203580 in controlling the symptom of DENV-induced liver injury and clarified the molecular mechanism by which SB203580 controls liver injury in a Balb/c mouse model of DENV infection [48].

Materials and Methods

DENV-infected mice and SB203580 treatment

Male Balb/c mice, aged 8 weeks and weighing 20–25 g, were purchased from the National Laboratory Animal Center, Mahidol University, Thailand. The animals were strictly maintained under highly sterile conditions, with four mice per cage, at 23 ± 2°C with a 12 h light/dark cycle, and given autoclaved pelleted food and water ad libitum. The animal health was monitored by a veterinarian throughout the study period. All the experiments were conducted in compliance with the institutional policies for animal care and the protocol was approved by the Siriraj Animal Care and Use Committee, Mahidol University (SI-ACUP 004/2556) and the Siriraj Biosafety Risk Management Taskforce, Mahidol University (SI-2013-11). DENV-2 (Thailand strain 16881) propagated in the mosquito cell line C6/36 (purchased from the American Type Culture Collection and further sub-cultured) was used in all experiments. The viral titers were determined with a standard protocol, the Focus Forming Unit (FFU) assay [56]. SB203580 was purchased from Abcam, Cambridge, UK (ab120162) and solubilized in 2% dimethyl sulfoxide (DMSO; Sigma-Aldrich, St. Louis, MO, USA). Mice were randomized into the experiments and were infected intravenously with 4×10^5 FFU/ml of DENV-2 through the lateral tail vein. Twelve mice were infected with DENV, and half of them were treated with the control vehicle, 2%DMSO (n = 6). The other six mice (n = 6) were treated with 5 mg/kg SB203580. Treatments with 2%DMSO alone or SB203580 dissolved in 2%DMSO were given 1 h before and 1 h and 24 h after DENV infection intravenously. In addition, other six mice, which were not infected with DENV, were treated with the control vehicle alone. The volume of all injections was 0.4 ml. At 7 days after infection, the mice were euthanized with an overdose intraperitoneal injection of sodium pentobarbital anesthesia. Intraperitonial injection of sodium pentobarbital anesthesia is applied to minimize animal sufferings. The blood samples for hematological analysis were processed instantly and the sera were prepared for clinical biochemical analysis. Liver tissues were collected and sliced into pieces for analysis. The liver tissues were weighed, and kept frozen in RNALater (Invitrogen, Carlsbad, CA, USA) or RPMI medium for the subsequent isolation of RNA and protein or the FFU assay, respectively. Duplicate independent experiments were performed. Therefore, a total of 36 mice were used in the experiments.

Quantification of DENV NS1 viral RNA with Real-Time Quantitative Reverse Transcription PCR (qRT-PCR)

In vitro transcription-derived DENV NS1 RNA with known copy number is served as a standard control for qRT-PCR [48]. Total RNA was extracted from the livers of 2%-DMSO-treated (n = 6), 2%-DMSO-treated DENV-infected (n = 6), and SB203580-treated DENV-infected mice (n = 6) with the Invitrap Spin Universal RNA Mini Kit (Stratec Molecular) and was quantified with a NanoDrop ND-1000 spectrophotometer. Equivalent amounts of RNA from each sample were converted to cDNA with SuperScript® III First-Strand Synthesis System (Invitrogen) with a reverse primer, NS1−R 5′ GCC ATC AAT GAG AAA GGT CTG G 3′. Amplification

was performed using the SYBR Green I reaction mix (Roche) in the presence of NS1 specific primers including NS1−F 5′ CCG GCC AGA TCT GGA GAC ATC AAA GGA ATC 3′ and the NS1-R in a Roche Light Cycler 480. The Ct of viral RNA was measured and compared to the standard control.

Determination of viral titers in liver homogenates with focus forming unit (FFU) assay

Seven days after DENV infection, the mice were euthanized and the liver tissues were collected from the 2%-DMSO-treated (n = 6), 2%-DMSO-treated DENV-infected (n = 6), and SB203580-treated DENV-infected (n = 6) mice under sterile conditions. The cropped tissues from each groups were equally-weighed. The collected tissues from individual mouse were separately stored in eppendroff tube containing pre-cooled RPMI medium and immediately stored at −80°C. The samples were homogenized in liquid nitrogen with a pestle, and all the samples from each group were centrifuged simultaneously for 5 min at 6,000 × g, and centrifugation was repeated until clear supernatants were obtained. All the centrifugation products were stored at 4°C and the supernatants were filter sterilized. An FFU assay was conducted to determine the viral titers in the centrifuged supernatants, with a previously established protocol [48, 56], and the results were presented as FFU/mg of liver tissue.

Hematology and measurement of liver enzymes

Blood was collected from the 2%-DMSO-treated (n = 12), 2%-DMSO-treated DENV-infected (n = 12), and SB203580-treated DENV-infected (n = 12) mice, stored in vacutainer tubes containing EDTA, and rapidly processed at the National Laboratory Animal Center, Mahidol University, Thailand. The complete blood count was analyzed with a CELL-DYN™ 3700 hematological auto analyzer (Abbott, Abbott Park, IL, USA). To prepare the sera, the blood samples were permitted to clot and then centrifuged. The serum ALT and AST levels were measured with an automated analyzer (Model 902, Hitachi Company, Japan).

Histopathology

Liver tissues from 2%-DMSO-treated (n = 3), 2%-DMSO-treated DENV-infected (n = 3), and SB203580-treated DENV-infected (n = 3) mice were fixed in 10% formalin in PBS and stored. The fixed tissues were paraffin embedded, sectioned, and conventionally stained with hematoxylin and eosin (H&E).

Expression of host mRNA with real-time PCR array

The Mouse Apoptosis RT^2 Profiler™ PCR Array (Qiagen, Valencia, CA, USA; cat. # PAMM-012) is a primer preset microarray widely used to analyze the roles of 84 genes involved in apoptosis. RNA was extracted from the liver tissues of the 2%-DMSO-treated, 2%-DMSO-treated DENV-infected, and SB203580-treated DENV-infected mice with the InviTrap Spin Universal RNA Mini Kit (Stratec Molecular). The concentration and purity of the total RNA were measured with a NanoDrop spectrophotometer and same amount of RNA from each group was converted to cDNA with the SuperScript® III First-Strand Synthesis System (Invitrogen). The samples were then mixed with SYBR Green RT^2 qPCR Mastermix (Qiagen), and equal volumes were aliquoted into each well of the real-time PCR arrays. The Roche LightCycler 480 instrument was used to run the PCR thermal cycling program. The Ct value for each gene was recorded on a Microsoft Excel spreadsheet and the data were uploaded to the web program http://pcrdataanalysis.sabiosciences.com/pcr/arrayanalysis.php for $2^{-\Delta\Delta Ct}$ analysis. The

calculated values were presented as fold increases or reductions compared relative to the control group value.

Cytokine and Chemokine mRNA expression by Real-time RT-PCR

Total RNA from the liver tissues of 2%DMSO treated (N = 3), DMSO treated DENV-infected (N = 3), and DENV-infected SB203580 treated (N = 3) mice was extracted using Invitrap Spin Universal RNA Mini Kit (Stratec Molecular) and converted to cDNA with SuperScript® III First-Strand Synthesis System (Invitrogen). Amplification was continued using specific primers (TNF-α: TNF-F 5′ CCC CCA GTC TGT ATC CTT CT 3′ and TNF-R 5′ TTT GAG TCC TTG ATG GTG GT 3′ , IL-6: IL-6-F 5′ AGT TGC CTT CTT GGG ACT GA 3′ and IL-6-R 5′ TCC ACG ATT TCC CAG AGA AC 3′ , IL-10: IL-10-F 5′ CCA AGC CTT ATC GGA AAT GA 3′ and IL-10-R 5′ TTT TCA CAG GGG AGA AAT CG 3′ , CCL-5: CCL-5-F 5′ CCC TCA CCA TCA TCC TCA CT 3′ and CCL-5-R 5′ CCT TCG AGT GAC AAA CAC GA 3′ , CXCL-10: CXCL-10-F 5′ GGA TGG CTG TCC TAG CTC TG 3′ and CXCL-10-R 5′ ATA ACC CCT TGG GAA GAT GG 3′ , GAPDH: GAPDH-F 5′ TGA ATA CGG CTA CAG CAA CA 3′ and GAPDH-R 5′ AGG CCC CTC CTG TTA TTA TG 3′) in a Roche Light Cycler 480 using SYBER Green I reaction mix (Roche). Threshold Ct value of each gene of interest and GAPDH (housekeeping gene) were measured and the differences between the gene of interest to the GAPDH (ΔCt) were calculated. The relative expression values ($2^{-\Delta\Delta Ct}$) were then determined. Results were obtained from three independent experiments for three independent mice per individual group.

Western blotting analysis

Total protein was extracted from the liver tissues of the 2%-DMSO-treated, 2%-DMSO treated DENV-infected, and SB203580-treated DENV-infected mice in RIPA buffer containing a protease inhibitor (Roche), and was subjected to western blotting analysis [57]. To detect the phosphorylated proteins, a phosphatase inhibitor cocktail (Roche) was also added. The concentrations of the extracted proteins were estimated with a Bradford Protein Assay (Bio-Rad Laboratories, Inc. Hercules, CA, USA). Equivalent protein concentrations from the individual groups were mixed with 4× loading dye (50 mM Tris-HCl [pH 6.8], 2% SDS, 0.1% bromophenol blue, and 10% glycerol) and denatured at 95°C for 5 min in a thermocycler. The samples were separated with SDS-PAGE and blotted onto nitrocellulose membrane (GE Healthcare Life Sciences, Freiburg, Germany). The membrane was blocked with 5% bovine serum albumin or 5% skim milk in Tris-buffered saline containing 0.1% Tween 20 (TBST) to restrict nonspecific binding. The membrane was washed three times and hybridized with rabbit anti-total p38 MAPK (Santa Cruz Biotechnology, Santa Cruz, CA, USA) at a dilution of 1:2000, or mouse anti-phosphorylated p38 MAPK (Santa Cruz Biotechnology) at a dilution of 1:1000, or rabbit anti-total HSP27 (Cell Signaling Technology, MA, USA) at a dilution of 1:1000, or rabbit anti-phosphorylated HSP27 (Cell Signaling) at a dilution of 1:1000, or rabbit anti-total MAPKAPK2 (Santa Cruz Biotechnology) at a dilution of 1:1000, or rabbit anti-phosphorylated MAPKAPK2 (Cell Signaling Technology) at a dilution of 1:2000, or rabbit anti-total ATF2 (Santa Cruz Biotechnology) at a dilution of 1:1000, or mouse anti-phosphorylated ATF2 (Santa Cruz Biotechnology) at a dilution of 1:1000, or goat anti-TNF-α (Santa Cruz Biotechnology) at a dilution of 1:2000, or rabbit anti-caspase 8 (Santa Cruz Biotechnology) at a dilution of 1:1000, or mouse anti-caspase 9 (Cell Signaling Technology) at a dilution of 1:1000, or rabbit anti-GGT1 antibody (Santa Cruz Biotechnology) at a dilution of 1:2500, or rabbit anti-GAPDH (Cell Signaling Technology) at a dilution of 1:2500, or rabbit anti-cleaved caspase 3 antibody (Cell Signaling Technology) at a dilution of 1:2000. The membrane was washed

three times with TBST and incubated for 1 h in the dark at room temperature with horseradish peroxidase (HRP)-conjugated secondary antibody, HRP-conjugated rabbit anti-mouse IgG antibody for phosphorylated p38 MAPK, phosphorylated ATF2 and Caspase 9 (Dako, Santa Clara, CA, USA), HRP-conjugated rabbit anti-goat IgG antibody for TNF-α (Dako, Santa Clara, CA, USA), or HRP-conjugated swine anti-rabbit IgG antibody for the all other proteins (Dako, Santa Clara, CA, USA). The membranes were washed three times with TBST in the dark and the immune complexes were detected with enhanced chemiluminescence (Super-Signal West Pico Chemiluminescent Substrate; Thermo Scientific, Waltham, MA, USA). GAPDH is used as the housekeeping gene for all the western blot analysis.

Statistical analysis

For the estimation of hematology and liver enzymes, the results were pooled from the two independent experiments (total of twelve mice per group from two independent experiments). For the quantification of viral NS1, a total of six mice per group were used. For the all other experiments, at least three independent experiments from three independent mice per individual group (n = 3) were performed. All the results were presented as means ± SEM and the data were analyzed using the GraphPad Prism Software version 5. Statistical analysis was conducted by One-way ANOVA and p value less than 0.05 were considered as statistically significant ($p < 0.05$).

Results

SB203580 treatment modulates hematological parameters in DENV-infected mice

In this study, Balb/c mice were intravenously injected with the vehicle control alone (2%DMSO) or were infected with DENV and treated with 2%DMSO or SB203580. All mice survived the challenge protocol, with no any clinical symptoms observed till the end of the protocol. However, the white blood cell (WBC) and platelet counts decreased significantly in the DENV-infected mice, suggesting leucopenia and thrombocytopenia, respectively. The hematological phenotype of the Balb/c mice was improved significantly by SB203580 treatment (Fig 1A and 1B).

SB203580 treatment reduces liver injury in DENV-infected mice

Mice were intravenously infected with DENV, and their liver transaminases ALT and AST were found to be significantly increased compared with those of the uninfected control group

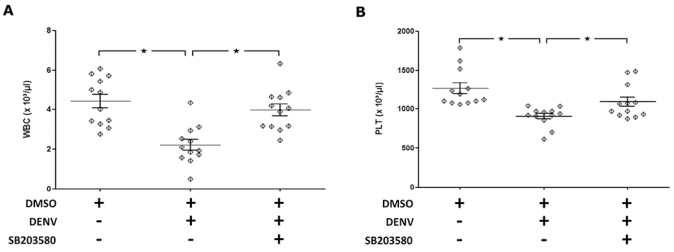

Fig 1. The hematological phenotype of the DENV-infected mice was improved by SB203580 treatment. Mice were infected with DENV and treated with 2%DMSO or SB203580. The uninfected control group was also treated with 2%DMSO alone. Seven days after infection, their blood was collected in EDTA tubes for hematological analysis. (A) WBC counts, and (B) platelet counts. The results were pooled from two independent experiments, and are presented as means ± SEM (a total of 12 mice per group from two independent experiments). The asterisks indicate statistically significant differences between groups ($p < 0.05$).

doi:10.1371/journal.pone.0149486.g001

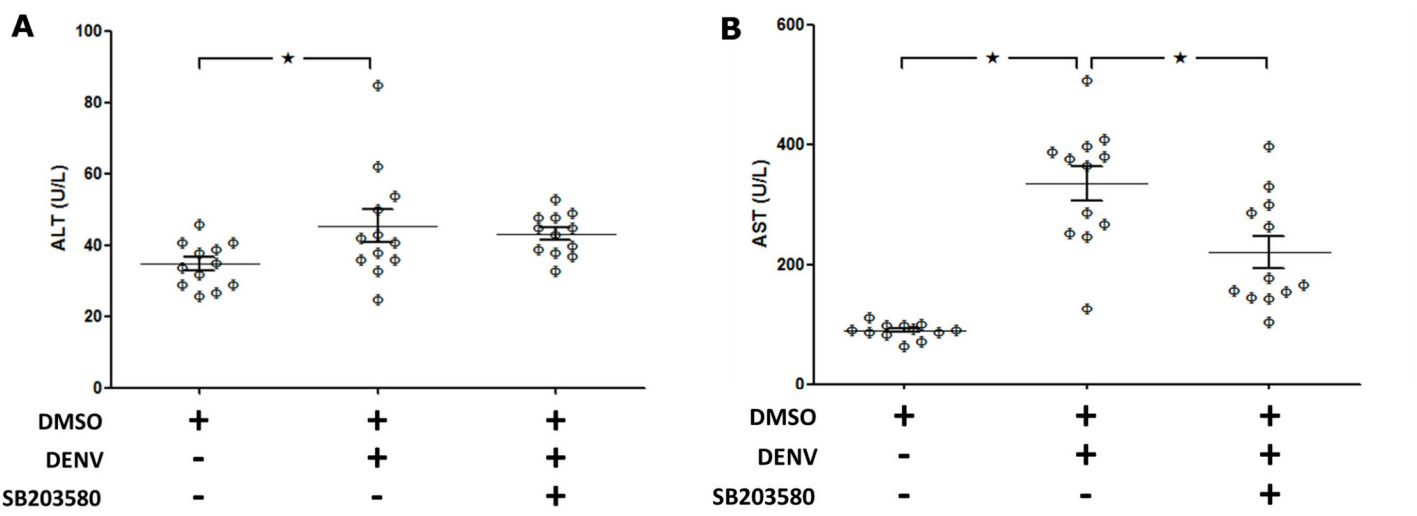

Fig 2. SB203580 treatment reduces liver enzymes in DENV-infected mice. Mice were infected with DENV and treated with 2%DMSO or SB203580. The uninfected control group was also treated with 2%DMSO. Seven days after infection, blood was collected and sera prepared to estimate liver transaminases. (A) ALT, and (B) AST. The pooled results of two independent experiments are presented as means ± SEM (12 mice per group in two independent experiments). The asterisks indicate statistically significant differences between the groups ($p < 0.05$).

doi:10.1371/journal.pone.0149486.g002

(Fig 2A and 2B) on day 7. However, after the DENV-infected mice were treated with SB203580, their liver AST levels were significantly reduced, but the changes in ALT were failed to reach statistical significance (Fig 2A and 2B).

Gamma-glutamyl transpeptidase (GGT) is reported as a biomarker for hepatocellular and cholestatic damage [58]. Elevated level of GGT was observed in various liver injuries [59–62]. Therefore, western blot analysis with antibody directed against GGT was conducted and normalized to GAPDH. The results show that the expression of GGT in liver of 2%DMSO treated DENV-infected mice was significantly higher than that of 2%DMSO treated mice (Fig 3A). Intravenous treatment of SB203580 reduced the GGT expression in livers of DENV-infected mice suggesting the decreased liver injury in SB203580 treated mice. Three independent experiments were conducted and densitometry analysis was conducted using ImageJ for three independent mice from each group (Fig 3B).

Histological analysis of the liver tissues of the uninfected 2%DMSO-treated mice (Fig 4A), 2%DMSO-treated DENV-infected mice (Fig 4B), and SB203580-treated DENV-infected mice (Fig 4C) was conducted. The 2%DMSO-treated DENV-infected mice showed classical signs of liver injury, with dilated sinusoid capillaries and numerous hyperplastic Kupffer cells around them, and the hepatocytes were enlarged by cytoplasmic vacuolization. Specifically, marked cellular necrosis and apoptosis were also noted in a histological analysis of the 2%DMSO-treated DENV-infected mice. Interestingly, the SB203580-treated DENV-infected mice showed less liver injury than that of the 2%DMSO-treated DENV-infected mice.

SB203580 does not reduce dengue virus production

To test whether SB203580 treatment modulates dengue virus production or host immune responses, the viral RNA copies in the liver of mice from each group were quantified. A known copy number of *in vitro*-transcribed DENV NS1 was used as the standard control PCR template. A standard curve was plotted with the Ct values for known copy numbers of DENV NS1, as shown in Fig 5A. The RNA from the liver tissue homogenates of mice treated with 2% DMSO alone, 2%DMSO-treated DENV-infected mice, and SB203580-treated DENV-infected

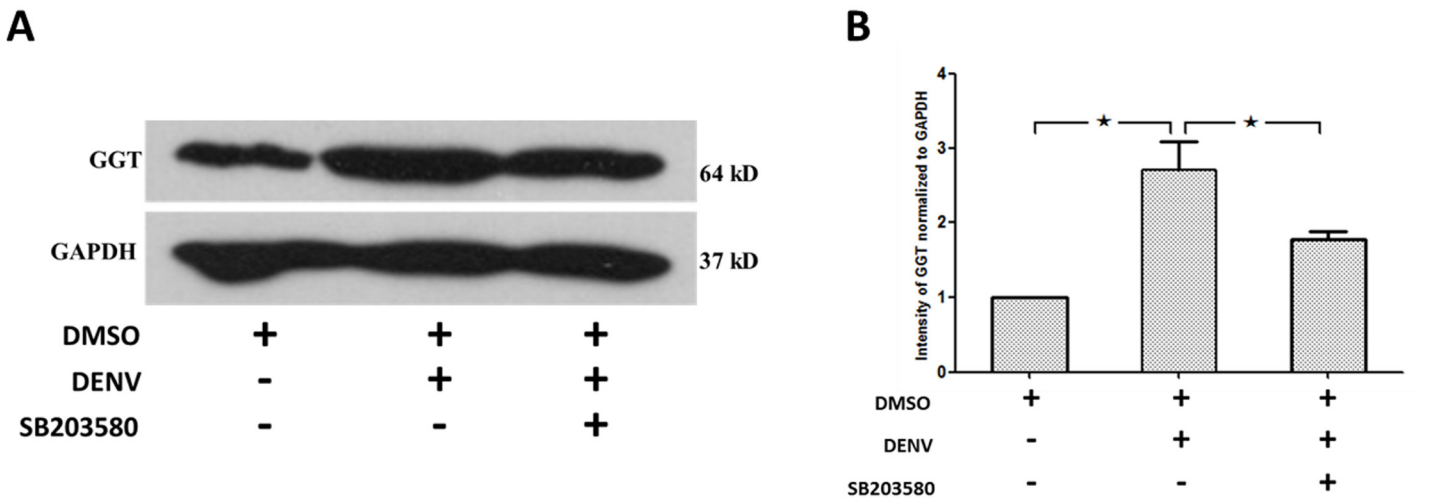

Fig 3. SB203580 treatment reduces GGT expression in DENV-infected mice. Mice were infected with 4×10^5 FFU/ml of DENV and treated with 2% DMSO (v/v) or SB203580 dissolved in 2%DMSO. The control (uninfected) group was treated with 2%DMSO (v/v) alone. Treatments were given 1 h before and after DENV infection and again at 24 h after infection. On day 7 after infection, the liver tissues were collected, and the proteins were extracted for western blotting analysis using antibody directed against (A) GGT normalized to GAPDH. The results shown are representatives of three independent experiments with three mice (n = 3) from each group. A densitometry analysis using the ImageJ software is shown in (B).

doi:10.1371/journal.pone.0149486.g003

mice was prepared and subjected to qRT–PCR with primers specific for DENV NS1. When six mice from each group were analyzed, 1 μg of total RNA from the 2%DMSO-treated DENV-infected mice contained an average of 3.843×10^8 DENV NS1 copies and that from SB203580-treated DENV-infected mice contained 3.147×10^8 DENV NS1 copies (Fig 5B). No DENV NS1 copies were detected in any mouse not infected with DENV and treated with 2% DMSO alone. The viral FFUs in the liver homogenates were determined with the FFU assay. The liver tissues from the 2%DMSO-alone-treated, 2%DMSO-treated DENV-infected, and SB203580-treated DENV-infected mice were collected on day 7 in RPMI medium. The

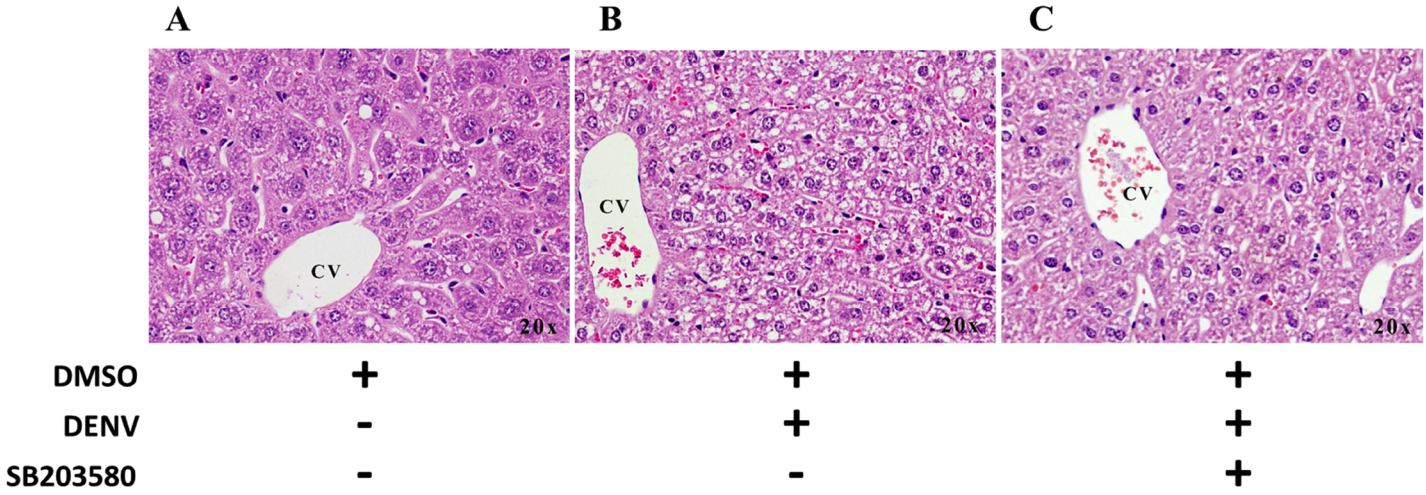

Fig 4. SB203580 treatment reduces DENV-induced liver pathology in DENV-infected mice. Mice were infected with DENV and treated with 2%DMSO or SB203580 dissolved in 2%DMSO. The uninfected control group was also treated with 2%DMSO. Seven days after infection, liver tissues were collected in 10% formalin for histopathological analysis and H&E staining. (A) 2%DMSO alone (B) 2%DMSO-treated DENV-infected (C) SB203580-treated DENV-infected. The results shown are representative of $\geq$ 3 mice from each group.

doi:10.1371/journal.pone.0149486.g004

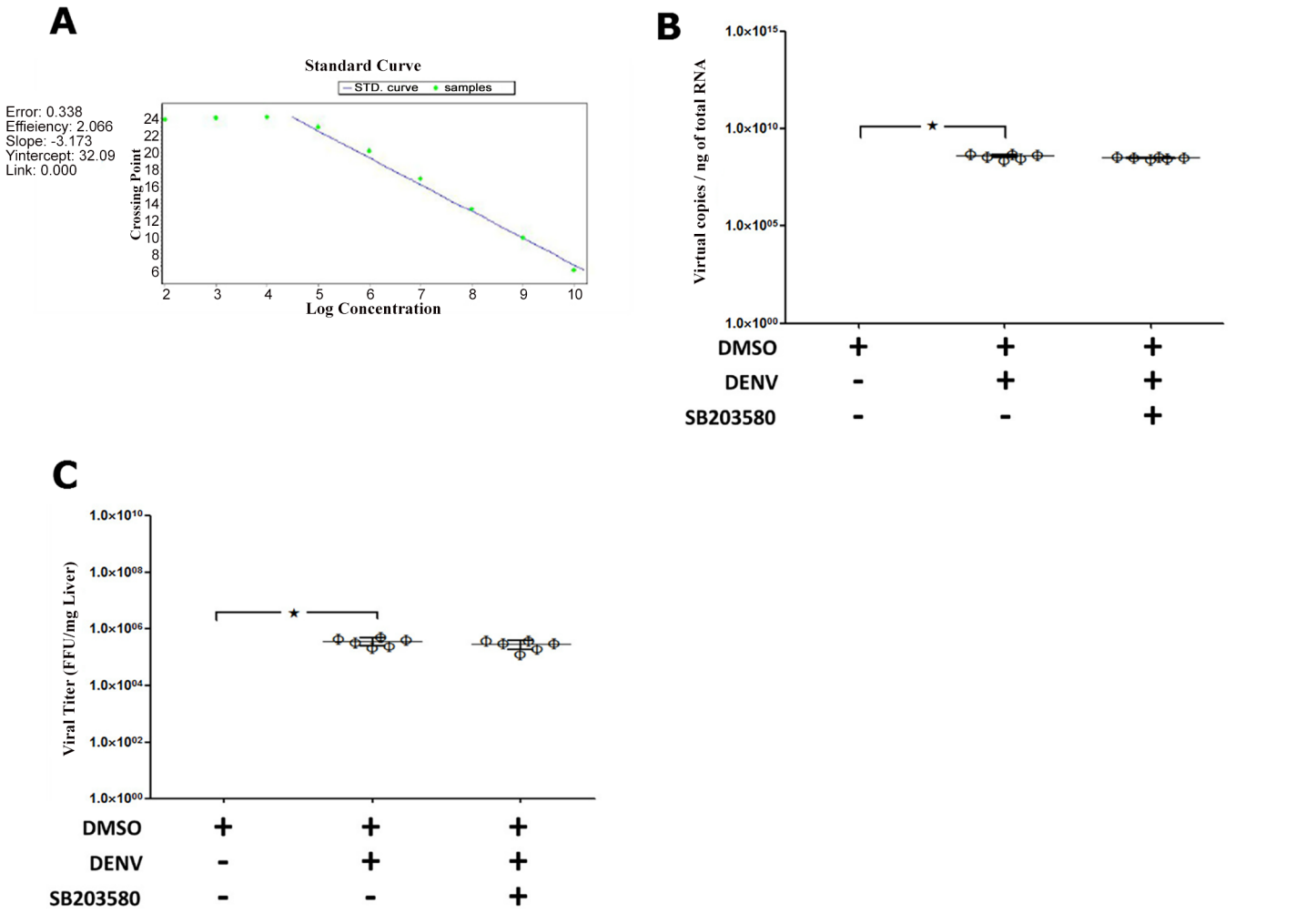

Fig 5. SB203580 does not reduce DENV production in DENV-infected mice. Mice were infected with 4×10^5 FFU/ml of DENV and treated with 2%DMSO alone or SB203580 in 2%DMSO. The uninfected control group was also treated with 2%DMSO. Seven days after infection, the liver tissues were collected, preserved in RNALater for the quantification of viral NS1, and in RPMI medium for an FFU assay. Total RNA was extracted to quantify viral NS1 with qRT–PCR. (A) Standard curve plotted from the Ct values for 10-fold serially diluted cDNA of known copy number (10^1–10^{10} copies). The dots represent the Ct values of each 10-fold dilution. (B) Viral NS1 copies in 1 μg of total RNA from 2%DMSO-treated (uninfected), 2%DMSO-treated DENV-infected, and SB203580-treated DENV-infected groups of mice (viral copies/μg). The supernatant was prepared from the liver tissue homogenates for the FFU assay. (C) Viral titers in the 2%DMSO-treated (uninfected), 2%DMSO-treated DENV-infected, and SB203580-treated DENV-infected groups of mice are expressed in FFU per milligram (FFU/mg). The results were obtained from six animals per group (n = 6). The data were analyzed with One-way ANOVA using GraphPad Prism 5 and are presented as means ± SEM. Asterisks show the level of significance ($p < 0.05$ is considered statistically significant).

doi:10.1371/journal.pone.0149486.g005

homogenates were prepared and centrifuged to obtain the supernatants, which were analyzed with FFU assay. There was no significant difference of in the liver homogenate FFUs of the SB203580-treated DENV-infected mice and those of 2%DMSO treated DENV-infected mice (Fig 5C).

SB203580 treatment modulates the apoptotic gene expression profile in DENV-infected mice

To explore the molecular mechanism by which SB203580 reduces liver damage, screening experiments were conducted with a commercially available Mouse Apoptosis RT^2 Profiler™ PCR Array System (Qiagen). Total RNA was isolated from the 2%DMSO-alone group, 2%

Table 1. Apoptotic gene expression profiles of DMSO-treated DENV-infected mice and SB203580 treated DENV-infected mice (both are normalized with those of DMSO-treated uninfected mice).

Gene	Gene Description	DMSO+DENV	DENV+SB203580
Apaf1	Apoptotic peptidase activating factor 1	2.5669	1.8404
Bax	Bcl2-associated X protein	3.3173	1.1729
Bcl2a1a	B-cell leukemia/lymphoma 2 related protein A1a	11.3924	6.4082
Casp1	Caspase 1	4.1411	5.4642
Casp12	Caspase 12	4.7899	2.1737
Casp14	Caspase 14	2.5491	1.1407
Casp2	Caspase 2	2.4284	1.8531
Casp3	Caspase 3	2.1886	1.8277
Casp8	Caspase 8	2.1140	1.9588
Casp9	Caspase 9	1.9588	1.1647
Cd40	CD40 antigen	3.0314	1.3850
Cd40lg	CD40 ligand	1.7411	0.5323
Cidea	Cell death-inducing DNA fragmentation factor, alpha subunit-like effector A	8.3977	2.3295
Cradd	CASP2 and RIPK1 domain containing adaptor with death domain	4.6268	2.4286
Fadd	Fas (TNFRSF6)-associated via death domain	2.4623	2.0705
Fasl	Fas ligand (TNF superfamily, member 6)	11.9588	7.8904
Il10	Interleukin 10	10.1261	1.0278
Pycard	PYD and CARD domain containing	3.3870	1.7413
Tnf	Tumor necrosis factor	2.5491	1.1407
Tnfsf10	Tumor necrosis factor (ligand) superfamily, member 10	11.3924	3.8370

doi:10.1371/journal.pone.0149486.t001

DMSO-treated DENV-infected group, and SB203580-treated DENV-infected group, converted to cDNA, and amplified with the LightCycler 480 PCR system. The full list of gene expression profile of the apoptosis related genes in DENV-infected mice and the effect of SB203580 treatment to those genes were separately shown in S1 Table. Table 1 lists the gene expression profile of the selected apoptosis related genes whose expression is increased in 2%DMSO-treated DENV infected mouse and reduced by SB203580-treated DENV-infected mouse, which is normalized to un-infected 2%DMSO treated mouse. Actin is used as the housekeeping gene for normalizing the expression profile.

SB203580 treatment reduces apoptosis

We confirmed the efficacy of SB203580 in modulating apoptosis in DENV-infected mice by western blot analysis. The expression of both pro and cleaved forms of caspase 3 in un-infected 2%DMSO treated, 2%DMSO-treated DENV-infected and SB203580 treated DENV-infected mice were evaluated. The pro-caspase 3 was decreased in 2%DMSO-treated DENV-infected mice (Fig 6A and 6B) compared to that of un-infected 2%DMSO-treated mice. Interestingly, SB203580-treated DENV-infected mice show significant increase in the pro-caspase 3. To further verify the results, an antibody that detects the cleaved form of caspase 3 was used in western blot analysis. The results show an increased expression of cleaved caspase 3 expression in the 2%DMSO-treated DENV-infected mice (Fig 6C and 6D) compared to that of un-infected 2%DMSO-treated control mice. A significant reduction in the expression of cleaved caspase 3 was observed in SB203580 treated DENV-infected mice (Fig 6C and 6D). Our results confirm that SB203580 treatment in DENV-infected mice restrict the cleavage of caspase 3 thereby reducing cellular apoptosis.

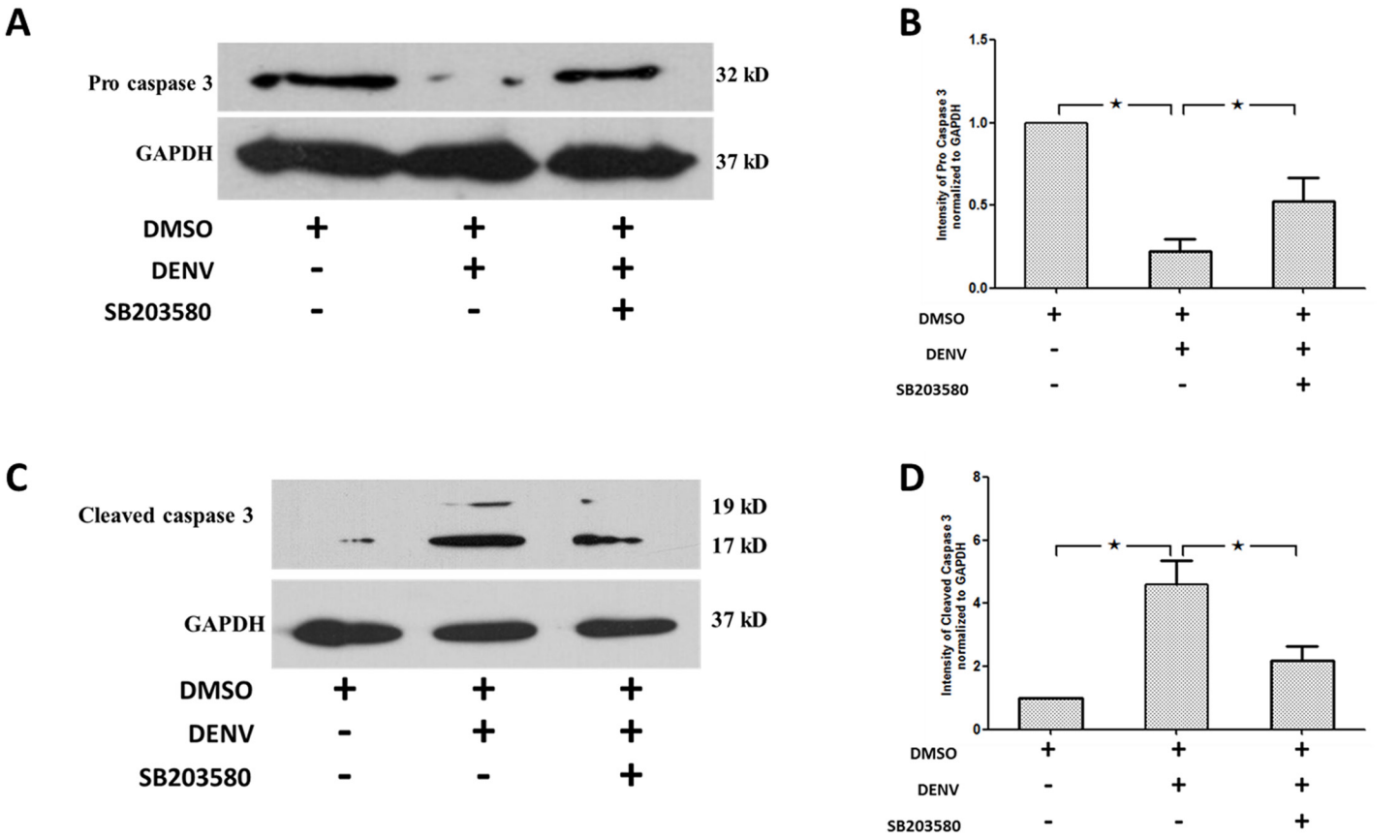

Fig 6. SB203580 treatment reduces caspase 3 expression. Mice were infected with 4×10^5 FFU/ml of DENV and treated with 2%DMSO (v/v) or SB203580 dissolved in 2%DMSO. The control (un-infected) group was treated with 2%DMSO (v/v) alone. Treatments were given 1 h before and after DENV infection and again at 24 h after infection. On day 7 after infection, the liver tissues were collected, and the proteins were extracted for western blotting analysis using antibodies directed against (A) pro caspase 3 and (C) cleaved caspase 3. The results shown are representative of three independent experiments with three mice (n = 3) from each group. A densitometry analysis using the ImageJ software is shown in (B) pro caspase 3 and (D) cleaved caspase 3.

doi:10.1371/journal.pone.0149486.g006

To further characterize in what way the apoptosis is controlled by SB203580 in DENV infected mice, we explored the specific markers for extrinsic and intrinsic apoptosis pathways. To characterize the extrinsic pathway, an antibody that detects both pro caspase 8 and cleaved caspase 8 was used for western blot analysis. Pro-caspase 8 in the 2%DMSO-treated DENV-infected mice was significantly less to that of un-infected mice treated with 2%DMSO alone (Fig 7A), whereas SB203580 treatment reversed the pro-caspase 8 of DENV-infected mice (Fig 7A). As expected, cleaved caspase 8 was activated in the 2%DMSO-treated DENV-infected mice (Fig 7A), whereas treatment with SB203580 reduced the cleaved caspase 8 expression (Fig 7A). Our results confirm that caspase 8 is activated in DENV infection and SB203580 treatment significantly restricts this activation, suggesting the role of SB203580 in reduction of the extrinsic pathway of apoptosis.

We further investigated the role of intrinsic pathway using an antibody against caspase 9, one of the classical markers for mitochondrial cell death. Pro caspase 9 was significantly reduced in 2%DMSO treated DENV infected mice compared to that of un-infected 2%DMSO control mice. SB203580 reversed the pro caspase 9 expression in DENV infected mice (Fig 8A). Interestingly, the cleaved caspase 9 was significantly higher in the 2%DMSO-treated DENV-infected mice than that of un-infected 2%DMSO treated control mice and SB203580 treatment

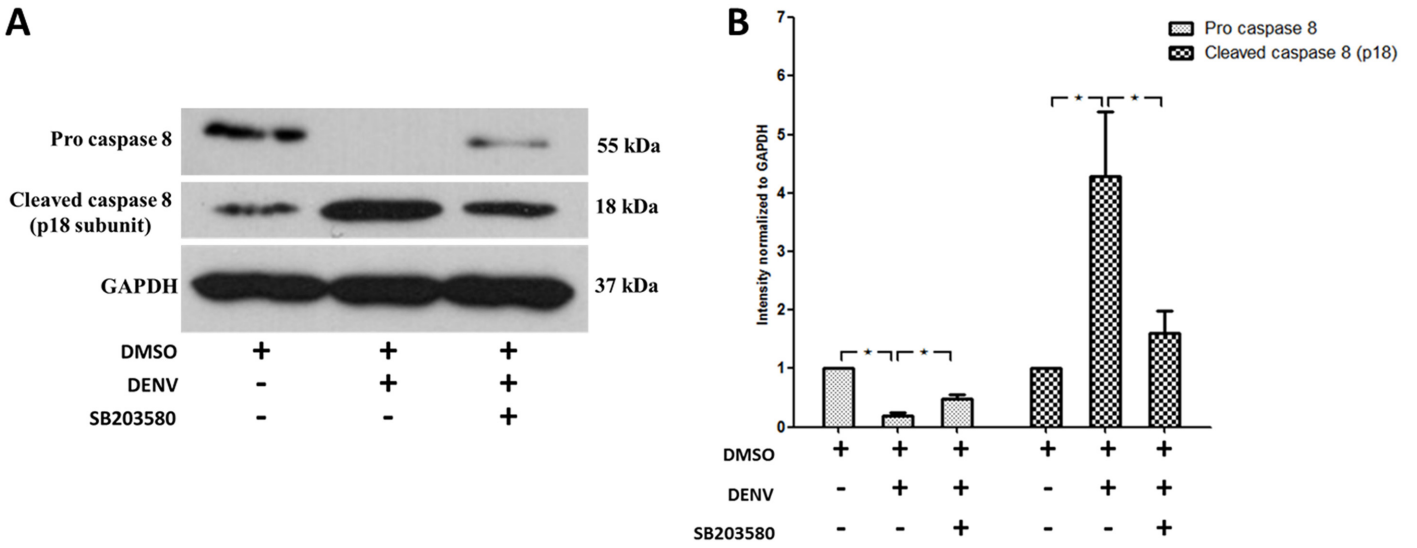

Fig 7. SB203580 treatment reduces caspase 8 expression. Mice were infected with 4×10^5 FFU/ml of DENV and treated with 2%DMSO (v/v) or SB203580 dissolved in 2%DMSO. The control (uninfected) group was treated with 2%DMSO (v/v) alone. Treatments were given 1 h before and after DENV infection and again at 24 h after infection. On day 7 after infection, the liver tissues were collected, and the proteins were extracted for western blotting analysis using antibody directed against the pro and p18 subunit of the cleaved form of (A) caspase 8. The results shown are representative of three independent experiments with three mice (n = 3) from each group. A densitometry analysis using the ImageJ software is shown in (B).

doi:10.1371/journal.pone.0149486.g007

reduced the cleaved caspase 9 expression in DENV infected mice (Fig 8A). The results shown are representative of three independent experiments with three mice (n = 3) from each group. A densitometry analysis using the ImageJ software is shown in (Fig 8B). Our results show that the reduced pro caspase 9 in 2%DMSO-treated DENV infected mice was found, as it is cleaved to 37 and 39 sub units of cleaved caspase 9 and SB203580 treatment restricted this cleavage and

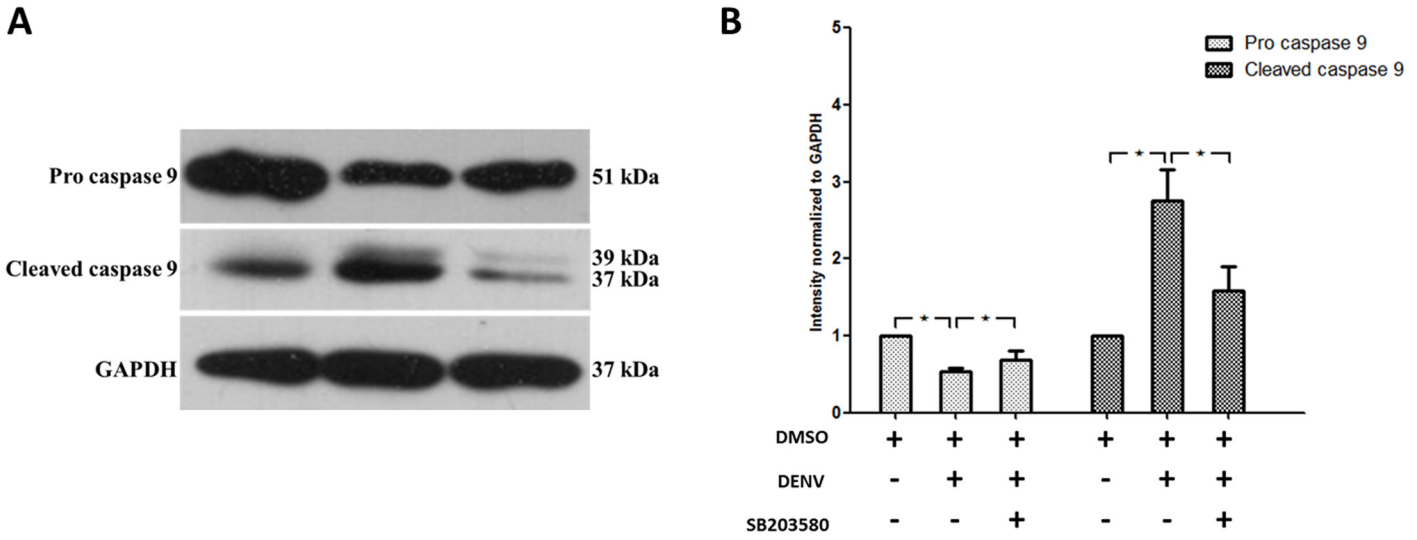

Fig 8. SB203580 treatment reduces caspase 9 expression. Mice were infected with 4×10^5 FFU/ml of DENV and treated with 2%DMSO (v/v) or SB203580 dissolved in 2%DMSO. The control (uninfected) group was treated with 2%DMSO (v/v) alone. Treatments were given 1 h before and after DENV infection and again at 24 h after infection. On day 7 after infection, the liver tissues were collected, and the proteins were extracted for western blotting analysis using antibodies directed against the pro and cleaved forms of (A) caspase 9. The results shown are representative of three independent experiments with three mice (n = 3) from each group. A densitometry analysis using the ImageJ software is shown in (B).

doi:10.1371/journal.pone.0149486.g008

modulated the caspase 9 expression in DENV-infected mice. Specifically, our results confirm that SB203580 modulate the intrinsic pathway of apoptosis in DENV-infected mice.

SB203580 treatment modulates the cytokine and chemokine gene expression profile in DENV-infected mice

The mRNA expression of cytokines including Tumor Necrosis Factor-α (TNF-α), IL-6 and IL-10, chemokines including CCL-5 (RANTES) and CXCL-10 (IP-10) were analyzed by RT-PCR. An mRNA expression of GAPDH is used to normalize the cytokine and chemokine expressions. The results were expressed in fold times to that of un-infected 2%DMSO control. DENV-infection resulted with significant up-regulation of cytokines and chemokines in DENV-infected mice on Day 7. Our results show up-regulated expression of cytokines including TNF-α (Fig 9A), IL-6 (Fig 9B) and IL-10 (Fig 9C) in 2%DMSO-treated DENV-infected mice and SB203580 treatment significantly reduced the TNF-α, IL-6 and IL-10 expression upon DENV-infection (Fig 9A, 9B and 9C). Similarly, the chemokines including CCL-5 (Fig 6D) and CXCL-10 (Fig 9E) were also up-regulated in 2%DMSO-treated DENV-infected mice and SB203580 treatment significantly reduced the mRNA expression of RANTES and IP-10 (Fig 9D and 9E). Interestingly, our results suggest the efficacy of SB203580 in controlling the cytokine and chemokine expression in DENV-infected mice.

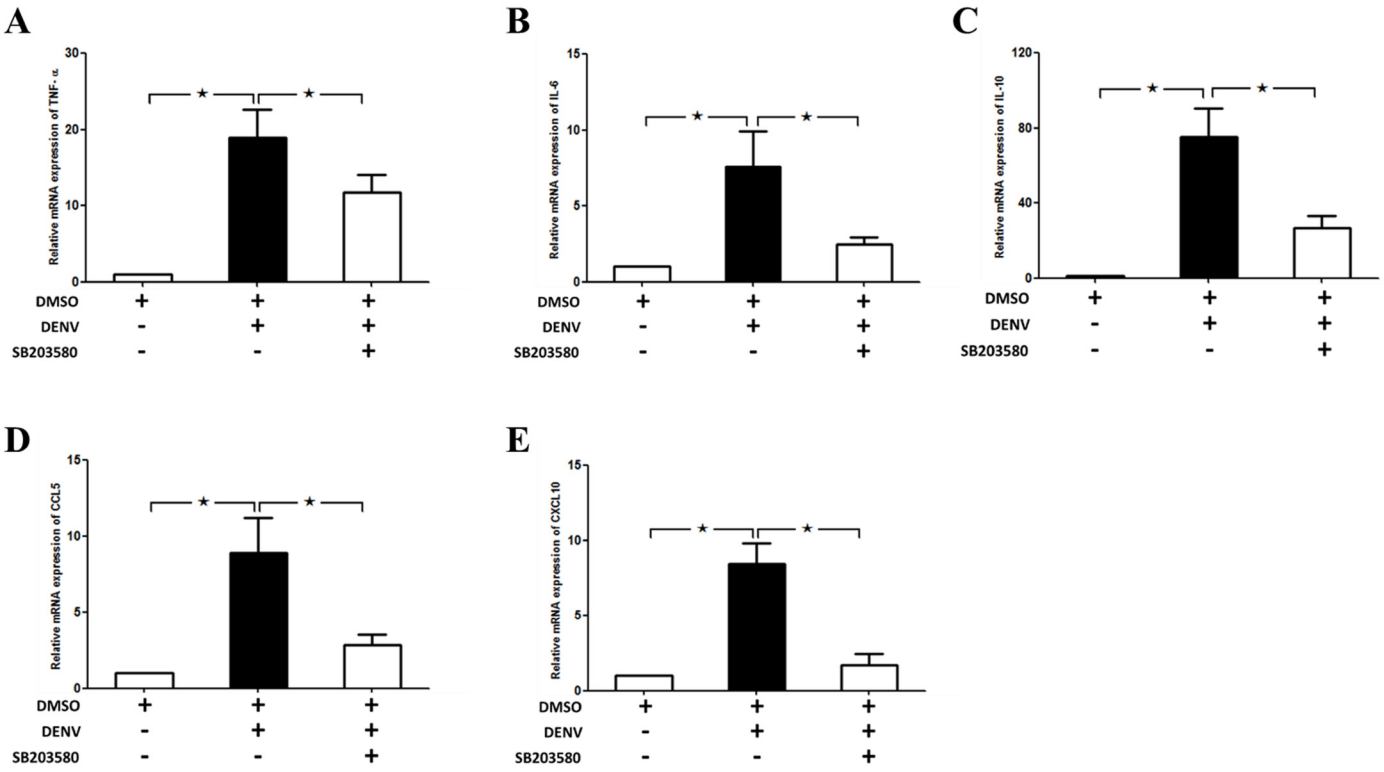

Fig 9. SB203580 modulates the cytokine and chemokine gene expressions in DENV infection Mice were infected with 4×10^5 FFU/ml of DENV and treated with 2%DMSO (v/v) or SB203580 dissolved in 2%DMSO. The control (uninfected) group was treated with 2%DMSO (v/v) alone. Treatments were given 1 h before and after DENV infection and again at 24 h after infection. On day 7 after infection, the liver tissues were collected, and RNA was extracted, cDNA were prepared and which undergone Real-time RT PCR analysis with individual primer set. GAPDH is used as the house keeping gene. The mRNA expression of (A) TNF-α (B) IL-6 (C) IL-10 (D) CCL-5 (E) CXCL-10 are shown. Results were represented in the graph by three independent experiments for at least 3 independent mice from each group. Statistical analysis is conducted by One Way ANOVA using GraphPad Prism Software Version 5. The asterisks indicate statistically significant differences between groups ($p < 0.05$).

doi:10.1371/journal.pone.0149486.g009

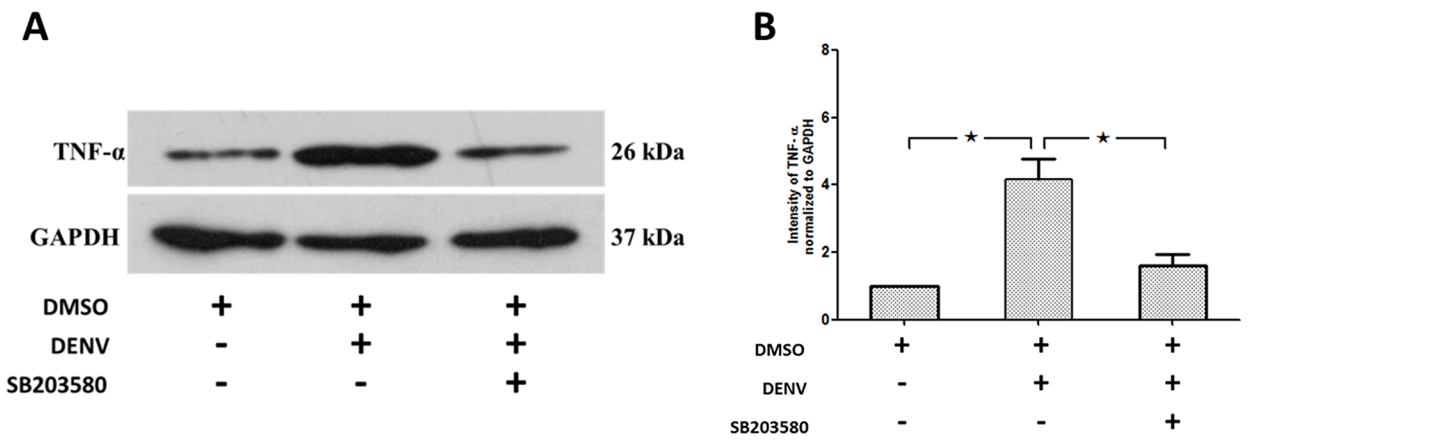

Fig 10. SB203580 treatment reduces TNF-α in DENV-infected mice. Mice were infected with 4×10^5 FFU/ml of DENV and treated with 2%DMSO (v/v) or SB203580 dissolved in 2%DMSO. The control (uninfected) group was treated with 2%DMSO (v/v) alone. Treatments were given 1 h before and after DENV infection and again at 24 h after infection. On day 7 after infection, the liver tissues were collected, and the proteins were extracted for western blotting analysis using antibodies directed against (A) TNF-α. The results shown are representative of three independent experiments with three mice (n = 3) from each group. A densitometry analysis using the ImageJ software is shown in (B).

doi:10.1371/journal.pone.0149486.g010

To validate the RT-PCR analysis, we investigated the protein expression of the prominent pro-inflammatory cytokine, TNF-α, in the liver tissue by western blot analysis. As expected, increased expression of TNF-α was observed in the 2%DMSO-treated DENV-infected mice (Fig 10A) compared to that of un-infected 2%DMSO treated mice and SB203580 significantly reduced the TNF-α production in the DENV-infected mice (Fig 10A). The results shown are representative of three independent experiments with three mice (n = 3) from each group. A densitometry analysis using the ImageJ software is shown in Fig 10B.

SB203580 does not reduce the phosphorylation of p38 MAPK

To explore the molecular mechanism by which the p38 MAPK inhibitor, SB203580 involves in the apoptotic pathways, we firstly tested whether DENV induces the phosphorylation of p38 MAPK in DENV-infected mice and further the ability of SB203580 to reduce the phosphorylated p38 MAPK. Our results show that DENV infection induced the phosphorylation of p38 MAPK and the treatment of with SB203580 in DENV-infected mice caused no reduction of p38 MAPK phosphorylation *in vivo* (Fig 11A). The total p38 MAPK remains equal in all group of mice (Fig 11B). The results were normalized to the house keeping gene GAPDH. The results were representative of at least three independent experiment obtained from three animals per group (n = 3). Densitometry analysis was conducted using ImageJ software and shown in Fig 11C.

SB203580 reduces phosphorylation of the downstream signaling molecules to p38 MAPK

Our results show that SB203580 treatment does not reduce the phosphorylated p38 MAPK in DENV-infected mice, we further examined how SB203580 reduces apoptosis in DENV-infected mice. We hypothesized whether the phosphorylation of any of the downstream signaling molecules to p38 MAPK is controlled by SB203580 treatment. We investigated whether DENV infection induces the phosphorylation of MAPKAPK2, the downstream target to p38 MAPK. Western blot analysis with antibodies directed against phosphorylated MAPKAPK2 and total MAPKAPK2 was conducted. We found that DENV infection induces

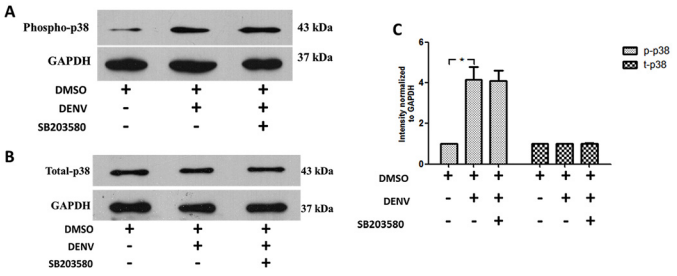

Fig 11. SB203580 does not reduce the phosphorylation of p38 MAPK. Proteins were extracted from the liver tissue samples of 2%DMSO-treated (uninfected), 2%DMSO-treated DENV-infected, and SB203580-treated DENV-infected groups of mice. An additional cocktail of phosphatase inhibitors was added for maintaining the phosphorylated proteins and subjected to western blot analysis with specific antibodies. Results were shown for (A) phosphorylated p38 MAPK and (B) total p38 MAPK. The results shown are representative of three independent experiments with three mice (n = 3) from each group. A densitometry analysis was conducted for the individual blots, normalized to the respective GAPDH, is shown in (C) phosphorylated p38 MAPK and total p38MAPK.

doi:10.1371/journal.pone.0149486.g011

phosphorylation of MAPKAPK2 (Fig 12A) and SB203580 is able to restrict the MAPKAPK2 phosphorylation. Our results confirm SB203580 treatment reduces the phosphorylated form of MAPKAPK2 in DENV infected mice (Fig 12A). The total MAPKAPK2 remains equal in each group of mice (Fig 12A). We suggest that the reduced phosphorylation of MAPKAPK2 by SB203580 treatment contributes to the reduced apoptosis in DENV-infected mice. We further investigated the downstream signaling molecules to MAPKAPK2, namely HSP-27. Western blot analysis with antibodies directed against phosphorylated HSP27 and total HSP27 was conducted. Our results show that DENV infection induces the phosphorylation of HSP27 (Fig 12C) in DENV-infected mice and SB203580 treatment reduces the phosphorylation of HSP27 (Fig 12C). The total HSP-27 remains equal in each group of mice (Fig 12C). Interestingly, we suggest that SB203580 didn't reduce the phosphorylation of p38 MAPK, but blocks the phosphorylation of its downstream signals including MAPKAPK2 and HSP-27. Individual blots were normalized to individual GAPDH. The results were representative of at least three

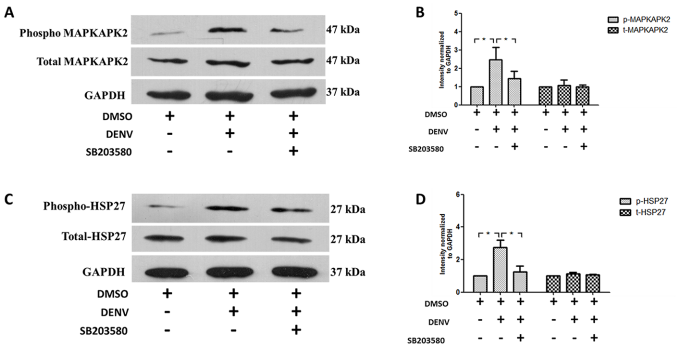

Fig 12. SB203580 treatment reduces the phosphorylation of MAPKAPK2 and HSP27. Proteins were extracted from the liver tissue samples of 2%DMSO-treated (un-infected), 2%DMSO-treated DENV-infected, and SB203580-treated DENV-infected groups of mice. An additional cocktail of phosphatase inhibitors was added for maintaining the phosphorylated proteins and allowed them to standard Western blot analysis with specific antibodies. The results were shown (A) phosphorylated MAPKAPK2 and total MAPKAPK2 and (C) phosphorylated HSP27 and total HSP27, which is normalized to their respective GAPDH. The results shown are representative of three independent experiments with three mice (n = 3) from each group. A densitometry analysis was conducted with the individual blots normalized to GAPDH and is shown in (B) phosphorylated MAPKAPK2 and total MAPKAPK2 and (D) phosphorylated HSP27 and total HSP27.

doi:10.1371/journal.pone.0149486.g012

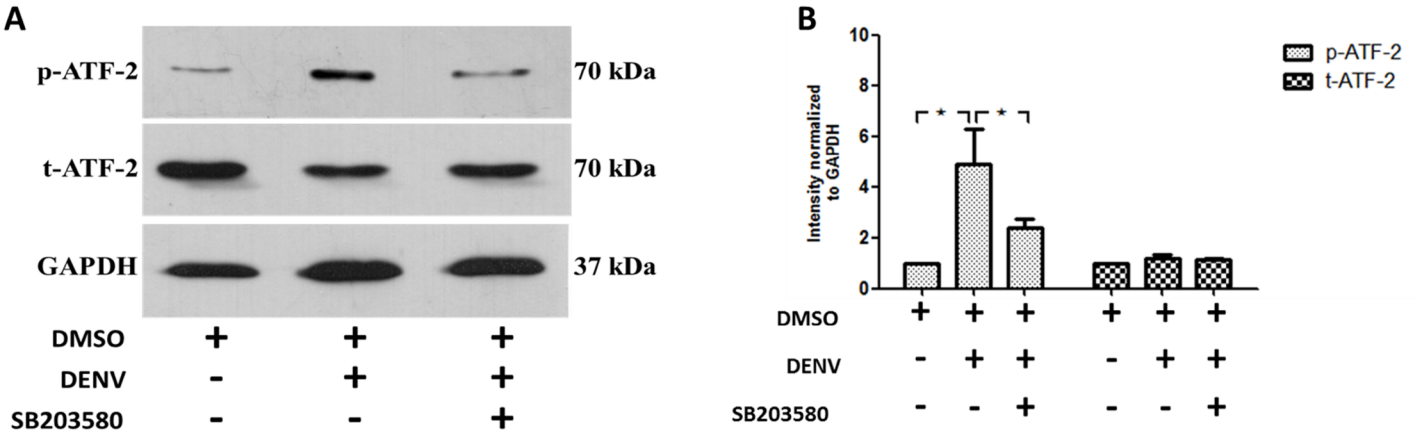

Fig 13. SB203580 treatment reduces the phosphorylation of ATF-2. Proteins were extracted from the liver tissue samples of 2%DMSO-treated (uninfected), 2%DMSO-treated DENV-infected, and SB203580-treated DENV-infected groups of mice. An additional cocktail of phosphatase inhibitors was added for maintaining the phosphorylated proteins and allowed them to standard Western blot analysis with specific antibodies. The result is shown (A) phosphorylated ATF-2 and total ATF-2 normalized to GAPDH. The results shown are representative of three independent experiments with three mice (n = 3) from each group. A densitometry analysis is conducted using the ImageJ software and is shown in (B).

doi:10.1371/journal.pone.0149486.g013

independent experiment obtained from three animals per group (n = 3). Densitometry analysis was conducted using ImageJ software and represented in Fig 12B and 12D.

We further explored the other downstream arm of p38 MAPK signaling, by investigating the role of ATF2, the downstream signaling molecules to p38 MAPK in DENV infection. Proteins were prepared from un-infected 2%DMSO treated, 2%DMSO-treated DENV-infected and SB203580-treated DENV-infected mice. Western blot analysis with antibodies directed against phosphorylated ATF2 and total ATF2 was conducted and normalized to GAPDH. Our results explains that DENV infection induced phosphorylation of ATF2 (Fig 13A) and SB203580 treatment in DENV-infected mice reduced expression of phosphorylated ATF2. The total ATF2 remains equal in each group of mice (Fig 13A). Densitometry analysis was also conducted and shown in Fig 13B.

We report here that DENV infection induces the phosphorylation of p38 MAPK, and the downstream signaling molecules to p38 MAPK including MAPKAPK2, HSP-27 and ATF-2 in DENV-infected mice (Fig 14). SB203580 didn't directly reduce the phosphorylation of p38 MAPK but actually modulates both MAPKAPK2/HSP27 and ATF-2 arms of p38 MAPK signaling. Therefore, the modulation of downstream signaling to p38 MAPK by SB203580 reduces the DENV-induced liver injury.

Discussion

Balb/c mice are susceptible to DENV infection and offer a convenient *in vivo* model of it [11–13]. An intravenous injection of DENV was used to study liver injury in Balb/c mice [11–13] because it produces prominent symptoms compared to DENV-infected mice infected by any other route [14, 48]. Viral particles were detectable in the liver and the classical markers of liver injury seen in patients were confirmed, including the elevation of liver transaminases and the characteristic histopathological changes. The WBC and platelet counts of the DENV-infected mice were reduced, suggesting leucopenia and thrombocytopenia, respectively, which are commonly seen in patients infected with DENV. These results are consistent with other models of DENV infection [63–65] and are similar to the symptoms in C57BL/6 mice [66] and human patients [67]. Although SB203580 improves the hematological profile, the levels of leucopenia and thrombocytopenia in the DENV-infected mice are still decreased relative to those in

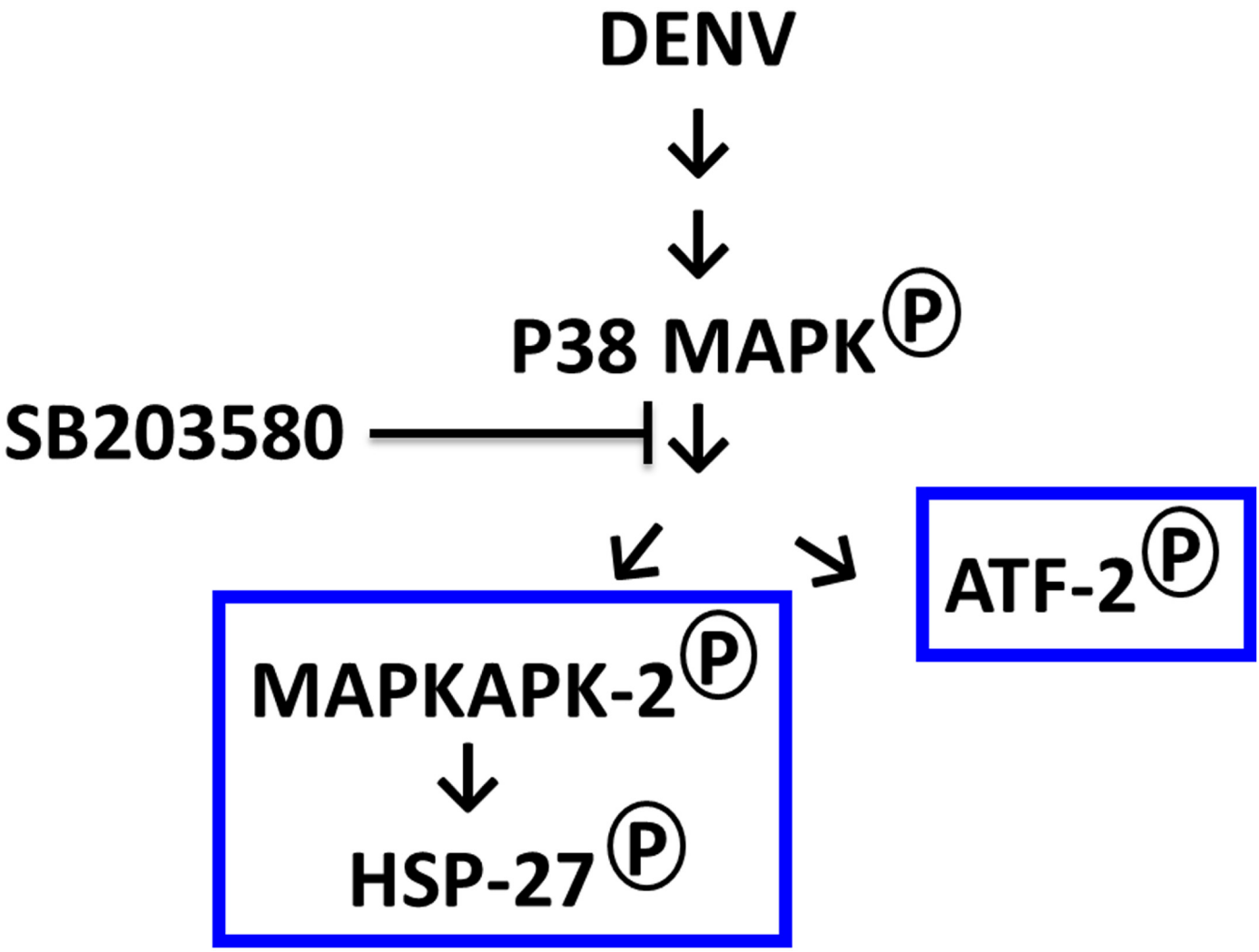

Fig 14. SB203580 does not directly reduce the phosphorylation of p38 MAPK but actually reduces both MAPKAPK2/HSP27 and ATF-2 arms of p38 MAPK signaling in DENV-infected mice.

doi:10.1371/journal.pone.0149486.g014

uninfected mice, similar to the results obtained with the chemical inhibitor of ERK1/2, FR180204 [48]. Therefore, SB203580 may be another option that can control the clinical parameters of DENV infection from the MAPK inhibitor family, but this requires confirmation by testing the additive or synergistic effects.

Elevated liver transaminases (ALT and AST) are used as clinical markers of the classical liver injury that occurs in mice infected with DENV, and are reported to be significantly elevated on day 7 after infection [11, 14, 68]. ALT and AST are also elevated in humans infected with DENV [69, 70]. No difference in ALT was seen with the addition of SB203580, though AST levels were altered in this study. It may be due to AST is more specific for liver inflammation than ALT, because the amount of AST in the liver is very much higher than that of ALT [8, 70, 71]. Elevated serum level of liver enzyme, gamma-glutamyl transpeptidase (GGT) was also correlated well with histology to study liver damage in alcoholism [72]. Similarly, in a mouse model of drug-induced chronic hepatitis GGT is significantly elevated [73]. A patient with DENV-induced fulminant hepatitis show increased GGT level [74]. The GGT expression

in the livers of DENV-infected mice in our study is consistent with the above findings. A histological analysis of the liver tissues from DMSO-treated DENV-infected mice shows the classical signs of liver injury seen in DENV-infected patients [13, 75, 76]. These conditions were alleviated by treatment with SB203580, suggesting the efficacy of SB203580 in controlling the liver injury induced by DENV infection.

We explored the molecular mechanism by which SB203580 controls this liver injury with a commercially available Mouse Apoptosis RT^2 Profiler™ PCR Array System (Qiagen). The increased pro-inflammatory cytokine expression induced by DENV is consistent with various other studies. The expression of TNF-α family increases in patients with severe DENV disease [24, 25, 77–80]. *In vitro* hepatic cell lines also show similar results for TRAIL [19, 81]. In DENV-infected HepG2 cells, TNF-α is increased and the inhibition of p38MAPK reduces TNF-α expression [20]. Interestingly, in the present study, *Cd40L* and *Cd40* mRNA expression is also up-regulated in the DENV-infected mice. An important TNF receptor family member, CD40, and its ligand, Cd40L, are important modulators of the antiviral immune responses [82–85]. In DENV-infected dendritic cells, CD40–CD40L signaling underlies the immune-mediated responses [86]. This finding requires further investigation primarily in hepatic cell line to determine the immuno-regulatory role of CD40–CD40L signaling in DENV-induced liver cell apoptosis. FAS/FASL pathway induces apoptosis in vascular endothelial cells [26]. FAS-mediated apoptosis is also induced DENV-infected HepG2 cells and the interaction of DENV capsid protein with DAXX is involved in this induction [27]. FAS-associated death domain (FADD) is also up-regulated during DENV infection, with concurrent increases of TNF-α and IL-10 expression [87]. Our results from mRNA expression profile suggest the involvement of FAS-mediated cell death in DENV-infected mice. The activation of the cytoplasmic apoptotic caspase was also observed in the present study. Increased cleaved caspase 3 expression is seen during DENV infection [88, 89] and explains the apoptosis and organ injury during DENV infection [83, 90–94]. We observed similar results of increased cleaved caspase 3 expression and SB203580 treatment restricted the cleaved caspase 3 expression, thereby decreasing the DENV -induced liver injury.

Very specifically, we questioned how the apoptotic signals were modulated by SB203580 treatment. Our results in DENV-infected mice confirmed increased expressions of caspase 8 and caspase 9, and we observed SB203580 treatment reduces the activation of both caspase 8 and caspase 9 in DENV-infected mice. In a previous *in vitro* study, DENV infection induced apoptosis through both intrinsic and extrinsic pathway, by the activation of caspase 8 and caspase 9 [95]. Our results were consistent in the liver tissues of DENV-infected mice and we show here that SB203580 is able to modulate apoptosis in both extrinsic and intrinsic pathways. Finally, we validated the previous findings, the apoptotic pathway by DENV infection in mice is in a caspase dependent manner and reports the efficacy of SB203580 in controlling the DENV induced apoptotic pathways.

Increased apoptosis is observed with increased pro-apoptotic cytokines including TNF-α, IL-6 and TRAIL [78]. In our study, mRNA expressions of cytokines including TNF-α, IL-6 and IL-10, and chemokines including RANTES and IP-10 are up-regulated in DENV-infected mice and SB203580 treatment reduces these expressions in DENV-induced liver injury. Our results are consistent with the inclined serum levels of IL-10 and IP-10 in patients with severe DENV infection and are associated with T cell apoptosis [96]. Children with DENV infection show increased levels of and IL-6, and IL-10 and correlates with the severity of disease progression [97], [98]. Increased IL-6 expression in the lung epithelial cells by DENV infection was found to be NF-kB dependent and is associated with RANTES expression [99]. Increased expression of RANTES in DENV-infected mice show liver damage, with leukocyte activation and increased IL-6 expression [66]. Increased expression of RANTES is observed in intra-cerebral

inoculation of DENV, which induces behavioral changes and encephalitis in C57BL/6 mice. Both RANTES and IP-10 were shown to be induced in human lung epithelial carcinoma cells (A549) infected with DENV [100]. Our research group also found similar results in DENV-infected HEK 293 cells and reported this is by NF-kB activation [101]. However, further information on these in *in vivo* models of DENV infection is still required. Interestingly, the efficacy of SB203580 in controlling the expression of other important cytokines involved in DENV infection also requires further investigations.

Increased apoptosis is also observed with increased cytokine expression of TNF-α, which contribute to increased phosphorylation of p38 MAPK in DENV infected HepG2 cells [20]. In DENV-infected HepG2 cells, SB203580 reduces the expression of RIPK2 and DENV-induced apoptosis [17]. Recently, SB203580 has been shown to improve the clinical manifestations and systemic inflammation in an animal model of DENV infection. This interesting study shows oral administration of SB203580 in immuno-competent AG129 mice, decreases the circulation of pro-inflammatory cytokines (TNF-α, IL-6 and MMP-9) and reduces the leakage resulting a better survival rate [54]. But interestingly, there is neither *in vitro* nor *in vivo* study which shows the mechanism by which SB203580 treatment modulates apoptosis in DENV infection.

To provide insight into this, we investigated whether DENV infection influences the phosphorylation of p38 MAPK in DENV-induced liver injury. We used the immuno-competent Balb/c mouse to understand the host immune responses, especially apoptosis in contribution to liver injury. Our results demonstrate that DENV infection induces the phosphorylation of p38 MAPK in mice and SB203580 treatment did not control the phosphorylation of p38 MAPK in DENV infected mice. This suggests SB203580 does not directly inhibit the phosphorylation of p38 MAPK. Similar results were observed in a cell-based system, treatment with TNF-α shows increased phosphorylation of p38 MAPK signaling, but treatment with SB203580 does not reduce the phosphorylation of p38 MAPK, but interestingly inhibits its downstream kinases, including MAPKAPK2 and ATF2 at both arms of p38 MAPK signaling [102].

We examined the same path, whether SB203580 reduces the phosphorylation of its downstream kinases including MAPKAPK2 and ATF-2 in DENV infection. We found that SB203580 treatment reduces the phosphorylation of both MAPKAPK2 and ATF-2 in DENV-induced liver injury. MAPKAPK2, is one of the direct downstream target of p38 MAPK signaling and its deficiency is reported as an important controlling factor in protecting brain from ischemic injury in mice [83]. The inhibition of MAPKAPK2 is also reported to block the p38 MAPK signaling on reperfusion, thereby reducing redox stress and apoptotic cell death [103]. Our results were consistent with these observations that DENV also induces p38 MAPK phosphorylation and we confirmed the ability of SB203580 to decrease the phosphorylation of MAPKAPK2 in DENV-induced liver injury. At the other arm of p38 MAPK signaling, ATF-2 is reported to be activated by signals from stress-activated protein kinases, including JNK and p38 MAPK [104]. In varicella-zoster virus infections, both p38 MAPK and JNK are activated, thereby activating of the downstream signal ATF2 [105]. In an animal model of *Human immunodeficiency virus* infection, ATF2 phosphorylation is also inhibited by SB203580 treatment without inhibiting the phosphorylation of p38 MAPK [106]. Our results explains in DENV-infected mice, where SB203580 treatment reduces the phosphorylation of ATF-2 at another arm of p38 MAPK pathway, which give us more clues for decreased liver injury observed in this study.

HSP27 is a member in the family of small heat shock proteins that act in various cellular responses, including apoptosis [107]. The activation of MAPKAPK2 is also reported to increase vascular permeability, together with activated HSP27, the direct downstream signal to MAPKAPK2 and SB203580 is reported to be effective in controlling vascular permeability [108]. In

another study of *respiratory syncytial virus* (RSV) infection, both p38 MAPK and HSP27 are required for increased human epithelial membrane permeability, and SB203580 controls the infectivity of RSV by attenuating this membrane permeability [109]. We also found increased phosphorylation of HSP27 in DENV-infected mice, which may directly come from the p38 MAPK and MAPKAPK2 phosphorylation signaling. SB203580 treatment decreases the phosphorylation of HSP27 by the inhibition of MAPKAPK2. As DENV infection also contributes to vascular permeability [110–113], this aspect needs further investigation.

Our results confirm that p38 MAPK and its downstream targets plays important roles in DENV-induced liver injury. DENV induces apoptosis by the induced phosphorylation of MAPKAPK2, HSP27 and ATF-2 and SB203580 treatment reduces the DENV-induced apoptosis, by inhibiting the phosphorylation of MAPKAPK2, HSP27 and ATF2. Since the inhibitor did not reduce p38 MAPK phosphorylation, there is a possibility that SB203580 may be acting directly on downstream molecules as well as p38 MAPK. Our study supports the previous studies, as p38 MAPK plays an important role in the induction of pro-inflammatory cytokine TNF-α during DENV infection [20] and modulation of inflammation and pathology in DENV infected mice by p38 MAPK inhibitor, SB203580 [54]. However, we open up the path to further investigate the downstream signals towards MAPK pathway, which is very important to better understand the pathogenesis of DENV infection.

Conclusion

The p38 MAPK inhibitor, SB203580 treatment in DENV-infected mice reverses the AST, GGT and histopathology of the liver and controls the cytokine and chemokine responses. The apoptosis signaling in DENV-infected mice via both intrinsic and extrinsic pathway is modulated by SB203580, by reducing the phosphorylation of downstream signaling molecules to p38 MAPK including MAPKAPK2, HSP27 and ATF-2.

Supporting Information

S1 Table. SB203580 treatment modulates the apoptotic gene expression profile in DENV-infected mice. To explore the molecular mechanism by which SB203580 reduces liver damage, screening experiments were conducted with a commercially available Mouse Apoptosis RT^2 Profiler™ PCR Array System (Qiagen). The full list of gene expression profile of the apoptosis related genes in DENV-infected mice and the effect of SB203580 treatment to those genes were shown in the S1 Table. The results were normalized to un-infected 2%DMSO-treated mouse. Actin is used as the housekeeping gene for normalizing the expression profile.
(PDF)

Author Contributions

Conceived and designed the experiments: TL GPS. Performed the experiments: GPS AC AS JP. Analyzed the data: GPS TL. Contributed reagents/materials/analysis tools: TL PY SN. Wrote the paper: GPS TL.

References

1. Viprakasit V, Ekwattanakit S, Chalaow N, Riolueang S, Wijit S, Tanyut P, et al. Clinical presentation and molecular identification of four uncommon alpha globin variants in Thailand. Initiation codon mutation of alpha2-globin Gene (HBA2:c.1delA), donor splice site mutation of alpha1-globin gene (IVSI-1, HBA1:c.95 + 1G>A), hemoglobin Queens Park/Chao Pra Ya (HBA1:c.98T>A) and hemoglobin Westmead (HBA2:c.369C>G). Acta Haematol. 2014; 131(2):88–94. Epub 2013/10/02. doi: 10.1159/000353119 PMID: 24081251.

2. Ramzan M, Yadav SP, Dinand V, Sachdeva A. Dengue fever causing febrile neutropenia in children with acute lymphoblastic leukemia: an unknown entity. Hematol Oncol Stem Cell Ther. 2013; 6(2): 65–67. Epub 2013/06/13. doi: 10.1016/j.hemonc.2013.05.005 PMID: 23756720.
3. Kharya G, Yadav SP, Katewa S, Sachdeva A. Management of severe refractory thrombocytopenia in dengue hemorrhagic fever with intravenous anti-D immune globulin. Pediatr Hematol Oncol. 2011; 28(8):727–732. Epub 2011/10/06. doi: 10.3109/08880018.2011.609581 PMID: 21970507.
4. Visuthranukul J, Bunworasate U, Lawasut P, Suankratay C. Dengue hemorrhagic fever in a peripheral blood stem cell transplant recipient: the first case report. Infect Dis Rep. 2009; 1(1):e3. Epub 2009/09/14. doi: 10.4081/idr.2009.e3 PMID: 24470881; PubMed Central PMCID: PMCPMC3892570.
5. de Castro RA, de Castro JA, Barez MY, Frias MV, Dixit J, Genereux M. Thrombocytopenia associated with dengue hemorrhagic fever responds to intravenous administration of anti-D (Rh(0)-D) immune globulin. Am J Trop Med Hyg. 2007; 76(4):737–742. Epub 2007/04/12. PMID: 17426181.
6. Wiwanitkit V, Manusvanich P. Can hematocrit and platelet determination on admission predict shock in hospitalized children with dengue hemorrhagic fever? A clinical observation from a small outbreak. Clin Appl Thromb Hemost. 2004; 10(1):65–67. Epub 2004/02/26. PMID: 14979408.
7. Trung DT, Thao le TT, Hien TT, Hung NT, Vinh NN, Hien PT, et al. Liver involvement associated with dengue infection in adults in Vietnam. Am J Trop Med Hyg. 2010; 83(4):774–780. doi: 10.4269/ajtmh.2010.10-0090 PMID: 20889864; PubMed Central PMCID: PMC2946741.
8. Chongsrisawat V, Hutagalung Y, Poovorawan Y. Liver function test results and outcomes in children with acute liver failure due to dengue infection. Southeast Asian J Trop Med Public Health. 2009; 40(1):47–53. PMID: 19323033.
9. Souza LJ, Alves JG, Nogueira RM, Gicovate Neto C, Bastos DA, Siqueira EW, et al. Aminotransferase changes and acute hepatitis in patients with dengue fever: analysis of 1,585 cases. Braz J Infect Dis. 2004; 8(2):156–163. /S1413-86702004000200006. PMID: 15361994.
10. Mohan B, Patwari AK, Anand VK. Hepatic dysfunction in childhood dengue infection. J Trop Pediatr. 2000; 46(1):40–43. PMID: 10730040.
11. Paes MV, Pinhao AT, Barreto DF, Costa SM, Oliveira MP, Nogueira AC, et al. Liver injury and viremia in mice infected with dengue-2 virus. Virology. 2005; 338(2):236–246. Epub 2005/06/18. S0042-6822(05)00270-9 [pii] doi: 10.1016/j.virol.2005.04.042 PMID: 15961136.
12. Barth OM, Barreto DF, Paes MV, Takiya CM, Pinhao AT, Schatzmayr HG. Morphological studies in a model for dengue-2 virus infection in mice. Mem Inst Oswaldo Cruz. 2006; 101(8):905–915. Epub 2007/02/13. S0074-02762006000800014 [pii]. PMID: 17293987.
13. Paes MV, Lenzi HL, Nogueira AC, Nuovo GJ, Pinhao AT, Mota EM, et al. Hepatic damage associated with dengue-2 virus replication in liver cells of BALB/c mice. Lab Invest. 2009; 89(10):1140–1151. doi: 10.1038/labinvest.2009.83 PMID: 19721415.
14. Franca RF, Zucoloto S, da Fonseca BA. A BALB/c mouse model shows that liver involvement in dengue disease is immune-mediated. Exp Mol Pathol. 2010; 89(3):321–326. Epub 2010/08/03. S0014-4800(10)00104-8 [pii] doi: 10.1016/j.yexmp.2010.07.007 PMID: 20673760.
15. Chen HC, Lai SY, Sung JM, Lee SH, Lin YC, Wang WK, et al. Lymphocyte activation and hepatic cellular infiltration in immunocompetent mice infected by dengue virus. J Med Virol. 2004; 73(3):419–431. doi: 10.1002/jmv.20108 PMID: 15170638.
16. Limonta D, Capo V, Torres G, Perez AB, Guzman MG. Apoptosis in tissues from fatal dengue shock syndrome. J Clin Virol. 2007; 40(1):50–54. doi: 10.1016/j.jcv.2007.04.024 PMID: 17693133.
17. Morchang A, Yasamut U, Netsawang J, Noisakran S, Wongwiwat W, Songprakhon P, et al. Cell death gene expression profile: role of RIPK2 in dengue virus-mediated apoptosis. Virus Res. 2011; 156(1–2):25–34. doi: 10.1016/j.virusres.2010.12.012 PMID: 21195733.
18. Thongtan T, Panyim S, Smith DR. Apoptosis in dengue virus infected liver cell lines HepG2 and Hep3B. J Med Virol. 2004; 72(3):436–444. doi: 10.1002/jmv.20004 PMID: 14748067.
19. Matsuda T, Almasan A, Tomita M, Tamaki K, Saito M, Tadano M, et al. Dengue virus-induced apoptosis in hepatic cells is partly mediated by Apo2 ligand/tumour necrosis factor-related apoptosis-inducing ligand. J Gen Virol. 2005; 86(Pt 4):1055–1065. doi: 10.1099/vir.0.80531-0 PMID: 15784899; PubMed Central PMCID: PMC2917180.
20. Nagila A, Netsawang J, Suttitheptumrong A, Morchang A, Khunchai S, Srisawat C, et al. Inhibition of p38MAPK and CD137 signaling reduce dengue virus-induced TNF-alpha secretion and apoptosis. Virol J. 2013; 10:105. doi: 10.1186/1743-422X-10-105 PMID: 23557259; PubMed Central PMCID: PMC3639879.
21. Alagarasu K, Mulay AP, Singh R, Gavade VB, Shah PS, Cecilia D. Association of HLA-DRB1 and TNF genotypes with dengue hemorrhagic fever. Hum Immunol. 2013; 74(5):610–617. doi: 10.1016/j.humimm.2013.01.027 PMID: 23380141.

22. Wati S, Rawlinson SM, Ivanov RA, Dorstyn L, Beard MR, Jans DA, et al. Tumour necrosis factor alpha (TNF-alpha) stimulation of cells with established dengue virus type 2 infection induces cell death that is accompanied by a reduced ability of TNF-alpha to activate nuclear factor kappaB and reduced sphingosine kinase-1 activity. J Gen Virol. 2011; 92(Pt 4):807–818. doi: 10.1099/vir.0.028159-0 PMID: 21148274.

23. Atrasheuskaya A, Petzelbauer P, Fredeking TM, Ignatyev G. Anti-TNF antibody treatment reduces mortality in experimental dengue virus infection. FEMS Immunol Med Microbiol. 2003; 35(1):33–42. PMID: 12589955.

24. Pinto LM, Oliveira SA, Braga EL, Nogueira RM, Kubelka CF. Increased pro-inflammatory cytokines (TNF-alpha and IL-6) and anti-inflammatory compounds (sTNFRp55 and sTNFRp75) in Brazilian patients during exanthematic dengue fever. Mem Inst Oswaldo Cruz. 1999; 94(3):387–394. PMID: 10348988.

25. Hober D, Poli L, Roblin B, Gestas P, Chungue E, Granic G, et al. Serum levels of tumor necrosis factor-alpha (TNF-alpha), interleukin-6 (IL-6), and interleukin-1 beta (IL-1 beta) in dengue-infected patients. Am J Trop Med Hyg. 1993; 48(3):324–331. PMID: 8470771.

26. Liao H, Xu J, Huang J. FasL/Fas pathway is involved in dengue virus induced apoptosis of the vascular endothelial cells. J Med Virol. 2010; 82(8):1392–1399. doi: 10.1002/jmv.21815 PMID: 20572077.

27. Limjindaporn T, Netsawang J, Noisakran S, Thiemmeca S, Wongwiwat W, Sudsaward S, et al. Sensitization to Fas-mediated apoptosis by dengue virus capsid protein. Biochem Biophys Res Commun. 2007; 362(2):334–339. doi: 10.1016/j.bbrc.2007.07.194 PMID: 17707345.

28. Nasirudeen AM, Liu DX. Gene expression profiling by microarray analysis reveals an important role for caspase-1 in dengue virus-induced p53-mediated apoptosis. J Med Virol. 2009; 81(6):1069–1081. doi: 10.1002/jmv.21486 PMID: 19382257.

29. Nasirudeen AM, Wang L, Liu DX. Induction of p53-dependent and mitochondria-mediated cell death pathway by dengue virus infection of human and animal cells. Microbes Infect. 2008; 10(10–11): 1124–1132. Epub 2008/07/09. doi: 10.1016/j.micinf.2008.06.005 PMID: 18606243.

30. Qi Y, Li Y, Zhang Y, Zhang L, Wang Z, Zhang X, et al. IFI6 Inhibits Apoptosis via Mitochondrial-Dependent Pathway in Dengue Virus 2 Infected Vascular Endothelial Cells. PLoS One. 2015; 10(8): e0132743. Epub 2015/08/06. doi: 10.1371/journal.pone.0132743 PMID: 26244642; PubMed Central PMCID: PMCPMC4526556.

31. Thepparit C, Khakpoor A, Khongwichit S, Wikan N, Fongsaran C, Chingsuwanrote P, et al. Dengue 2 infection of HepG2 liver cells results in endoplasmic reticulum stress and induction of multiple pathways of cell death. BMC Res Notes. 2013; 6:372. Epub 2013/09/17. doi: 10.1186/1756-0500-6-372 PMID: 24034452; PubMed Central PMCID: PMCPMC3847886.

32. Lee CJ, Liao CL, Lin YL. Flavivirus activates phosphatidylinositol 3-kinase signaling to block caspase-dependent apoptotic cell death at the early stage of virus infection. J Virol. 2005; 79(13):8388–8399. Epub 2005/06/16. doi: 10.1128/JVI.79.13.8388-8399.2005 PMID: 15956583; PubMed Central PMCID: PMCPMC1143730.

33. Cross TG, Scheel-Toellner D, Henriquez NV, Deacon E, Salmon M, Lord JM. Serine/threonine protein kinases and apoptosis. Exp Cell Res. 2000; 256(1):34–41. Epub 2000/03/31. doi: 10.1006/excr.2000.4836 PMID: 10739649.

34. Hui KP, Lee SM, Cheung CY, Ng IH, Poon LL, Guan Y, et al. Induction of proinflammatory cytokines in primary human macrophages by influenza A virus (H5N1) is selectively regulated by IFN regulatory factor 3 and p38 MAPK. J Immunol. 2009; 182(2):1088–1098. PMID: 19124752.

35. Rajendra Kumar P, Singhal PK, Subba Rao MR, Mahalingam S. Phosphorylation by MAPK regulates simian immunodeficiency virus Vpx protein nuclear import and virus infectivity. J Biol Chem. 2005; 280(9):8553–8563. doi: 10.1074/jbc.M407863200 PMID: 15556948.

36. Regan AD, Cohen RD, Whittaker GR. Activation of p38 MAPK by feline infectious peritonitis virus regulates pro-inflammatory cytokine production in primary blood-derived feline mononuclear cells. Virology. 2009; 384(1):135–143. doi: 10.1016/j.virol.2008.11.006 PMID: 19058829.

37. Lin CF, Wan SW, Chen MC, Lin SC, Cheng CC, Chiu SC, et al. Liver injury caused by antibodies against dengue virus nonstructural protein 1 in a murine model. Lab Invest. 2008; 88(10):1079–1089. doi: 10.1038/labinvest.2008.70 PMID: 18679379.

38. Han J, Lee JD, Jiang Y, Li Z, Feng L, Ulevitch RJ. Characterization of the structure and function of a novel MAP kinase kinase (MKK6). J Biol Chem. 1996; 271(6):2886–2891. PMID: 8621675.

39. Stein B, Brady H, Yang MX, Young DB, Barbosa MS. Cloning and characterization of MEK6, a novel member of the mitogen-activated protein kinase kinase cascade. J Biol Chem. 1996; 271(19): 11427–11433. PMID: 8626699.

40. Enslen H, Raingeaud J, Davis RJ. Selective activation of p38 mitogen-activated protein (MAP) kinase isoforms by the MAP kinase kinases MKK3 and MKK6. J Biol Chem. 1998; 273(3):1741–1748. PMID: 9430721.

41. Rouse J, Cohen P, Trigon S, Morange M, Alonso-Llamazares A, Zamanillo D, et al. A novel kinase cascade triggered by stress and heat shock that stimulates MAPKAP kinase-2 and phosphorylation of the small heat shock proteins. Cell. 1994; 78(6):1027–1037. PMID: 7923353.

42. Raingeaud J, Gupta S, Rogers JS, Dickens M, Han J, Ulevitch RJ, et al. Pro-inflammatory cytokines and environmental stress cause p38 mitogen-activated protein kinase activation by dual phosphorylation on tyrosine and threonine. J Biol Chem. 1995; 270(13):7420–7426. PMID: 7535770.

43. Liew KJ, Chow VT. Microarray and real-time RT-PCR analyses of a novel set of differentially expressed human genes in ECV304 endothelial-like cells infected with dengue virus type 2. J Virol Methods. 2006; 131(1):47–57. Epub 2005/08/23. doi: 10.1016/j.jviromet.2005.07.003 PMID: 16112753.

44. Cabello-Gutierrez C, Manjarrez-Zavala ME, Huerta-Zepeda A, Cime-Castillo J, Monroy-Martinez V, Correa BB, et al. Modification of the cytoprotective protein C pathway during Dengue virus infection of human endothelial vascular cells. Thromb Haemost. 2009; 101(5):916–928. PMID: 19404546.

45. Ceballos-Olvera I, Chavez-Salinas S, Medina F, Ludert JE, del Angel RM. JNK phosphorylation, induced during dengue virus infection, is important for viral infection and requires the presence of cholesterol. Virology. 2010; 396(1):30–36. Epub 2009/11/10. S0042-6822(09)00642-4 [pii] doi: 10.1016/j.virol.2009.10.019 PMID: 19897220.

46. Huerta-Zepeda A, Cabello-Gutierrez C, Cime-Castillo J, Monroy-Martinez V, Manjarrez-Zavala ME, Gutierrez-Rodriguez M, et al. Crosstalk between coagulation and inflammation during Dengue virus infection. Thromb Haemost. 2008; 99(5):936–943. doi: 10.1160/TH07-08-0438 PMID: 18449425.

47. Albarnaz JD, De Oliveira LC, Torres AA, Palhares RM, Casteluber MC, Rodrigues CM, et al. MEK/ERK activation plays a decisive role in yellow fever virus replication: Implication as an antiviral therapeutic target. Antiviral Res. 2014; 111C:82–92. doi: 10.1016/j.antiviral.2014.09.004 PMID: 25241249.

48. Sreekanth GP, Chuncharunee A, Sirimontaporn A, Panaampon J, Srisawat C, Morchang A, et al. Role of ERK1/2 signaling in dengue virus-induced liver injury. Virus Res. 2014; 188:15–26. doi: 10.1016/j.virusres.2014.03.025 PMID: 24704674.

49. Liu XW, Ji EF, He P, Xing RX, Tian BX, Li XD. Protective effects of the p38 MAPK inhibitor SB203580 on NMDAinduced injury in primary cerebral cortical neurons. Mol Med Rep. 2014; 10(4):1942–1948. doi: 10.3892/mmr.2014.2402 PMID: 25051190.

50. Stirling DP, Liu J, Plunet W, Steeves JD, Tetzlaff W. SB203580, a p38 mitogen-activated protein kinase inhibitor, fails to improve functional outcome following a moderate spinal cord injury in rat. Neuroscience. 2008; 155(1):128–137. doi: 10.1016/j.neuroscience.2008.05.007 PMID: 18562123.

51. Morley SJ, Naegele S. Phosphorylation of initiation factor 4E is resistant to SB203580 in cells expressing a drug-resistant mutant of stress-activated protein kinase 2a/p38. Cell Signal. 2003; 15(8):741–749. PMID: 12781867.

52. Lahti A, Kankaanranta H, Moilanen E. P38 mitogen-activated protein kinase inhibitor SB203580 has a bi-directional effect on iNOS expression and NO production. Eur J Pharmacol. 2002; 454(2–3):115–123. PMID: 12421638.

53. Johnson JC, Martinez O, Honko AN, Hensley LE, Olinger GG, Basler CF. Pyridinyl imidazole inhibitors of p38 MAP kinase impair viral entry and reduce cytokine induction by Zaire ebolavirus in human dendritic cells. Antiviral Res. 2014; 107:102–109. doi: 10.1016/j.antiviral.2014.04.014 PMID: 24815087; PubMed Central PMCID: PMC4103912.

54. Fu Y, Yip A, Seah PG, Blasco F, Shi PY, Herve M. Modulation of inflammation and pathology during dengue virus infection by p38 MAPK inhibitor SB203580. Antiviral Res. 2014; 110:151–157. doi: 10.1016/j.antiviral.2014.08.004 PMID: 25131378.

55. Oliveira ER, Amorim JF, Paes MV, Azevedo AS, Goncalves AJ, Costa SM, et al. Peripheral effects induced in BALB/c mice infected with DENV by the intracerebral route. Virology. 2015; 489:95–107. Epub 2016/01/10. doi: 10.1016/j.virol.2015.12.006 PMID: 26748331.

56. Jirakanjanakit N, Sanohsomneing T, Yoksan S, Bhamarapravati N. The micro-focus reduction neutralization test for determining dengue and Japanese encephalitis neutralizing antibodies in volunteers vaccinated against dengue. Trans R Soc Trop Med Hyg. 1997; 91(5):614–617. Epub 1998/02/17. PMID: 9463684.

57. Towbin H, Staehelin T, Gordon J. Electrophoretic transfer of proteins from polyacrylamide gels to nitrocellulose sheets: procedure and some applications. Proc Natl Acad Sci U S A. 1979; 76(9):4350–4354. Epub 1979/09/01. PMID: 388439.

58. Robles-Diaz M, Garcia-Cortes M, Medina-Caliz I, Gonzalez-Jimenez A, Gonzalez-Grande R, Navarro JM, et al. The value of serum aspartate aminotransferase and gamma-glutamyl transpetidase as

biomarkers in hepatotoxicity. Liver Int. 2015; 35(11):2474–2482. Epub 2015/03/27. doi: 10.1111/liv.12834 PMID: 25809419.

59. Yu G, Chi X, Wu R, Wang X, Gao X, Kong F, et al. Replication Inhibition of Hepatitis B Virus and Hepatitis C Virus in Co-Infected Patients in Chinese Population. PLoS One. 2015; 10(9):e0139015. Epub 2015/10/01. doi: 10.1371/journal.pone.0139015 PMID: 26422607; PubMed Central PMCID: PMCPMC4589515.

60. Li R, Mi Y, Tan G, Zhang W, Li G, Sun X. A novel in situ model of liver cold ischemia-reperfusion in rats. J Surg Res. 2014; 192(1):195–199. Epub 2014/06/24. doi: 10.1016/j.jss.2014.05.042 PMID: 24953989.

61. Kim E, Yang J, Lee H, Park JR, Hong SH, Woo HM, et al. Gamma-glutamyl transferase as an early and sensitive marker in ethanol-induced liver injury of rats. Transplant Proc. 2014; 46(4):1180–1185. Epub 2014/05/13. doi: 10.1016/j.transproceed.2013.11.028 PMID: 24815155.

62. Tian Z, Liu H, Su X, Fang Z, Dong Z, Yu C, et al. Role of elevated liver transaminase levels in the diagnosis of liver injury after blunt abdominal trauma. Exp Ther Med. 2012; 4(2):255–260. Epub 2012/11/10. doi: 10.3892/etm.2012.575 PMID: 23139714; PubMed Central PMCID: PMCPMC3460295.

63. Rajmane Y, Shaikh S, Basha K, Reddy GE, Nair S, Kamath S, et al. Infant mouse brain passaged Dengue serotype 2 virus induces non-neurological disease with inflammatory spleen collapse in AG129 mice after splenic adaptation. Virus Res. 2013; 173(2):386–397. doi: 10.1016/j.virusres.2013.01.002 PMID: 23337909.

64. Sarathy VV, White M, Li L, Gorder SR, Pyles RB, Campbell GA, et al. A Lethal Murine Infection Model for Dengue Virus 3 in AG129 Mice Deficient in Type I and II Interferon Receptors Leads to Systemic Disease. J Virol. 2015; 89(2):1254–1266. doi: 10.1128/JVI.01320-14 PMID: 25392217.

65. Sridharan A, Chen Q, Tang KF, Ooi EE, Hibberd ML, Chen J. Inhibition of megakaryocyte development in the bone marrow underlies dengue virus-induced thrombocytopenia in humanized mice. J Virol. 2013; 87(21):11648–11658. doi: 10.1128/JVI.01156-13 PMID: 23966397; PubMed Central PMCID: PMC3807371.

66. Guabiraba R, Marques RE, Besnard AG, Fagundes CT, Souza DG, Ryffel B, et al. Role of the chemokine receptors CCR1, CCR2 and CCR4 in the pathogenesis of experimental dengue infection in mice. PLoS One. 2010; 5(12):e15680. doi: 10.1371/journal.pone.0015680 PMID: 21206747; PubMed Central PMCID: PMC3012079.

67. Binh PT, Matheus S, Huong VT, Deparis X, Marechal V. Early clinical and biological features of severe clinical manifestations of dengue in Vietnamese adults. J Clin Virol. 2009; 45(4):276–280. doi: 10.1016/j.jcv.2009.04.004 PMID: 19451025.

68. Butt N, Abbassi A, Munir SM, Ahmad SM, Sheikh QH. Haematological and biochemical indicators for the early diagnosis of dengue viral infection. J Coll Physicians Surg Pak. 2008; 18(5):282–285. 05.2008/JCPSP.282285. PMID: 18541082.

69. Kalayanarooj S, Nimmannitya S. Clinical presentations of dengue hemorrhagic fever in infants compared to children. J Med Assoc Thai. 2003; 86 Suppl 3:S673–680. PMID: 14700166.

70. Kuo CH, Tai DI, Chang-Chien CS, Lan CK, Chiou SS, Liaw YF. Liver biochemical tests and dengue fever. Am J Trop Med Hyg. 1992; 47(3):265–270. PMID: 1355950.

71. Nguyen TL, Nguyen TH, Tieu NT. The impact of dengue haemorrhagic fever on liver function. Res Virol. 1997; 148(4):273–277. PMID: 9272578.

72. Wu A, Slavin G, Levi AJ. Elevated serum gamma-glutamyl-transferase (transpeptidase) and histological liver damage in alcoholism. Am J Gastroenterol. 1976; 65(4):318–323. PMID: 7137.

73. French SW, Bardag-Gorce F, French BA, Li J, Oliva J. The role of innate immunity in the pathogenesis of preneoplasia in drug-induced chronic hepatitis based on a mouse model. Exp Mol Pathol. 2011; 91(3):653–659. Epub 2011/09/29. doi: 10.1016/j.yexmp.2011.07.004 PMID: 21820428; PubMed Central PMCID: PMCPMC3482129.

74. Ling LM, Wilder-Smith A, Leo YS. Fulminant hepatitis in dengue haemorrhagic fever. J Clin Virol. 2007; 38(3):265–268. Epub 2007/02/20. doi: 10.1016/j.jcv.2006.12.011 PMID: 17306619.

75. Povoa TF, Alves AM, Oliveira CA, Nuovo GJ, Chagas VL, Paes MV. The pathology of severe dengue in multiple organs of human fatal cases: histopathology, ultrastructure and virus replication. PLoS One. 2014; 9(4):e83386. doi: 10.1371/journal.pone.0083386 PMID: 24736395; PubMed Central PMCID: PMC3987999.

76. Barreto DF, Takiya CM, Paes MV, Farias-Filho J, Pinhao AT, Alves AM, et al. Histopathological aspects of Dengue-2 virus infected mice tissues and complementary virus isolation. J Submicrosc Cytol Pathol. 2004; 36(2):121–130. PMID: 15554498.

77. Villar LA, Gelvez RM, Rodriguez JA, Salgado D, Parra B, Osorio L, et al. [Biomarkers for the prognosis of severe dengue]. Biomedica. 2013; 33 Suppl 1:108–116. PMID: 24652255.

78. Arias J, Valero N, Mosquera J, Montiel M, Reyes E, Larreal Y, et al. Increased expression of cytokines, soluble cytokine receptors, soluble apoptosis ligand and apoptosis in dengue. Virology. 2014; 452–453:42–51. doi: 10.1016/j.virol.2013.12.027 PMID: 24606681.

79. Cardier JE, Marino E, Romano E, Taylor P, Liprandi F, Bosch N, et al. Proinflammatory factors present in sera from patients with acute dengue infection induce activation and apoptosis of human microvascular endothelial cells: possible role of TNF-alpha in endothelial cell damage in dengue. Cytokine. 2005; 30(6):359–365. PMID: 15935956.

80. Fernandez-Mestre MT, Gendzekhadze K, Rivas-Vetencourt P, Layrisse Z. TNF-alpha-308A allele, a possible severity risk factor of hemorrhagic manifestation in dengue fever patients. Tissue Antigens. 2004; 64(4):469–472. doi: 10.1111/j.1399-0039.2004.00304.x PMID: 15361124.

81. Suksanpaisan L, Cabrera-Hernandez A, Smith DR. Infection of human primary hepatocytes with dengue virus serotype 2. J Med Virol. 2007; 79(3):300–307. doi: 10.1002/jmv.20798 PMID: 17245728.

82. Zickovich JM, Meyer SI, Yagita H, Obar JJ. Agonistic anti-CD40 enhances the CD8+ T cell response during vesicular stomatitis virus infection. PLoS One. 2014; 9(8):e106060. doi: 10.1371/journal.pone.0106060 PMID: 25166494; PubMed Central PMCID: PMC4148391.

83. Hashem AM, Gravel C, Chen Z, Yi Y, Tocchi M, Jaentschke B, et al. CD40 ligand preferentially modulates immune response and enhances protection against influenza virus. J Immunol. 2014; 193(2): 722–734. doi: 10.4049/jimmunol.1300093 PMID: 24928989.

84. Otahal P, Knowles BB, Tevethia SS, Schell TD. Anti-CD40 conditioning enhances the T(CD8) response to a highly tolerogenic epitope and subsequent immunotherapy of simian virus 40 T antigen-induced pancreatic tumors. J Immunol. 2007; 179(10):6686–6695. PMID: 17982058.

85. Sitati E, McCandless EE, Klein RS, Diamond MS. CD40-CD40 ligand interactions promote trafficking of CD8+ T cells into the brain and protection against West Nile virus encephalitis. J Virol. 2007; 81(18):9801–9811. doi: 10.1128/JVI.00941-07 PMID: 17626103; PubMed Central PMCID: PMC2045405.

86. Sun P, Celluzzi CM, Marovich M, Subramanian H, Eller M, Widjaja S, et al. CD40 ligand enhances dengue viral infection of dendritic cells: a possible mechanism for T cell-mediated immunopathology. J Immunol. 2006; 177(9):6497–6503. Epub 2006/10/24. PMID: 17056582.

87. Torrentes-Carvalho A, Azeredo EL, Reis SR, Miranda AS, Gandini M, Barbosa LS, et al. Dengue-2 infection and the induction of apoptosis in human primary monocytes. Mem Inst Oswaldo Cruz. 2009; 104(8):1091–1099. PMID: 20140369.

88. de Miranda AS, Rodrigues DH, Amaral DC, de Lima Campos RD, Cisalpino D, Vilela MC, et al. Dengue-3 encephalitis promotes anxiety-like behavior in mice. Behav Brain Res. 2012; 230(1): 237–242. doi: 10.1016/j.bbr.2012.02.020 PMID: 22366269.

89. Vasquez Ochoa M, Garcia Cordero J, Gutierrez Castaneda B, Santos Argumedo L, Villegas Sepulveda N, Cedillo Barron L. A clinical isolate of dengue virus and its proteins induce apoptosis in HMEC-1 cells: a possible implication in pathogenesis. Arch Virol. 2009; 154(6):919–928. doi: 10.1007/s00705-009-0396-7 PMID: 19440830.

90. Vincenzo D, Morabito V, Andreola F, Pieri G, Luong TV, Dhillon A, et al. Mechanism of cell-death in acute on chronic liver failure: A clinico-pathologic-biomarker study. Liver Int. 2015. doi: 10.1111/liv.12850.

91. Chuturgoon AA, Phulukdaree A, Moodley D. Fumonisin B inhibits apoptosis in HepG2 cells by inducing Birc-8/ILP-2. Toxicol Lett. 2015; 235(2):67–74. PMID: 25800559.

92. Sheng M, Zhou Y, Yu W, Weng Y, Xu R, Du H. Protective effect of berberine pretreatment in hepatic ischemia/reperfusion injury of rat. Transplant Proc. 2015; 47(2):275–282. doi: 10.1016/j.transproceed.2015.01.010 PMID: 25769560.

93. Zhang F, Wang X, Qiu X, Wang J, Fang H, Wang Z, et al. The protective effect of esculentoside a on experimental acute liver injury in mice. PLoS One. 2014; 9(11):e113107. doi: 10.1371/journal.pone.0113107 PMID: 25405982; PubMed Central PMCID: PMC4236201.

94. Lim EJ, El Khobar K, Chin R, Earnest-Silveira L, Angus PW, Bock CT, et al. Hepatitis C virus-induced hepatocyte cell death and protection by inhibition of apoptosis. J Gen Virol. 2014; 95(Pt 10): 2204–2215. doi: 10.1099/vir.0.065862-0 PMID: 24973240.

95. Klomporn P, Panyasrivanit M, Wikan N, Smith DR. Dengue infection of monocytic cells activates ER stress pathways, but apoptosis is induced through both extrinsic and intrinsic pathways. Virology. 2011; 409(2):189–197. Epub 2010/11/05. doi: 10.1016/j.virol.2010.10.010 PMID: 21047664.

96. Malavige GN, Huang LC, Salimi M, Gomes L, Jayaratne SD, Ogg GS. Cellular and cytokine correlates of severe dengue infection. PLoS One. 2012; 7(11):e50387. Epub 2012/12/05. doi: 10.1371/journal.pone.0050387 PMID: 23209731; PubMed Central PMCID: PMCPMC3510251.

97. Green S, Vaughn DW, Kalayanarooj S, Nimmannitya S, Suntayakorn S, Nisalak A, et al. Elevated plasma interleukin-10 levels in acute dengue correlate with disease severity. J Med Virol. 1999; 59(3):329–334. PMID: 10502265.

98. Juffrie M, Meer GM, Hack CE, Haasnoot K, Sutaryo, Veerman AJ, et al. Inflammatory mediators in dengue virus infection in children: interleukin-6 and its relation to C-reactive protein and secretory phospholipase A2. Am J Trop Med Hyg. 2001; 65(1):70–75. PMID: 11504411.

99. Lee YR, Su CY, Chow NH, Lai WW, Lei HY, Chang CL, et al. Dengue viruses can infect human primary lung epithelia as well as lung carcinoma cells, and can also induce the secretion of IL-6 and RANTES. Virus Res. 2007; 126(1–2):216–225. Epub 2007/04/10. doi: 10.1016/j.virusres.2007.03.003 PMID: 17416433.

100. Rattanaburee T, Junking M, Panya A, Sawasdee N, Songprakhon P, Suttitheptumrong A, et al. Inhibition of dengue virus production and cytokine/chemokine expression by ribavirin and compound A. Antiviral Res. 2015; 124:83–92. Epub 2015/11/07. doi: 10.1016/j.antiviral.2015.10.005 PMID: 26542647.

101. Khunchai S, Junking M, Suttitheptumrong A, Kooptiwut S, Haegeman G, Limjindaporn T, et al. NF-kappaB is required for dengue virus NS5-induced RANTES expression. Virus Res. 2015; 197:92–100. Epub 2014/12/20. PMID: 25523420.

102. Kumar S, Jiang MS, Adams JL, Lee JC. Pyridinylimidazole compound SB 203580 inhibits the activity but not the activation of p38 mitogen-activated protein kinase. Biochem Biophys Res Commun. 1999; 263(3):825–831. doi: 10.1006/bbrc.1999.1454 PMID: 10512765.

103. Ashraf MI, Ebner M, Wallner C, Haller M, Khalid S, Schwelberger H, et al. A p38MAPK/MK2 signaling pathway leading to redox stress, cell death and ischemia/reperfusion injury. Cell Commun Signal. 2014; 12:6. doi: 10.1186/1478-811X-12-6 PMID: 24423080; PubMed Central PMCID: PMC3896752.

104. Reimold AM, Kim J, Finberg R, Glimcher LH. Decreased immediate inflammatory gene induction in activating transcription factor-2 mutant mice. Int Immunol. 2001; 13(2):241–248. PMID: 11157857.

105. Rahaus M, Desloges N, Wolff MH. Replication of varicella-zoster virus is influenced by the levels of JNK/SAPK and p38/MAPK activation. J Gen Virol. 2004; 85(Pt 12):3529–3540. doi: 10.1099/vir.0.80347-0 PMID: 15557226.

106. Kan H, Xie Z, Finkel MS. p38 MAP kinase-mediated negative inotropic effect of HIV gp120 on cardiac myocytes. Am J Physiol Cell Physiol. 2004; 286(1):C1–7. doi: 10.1152/ajpcell.00059.2003 PMID: 14660488.

107. Gusev NB, Bogatcheva NV, Marston SB. Structure and properties of small heat shock proteins (sHsp) and their interaction with cytoskeleton proteins. Biochemistry (Mosc). 2002; 67(5):511–519. PMID: 12059769.

108. Hsu YL, Shi SF, Wu WL, Ho LJ, Lai JH. Protective roles of interferon-induced protein with tetratricopeptide repeats 3 (IFIT3) in dengue virus infection of human lung epithelial cells. PLoS One. 2013; 8(11):e79518. doi: 10.1371/journal.pone.0079518 PMID: 24223959; PubMed Central PMCID: PMC3817122.

109. Singh D, McCann KL, Imani F. MAPK and heat shock protein 27 activation are associated with respiratory syncytial virus induction of human bronchial epithelial monolayer disruption. Am J Physiol Lung Cell Mol Physiol. 2007; 293(2):L436–445. doi: 10.1152/ajplung.00097.2007 PMID: 17557802; PubMed Central PMCID: PMC2231338.

110. Srikiatkhachorn A, Spiropoulou CF. Vascular events in viral hemorrhagic fevers: a comparative study of dengue and hantaviruses. Cell Tissue Res. 2014; 355(3):621–633. Epub 2014/03/14. doi: 10.1007/s00441-014-1841-9 PMID: 24623445; PubMed Central PMCID: PMCPMC3972431.

111. Halstead SB. Dengue vascular permeability syndrome: what, no T cells? Clin Infect Dis. 2013; 56(6): 900–901. Epub 2012/12/18. doi: 10.1093/cid/cis1047 PMID: 23243186.

112. Limonta D, Torres G, Capo V, Guzman MG. Apoptosis, vascular leakage and increased risk of severe dengue in a type 2 diabetes mellitus patient. Diab Vasc Dis Res. 2008; 5(3):213–214. Epub 2008/09/09. doi: 10.3132/dvdr.2008.034 PMID: 18777495.

113. Avirutnan P, Punyadee N, Noisakran S, Komoltri C, Thiemmeca S, Auethavornanan K, et al. Vascular leakage in severe dengue virus infections: a potential role for the nonstructural viral protein NS1 and complement. J Infect Dis. 2006; 193(8):1078–1088. Epub 2006/03/18. doi: 10.1086/500949 PMID: 16544248.

Antiviral Research 141 (2017) 7–18

Contents lists available at ScienceDirect

Antiviral Research

journal homepage: www.elsevier.com/locate/antiviral

JNK1/2 inhibitor reduces dengue virus-induced liver injury

Gopinathan Pillai Sreekanth [a, b], Aporn Chuncharunee [a], Boonyarit Cheunsuchon [c], Sansanee Noisakran [d], Pa-thai Yenchitsomanus [b], Thawornchai Limjindaporn [a, b, *]

[a] Department of Anatomy, Faculty of Medicine Siriraj Hospital, Mahidol University, Bangkok, Thailand
[b] Division of Molecular Medicine, Department of Research and Development, Faculty of Medicine Siriraj Hospital, Mahidol University, Bangkok, Thailand
[c] Department of Pathology, Faculty of Medicine Siriraj Hospital, Mahidol University, Bangkok, Thailand
[d] Medical Biotechnology Research Unit, National Center for Genetic Engineering and Biotechnology, National Science and Technology Development Agency, Bangkok, Thailand

ARTICLE INFO

Article history:
Received 1 November 2016
Received in revised form
26 January 2017
Accepted 5 February 2017
Available online 7 February 2017

Keywords:
Dengue virus
JNK
Liver injury
Apoptosis
SP600125

ABSTRACT

High viral load with liver injury is exhibited in severe dengue virus (DENV) infection. Mitogen activated protein kinases (MAPKs) including ERK1/2 and p38 MAPK were previously found to be involved in the animal models of DENV-induced liver injury. However, the role of JNK1/2 signaling in DENV-induced liver injury has never been investigated. JNK1/2 inhibitor, SP600125, was used to investigate the role of JNK1/2 signaling in the BALB/c mouse model of DENV-induced liver injury. SP600125-treated DENV-infected mice ameliorated leucopenia, thrombocytopenia, hemoconcentration, liver transaminases and liver histopathology. DENV-induced liver injury exhibited induced phosphorylation of JNK1/2, whereas SP600125 reduced this phosphorylation. An apoptotic real-time PCR array profiler was used to screen how SP600125 affects the expression of 84 cell death-associated genes to minimize DENV-induced liver injury. Modulation of caspase-3, caspase-8 and caspase-9 expressions by SP600125 in DENV-infected mice suggests its efficiency in restricting apoptosis via both extrinsic and intrinsic pathways. Reduced expressions of TNF-α and TRAIL are suggestive to modulate the extrinsic apoptotic signals, where reduced p53 phosphorylation and induced anti-apoptotic Bcl-2 expression indicate the involvement of the intrinsic apoptotic pathway. This study thus demonstrates the pivotal role of JNK1/2 signaling in DENV-induced liver injury and how SP600125 modulates this pathogenesis.

1. Introduction

Dengue virus (DENV) infection is one of the most important arbo-viral diseases of the 21st century, most prevalent in tropical and sub-tropical countries (Gubler, 2002). DENV-infected patients show different levels of disease severity; dengue fever, dengue hemorrhagic fever, or the most severe dengue shock syndrome. The hemorrhage signs of DENV infection are represented by plasma leakage and hematologic disorders. Severe infection may lead to hypovolemic shock in DENV infection (Halstead, 2007) with multiple organ injuries (Ghosh et al., 2011; Schmitz et al., 2011).

Liver injury is reported in severe DENV-infected patients (Trung et al., 2010) where apoptosis is evident (Limonta et al., 2007). Elevated alanine transaminase (ALT) and aspartate transaminase (AST) are observed in the patients (Arora et al., 2015; Nguyen et al., 1997; Treeprasertsuk and Kittitrakul, 2015) and animal models (Franca et al., 2010; Paes et al., 2005, 2009; Sreekanth et al., 2016; Sreekanth et al., 2014) of DENV infection. Histopathology correlated with transaminase level is used to understand the severity of liver injury (de Macedo et al., 2006; Huerre et al., 2001). Histopathology of DENV-induced liver injury in Balb/C mice was thoroughly studied (Sakinah et al., 2016). DENV infection induces apoptosis in HepG2 cells (Morchang et al., 2011; Thepparit et al., 2013; Thongtan et al., 2004). DENV infection undergoes apoptosis via activated caspase-8 (Liao et al., 2010), and overexpression of pro-inflammatory cytokines and chemokines including TNF-α, IL-8 and RANTES leads to vascular permeability in DENV-infected patients (Chareonsirisuthigul et al., 2007; Pang et al., 2007). DENV-induced TNF-α mediates apoptosis (Cardier et al., 2005), and TNF-related apoptosis-inducing ligand (TRAIL) modulates type I and

* Corresponding author. Department of Anatomy, Faculty of Medicine Siriraj Hospital, Mahidol University, Bangkok 10700, Thailand. Tel.: +66 2 419 2754; fax: +66 2 411 0169.
E-mail address: thawornchai.lim@mahidol.ac.th (T. Limjindaporn).

http://dx.doi.org/10.1016/j.antiviral.2017.02.003
0166-3542/

type II interferon responses (Warke et al., 2008). The role of p53 in cellular functions including apoptosis is studied (Yan et al., 2016). The anti-apoptotic protein Bcl-2 depletion promotes death signals in DENV-infected HepG2 cells via the mitochondrial pathway of apoptosis (Catteau et al., 2003).

Mitogen-activated protein kinases (MAPKs) including p38 MAPK, JNK (c-Jun N-terminal kinase) and ERK1/2 (Extracellular-signal Regulated Kinase) are involved in apoptosis and cytokine responses. Phosphorylation of ERK1/2 and p38 induces liver injury in DENV-infected mice and treatments with ERK1/2 and p38 inhibitors minimized the liver injury (Sreekanth et al., 2014, 2016). JNK, the stress-activated protein kinase, is phosphorylated during inflammatory responses and an anthrapyrazolone inhibitor of JNK1/2, SP600125 was reported to inhibit this phosphorylation (Bennett et al., 2001). JNK phosphorylation is vital for DENV infection in human monocyte-derived macrophages (Ceballos-Olvera et al., 2010). However, the role of JNK1/2 in animal models of DENV-induced liver injury has never been investigated. We therefore investigated the effect of SP600125 on the inhibition of JNK1/2 and its molecular signaling in DENV-induced liver injury.

2. Materials and methods

2.1. Mouse infection, SP600125 treatment and sample collection

Male BALB/c mice were purchased from National Laboratory Animal Center (NLAC), Mahidol University, Thailand, and experiments were performed in compliance with ethics principles and institutional policies, with the protocol approved by the Siriraj Animal Care and Use Committee, Mahidol University (SI-ACUP 004/2556) and Siriraj Biosafety Risk Management Taskforce, Mahidol University (SI-2013-11). Eight week-old mice were infected with 4×10^5 FFU of DENV-2 (Strain 16881) intravenously via lateral tail vein. An un-infected group of mice is maintained with 2%-dimethyl sulfoxide (DMSO) treatment via the same route. DENV-infected mice were treated with 2%-DMSO (v/v) or SP600125 (dose of 20 mg/kg dissolved in 2%-DMSO). The volume of all injections was 0.4 ml and the SP600125 treatment was given 1 h before and 1 h and 24 h after DENV-infection. Blood samples were collected on both day 3 and 7 for serum preparations. At day 7 post-infection, the mice were euthanized with an intraperitoneal injection of sodium pentobarbital and liver tissues were collected and stored. For a total of three groups, six mice per group were challenged. Two independent experiments were conducted with a total of 36 mice.

2.2. DENV-NS1 viral RNA quantification and focus forming unit (FFU) assay

RNA was extracted from the serum and livers of uninfected, DENV-infected, and DENV-infected and SP600125-treated mice. DENV-NS1 viral RNA was quantified by real-time quantitative reverse transcription polymerase chain reaction (qRT-PCR) using specific primers as previously described (Sreekanth et al., 2016). For FFU assay, liver tissues were homogenized in RPMI medium and centrifuged at 6000×*g* for 5 min repeatedly till clear supernatants were obtained. Supernatants were filter-sterilized for standard FFU assay (Jirakanjanakit et al., 1997).

Table 1
The specific primer set for each individual gene of interest.

Primer	Gene description
TNF-α F	5′ CCC CCA GTC TGT ATC CTT CT 3′
TNF-α R	5′ TTT GAG TCC TTG ATG GTG GT 3′
TRAIL F	5′ GAT GTT GGT GCC TGG AGT TT 3′
TRAIL R	5′ AAG CAA AGG GCA GAA AGT CA 3′
GAPDH F	5′ TGA ATA CGG CTA CAG CAA CA 3′
GAPDH R	5′ AGG CCC CTC CTG TTA TTA TG 3′

2.3. Histopathology and immunohistochemistry

Liver tissues were fixed in 10% formalin and paraffin embedded. Hematoxylin and eosin (H&E) staining was conducted for histopathology. The paraffin embedded liver tissues were allowed for standard immunohistochemistry staining with DENV-E antigen as previously mentioned (Aye et al., 2014).

2.4. Apoptotic mRNA expression profiler

RNA samples extracted from the liver tissues were converted to cDNA using SuperScript® III First-Strand Synthesis System (Invitrogen). The cDNA was further mixed with SYBR Green RT^2 qPCR Mastermix (Qiagen), and were aliquoted into the Mouse Apoptosis RT^2 Profiler™ PCR Array (Qiagen) containing 84 apoptosis related genes. The PCR amplification steps were performed in a Roche LightCycler 480 instrument and Ct values were copied and uploaded to the web program http://pcrdataanalysis.sabiosciences.com/pcr/arrayanalysis.php for $2^{-\Delta\Delta Ct}$ analysis using β-actin as housekeeping gene control. The results were presented as fold increased or decreased compared to those of the uninfected group of mice.

2.5. Expression of pro-inflammatory cytokines by real-time RT-PCR

RNA samples were prepared from the liver tissues and reverse transcribed to cDNA, allowed to mix with LightCycler® 480 SYBR Green Mastermix (Invitrogen) and the specific primer set for each individual gene of interest (Table 1). The reactions were allowed to run in a Roche LightCycler 480 instrument for the Ct values. GAPDH (house-keeping gene control) was used to normalize the Ct values. The results were further analyzed by $2^{-\Delta\Delta Ct}$ analysis and the expressions were represented as fold increased or decreased.

2.6. Western blot analysis

Proteins from the livers were extracted in protease inhibitor premixed RIPA buffer and a cocktail of phosphatase inhibitor was added to detect phosphorylated proteins. Bradford assay (Bio-Rad Laboratories) was used to estimate the protein concentration. Proteins were separated with SDS-PAGE, blotted onto nitrocellulose membrane and further blocked with 5%-BSA or 5%-skim milk. Membranes were incubated overnight with rabbit anti-total JNK1/2 or mouse anti-phosphorylated JNK1/2 or rabbit anti-total p53 or rabbit anti-phosphorylated p53 (ser15) or rabbit anti-total p38 MAPK or mouse anti-phosphorylated p38 MAPK or mouse anti-total ERK1/2 or rabbit anti-phosphorylated ERK1/2 or goat anti-TNF-α or rabbit anti-caspase-8 or mouse anti-caspase-9 or goat anti-pro caspase-3 or rabbit anti-cleaved caspase-3 or rabbit anti-

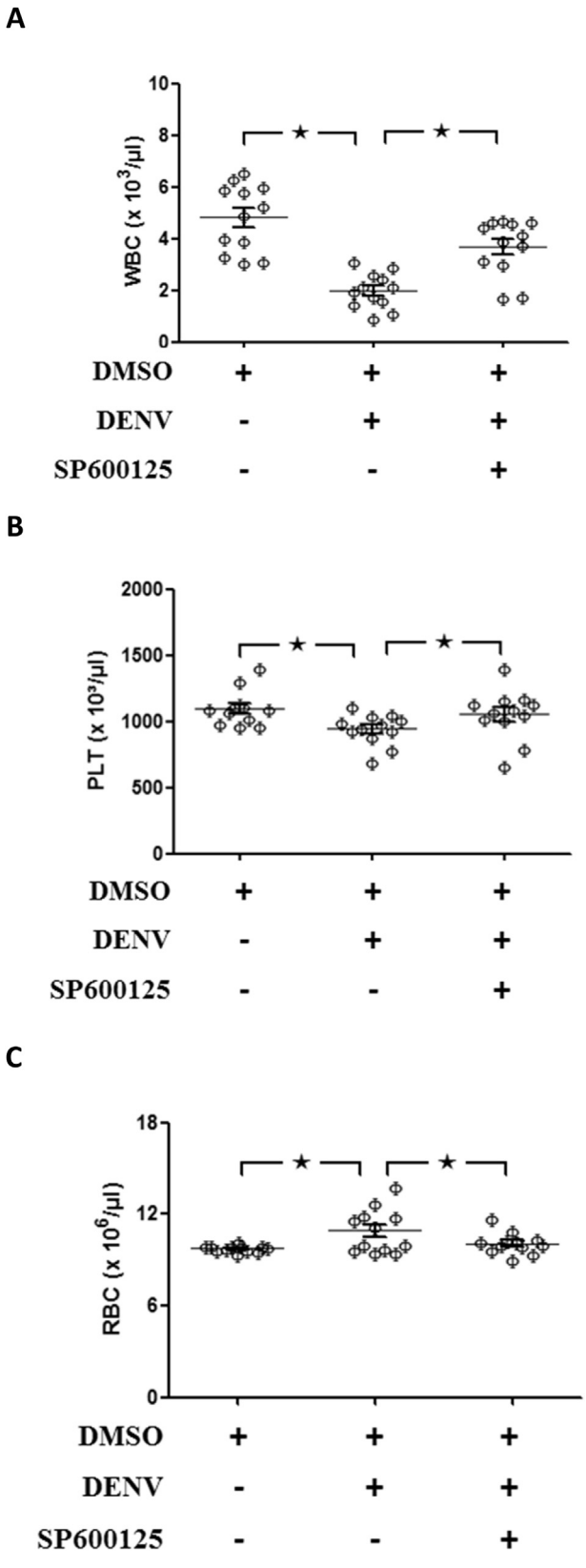

Fig. 1. SP600125 treatment modulated the hematology of DENV-infected mice. Balb/c mice were infected with 4×10^5 FFU/ml of DENV and treated with 2% DMSO alone or SP600125 dissolved in 2% DMSO. The uninfected 2% DMSO alone treated control group was also maintained. Seven-day post infection; blood sample was collected for hematological analysis. (A) WBC (B) PLT and (C) RBC. The results were obtained from two independent experiments and the values were pooled together as Mean ± SEM (12 mice per individual group from two independent experiments). The asterisks indicate statistically significant differences between groups ($p < 0.05$).

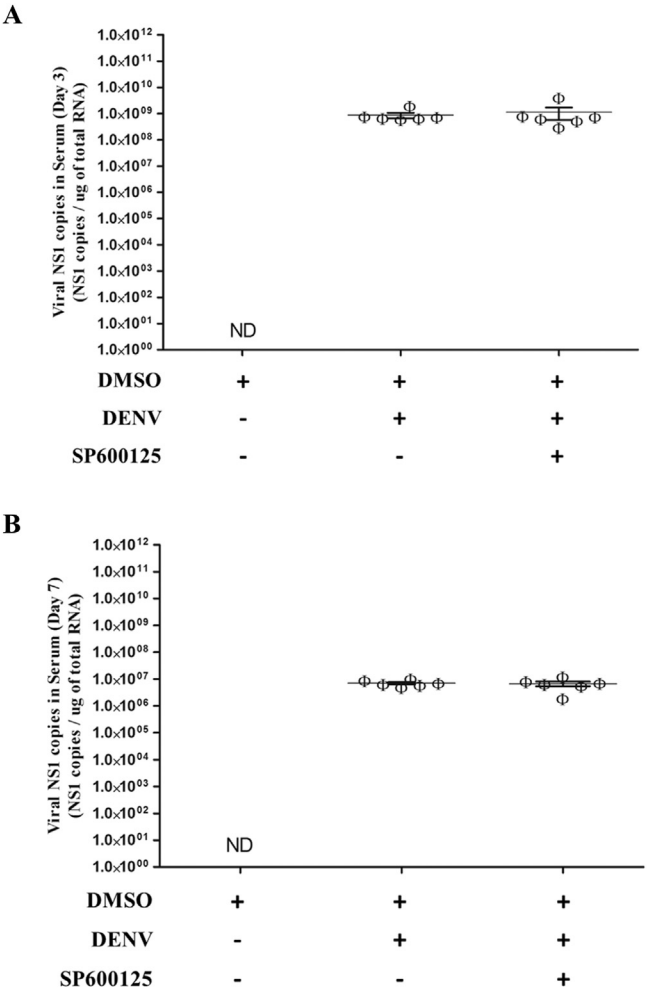

Fig. 2. SP600125 treatment did not reduce DENV in the serum. Mice were infected with 4×10^5 FFU/ml of DENV and treated with 2% DMSO or SP600125 dissolved in 2% DMSO. An uninfected 2% DMSO alone treated control group was also maintained. Blood was collected on three and seven-day post infection, serum was prepared and DENV-NS1 was quantified. Viral NS1 copies in the serum on (A) Day 3 and (B) Day 7 is shown. Results were obtained from six animals from each group (n = 6). ND shows Not Detected.

Bcl-2 which were purchased from either Cell Signaling Technology or Santa Cruz Biotechnology. The membrane was further incubated for 1 h in the dark at room temperature with horseradish peroxidase (HRP)-conjugated secondary antibody. For the blots with a primary antibody generated from rabbit, mouse, and goat, the secondary antibodies were HRP-conjugated swine anti-rabbit IgG antibody, HRP-conjugated rabbit anti-mouse IgG antibody and HRP-conjugated rabbit anti-goat IgG antibody (Dako, Santa Clara, CA, USA), respectively. The immune complexes were detected by enhanced chemiluminescence (SuperSignal West Pico Chemiluminescent Substrate; Thermo Scientific, Waltham, MA, USA). GAPDH was used as the housekeeping gene control and the results were represented from at least three independent mice from each group. Densitometry analysis normalized with GAPDH was conducted using ImageJ software (National Institutes of Health, Bethesda, MD, USA).

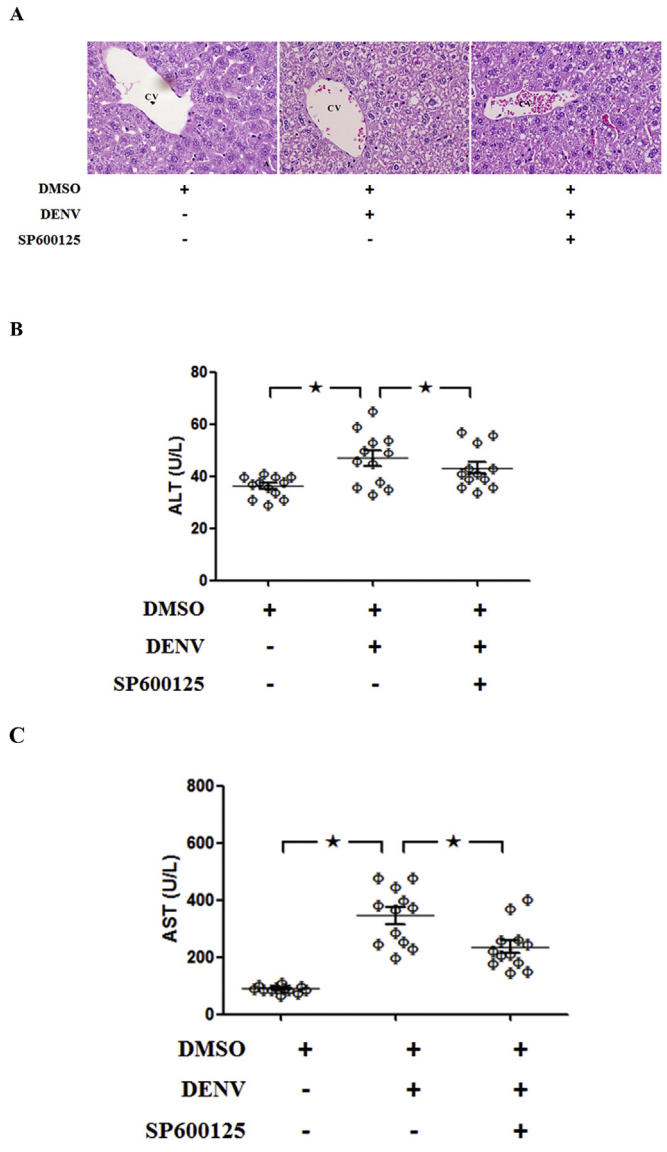

Fig. 3. SP600125 treatment minimized the DENV-induced liver injury. Mice were infected with 4 × 10^5 FFU/ml of DENV and treated with 2% DMSO or SP600125 dissolved in 2% DMSO. An uninfected 2% DMSO alone treated control group was also maintained. Seven-day post infection; blood was collected for serum preparations and liver tissues were fixed in 10% Formalin for histopathology analysis and H&E Staining. (A) Histopathology analysis (B) ALT and (C) AST is shown. For (A), the result shown is a representative of ≥3 independent mice from individual group. For (B) and (C), the results were obtained from two independent experiments and the values were pooled together as Mean ± SEM (12 mice per individual group from two independent experiments). The asterisks indicate statistically significant differences between groups ($p < 0.05$).

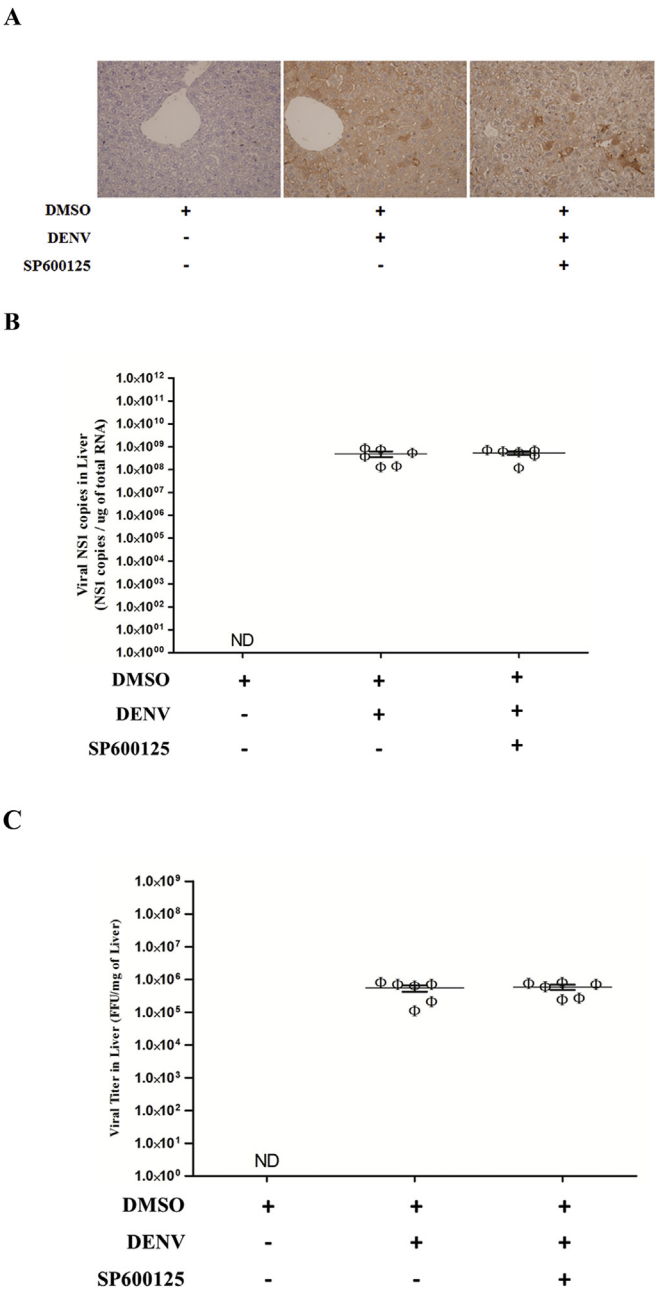

Fig. 4. SP600125 treatment did not reduce DENV in the liver. Mice were infected with 4 × 10^5 FFU/ml of DENV and treated with 2% DMSO or SP600125 dissolved in 2% DMSO. An uninfected 2% DMSO alone treated control group was also maintained. Seven-day post infection, animals were sacrificed, liver tissues were harvested and stored. (A) Immunohistochemistry staining with DENV-E antigen (B) DENV-NS1 quantification and (C) FFU assay is shown. Results were obtained from six animals from each group (n = 6). ND shows Not Detected.

2.7. Statistical analysis

The results were analyzed by either One-Way ANOVA or unpaired *t*-test, using GraphPad Prism Software and represented as mean ± SEM. The p value less than 0.05 was considered to be statistically significant difference between groups ($p < 0.05$).

3. Results

3.1. SP600125, improved hematology parameters in DENV-infected mice

Mice were infected with DENV-2 intravenously and 2%-DMSO or SP600125 treatments were given intravenously. An un-

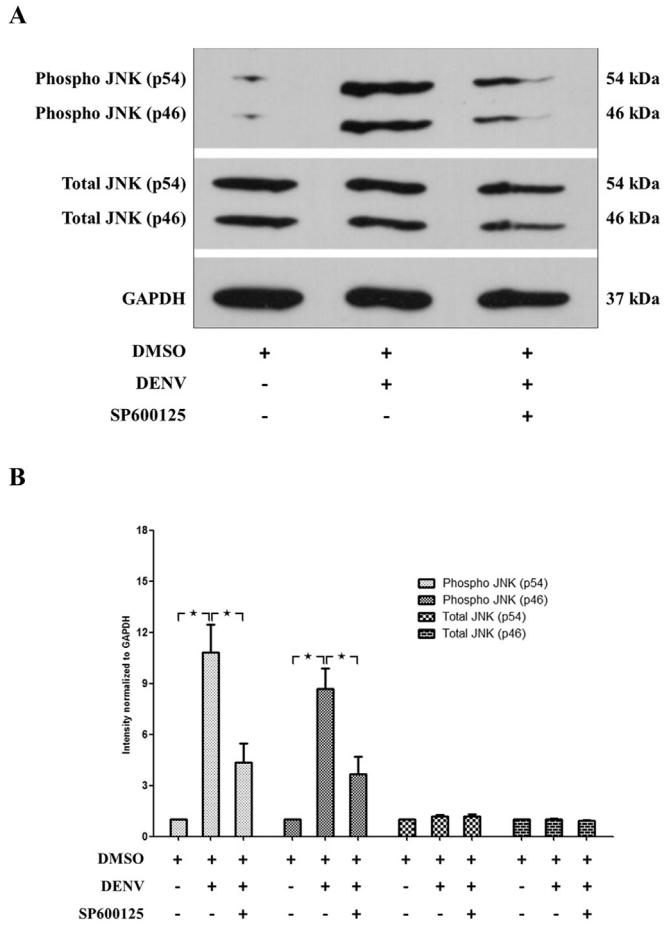

Fig. 5. SP600125 treatment reduced the phosphorylation of JNK in the liver of DENV-infected mice. Mice were infected with DENV at a dose of 4×10^5 FFU and treated with 2% DMSO (v/v) or SP600125 in 2% DMSO. The un-infected control group of 2% DMSO (v/v) alone was also maintained. At day 7 post infection, liver tissues were harvested, homogenized for protein preparation and Western blot analysis. GAPDH was used as the housekeeping gene. Results shown are representative from 3 independent experiments from 3 independent mice (n = 3) for each group. Densitometry analysis was conducted for individual blots and normalized with GAPDH. (A) Western blot analysis of phosphorylated JNK1/2 and total JNK1/2 normalized to GAPDH (B) Densitometry analysis of phosphorylated JNK1/2 and total JNK1/2.

Table 2
The selected apoptosis-related gene expression profile normalized to β-actin before and after SP600125 treatment.

Gene Name	Gene description	Fold times to DMSO (uninfected)	
		DMSO + DENV	DENV + SP600125
Aifm1	Apoptosis-inducing factor, mitochondrion-associated 1	4.6935	2.5315
Apaf1	Apoptotic peptidase activating factor 1	5.9053	1.8658
Api5	Apoptosis inhibitor 5	0.5476	0.8467
Bax	Bcl2-associated X protein	4.0279	1.6598
Bcl2	B-cell leukemia/lymphoma 2	0.3320	0.6137
Bid	BH3 interacting domain death agonist	1.9453	1.0994
Casp12	Caspase 12	2.9849	1.4044
Casp3	Caspase 3	3.9862	1.9727
Casp7	Caspase 7	1.9096	1.3526
Casp8	Caspase 8	3.0943	2.0867
Casp9	Caspase 9	2.2226	1.3737
Cd40	CD40 antigen	2.6139	1.4506
Cd40lg	CD40 ligand	1.5801	1.2381
Cflar	CASP8 and FADD-like apoptosis regulator	2.9659	1.8827
Cidea	Cell death-inducing DNA fragmentation factor, alpha subunit-like effector A	6.9013	4.4204
Cideb	Cell death-inducing DNA fragmentation factor, alpha subunit-like effector B	2.8950	1.9993
Cradd	CASP2 and RIPK1 domain containing adaptor with death domain	5.8123	1.6373
Dad1	Defender against cell death 1	0.1141	0.8975
Dapk1	Death associated protein kinase 1	3.4641	1.8236
Fadd	Fas (TNFRSF6)-associated via death domain	6.0121	2.7071
Fas	Fas (TNF receptor superfamily member 6)	2.8967	1.3526
Fasl	Fas ligand (TNF superfamily, member 6)	14.5157	5.3404
Il10	Interleukin 10	16.4641	9.9381
Naip1	NLR family, apoptosis inhibitory protein 1	0.5322	3.0525
Naip2	NLR family, apoptosis inhibitory protein 2	0.4340	0.6329
Nfkb1	Nuclear factor of kappa light polypeptide gene enhancer in B-cells 1, p105	2.8351	1.6598
Pycard	PYD and CARD domain containing	3.8701	1.4719
Tnf	Tumor necrosis factor	3.5404	2.0630
Tnfsf10	Tumor necrosis factor (ligand) superfamily, member 10	5.4581	2.0279
Xiap	X-linked inhibitor of apoptosis	0.5692	0.9013

infected 2%-DMSO-treated group of mice was also maintained. All the mice survived the challenge protocol. However, the hematology analysis show decreased white blood cell (WBC) and platelet count in DENV-infected mice compared to that of un-infected mice (Fig. 1A and B). These results suggest that DENV-infected mice exhibited leucopenia and thrombocytopenia, respectively. JNK1/2 inhibitor-SP600125 treatment improved the leucopenia and thrombocytopenia in DENV-infected mice (Fig. 1A and B). In addition, DENV-infected mice exhibited a significant rise in red blood cell (RBC) count and SP600125 reduced it in DENV-infected mice (Fig. 1C).

3.2. SP600125 did not reduce the DENV production in the serum

DENV-NS1 viral RNA from the serum samples (day 3 and day 7) of DENV-infected as well as DENV-infected and SP600125-treated mice were quantified. An *in vitro*-transcribed DENV-NS1 standard with known copy number was ten-fold serially diluted and obtained Ct values were used to plot the standard curve (data not shown). No reduction in the DENV-NS1 copies in the serum collected either on day 3 or day 7 (Fig. 2A and B) was observed upon SP600125 treatment in DENV-infected mice. Although no reduction in DENV between groups of mouse, we observed a significant reduction of virus on day 7 compared to day 3 (Fig. 2A and B).

3.3. SP600125, improved liver injury in DENV-infected mice

Histopathology analysis of DENV-infected mice exhibited signs of liver injury including widespread tumefaction of hepatocytes and focal mononuclear inflammatory cell infiltration in portal triads compared to that of un-infected mice (Fig. 3A). DENV-infected and SP600125-treated mice showed lesser degree of hepatocyte

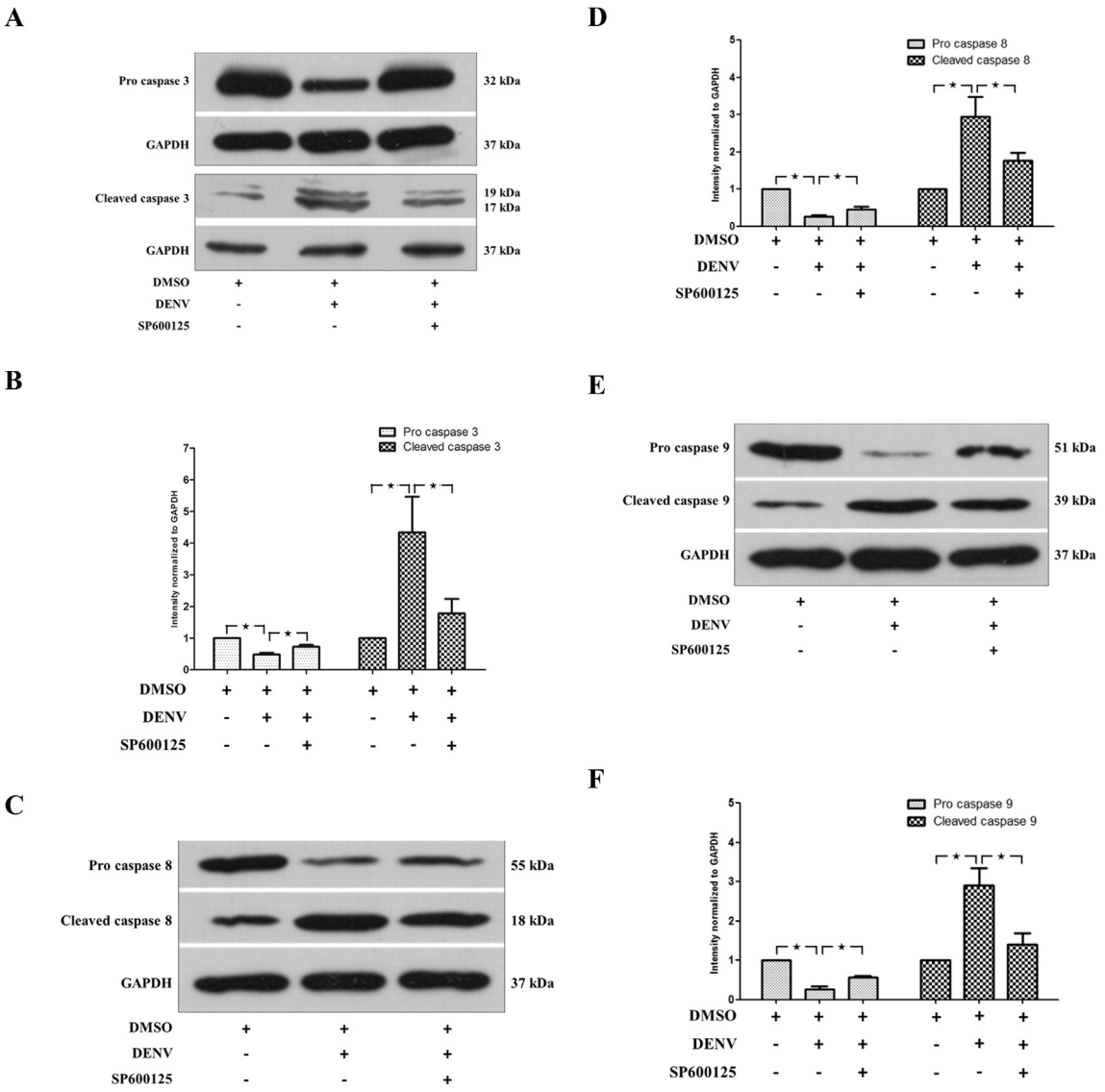

Fig. 6. SP600125 treatment reduced both extrinsic and intrinsic pathways of apoptosis during DENV-induced liver injury. Liver tissues were harvested and proteins were extracted from un-infected control mice of 2% DMSO (v/v) alone treated and from two other groups of mice infected with DENV at a dose of 4×10^5 FFU, those were treated with either 2% DMSO (v/v) or SP600125 dissolved in 2% DMSO (v/v). Western blot analysis and densitometry analysis normalized to GAPDH was conducted. Western blot analysis of (A) Pro-caspase-3 and Cleaved caspase-3 (C) Pro-caspase-8 and Cleaved caspase-8 and (E) Pro-caspase-9 and Cleaved caspase-9. Densitometry analysis of (B) Pro-caspase-3 and Cleaved caspase-3 (D) Pro-caspase-8 and Cleaved caspase-8, and (F) Pro-caspase-9 and Cleaved caspase-9 is shown. Results were represented from at least 3 independent experiments from 3 independent mice (n = 3).

tumefaction (Fig. 3A). The liver transaminases (ALT, AST) were elevated in DENV-infected mice and SP600125 treatment reduced both transaminases (Fig. 3B and C).

3.4. SP600125 did not reduce the DENV production in the liver

DENV-E antigen was detected in the liver of both DENV-infected as well as SP600125-treated DENV-infected mice (Fig. 4A). Immunostaining shows DENV-infected hepatocytes and Kupffer cells. A bundle of positive staining was observed in the spleen compared to that of liver (data not shown). Upon quantification of DENV-NS1, we did not observe any significant reduction of virus in the liver of DENV-infected or SP600125-treated DENV-infected mice (Fig. 4B). FFU assay confirmed that SP600125 treatment in DENV-infected mice did not reduce virus production in the liver on day 7 post-infection (Fig. 4C).

3.5. SP600125 reduced JNK1/2 phosphorylation to decrease DENV-induced liver injury

We investigated how the JNK signaling contributes to liver injury in DENV-infected mice. Western blot analysis shows that the phosphorylated JNK1/2 of DENV-infected mice was higher than that of control mice, while SP600125 treated mice exhibited a

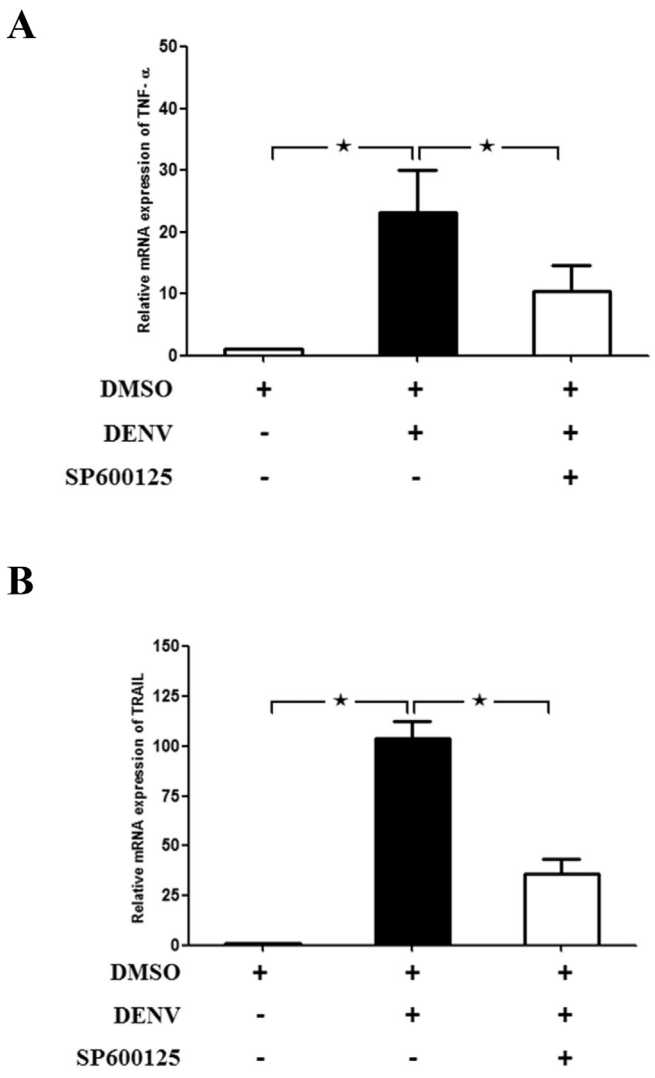

Fig. 7. SP600125 modulated pro-inflammatory cytokines in the liver of DENV-infected mice. Mice were infected with DENV and treated with 2% DMSO or SP600125 dissolved in 2% DMSO. The uninfected 2% DMSO alone treated control group were also maintained. RNA is extracted from the liver tissues which were converted to cDNA and further undergone Real-time RT-PCR analysis using individual set of primer for each gene of interest. GAPDH was used as the house keeping gene. The mRNA expression of (A) TNF-α and (B) TRAIL is represented. Results were obtained from three independent experiments, for 3 independent mice from each group. The asterisks indicate statistically significant differences between groups ($p < 0.05$).

reduced expression of the phosphorylated JNK1/2 (Fig. 5A). No significant change in the total JNK1/2 expressions between groups of mice was observed. Densitometry analysis is shown in Fig. 5B. Our result shows that JNK1/2 phosphorylation induced liver injury in DENV-infected mice, and JNK1/2 inhibitor-SP600125 was able to reduce this phosphorylation.

3.6. SP600125 restricted apoptotic signals in the liver of DENV-infected mice via both extrinsic and intrinsic pathways

To identify the mechanism by which SP600125 reduced liver injury in DENV-infected mice, 84 apoptosis-related gene expression profile normalized to β-actin gene expression was conducted and the most remarkable fold changes are shown in Table 2. A detailed gene expression list is available in Supplementary Table 1.

We further investigated the caspase-3 expression to well-explain the efficacy of SP600125 in inhibiting DENV-induced apoptosis. Reduced pro-caspase-3 and higher cleaved caspase-3 (Fig. 6A) expression were observed in DENV-infected mice. Interestingly, SP600125 treatment reduced the caspase-3 cleavage and existed as pro-form (Fig. 6A). Densitometry analysis is shown in Fig. 6B. The expressions of both pro and active forms of caspase-8 protein were studied to examine the role of SP600125 in the extrinsic pathway of apoptosis. DENV-infected mice exhibited reduced pro and elevated active forms of caspase-8 protein (Fig. 6C). SP600125 could reverse this finding in DENV-infected mice (Fig. 6C). Densitometry analysis is shown in Fig. 6D. Expressions of both pro and active forms of caspase-9 protein were used to investigate the efficiency of SP600125 in regulating the intrinsic pathway of apoptosis. DENV-infected mice presented with reduced pro form of caspase-9 and increased active form of caspase-9, whereas the treatment with SP600125 reversed these situations indicating its inhibition of the intrinsic pathway of apoptosis (Fig. 6E). Densitometry analysis is shown in Fig. 6F.

3.7. SP600125 modulated the pro-inflammatory cytokines in the liver of DENV-infected mice

The mRNA expressions of prominent pro-inflammatory cytokines including TNF-α and TRAIL were investigated by using the primer sets as shown in Table 1. In DENV-infected mice exhibiting liver injury, TNF-α (Fig. 7A) and TRAIL (Fig. 7B), were up-regulated, while SP600125 treatment reduced their expressions. Similarly, the protein expressions of these cytokines in the liver of SP600125-treated mice upon DENV-infection were reduced to those of DENV-infected controls (Fig. 8A–D).

3.8. SP600125 reduced p53 phosphorylation in the liver of DENV-infected mice

The protein expressions of phosphorylated and total forms of p53 were investigated. An increased phosphorylation of p53 in DENV-infected mice (Fig. 9A) was observed, however, upon SP600125 treatment the phosphorylated p53 was decreased (Fig. 9A). No significant change in the total p53 expressions between any groups of mice was observed (Fig. 9A). Densitometry analysis is shown in Fig. 9B.

3.9. SP600125 modulated the anti-apoptotic Bcl-2 expression in the liver of DENV-infected mice

To additionally characterize the intrinsic pathway of apoptosis, the protein expression of Bcl-2 was investigated. DENV-infection in mice reduced the Bcl-2 expression, whereas SP600125 treatment reversed the Bcl-2 expression close to the normal level (Fig. 10A and B).

3.10. SP600125 reduced the phosphorylation of p38 MAPK, but not the phosphorylation of ERK1/2

To insight into the cross reactivity of SP600125 towards other classical MAPKs including p38 MAPK and ERK1/2, western blot analysis was performed. Increased phosphorylation of p38 MAPK was observed in DENV-infected mice and SP600125 treatment could reduce this phosphorylation (Fig. 11A and B). However, no reduction in the ERK1/2 phosphorylation was seen upon SP600125 treatment in DENV-infected mice suggesting its inefficiency to

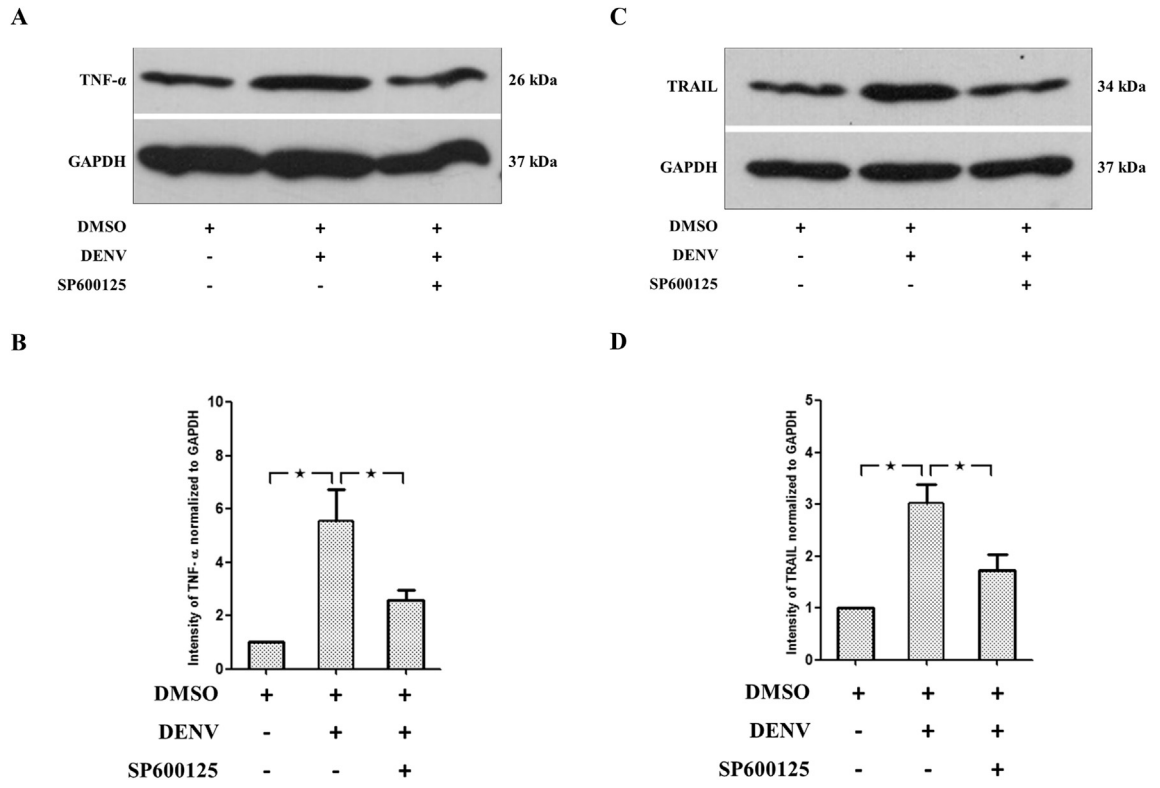

Fig. 8. SP600125 treatment modulated the TNF-α and TRAIL protein expression in the liver of DENV-infected mice. Mice were infected with DENV at a dose of 4×10^5 FFU and treated with 2% DMSO (v/v) or SP600125 in 2% DMSO. The un-infected control group of 2% DMSO (v/v) alone was also maintained. Liver tissues were harvested and proteins were extracted for western blot analysis, and densitometry analysis normalized to GAPDH was conducted. Western blot analysis of (A) TNF-α and (C) TRAIL normalized to individual GAPDH. The densitometry analysis of (B) TNF-α and (D) TRAIL expression is shown. Results are representative from 3 independent experiments for 3 independent mice (n = 3) from individual group.

block the ERK1/2 phosphorylation (Fig. 11C and D).

4. Discussion

Liver involvement in DENV infection is more evidently reported in BALB/c mouse models (Barreto et al., 2004; Franca et al., 2010; Paes et al., 2005, 2009), which is persistent with our previously established mouse model (Sreekanth et al., 2014). Leucopenia, thrombocytopenia, polycythemia and increased liver transaminases are observed in DENV-infected mice which were consistent with the DENV-infected patients (Azin et al., 2012; Binh et al., 2009; Kalayanarooj and Nimmannitya, 2003; Kittitrakul et al., 2015; Lee et al., 2012; Rathakrishnan et al., 2012). Liver histopathology with classical signs of injury was evident in DENV-infected patients as well as in animal models (Franca et al., 2010; Goncalves et al., 2012; Povoa et al., 2014; Sarathy et al., 2015; Sreekanth et al., 2014; Tan et al., 2010). Liver injury in DENV-infected mice was evident on Day 7, but a high level of viremia was observed in the serum on Day 3 compared to that of Day 7. Improved laboratory parameters on Day 7 post infection suggest the efficacy of SP600125 in DENV-induced liver injury. Other MAPK inhibitors reported similarly (Fu et al., 2014; Sreekanth et al., 2014, 2016), suggesting SP600125 as a compound for reducing the liver injury in DENV infection; however, this requires proper validation in clinical trial before using in clinical setup.

The amelioration of liver injury did not result from the reduction of DENV, but it is likely to be due to the modulation of host immune responses. Without reducing the number of viral particles, SB203580 reduces apoptosis, inflammation and liver injuries in DENV-infected mice (Fu et al., 2014; Sreekanth et al., 2016). An ERK1/2 inhibitor, FR180204, also suppressed the ERK1/2 phosphorylation to reduce DENV-induced liver injury without influencing the virus (Sreekanth et al., 2014). Induced JNK phosphorylation and viral load were shown in DENV-infected macrophages, where SP600125 inhibited JNK phosphorylation with a clearance in the virus titer (Ceballos-Olvera et al., 2010). Similarly, induced JNK phosphorylation was observed in DENV-induced liver injury in this study. However, SP600125 did not show any reduction in DENV production either in serum or liver samples. However, our finding is consistent with the observation in another mosquito-borne flavivirus, JEV where SP600125 increased cell viability and reduced cell apoptosis but did not alter viral replication (Huang et al., 2016).

JNK phosphorylation associated with apoptosis is observed in pseudorabies virus (Yeh et al., 2008) and rabbit hemorrhagic disease virus (Garcia-Lastra et al., 2010). Apoptosis and phagocytic cell activation in DENV infection causes tissue injury or transient imbalance in the homeostasis (Marianneau et al., 1998). We characterized how SP600125 affects the expression of 84 apoptosis-related genes in DENV-infection. DENV-infection induces cleaved caspase-3 (de Miranda et al., 2012; Sung et al.,

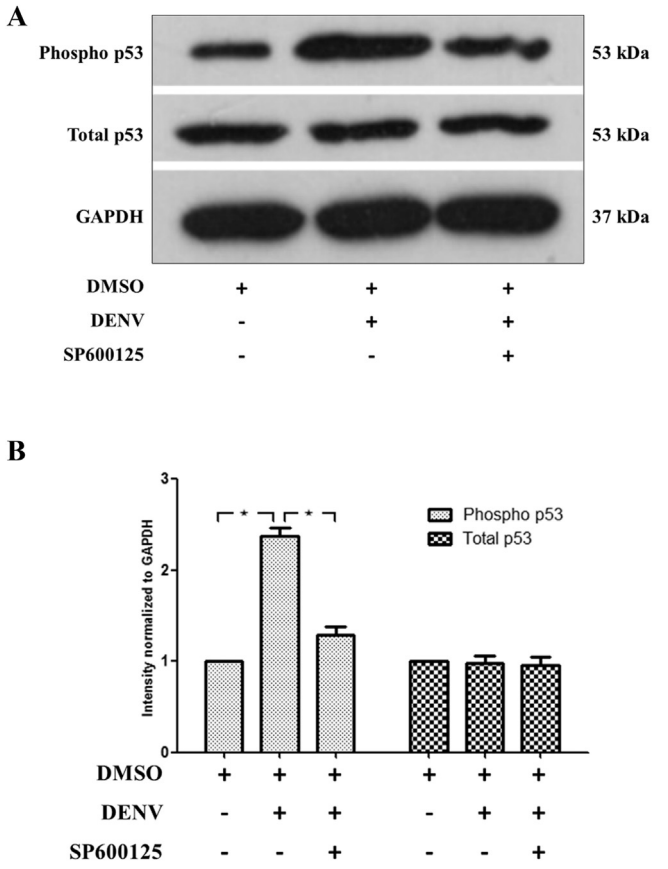

Fig. 9. SP600125 restricted the phosphorylation of p53 in the liver of DENV-infected mice. Liver tissues were harvested and proteins were extracted from un-infected control mice of 2% DMSO (v/v) alone treated and from two other groups of mice infected with DENV at a dose of 4×10^5 FFU, those were treated with either 2% DMSO (v/v) or SP600125 dissolved in 2% DMSO (v/v). Western blot analysis was conducted and results shown are representative from 3 independent experiments from at least 3 independent mice (n = 3) from each group. Densitometry analysis was conducted and normalized with GAPDH. (A) Western blot analysis of phosphorylated p53 and total p53 normalized to GAPDH (B) Densitometry analysis of phosphorylated p53 and total p53 normalized to GAPDH.

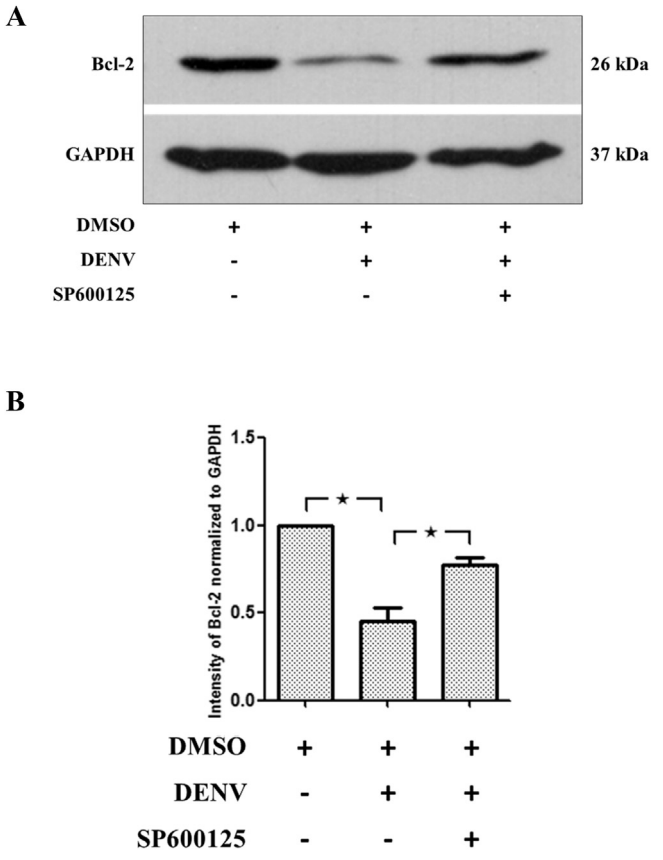

Fig. 10. SP600125 treatment modulated the anti-apoptotic Bcl-2 expressions in the liver of DENV-infected mice. Mice were infected with DENV at a dose of 4×10^5 FFU and treated with 2% DMSO (v/v) or SP600125 in 2% DMSO. An un-infected control group of 2% DMSO (v/v) alone is also maintained. Proteins were extracted from the liver tissue for Western blot analysis. Densitometry analysis normalized to GAPDH was conducted using ImageJ software. (A) Western blot analysis of Bcl-2 normalized to GAPDH, and (B) Densitometry analysis of Bcl-2 is shown. Results are representative from 3 independent experiments for 3 independent mice (n = 3) from individual group.

2012; Vasquez Ochoa et al., 2009) and DENV-infected HepG2 cells associates to multiple apoptotic pathways (Limonta et al., 2007; Marianneau et al., 1997; Netsawang et al., 2010; Thepparit et al., 2013). DENV-induced overexpression of caspase-9 reduced mitochondrial membrane potential (Qi et al., 2015), which can contribute to vascular pathology (Lin et al., 2004). WNV is reported to induce caspase-3 and caspase-9 to initiate mitochondrial pathway of apoptosis (Chu and Ng, 2003). The reduction of active caspase-8 and caspase-9 in our study indicates the ability of SP600125 in modulating both extrinsic and intrinsic pathways of apoptosis.

Phosphorylation of MAPKs induces cytokine production (Hui et al., 2009; Lin et al., 2008; Rajendra Kumar et al., 2005; Regan et al., 2009), which was reported in various viral diseases (Garcia-Lastra et al., 2010; Rahaus et al., 2004; Rajendra Kumar et al., 2005; Strong et al., 2008; Wei et al., 2014; Yang et al., 2010). Excessive cytokine production may lead to DENV-induced liver injury and increase vascular permeability (Pagliari et al., 2014). The increased expressions of TNF-α and TRAIL are associated with DENV-induced apoptosis, which may increase the disease severity (Arias et al., 2014; Suksanpaisan et al., 2007). Increased TRAIL expression is observed in DENV-infected hepatic cells, immune cells (Matsuda et al., 2005; Suksanpaisan et al., 2007; Warke et al., 2008) and patients (Limonta et al., 2014). TNF-α, and TRAIL initiates apoptosis via the activation of Fas and caspase-8, suggesting the involvement of extrinsic pathway (Liao et al., 2010; Torrentes-Carvalho et al., 2009). We report here the role of SP600125 in modulating the DENV-induced extrinsic pathway of apoptosis by decreasing the expressions of TNF-α and TRAIL.

Serine/threonine kinases including stress activating kinases are reported to phosphorylate p53 at multiple sites (Brooks and Gu, 2003), which was evident in UVB-induced JNK activation (She et al., 2002). In avian reo-virus (ARV) -induced apoptosis, SP600125 blocked the JNK1/2 induced p53 phosphorylation (Lin et al., 2009). Overexpression of bcl-2 is reported to delay apoptosis in DENV-infected fibroblast-like BHK-21 cells and allows the surviving cells to be persistent to infection (Su et al., 2001). Bcl-2 protects HepG2 cells from DENV M-ecto-domain-induced

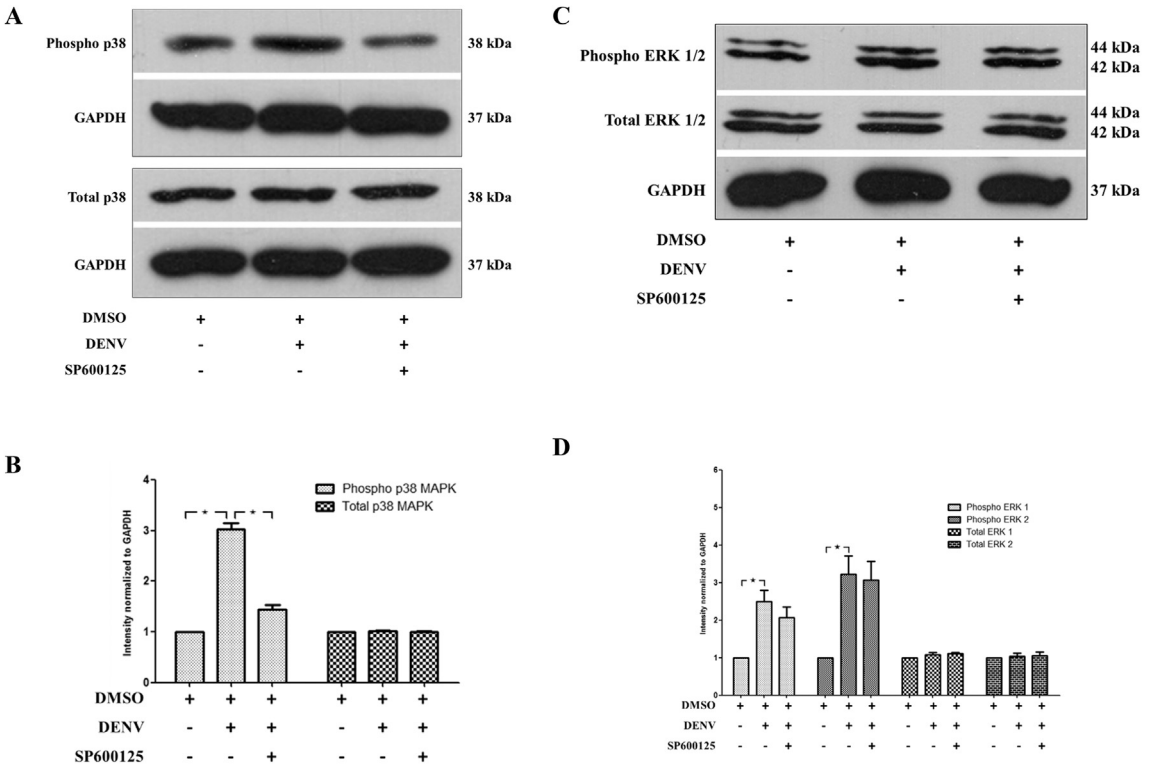

Fig. 11. SP600125 restricted the phosphorylation of p38 MAPK but not the ERK1/2 phosphorylation in the liver of DENV-infected mice. Liver tissues were harvested and proteins were extracted from un-infected control mice of 2% DMSO (v/v) alone treated and from two other groups of mice infected with DENV at a dose of 4×10^5 FFU, those were treated with either 2% DMSO (v/v) or SP600125 dissolved in 2% DMSO (v/v). Western blot analysis was conducted and results were normalized to GAPDH. The results shown are representative from 3 independent experiments from at least 3 independent mice (n = 3) from each group. Densitometry analysis was conducted and normalized with individual GAPDH. (A) Western blot analysis of phosphorylated p38 MAPK and total p38 MAPK (B) Densitometry analysis of phosphorylated p38 MAPK and total p38 MAPK (C) Western blot analysis of phosphorylated ERK1/2 and total ERK1/2 (D) Densitometry analysis of phosphorylated ERK1/2 and total ERK1/2 is shown.

apoptosis suggesting its anti-apoptotic role (Catteau et al., 2003). In hepatic ischemia-reperfusion injury, overexpressed Bcl-2 influences the JNK signaling to modulate apoptosis (Wang et al., 2014). Induced JNK and p53 phosphorylation reduces the Bcl-2 expression and this is responsible for the mitochondrial cytochrome-c release, and caspase-3 activation (Sarker et al., 2003). The involvement of mitochondria-mediated apoptosis via p53 has been reported in DENV-infected cell lines (Nasirudeen et al., 2008). We found that induced p53 phosphorylation contributes to DENV-induced liver injury and SP600125 treatment reduced this effect, which is consistent with the findings in ARV infection (Lin et al., 2009).

DENV infection in mice induces phosphorylation of p38 MAPK, the p38 MAPK inhibitor (SB203580) treatment did not directly reduce the phosphorylated form of p38, but modulates its downstream signals including MAPK-Activated Protein Kinse-2/Heat Shock Protein-27 (MAPKAPK2/HSP27) and Activating Transcription Factor-2 (ATF-2) to reduce DENV-induced liver injury (Sreekanth et al., 2016). Although SB203580 is inefficient to reduce the phosphorylation of p38 MAPK, SP600125 was found to be promising to reduce the phosphorylation of p38 MAPK. ERK1/2 phosphorylation contributes to DENV-induced liver injury in both DENV-infected HepG2 cells and mice (Leela et al., 2016; Sreekanth et al., 2014); however, no change in the DENV-induced ERK1/2 phosphorylation was observed with SP600125 treatment. Even though we clarified the cross reactivity of SP600125 in controlling other MAPKs including p38 MAPK, further studies in DENV-induced liver injury of knock out mice may be needed to clearly understand the specificity of each MAPK in modulation of DENV induced organ injury.

In this study, we elucidate the molecular mechanism by which JNK1/2 contributes to DENV-induced liver injury (Fig. 12A) and the effect of JNK1/2 inhibitor, SP600125 in modulating the liver injury in DENV infection (Fig. 12B). Even though, our effort was to find out the role of JNK signaling in DENV-induced liver injury and to sort out the contribution of SP600125 towards DENV-induced apoptotic cell death, further functional studies with causations are required to clearly clarify the pathogenesis.

5. Conclusion

DENV infection increases phosphorylation of JNK1/2 and p38 MAPK to induce liver injury via both intrinsic and extrinsic apoptotic pathways and SP600125 treatment reduces apoptosis via inhibiting phosphorylation of JNK1/2 and p38 MAPK, thereby curtailing the DENV-induced liver injury.

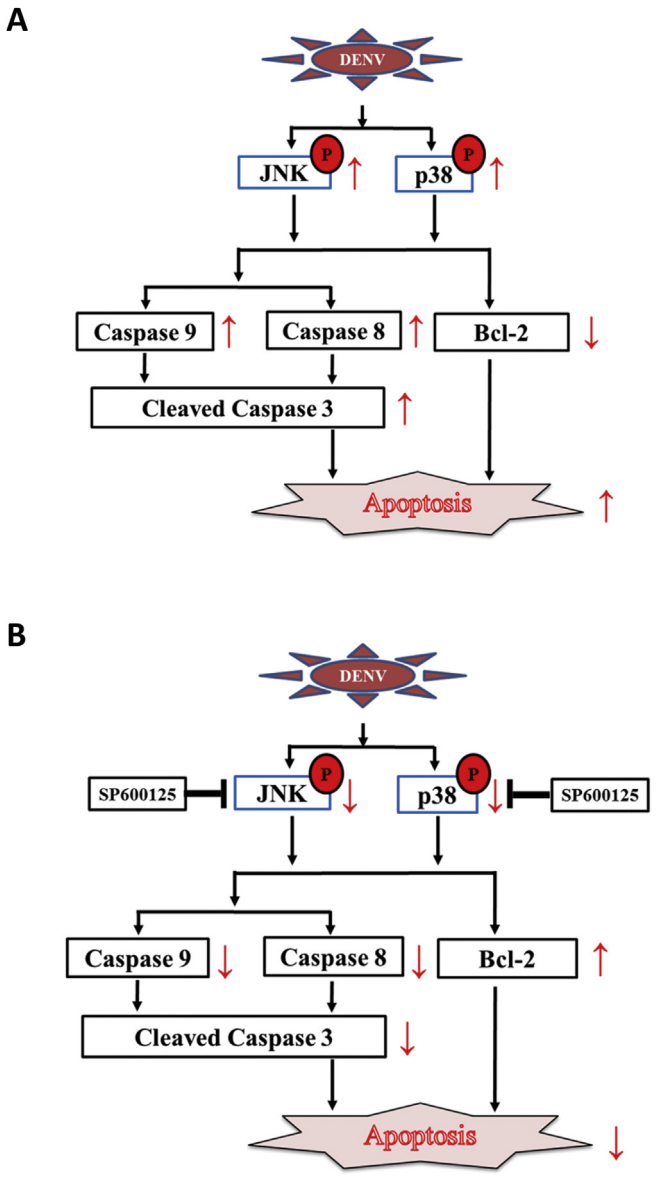

Fig. 12. Role of JNK signaling and effect of JNK1/2 inhibitor-SP600125 in DENV-induced liver injury. (A) JNK signaling in DENV-induced liver injury (B) SP600125 modulates the DENV-induced liver injury.

Acknowledgements

We sincerely thank Aunchalee Sirimontapon, Chalermporn Jompayao, Rapeephan Cholkate and Jutatip Panaampon for their technical supports. GPS was supported by Faculty of Medicine Siriraj Hospital, Mahidol University, Thailand. This study was supported by Mahidol University Grant No. R015810002 to TL.

Appendix A. Supplementary data

Supplementary data related to this article can be found at http://dx.doi.org/10.1016/j.antiviral.2017.02.003.

References

Arias, J., Valero, N., Mosquera, J., Montiel, M., Reyes, E., Larreal, Y., Alvarez-Mon, M., 2014. Increased expression of cytokines, soluble cytokine receptors, soluble apoptosis ligand and apoptosis in dengue. Virology 452–453, 42–51.

Arora, S., Nathaniel, S.D., Paul, J.C., Hansdak, S.G., 2015. Acute liver failure in dengue haemorrhagic fever. BMJ Case Rep. 2015.

Aye, K.S., Charngkaew, K., Win, N., Wai, K.Z., Moe, K., Punyadee, N., Thiemmeca, S., Suttitheptumrong, A., Sukpanichnant, S., Prida, M., Halstead, S.B., 2014. Pathologic highlights of dengue hemorrhagic fever in 13 autopsy cases from Myanmar. Hum. Pathol. 45, 1221–1233.

Azin, F.R., Goncalves, R.P., Pitombeira, M.H., Lima, D.M., Branco, I.C., 2012. Dengue: profile of hematological and biochemical dynamics. Rev. Bras. Hematol. Hemoter. 34, 36–41.

Barreto, D.F., Takiya, C.M., Paes, M.V., Farias-Filho, J., Pinhao, A.T., Alves, A.M., Costa, S.M., Barth, O.M., 2004. Histopathological aspects of Dengue-2 virus infected mice tissues and complementary virus isolation. J. Submicrosc. Cytol. Pathol. 36, 121–130.

Bennett, B.L., Sasaki, D.T., Murray, B.W., O'Leary, E.C., Sakata, S.T., Xu, W., Leisten, J.C., Motiwala, A., Pierce, S., Satoh, Y., Bhagwat, S.S., Manning, A.M., Anderson, D.W., 2001. SP600125, an anthrapyrazolone inhibitor of Jun N-terminal kinase. Proc. Natl. Acad. Sci. U. S. A. 98, 13681–13686.

Binh, P.T., Matheus, S., Huong, V.T., Deparis, X., Marechal, V., 2009. Early clinical and biological features of severe clinical manifestations of dengue in Vietnamese adults. J. Clin. Virol. Off. Publ. Pan Am. Soc. Clin. Virol. 45, 276–280.

Brooks, C.L., Gu, W., 2003. Ubiquitination, phosphorylation and acetylation: the molecular basis for p53 regulation. Curr. Opin. Cell Biol. 15, 164–171.

Cardier, J.E., Marino, E., Romano, E., Taylor, P., Liprandi, F., Bosch, N., Rothman, A.L., 2005. Proinflammatory factors present in sera from patients with acute dengue infection induce activation and apoptosis of human microvascular endothelial cells: possible role of TNF-alpha in endothelial cell damage in dengue. Cytokine 30, 359–365.

Catteau, A., Kalinina, O., Wagner, M.C., Deubel, V., Courageot, M.P., Despres, P., 2003. Dengue virus M protein contains a proapoptotic sequence referred to as ApoptoM. J. General Virol. 84, 2781–2793.

Ceballos-Olvera, I., Chavez-Salinas, S., Medina, F., Ludert, J.E., del Angel, R.M., 2010. JNK phosphorylation, induced during dengue virus infection, is important for viral infection and requires the presence of cholesterol. Virology 396, 30–36.

Chareonsirisuthigul, T., Kalayanarooj, S., Ubol, S., 2007. Dengue virus (DENV) antibody-dependent enhancement of infection upregulates the production of anti-inflammatory cytokines, but suppresses anti-DENV free radical and pro-inflammatory cytokine production, in THP-1 cells. J. General Virol. 88, 365–375.

Chu, J.J., Ng, M.L., 2003. The mechanism of cell death during West Nile virus infection is dependent on initial infectious dose. J. General Virol. 84, 3305–3314.

de Macedo, F.C., Nicol, A.F., Cooper, L.D., Yearsley, M., Pires, A.R., Nuovo, G.J., 2006. Histologic, viral, and molecular correlates of dengue fever infection of the liver using highly sensitive immunohistochemistry. Diag. Mol. Pathol. Am. J. Surg. Pathol. Part B 15, 223–228.

de Miranda, A.S., Rodrigues, D.H., Amaral, D.C., de Lima Campos, R.D., Cisalpino, D., Vilela, M.C., Lacerda-Queiroz, N., de Souza, K.P., Vago, J.P., Campos, M.A., Kroon, E.G., da Gloria de Souza, D., Teixeira, M.M., Teixeira, A.L., Rachid, M.A., 2012. Dengue-3 encephalitis promotes anxiety-like behavior in mice. Behav. Brain Res. 230, 237–242.

Franca, R.F., Zucoloto, S., da Fonseca, B.A., 2010. A BALB/c mouse model shows that liver involvement in dengue disease is immune-mediated. Exp. Mol. Pathol. 89, 321–326.

Fu, Y., Yip, A., Seah, P.G., Blasco, F., Shi, P.Y., Herve, M., 2014. Modulation of inflammation and pathology during dengue virus infection by p38 MAPK inhibitor SB203580. Antivir. Res. 110, 151–157.

Garcia-Lastra, R., San-Miguel, B., Crespo, I., Jorquera, F., Alvarez, M., Gonzalez-Gallego, J., Tunon, M.J., 2010. Signaling pathways involved in liver injury and regeneration in rabbit hemorrhagic disease, an animal model of virally-induced fulminant hepatic failure. Veterinary Res. 41, 2.

Ghosh, M., Banerjee, M., Das, S., Chakraborty, S., 2011. Dengue infection with multi-organ involvement. Scand. J. Infect. Dis. 43, 316–318.

Goncalves, D., de Queiroz Prado, R., Almeida Xavier, E., Cristina de Oliveira, N., da Matta Guedes, P.M., da Silva, J.S., Moraes Figueiredo, L.T., Aquino, V.H., 2012. Imunocompetent mice model for dengue virus infection. Sci. J. 2012, 525947.

Gubler, D.J., 2002. Epidemic dengue/dengue hemorrhagic fever as a public health, social and economic problem in the 21st century. Trends Microbiol. 10, 100–103.

Halstead, S.B., 2007. Dengue. Lancet 370, 1644–1652.

Huang, M., Xu, A., Wu, X., Zhang, Y., Guo, Y., Guo, F., Pan, Z., Kong, L., 2016. Japanese encephalitis virus induces apoptosis by the IRE1/JNK pathway of ER stress response in BHK-21 cells. Arch. Virol. 161, 699–703.

Huerre, M.R., Lan, N.T., Marianneau, P., Hue, N.B., Khun, H., Hung, N.T., Khen, N.T., Drouet, M.T., Huong, V.T., Ha, D.Q., Buisson, Y., Deubel, V., 2001. Liver histopathology and biological correlates in five cases of fatal dengue fever in Vietnamese children. Virchows Arch. Int. J. Pathol. 438, 107–115.

Hui, K.P., Lee, S.M., Cheung, C.Y., Ng, I.H., Poon, L.L., Guan, Y., Ip, N.Y., Lau, A.S., Peiris, J.S., 2009. Induction of proinflammatory cytokines in primary human macrophages by influenza A virus (H5N1) is selectively regulated by IFN regulatory factor 3 and p38 MAPK. J. Immunol. 182, 1088–1098.

Jirakanjanakit, N., Sanohsomneing, T., Yoksan, S., Bhamarapravati, N., 1997. The micro-focus reduction neutralization test for determining dengue and Japanese encephalitis neutralizing antibodies in volunteers vaccinated against dengue. Trans. R. Soc. Trop. Med. Hyg. 91, 614–617.

Kalayanarooj, S., Nimmannitya, S., 2003. Clinical presentations of dengue hemorrhagic fever in infants compared to children. J. Med. Assoc. Thail. = Chotmaihet

thangphaet 86 (Suppl. 3), S673–S680.
Kittitrakul, C., Silachamroon, U., Phumratanaprapin, W., Krudsood, S., Wilairatana, P., Treeprasertsuk, S., 2015. Liver function tests abnormality and clinical severity of dengue infection in adult patients. J. Med. Assoc. Thail. = Chotmaihet thangphaet 98 (Suppl. 1), S1–S8.
Lee, L.K., Gan, V.C., Lee, V.J., Tan, A.S., Leo, Y.S., Lye, D.C., 2012. Clinical relevance and discriminatory value of elevated liver aminotransferase levels for dengue severity. PLoS Neglected Trop. Dis. 6, e1676.
Leela, S.L., Srisawat, C., Sreekanth, G.P., Noisakran, S., Yenchitsomanus, P.T., Limjindaporn, T., 2016. Drug repurposing of minocycline against dengue virus infection. Biochem. Biophys. Res. Commun. 478, 410–416.
Liao, H., Xu, J., Huang, J., 2010. FasL/Fas pathway is involved in dengue virus induced apoptosis of the vascular endothelial cells. J. Med. Virol. 82, 1392–1399.
Limonta, D., Capo, V., Torres, G., Perez, A.B., Guzman, M.G., 2007. Apoptosis in tissues from fatal dengue shock syndrome. J. Clin. Virol. Off. Publ. Pan Am. Soc. Clin. Virol. 40, 50–54.
Limonta, D., Torrentes-Carvalho, A., Marinho, C.F., de Azeredo, E.L., de Souza, L.J., Motta-Castro, A.R., da Cunha, R.V., Kubelka, C.F., Nogueira, R.M., de-Oliveira-Pinto, L.M., 2014. Apoptotic mediators in patients with severe and non-severe dengue from Brazil. J. Med. Virol. 86, 1437–1447.
Lin, C.F., Wan, S.W., Chen, M.C., Lin, S.C., Cheng, C.C., Chiu, S.C., Hsiao, Y.L., Lei, H.Y., Liu, H.S., Yeh, T.M., Lin, Y.S., 2008. Liver injury caused by antibodies against dengue virus nonstructural protein 1 in a murine model. Lab. Investig. J. Tech. Methods Pathol. 88, 1079–1089.
Lin, P.Y., Lee, J.W., Liao, M.H., Hsu, H.Y., Chiu, S.J., Liu, H.J., Shih, W.L., 2009. Modulation of p53 by mitogen-activated protein kinase pathways and protein kinase C delta during avian reovirus S1133-induced apoptosis. Virology 385, 323–334.
Lin, Y.S., Lin, C.F., Lei, H.Y., Liu, H.S., Yeh, T.M., Chen, S.H., Liu, C.C., 2004. Antibody-mediated endothelial cell damage via nitric oxide. Curr. Pharm. Des. 10, 213–221.
Marianneau, P., Cardona, A., Edelman, L., Deubel, V., Despres, P., 1997. Dengue virus replication in human hepatoma cells activates NF-kappaB which in turn induces apoptotic cell death. J. Virol. 71, 3244–3249.
Marianneau, P., Flamand, M., Deubel, V., Despres, P., 1998. Apoptotic cell death in response to dengue virus infection: the pathogenesis of dengue haemorrhagic fever revisited. Clin. Diag. Virol. 10, 113–119.
Matsuda, T., Almasan, A., Tomita, M., Tamaki, K., Saito, M., Tadano, M., Yagita, H., Ohta, T., Mori, N., 2005. Dengue virus-induced apoptosis in hepatic cells is partly mediated by Apo2 ligand/tumour necrosis factor-related apoptosis-inducing ligand. J. General Virol. 86, 1055–1065.
Morchang, A., Yasamut, U., Netsawang, J., Noisakran, S., Wongwiwat, W., Songprakhon, P., Srisawat, C., Puttikhunt, C., Kasinrerk, W., Malasit, P., Yenchitsomanus, P.T., Limjindaporn, T., 2011. Cell death gene expression profile: role of RIPK2 in dengue virus-mediated apoptosis. Virus Res. 156, 25–34.
Nasirudeen, A.M., Wang, L., Liu, D.X., 2008. Induction of p53-dependent and mitochondria-mediated cell death pathway by dengue virus infection of human and animal cells. Microb. Infect. Inst. Pasteur 10, 1124–1132.
Netsawang, J., Noisakran, S., Puttikhunt, C., Kasinrerk, W., Wongwiwat, W., Malasit, P., Yenchitsomanus, P.T., Limjindaporn, T., 2010. Nuclear localization of dengue virus capsid protein is required for DAXX interaction and apoptosis. Virus Res. 147, 275–283.
Nguyen, T.L., Nguyen, T.H., Tieu, N.T., 1997. The impact of dengue haemorrhagic fever on liver function. Res. Virol. 148, 273–277.
Paes, M.V., Lenzi, H.L., Nogueira, A.C., Nuovo, G.J., Pinhao, A.T., Mota, E.M., Basilio-de-Oliveira, C.A., Schatzmayr, H., Barth, O.M., Alves, A.M., 2009. Hepatic damage associated with dengue-2 virus replication in liver cells of BALB/c mice. Lab. Investig. J. Tech. Methods Pathol. 89, 1140–1151.
Paes, M.V., Pinhao, A.T., Barreto, D.F., Costa, S.M., Oliveira, M.P., Nogueira, A.C., Takiya, C.M., Farias-Filho, J.C., Schatzmayr, H.G., Alves, A.M., Barth, O.M., 2005. Liver injury and viremia in mice infected with dengue-2 virus. Virology 338, 236–246.
Pagliari, C., Quaresma, J.A., Fernandes, E.R., Stegun, F.W., Brasil, R.A., de Andrade Jr., H.F., Barros, V., Vasconcelos, P.F., Duarte, M.I., 2014. Immunopathogenesis of dengue hemorrhagic fever: contribution to the study of human liver lesions. J. Med. Virol. 86, 1193–1197.
Pang, T., Cardosa, M.J., Guzman, M.G., 2007. Of cascades and perfect storms: the immunopathogenesis of dengue haemorrhagic fever-dengue shock syndrome (DHF/DSS). Immunol. Cell Biol. 85, 43–45.
Povoa, T.F., Alves, A.M., Oliveira, C.A., Nuovo, G.J., Chagas, V.L., Paes, M.V., 2014. The pathology of severe dengue in multiple organs of human fatal cases: histopathology, ultrastructure and virus replication. PloS One 9, e83386.
Qi, Y., Li, Y., Zhang, Y., Zhang, L., Wang, Z., Zhang, X., Gui, L., Huang, J., 2015. IFI6 inhibits apoptosis via mitochondrial-dependent pathway in dengue virus 2 infected vascular endothelial cells. PloS One 10, e0132743.
Rahaus, M., Desloges, N., Wolff, M.H., 2004. Replication of varicella-zoster virus is influenced by the levels of JNK/SAPK and p38/MAPK activation. J. General Virol. 85, 3529–3540.
Rajendra Kumar, P., Singhal, P.K., Subba Rao, M.R., Mahalingam, S., 2005. Phosphorylation by MAPK regulates simian immunodeficiency virus Vpx protein nuclear import and virus infectivity. J. Biol. Chem. 280, 8553–8563.
Rathakrishnan, A., Wang, S.M., Hu, Y., Khan, A.M., Ponnampalavanar, S., Lum, L.C., Manikam, R., Sekaran, S.D., 2012. Cytokine expression profile of dengue patients at different phases of illness. PloS One 7, e52215.
Regan, A.D., Cohen, R.D., Whittaker, G.R., 2009. Activation of p38 MAPK by feline infectious peritonitis virus regulates pro-inflammatory cytokine production in primary blood-derived feline mononuclear cells. Virology 384, 135–143.
Sakinah, S., Priya, S.P., Kumari, S., Amira, F., K, P., Alsaeedy, H., Ling, M.P., Chee, H.Y., Higuchi, A., Alarfaj, A.A., Munusamy, M.A., Murugan, K., Taib, C.N., Arulselvan, P., Rajan, M., Neela, V.K., Hamat, R.A., Benelli, G., Kumar, S.S., 2016. Impact of dengue virus (serotype DENV-2) infection on liver of BALB/c mice: a histopathological analysis. Tissue & Cell 49, 86–94.
Sarathy, V.V., White, M., Li, L., Gorder, S.R., Pyles, R.B., Campbell, G.A., Milligan, G.N., Bourne, N., Barrett, A.D., 2015. A lethal murine infection model for dengue virus 3 in AG129 mice deficient in type I and II interferon receptors leads to systemic disease. J. Virol. 89, 1254–1266.
Sarker, K.P., Biswas, K.K., Rosales, J.L., Yamaji, K., Hashiguchi, T., Lee, K.Y., Maruyama, I., 2003. Ebselen inhibits NO-induced apoptosis of differentiated PC12 cells via inhibition of ASK1-p38 MAPK-p53 and JNK signaling and activation of p44/42 MAPK and Bcl-2. J. Neurochem. 87, 1345–1353.
Schmitz, L., Prayag, S., Varghese, S., Jog, S., Bhargav-Patil, P., Yadav, A., Salunke, D., Vincent, J.L., 2011. Nonhematological organ dysfunction and positive fluid balance are important determinants of outcome in adults with severe dengue infection: a multicenter study from India. J. Crit. Care 26, 441–448.
She, Q.B., Ma, W.Y., Dong, Z., 2002. Role of MAP kinases in UVB-induced phosphorylation of p53 at serine 20. Oncogene 21, 1580–1589.
Sreekanth, G.P., Chuncharunee, A., Sirimontaporn, A., Panaampon, J., Noisakran, S., Yenchitsomanus, P.T., Limjindaporn, T., 2016. SB203580 modulates p38 MAPK signaling and dengue virus-induced liver injury by reducing MAPKAPK2, HSP27, and ATF2 phosphorylation. PloS One 11, e0149486.
Sreekanth, G.P., Chuncharunee, A., Sirimontaporn, A., Panaampon, J., Srisawat, C., Morchang, A., Malakar, S., Thuwajit, P., Kooptiwut, S., Suttitheptumrong, A., Songprakhon, P., Noisakran, S., Yenchitsomanus, P.T., Limjindaporn, T., 2014. Role of ERK1/2 signaling in dengue virus-induced liver injury. Virus Res. 188, 15–26.
Strong, J.E., Wong, G., Jones, S.E., Grolla, A., Theriault, S., Kobinger, G.P., Feldmann, H., 2008. Stimulation of Ebola virus production from persistent infection through activation of the Ras/MAPK pathway. Proc. Natl. Acad. Sci. U. S. A. 105, 17982–17987.
Su, H.L., Lin, Y.L., Yu, H.P., Tsao, C.H., Chen, L.K., Liu, Y.T., Liao, C.L., 2001. The effect of human bcl-2 and bcl-X genes on dengue virus-induced apoptosis in cultured cells. Virology 282, 141–153.
Suksanpaisan, L., Cabrera-Hernandez, A., Smith, D.R., 2007. Infection of human primary hepatocytes with dengue virus serotype 2. J. Med. Virol. 79, 300–307.
Sung, J.M., Lee, C.K., Wu-Hsieh, B.A., 2012. Intrahepatic infiltrating NK and CD8 T cells cause liver cell death in different phases of dengue virus infection. PloS One 7, e46292.
Tan, G.K., Ng, J.K., Trasti, S.L., Schul, W., Yip, G., Alonso, S., 2010. A non mouse-adapted dengue virus strain as a new model of severe dengue infection in AG129 mice. PLoS Neglected Trop. Dis. 4, e672.
Thepparit, C., Khakpoor, A., Khongwichit, S., Wikan, N., Fongsaran, C., Chingsuwanrote, P., Panraksa, P., Smith, D.R., 2013. Dengue 2 infection of HepG2 liver cells results in endoplasmic reticulum stress and induction of multiple pathways of cell death. BMC Res. Notes 6, 372.
Thongtan, T., Panyim, S., Smith, D.R., 2004. Apoptosis in dengue virus infected liver cell lines HepG2 and Hep3B. J. Med. Virol. 72, 436–444.
Torrentes-Carvalho, A., Azeredo, E.L., Reis, S.R., Miranda, A.S., Gandini, M., Barbosa, L.S., Kubelka, C.F., 2009. Dengue-2 infection and the induction of apoptosis in human primary monocytes. Mem. do Inst. Oswaldo Cruz 104, 1091–1099.
Treeprasertsuk, S., Kittitrakul, C., 2015. Liver complications in adult dengue and current management. Southeast Asian J. Trop. Med. Public Health 46 (Suppl. 1), 99–107.
Trung, D.T., Thao le, T.T., Hien, T.T., Hung, N.T., Vinh, N.N., Hien, P.T., Chinh, N.T., Simmons, C., Wills, B., 2010. Liver involvement associated with dengue infection in adults in Vietnam. Am. J. Trop. Med. Hyg. 83, 774–780.
Vasquez Ochoa, M., Garcia Cordero, J., Gutierrez Castaneda, B., Santos Argumedo, L., Villegas Sepulveda, N., Cedillo Barron, L., 2009. A clinical isolate of dengue virus and its proteins induce apoptosis in HMEC-1 cells: a possible implication in pathogenesis. Arch. Virol. 154, 919–928.
Wang, C., Chen, K., Xia, Y., Dai, W., Wang, F., Shen, M., Cheng, P., Wang, J., Lu, J., Zhang, Y., Yang, J., Zhu, R., Zhang, H., Li, J., Zheng, Y., Zhou, Y., Guo, C., 2014. N-acetylcysteine attenuates ischemia-reperfusion-induced apoptosis and autophagy in mouse liver via regulation of the ROS/JNK/Bcl-2 pathway. PloS One 9, e108855.
Warke, R.V., Martin, K.J., Giaya, K., Shaw, S.K., Rothman, A.L., Bosch, I., 2008. TRAIL is a novel antiviral protein against dengue virus. J. Virol. 82, 555–564.
Wei, D., Huang, Z.H., Zhang, R.H., Wang, C.L., Xu, M.J., Liu, B.J., Wang, G.H., Xu, T., 2014. Roles of p38 MAPK in the regulation of the inflammatory response to swine influenza virus-induced acute lung injury in mice. Acta Virol. 58, 374–379.
Yan, D., An, G., Kuo, M.T., 2016. C-Jun N-terminal kinase signalling pathway in response to cisplatin. J. Cell. Mol. Med. 20, 2013–2019.
Yang, T.C., Lai, C.C., Shiu, S.L., Chuang, P.H., Tzou, B.C., Lin, Y.Y., Tsai, F.J., Lin, C.W., 2010. Japanese encephalitis virus down-regulates thioredoxin and induces ROS-mediated ASK1-ERK/p38 MAPK activation in human promonocyte cells. Microb. Infect. Inst. Pasteur 12, 643–651.
Yeh, C.J., Lin, P.Y., Liao, M.H., Liu, H.J., Lee, J.W., Chiu, S.J., Hsu, H.Y., Shih, W.L., 2008. TNF-alpha mediates pseudorabies virus-induced apoptosis via the activation of p38 MAPK and JNK/SAPK signaling. Virology 381, 55–66.